GROUNDWATER RESOURCES PROGRAM

Conceptual Model of the Great Basin Carbonate and Alluvial Aquifer System

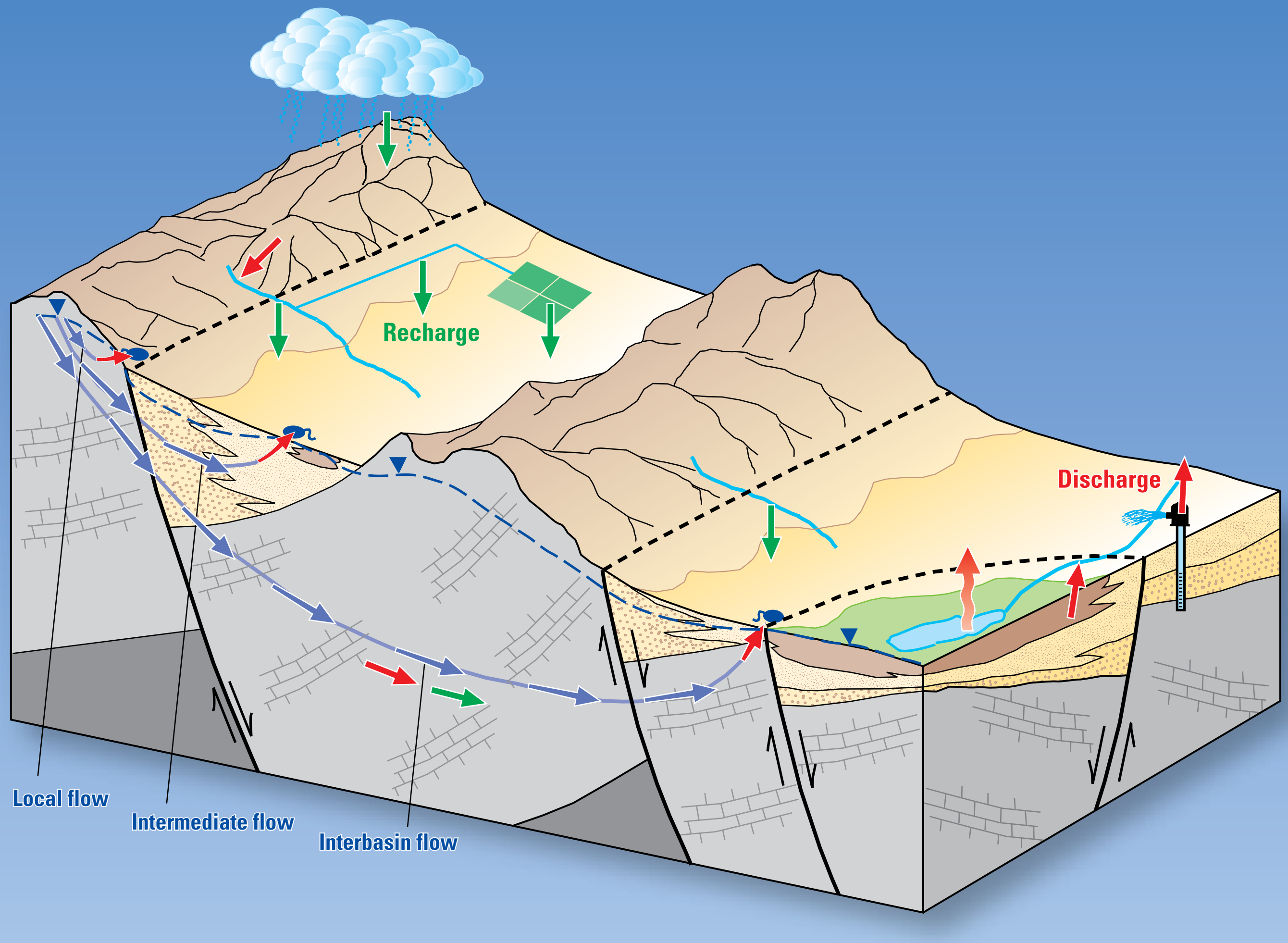

Scientific Investigations Report 2010–5193

U.S. Department of the Interior
U.S. Geological Survey

Conceptual Model of the Great Basin Carbonate and Alluvial Aquifer System

By Victor M. Heilweil, and Lynette E. Brooks, editors

Scientific Investigations Report 2010–5193

U.S. Department of the Interior
U.S. Geological Survey

U.S. Department of the Interior
KEN SALAZAR, Secretary

U.S. Geological Survey
Marcia K. McNutt, Director

U.S. Geological Survey, Reston, Virginia: 2011

For more information on the USGS—the Federal source for science about the Earth, its natural and living resources, natural hazards, and the environment, visit http://www.usgs.gov or call 1-888-ASK-USGS

For an overview of USGS information products, including maps, imagery, and publications, visit http://www.usgs.gov/pubprod

To order this and other USGS information products, visit http://store.usgs.gov

Suggested citation:
Heilweil, V.M., and Brooks, L.E., eds., 2011, Conceptual model of the Great Basin carbonate and alluvial aquifer system: U.S. Geological Survey Scientific Investigations Report 2010-5193, 191 p.

Contents

Figures

Tables

Conversion Factors

Inch/Pound to SI

Multiply	By	To obtain
	Length	
inch (in.)	2.54	centimeter (cm)
inch (in.)	25.4	millimeter (mm)
foot (ft)	0.3048	meter (m)
mile (mi)	1.609	kilometer (km)
	Area	
acre	4,047	square meter (m^2)
acre	0.4047	hectare (ha)
square mile (mi^2)	2.590	square kilometer (km^2)
	Volume	
gallon (gal)	3.785	liter (L)
gallon (gal)	0.003785	cubic meter (m^3)
gallon (gal)	3.785	cubic decimeter (dm^3)
cubic foot (ft^3)	28.32	cubic decimeter (dm^3)
cubic foot (ft^3)	0.02832	cubic meter (m^3)
acre-foot (acre-ft)	1,233	cubic meter (m^3)
acre-foot (acre-ft)	0.001233	cubic hectometer (hm^3)
	Flow rate	
acre-foot per year (acre-ft/yr)	1,233	cubic meter per year (m^3/yr)
acre-foot per year (acre-ft/yr)	0.001233	cubic hectometer per year (hm^3/yr)
foot per year (ft/yr)	0.3048	meter per year (m/yr)
cubic foot per second (ft^3/s)	0.02832	cubic meter per second (m^3/s)
cubic foot per day (ft^3/d)	0.02832	cubic meter per day (m^3/d)
gallon per minute (gal/min)	0.06309	liter per second (L/s)
	Hydraulic conductivity	
foot per day (ft/d)	0.3048	meter per day (m/d)
inch per day (in./d)	25.38	millimeter per day (mm/d)
	Transmissivity*	
foot squared per day (ft^2/d)	0.09290	meter squared per day (m^2/d)

Note: The conversion factors given above are for the entire report. Not all listed conversion factors will be in any given chapter of this report.

Temperature in degrees Celsius (°C) may be converted to degrees Fahrenheit (°F) as follows:
°F=(1.8×°C)+32

Temperature in degrees Fahrenheit (°F) may be converted to degrees Celsius (°C) as follows:
°C=(°F-32)/1.8

Temperature in kelvin (K) may be converted to degrees Fahrenheit (°F) as follows:
°F=1.8K-459.67

Temperature in kelvin (K) may be converted to degrees Celsius (°C) as follows:
°C=K-273.15

Vertical coordinate information is referenced to the North American Vertical Datum of 1988 (NAVD 88).

Horizontal coordinate information is referenced to the North American Datum of 1983 (NAD 83).

Altitude, as used in this report, refers to distance above the vertical datum.

*Transmissivity: The standard unit for transmissivity is cubic foot per day per square foot times foot of aquifer thickness [(ft^3/d)/ft^2]ft. In this report, the mathematically reduced form, foot squared per day (ft^2/d), is used for convenience.

Abstract

A conceptual model of the Great Basin carbonate and alluvial aquifer system (GBCAAS) was developed by the U.S. Geological Survey (USGS) for a regional assessment of groundwater availability as part of a national water census. The study area is an expansion of a previous USGS Regional Aquifer Systems Analysis (RASA) study conducted during the 1980s and 1990s of the carbonate-rock province of the Great Basin. The geographic extent of the study area is 110,000 mi^2, predominantly in eastern Nevada and western Utah, and includes 165 hydrographic areas (HAs) and 17 regional groundwater flow systems.

A three-dimensional hydrogeologic framework was constructed that defines the physical geometry and rock types through which groundwater moves. The diverse sedimentary units of the GBCAAS study area are grouped into hydrogeologic units (HGUs) that are inferred to have reasonably distinct hydrologic properties due to their physical characteristics. These HGUs are commonly disrupted by large-magnitude offset thrust, strike-slip, and normal faults, and locally affected by caldera formation. The most permeable aquifer materials within the study area include Cenozoic unconsolidated sediments and volcanic rocks, along with Mesozoic and Paleozoic carbonate rocks. The framework was built by extracting and combining information from digital elevation models, geologic maps, cross sections, drill hole logs, existing hydrogeologic frameworks, and geophysical data.

Most groundwater flow occurs at local and intermediate scales within each HA, but previous studies have suggested interbasin flow on the basis of groundwater budget imbalances, isotopic studies, and numerical modeling. A regional potentiometric-surface map of the GBCAAS study area was developed based on water-level data from wells, springs, and perennial mountain streams. This map indicates that groundwater levels and hydraulic gradients within each HA generally follow topography and flow from areas of high land-surface altitude to areas of lower altitude. At the regional scale, groundwater flow between HAs may occur where (1) a hydraulic gradient exists, (2) the intervening mountains are comprised of rocks permeable enough to permit groundwater flow, and (3) substantial groundwater mounding from mountain-block recharge does not occur. The potentiometric-surface map indicates general groundwater movement from mountainous areas to the Great Salt Lake Desert, the Humboldt River, the Colorado River, and Death Valley.

Hydrologic data from previous investigations were compiled and reinterpreted to quantify groundwater recharge- and discharge-budget components. The Basin Characterization Model (BCM), a distributed-parameter water-balance-accounting model, was used to estimate recharge from precipitation. Prior to groundwater development beginning largely in the 1940s, total recharge was estimated to be 4,500,000 acre-ft/yr with an uncertainty of ± 50 percent (± 2,200,000 acre-ft/yr). The primary source of groundwater recharge to the GBCAAS is direct infiltration of precipitation. The estimated average 1940–2006 in-place recharge from precipitation is 2,900,000 acre-ft/yr. Other forms of recharge include infiltration of surface-water runoff including irrigation return flow (570,000 acre-ft/yr), recharge from mountain streams (130,000 acre-ft/yr), recharge from imported surface water (990,000 acre-ft/yr), and subsurface inflow (not estimated).

Prior to groundwater development, total groundwater discharge was estimated to be 4,200,000 acre-ft/yr with an uncertainty of ± 30 percent (± 1,300,000 acre-ft/yr). The two major components of discharge are evapotranspiration and springs. Estimated groundwater discharge to evapotranspiration and springs for predevelopment conditions was 1,800,000 acre-ft/yr and 990,000 acre-ft/yr, respectively. Other forms of discharge include discharge to basin-fill streams/lakes/reservoirs (660,000 acre-ft/yr), discharge to mountain streams (450,000 acre-ft/yr), and subsurface outflow (not estimated). Some previously reported estimates of discharge to evapotranspiration and springs were made while groundwater withdrawals were occurring; an additional 330,000 acre-ft/yr adjustment to natural discharge for well withdrawals was estimated for the predevelopment groundwater budget.

Between 1940 and 2006, groundwater development occurred in various parts of the GBCAAS, with estimated total well withdrawals increasing from less than 300,000 acre-ft/yr in 1940 to almost 1,300,000 acre-ft/yr in the late 1970s. Since the late 1970s, well withdrawals have fluctuated between about 1,100,000 and 1,500,000 acre-ft/yr. Although well withdrawals have been minimal in the majority of HAs and groundwater flow systems, some areas have undergone substantial development, sometimes causing significant water-level declines. Although the majority of well withdrawals are used for irrigation, there has been a general increase in withdrawals for public supply and a decrease in

withdrawals for agriculture since the late 1970s. In addition to the estimated predevelopment groundwater recharge of 4,500,000 acre-ft/yr, the recent (year 2000) groundwater budget for the GBCAAS study area also includes recharge from unconsumed irrigation and public supply water from well withdrawals (470,000 acre-ft). The estimated decrease in combined natural discharge and groundwater storage within the GBCAAS study area caused by well withdrawals for the year 2000 was 990,000 acre-ft, including a minimum decrease of 67,000 acre-ft in groundwater storage.

Chapter A: Introduction

By Victor M. Heilweil, Donald S. Sweetkind, and David D. Susong

This study assesses groundwater resources in the complex Great Basin carbonate and alluvial aquifer system (GBCAAS). Located within the Basin and Range Physiographic Province, the Great Basin carbonate and alluvial aquifer system covers an area of approximately 110,000 mi^2 (fig. A–1), predominantly in eastern Nevada and western Utah. The study area encompasses the Basin and Range carbonate-rock aquifers and Southern Nevada volcanic-rock aquifers and includes a large portion of the Basin and Range basin-fill aquifers (Reilly and others, 2008, fig. 2). The aquifer system generally comprises aquifers and confining units in unconsolidated basin fill and volcanic deposits in the basins, and carbonate and other bedrock in the mountain ranges separating the basins. These same bedrock units often underlie the basins. The aquifers are, in some areas, hydraulically connected between basins. Harrill and Prudic (1998) note that because of this connectivity, the aquifers of the eastern Great Basin "collectively constitute a significant regional ground-water resource." Some mountain ranges in the study area, however, consist of less permeable rock that may impede groundwater flow between basins.

The GBCAAS study area is experiencing rapid population growth and has some of the highest per capita water use in the Nation, resulting in increasing demand for groundwater. The U.S. Census Bureau (2005) found that Nevada and Utah were among the fastest growing states in the United States, with a projected increase in population of more than 50 percent between 2000 and 2030. Growing urban areas include Las Vegas in the southern part of the study area and the Wasatch Front (extending from Cache County to Iron County, Utah) along the eastern margin of the study area (fig. A–1). A 1990 comparison of water use by states found that Utah and Nevada had per capita water uses of 308 and 344 gallons per person per day, respectively (Bergquist, 1994). These rates are the highest in the United States and nearly twice the national average of 185 gallons per person per day. The alluvial aquifers of the GBCAAS are considered part of the Basin and Range basin-fill aquifer system—the fourth most heavily pumped regional aquifer in the United States (Reilly and others, 2008). The combination of rapid population growth, high water use, and arid climate has led to an increased dependence upon groundwater resources during the past 60 years (Gates, 2004) and predictions of future water shortages (U.S. Water News, June 2005). Severe groundwater depletion, along with declining groundwater levels and spring discharge, has occurred in several basins within the study area (Hurlow and Burke, 2008; L. Konikow, U.S. Geological Survey, written commun., 2009).

Because of its regional extent and large reliance upon groundwater resources as water supplies for urban populations, agriculture, and native habitats, the GBCAAS was selected for assessment by the U.S. Geological Survey National Water Census Initiative to evaluate the nation's groundwater availability. Groundwater availability includes an understanding of the groundwater-budget components, along with other considerations such as water quality, regulations, and socioeconomic factors that control its demand and use (Reilly and others, 2008, p. 3). Within the context of the national groundwater availability assessment, the goals of regional assessments (such as the GBCAAS) are the development of (1) water budgets for the aquifer system (recharge and discharge components); (2) current estimates and historic trends in groundwater use, storage, recharge, and discharge; (3) numerical modeling tools to provide a regional context for groundwater availability and for future projections of groundwater availability; (4) regional estimates of important hydrologic variables (e.g. aquifer properties); (5) evaluation of existing groundwater monitoring networks; and (6) new approaches for regional groundwater resources analysis (Reilly and others, 2008, p. 37).

Purpose and Scope

The purpose of this report is to present an updated conceptual model of the GBCAAS for evaluating regional groundwater availability. The report provides an update to the previous Regional Aquifer-System Analysis (RASA) conceptual model (Prudic and others, 1995), integrating newer findings from several recent basin-scale studies, the Death Valley Regional Flow System (DVRFS) study (Belcher, 2004), and the Basin and Range Carbonate Aquifer System (BARCAS) study (Welch and others, 2007). Specifically, this report addresses objectives 1, 2, and 4 of the national groundwater availability assessment described in the previous section. This conceptual model includes the delineation of hydrogeologic units on the basis of lithology and hydraulic properties, construction of a detailed three-dimensional hydrogeologic framework, development of a potentiometric-surface map of the aquifer system, an evaluation of interbasin

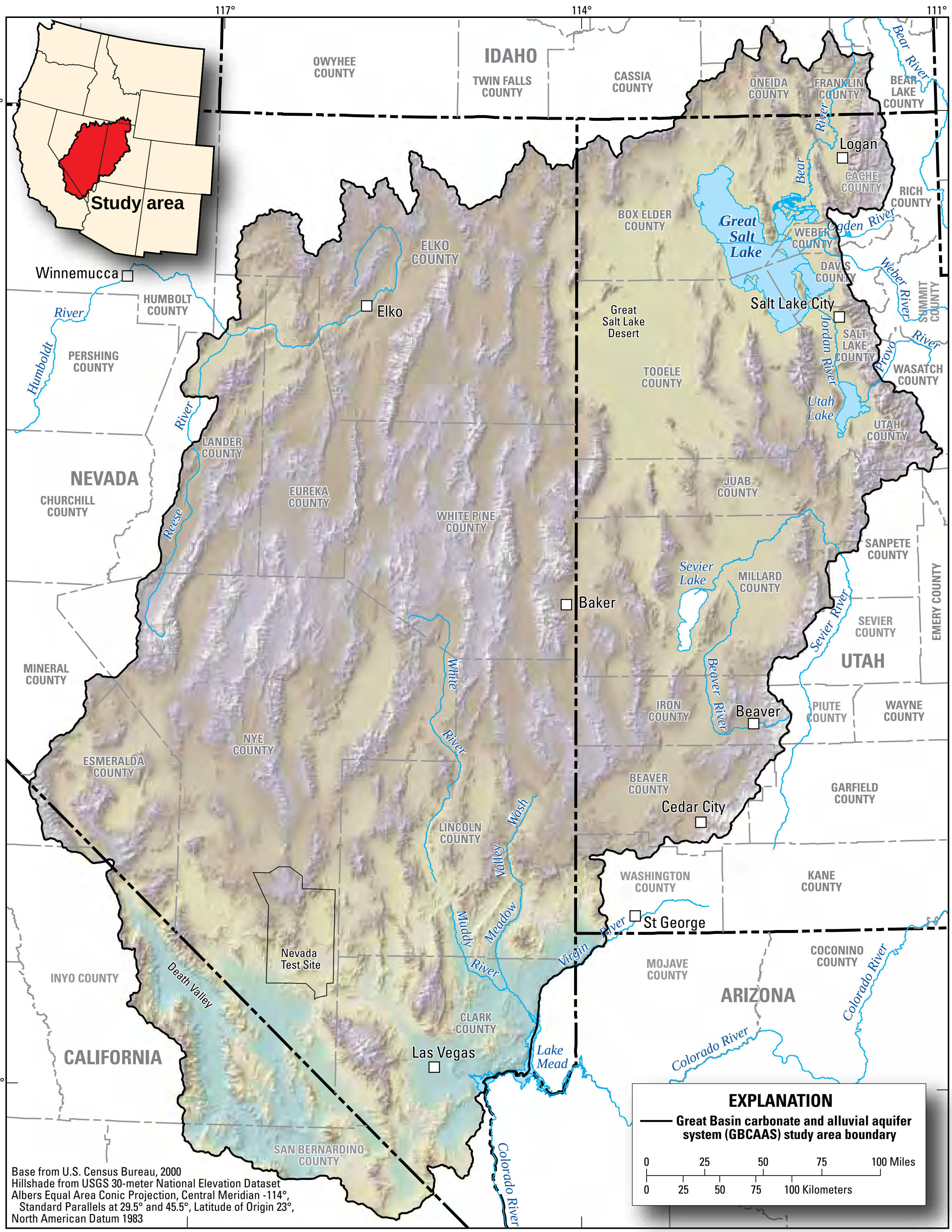

Figure A–1. Location map of the Great Basin carbonate and alluvial aquifer system study area.

bedrock hydraulic connectivity and regional groundwater flow directions, and a synthesis/interpretation of both predevelopment and recent groundwater recharge- and discharge-budget components.

The current study area is larger than that of a previous hydrogeologic study of the eastern Great Basin Carbonate-Rock Province (GB/CRP) conducted during 1981–87 as part of the U.S. Geological Survey's RASA program (fig. A–2; Prudic and others, 1995). The RASA–GB/CRP study area boundary was based on the occurrence of thick sequences of permeable carbonate and volcanic consolidated bedrock, but excluded the northern and eastern parts of the Great Salt Lake drainage area in Cache, Weber, Davis, Salt Lake, and Utah Counties (figs. A–1, A–2). Because these areas contain thick sequences of carbonate rocks, they are included in the GBCAAS study area. The GBCAAS study area also extends beyond the RASA–GB/CRP study area (1) to the northwest to include a larger portion of the Humboldt River drainage which also contains relatively thick sequences of carbonate rocks, and (2) to the west and southwest for consistency with watershed boundaries and with the DVRFS model area boundary (Belcher, 2004) (fig. A–2).

The temporal extent of data compiled for this study generally includes information through 2006. Data prior to the 1940s are scarce because (1) substantial groundwater development (well withdrawals) within the GBCAAS area did not begin until the widespread use of the deep-well turbine pump beginning in the 1940s, and (2) there were few quantitative hydrologic studies of individual basins within the study area prior to the 1940s.

This report presents components of the conceptual groundwater model within the GBCAAS study area in three subsequent chapters. Chapter B describes the stratigraphy and structure of the region in terms of the geologic setting and geologic history of the eastern Great Basin and defines hydrogeologic units used for describing aquifers and confining units. These hydrogeologic units provide the basis for the construction of a three-dimensional hydrogeologic framework of the aquifer system, described in Chapter B and detailed in Appendix 1. Chapter C describes (1) a conceptual model of groundwater flow through both bedrock and alluvial aquifers, (2) how geologic layers and structures control groundwater movement, and (3) the construction of a regional potentiometric map that is used for evaluating directions of groundwater flow. Chapter D describes the approach used for compiling and interpreting groundwater recharge- and discharge-budget components, and provides detailed groundwater-budget data for the entire study area. This includes a description of the Basin Characterization Model (BCM) used for estimating recharge from precipitation (further described in Appendix 3). Appendixes 6 and 8 describe the spatial datasets associated with this report and methods for estimating historical well withdrawals, respectively. The other appendixes are tables detailing descriptive information for each hydrographic area (HA) (Appendix 2), current study recharge and discharge estimates for predevelopment conditions (Appendixes 4 and 5, respectively), and predevelopment and recent groundwater-budget estimates for each HA (Appendix 7). In general, HA boundaries coincide with topographic basin divides that form the basis for defining watersheds; however, some divisions are arbitrary and lack topographic basis (Welch and others, 2007). Most HAs represent a single watershed, including both basin fill and adjacent mountain blocks up to the topographic divide (Harrill and Prudic, 1998).

Previous Studies

Two regional groundwater studies and two subregional groundwater studies were previously completed by the U.S. Geological Survey (USGS) within the GBCAAS study area. In the 1980s, the USGS RASA program assessed the Nation's major aquifer systems and made two regional studies as part of the Great Basin RASA: (1) delineation of aquifer systems in the Great Basin region (RASA–GB; Harrill and Prudic, 1998), and (2) a conceptual evaluation of regional groundwater flow in the Carbonate-Rock Province of the Great Basin (RASA–GB/CRP; Prudic and others, 1995). The two subregional studies include (1) the DVRFS study in the Death Valley area (Belcher, 2004) of southern Nevada and southeastern California, and (2) the BARCAS study (Welch and others, 2007) in east central Nevada and western Utah (fig. A–2).

The RASA–GB study focused on two important aquifer systems in the Great Basin, one composed of basin-fill aquifers and the other of consolidated carbonate-rock aquifers (Harrill and Prudic, 1998). Because the study area was large, encompassing 260 individual HAs or subareas, the study investigated small "type areas" (for example, Prudic and Herman, 1996; Mason, 1998; Harrill and Preissler, 1994) that were thought to be representative of larger parts of the region and assumed to have transfer value in terms of critical components of the groundwater flow system. The study also included regional assessments of hydrogeology (Plume and Carlton, 1988), geochemistry (Thomas and others, 1996), and hydrology (Thomas and others, 1986; Harrill and others, 1988). As part of the RASA–GB, the RASA–GB/CRP study included a groundwater flow model (Prudic and others, 1995). The results of the RASA studies form the basis for most subsequent conceptualizations of groundwater flow in the Great Basin. Important conclusions pertinent to the GBCAAS study area were (1) most groundwater flow moves from recharge areas in the mountains to discharge areas in adjacent valleys; (2) interbasin groundwater flow is predominantly through thick and continuous carbonate rocks; (3) not all carbonate rocks are highly permeable; (4) some highly permeable carbonate aquifers are hydraulically disconnected from shallower alluvial aquifers by low-permeability confining units; (5) while there are some long and deep interbasin groundwater flow paths to terminal sinks such as the Great Salt Lake, Great Salt lake Desert, Death Valley, and the Colorado River, most discharge along these flow paths occurs

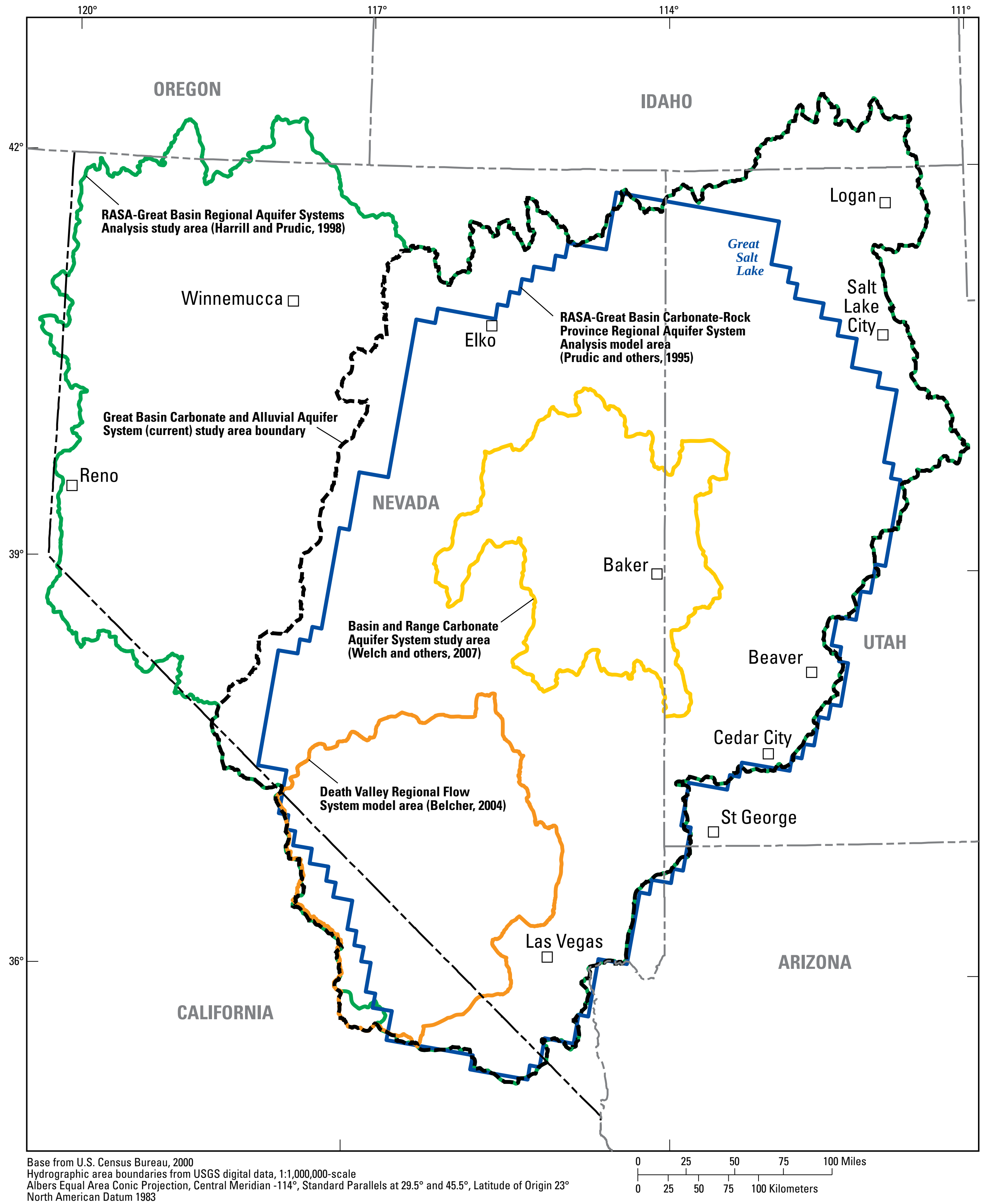

Figure A–2. Location of previous regional groundwater study and model areas within the Great Basin carbonate and alluvial aquifer system study area.

at intermediary locations as springflow and evapotranspiration (Harrill and Prudic, 1998, p. A39).

The DVRFS study, located within the southern part of the GBCAAS study area (fig. A–2), was completed by the U.S. Geological Survey in support of the U.S. Department of Energy (DOE) programs at the Nevada Test Site and at Yucca Mountain Repository, which is adjacent to the Nevada Test Site in southwestern Nevada. The study updated estimates of discharge and integrated all available information in the region to develop a numerical three-dimensional transient groundwater flow model of the Death Valley region (Belcher, 2004). The DVRFS study provided an improved understanding of regional groundwater flow in southern Nevada and the Death Valley region in California—a critical objective of the DOE program concerned with potential movement of radioactive material away from the Nevada Test Site and characterizing the groundwater flow system in the vicinity of the proposed high-level radioactive waste repository at Yucca Mountain, Nevada (Hanks and others, 1999).

The BARCAS study, located within the central part of the GBCAAS study area (fig. A–2), was completed by the U.S. Geological Survey and the Desert Research Institute in support of federal legislation to investigate the groundwater flow system underlying White Pine County and adjacent counties in Nevada and Utah (Section 131 of the Lincoln County Conservation, Recreation, and Development Act of 2004). The BARCAS study developed potentiometric-surface maps showing groundwater flow directions in both alluvial and carbonate aquifers, derived new estimates of groundwater recharge and discharge for HAs in White Pine County, Nevada, and adjacent areas in Nevada and Utah, and assessed inter-basin groundwater flow on the basis of a combination of deuterium mass-balance modeling, basin-boundary geology, hydraulic heads, and geochemistry. Findings of the BARCAS study are available in a summary report (Welch and others, 2007) and individual reports that describe the specific methods and water-budget components used in the analysis of the groundwater flow system (Cablk and Kratt, 2007; Flint and Flint, 2007; Hershey and others, 2007; Lundmark, 2007; Lundmark and others, 2007; Mizell and others, 2007; Moreo and others, 2007; Pavelko, 2007; Smith and others, 2007; Welborn and Moreo, 2007; Wilson, 2007; Zhu and others, 2007).

In addition to the previous regional groundwater studies, several other studies focused on the distribution of carbonate-rock aquifers and their potential for groundwater development (Dettinger and others, 1995; Burbey, 1997), and on estimating groundwater recharge (Watson and others, 1976; Dettinger, 1989; Kirk and Campana, 1990; Nichols, 2000; Thomas and others, 2001; Epstein, 2004). Numerous other previous groundwater studies have focused on individual basins in Nevada and Utah (listed in Auxiliary 2).

The previous studies and the current GBCAAS study refer to HAs, especially when discussing locations and groundwater budgets. HAs in Nevada were delineated systematically by the USGS and Nevada Division of Water Resources (NDWR) in the late 1960s (Cardinalli and others, 1968; Rush, 1968) for scientific and administrative purposes.

Basis for Developing a Three-Dimensional Hydrogeologic Framework

The GBCAAS study area comprises many types of rocks that have been subjected to a variety of structural disruptions and, as a result, the regional geology is stratigraphically and structurally complex. These rocks form a complex, three-dimensional hydrogeologic framework that can be subdivided into multiple aquifers and confining units on the basis of their capacity to store and transmit water. The RASA–GB/CRP numerical groundwater flow model (Prudic and others, 1995) represented this complex regional geology as a two-layer hydrogeologic system: an upper model layer primarily used to represent basin-fill aquifers and adjacent mountain ranges to depths of a few thousand feet, and a lower model layer generally used to represent deeper carbonate-rock aquifers. This simplified mathematical representation of the complex geology and hydrogeology in the region was developed because of large uncertainty in the thickness of hydrogeologic units, sparse data, and limited computing resources available at that time. Since the RASA–GB/CRP model was completed, the increase in computing power and advances in numerical modeling allow the incorporation of more geologic detail in three-dimensional hydrogeologic frameworks and groundwater flow models. Subsequent conceptual models (e.g., Laczniak and others, 1996; Welch and others, 2007; Cederberg and others, 2008) and numerical groundwater flow models (Belcher, 2004; Brooks and Mason, 2005; Gardner, 2009) of parts of the region have incorporated greater geologic detail, which has resulted in finer scale, more sophisticated models that are more representative of the groundwater flow systems.

A hydrogeologic framework defines the physical geometry and rock types in the subsurface. The complex stratigraphy and structure of the GBCAAS study area significantly influences the location and direction of groundwater flow. The occurrence and juxtaposition of permeable aquifer units or impermeable confining units in three dimensions are critical factors that determine the potential for groundwater flow across HA boundaries. Thus, the development of a three-dimensional hydrogeologic framework of the GBCAAS study area is a necessary and significant step in improving the conceptualization of groundwater flow in the Great Basin, and in providing a foundation for the development of future groundwater flow models. The three-dimensional hydrogeologic framework presented in this report is a representation of the regional hydrogeology in digital form, including the spatial extent and thickness of aquifers and confining units and the geometry of major structures. The hydrogeologic framework was built by combining and extracting information from a variety of data sets, including elevation models, geologic maps, borehole logs, cross sections, and other digital frameworks. This information was combined into an integrated three-dimensional framework of the aquifer system. This framework will be used both for an improved conceptual understanding of groundwater flow in the GBCAAS study area (Chapter C) and as the three-dimensional framework for a numerical groundwater flow model of the entire area (subsequent report).

The framework incorporates abundant geologic data and information that were developed during, or subsequent to, the Great Basin RASA studies. These include advances in the understanding of the style and magnitude of Great Basin extension (for example Snow and Wernicke, 2000), the relation between extension and caldera-related volcanism (Axen and others, 1993), and an increased understanding of the role of regional-scale transverse structures (Faulds and Stewart, 1998). New geophysical methods and data have been developed to estimate the shape and size of Cenozoic basins, including the gravity-derived depth-to-basement method (Saltus and Jachens, 1995) and regional-scale seismic data (Allmendinger and others, 1987), which are used to develop a crustal cross section across the entire GBCAAS study area. Map compilations and three-dimensional hydrogeologic frameworks for the Death Valley and Nevada Test Site areas (Workman and others, 2002; Faunt and others, 2004) and lower White River/Meadow Valley Wash areas (Page and others, 2005; 2006) provide new data on the surface and subsurface extent of geologic units. Collectively, updated interpretations of subsurface geology, new surface geologic mapping, advances in geophysical methods, an improved understanding of hydraulic properties of geologic units, the development of subregional hydrogeologic frameworks, and advances in software and computing power provide the foundation for the development of a more complex, finer scale, and multi-layer hydrogeologic framework for the aquifer system.

Basis for Updating the Conceptual Groundwater Model

Recent data and interpretation of hydraulic properties in carbonate rocks (Dettinger and others, 1995; Dettinger and Schaefer, 1996) and in volcanic rocks and basin fill (Belcher and others, 2001) have advanced the understanding of the major aquifers of the eastern Great Basin. Since the RASA–GB study, developments in groundwater budget estimates include improved methods for estimating evapotranspiration and for estimating the magnitude and distribution of recharge and runoff (Flint and Flint, 2007). Subsequent to the RASA–GB study, conceptual models (e.g., Laczniak and others, 1996; Welch and others, 2007; Cederberg and others, 2008) and numerical groundwater flow models (Belcher, 2004; Brooks and Mason, 2005; Gardner, 2009) of parts of the region have incorporated greater geologic detail, which has resulted in finer scale, more sophisticated models that are more representative of the groundwater flow systems.

Another important improvement since the RASA–GB study is the development of a watershed approach to understanding Great Basin groundwater systems (Cederberg and others, 2008; Gardner, 2009; Stolp and Brooks, 2009), wherein the hydrology of both mountain-block and basin-fill aquifers are explicitly defined and linked, allowing a more comprehensive representation of groundwater recharge and discharge components (such as groundwater discharge to mountain springs and streams). Also, the availability of (1) new and higher resolution remotely-sensed data for vegetation, soil moisture, and snowpack; (2) new techniques for mapping the distribution of precipitation such as PRISM (Parameter-elevation Regressions on Independent Slopes Model; Daly and others, 1994); and (3) digital data sets of topography, soils, and geology all permit a more precise determination of the spatial variability of input data for regional groundwater studies such as the GBCAAS. The improved conceptual understanding of groundwater flow and interbasin hydraulic connections, along with the advances in water-budget estimation methods and recently collected hydrologic data, all contribute to the updated conceptual model and groundwater budgets of the GBCAAS.

Geographic Setting

The GBCAAS study area extends across the eastern two-thirds of the Great Basin, a subprovince of the Basin and Range physiographic province (Fenneman, 1931), including most of eastern Nevada and western Utah, parts of southeastern California and Idaho, and a small corner of northwestern Arizona (fig. A–1). The area is generally bounded by latitudes of about 35° to 42°N and longitudes of about 111° to 118 °W. The physical geography of the study area is characterized by north or northeast trending mountain ranges separated by broad basins (fig. A–1). Mountain ranges typically are 5–15 mi wide and can be as long as 50 mi or more. Basins typically are 5–10 mi wide and 35–70 mi long, although some are as long as 150 mi. The longer basins, like Snake Valley (150 mi; pl. 1), are bordered by multiple mountain ranges. Where mountain ranges are bounded by extensive normal faults, the mountain fronts are steep and abruptly transition to alluvial fans that extend into the basins. Topographic relief between the mountain crests and basin floors typically ranges from 1,000 to 6,000 ft, with a few areas exceeding 8,000 ft. The altitude of the basin floor is below sea level in Death Valley, but typically ranges from 3,000 to 6,000 ft above sea level elsewhere. Steptoe Valley in the north-central part of the study area (pl. 1) has the highest altitude of all basin floors (approximately 6,300 ft), and basin altitude generally decreases in all directions. Mountain altitudes commonly range from 8,000 to 11,000 ft, with a few peaks exceeding 13,000 ft (for example Wheeler Peak in the Snake Range at 13,063 ft and White Mountain Peak in the White Mountains west of Fish Lake Valley at 14,246 ft (pl. 1)).

The GBCAAS study area includes numerous public lands, including two national parks, multiple national and state wildlife refuges, national conservation and wilderness areas, national and state monuments, national historic sites, national and state recreation areas, and state parks (fig. A–3). About 90 percent of the land in the study area is managed by federal and state agencies.

Climate

The climate of the GBCAAS study area varies substantially with both land-surface altitude and latitude. The eastern Great Basin is generally categorized as having a dry, mid-latitude “semi-arid” or “steppe” climate. This climate zone includes areas between latitudes of 35° to 55° N having a range in average daily temperature of about 25°C and annual precipitation from less than 4 in. to more than 20 in. (Strahler, 1989). More detailed climate zones have been described for the region, and the majority of the GBCAAS study area is within the “Great Basin Woodland and Desert” climatic zone. The southernmost portion of the study area, including the Las Vegas area and the southern part of the Death Valley region, is located within the warmer and drier “Mohave Desert” climate zone. A narrow east-west band north of Las Vegas and south of Cedar City is categorized as the “Transition Desert” climatic zone (Belcher, 2004). The highest mountains within the study area are categorized as the “Highland Climate/Alpine Biome” zone (Strahler, 1989).

Average annual precipitation within the GBCAAS study area between 1940 and 2006 ranged from 1.5 in. in Death Valley National Park to 70 in. in the Wasatch Range east of Salt Lake City and Logan, Utah (Daly and others, 2004; 2008). Precipitation data were evaluated beginning in 1940 to be consistent with the compilation of other hydrologic data, which are generally available back to the 1940s. Most of the precipitation in the study area falls as snow in the mountains at higher latitudes. Less precipitation falls in the valley bottoms and at lower latitudes and typically occurs as rainfall. Precipitation predominantly occurs in winter and early spring, with moisture coming along storm tracks from the Pacific Ocean. A second period of higher precipitation during late summer and early fall is associated with the summer monsoonal moisture from the Gulf of California and the Gulf of Mexico (Brenner, 1974; Weng and Jackson, 1999). This monsoonal precipitation is more pronounced in the southern part of the study area.

During the 20th century, greater-than-average precipitation occurred from 1977 through 1998, possibly linked with the positive warm phase of the Pacific Decadal Oscillation (PDO) and a cool phase of the Atlantic Multidecadal Oscillation (AMO; Gray and others, 2003). This conclusion is supported by tree-ring based precipitation reconstructions spanning the period 1226–2001 in the Uinta Basin of Duchesne County, Utah (east of the GBCAAS study area; fig. A–1) that show the period 1960–2000 was the second-wettest multi-decadal period of the past 775 years (Gray and others, 2004).

Surface-Water Hydrology

Because of the generally semi-arid climate within the GBCAAS study area, surface-water resources are limited and unevenly distributed across the study area. About one dozen rivers and many smaller perennial streams either originate in or flow through the GBCAAS study area (fig. A–1; pl. 1). Four of the larger rivers (the Bear, Ogden, Weber, and Provo Rivers) originate in mountains east of the study area and flow westward through the Wasatch Range. Canals and aqueducts (transbasin diversions) also bring surface water through the Wasatch Range into the study area. Rivers originating in the Wasatch Range include the Jordan, Sevier, and Beaver Rivers. All of the basins associated with these rivers drain internally within the GBCAAS study area and the rivers terminate in either Great Salt Lake or Sevier Lake (commonly a dry playa), where evaporation is the only form of discharge. These terminal lake/playa systems are saline remnants of ancestral Lake Bonneville, which inundated most of the basins in the northeast part of the study area during the Pleistocene. The areas and stages of these lakes fluctuate in tandem with pluvial cycles (Stephens and Arnow, 1987). In Nevada, the Reese River and other tributaries to the Humboldt River are fed predominantly by snowmelt that runs off various mountain ranges in the north-central part of the state. These rivers join to form the Humboldt River near where it flows through the northwestern boundary of the study area and into the lower Humboldt watershed. In southeastern Nevada, the White River, Muddy River, and Meadow Valley Wash flow southward. Both the White River and Meadow Valley Wash cease flowing towards the south, owing to evapotranspiration and (or) seepage losses. The Muddy River discharges to the Virgin River along the southeastern boundary of the study area just above Lake Mead of the Colorado River system (fig. A–1). Flow in the Muddy River is derived almost entirely from Muddy River Springs at the beginning of the river (pl. 1).

As a result of the arid climate and basin-and-range topography, surface water generally does not flow between basins. The exceptions are the larger river systems, including the Bear, Beaver, Humboldt, Jordan, Muddy, Reese, Sevier, and White Rivers (fig. A–1). Transbasin diversions also move surface water between basins. Other than Lake Mead along the lower Colorado River, most of the larger lakes in the study area are located along the Wasatch Front and include Great Salt Lake, Utah Lake, and Sevier Lake. Playas are found in some internally drained basins. Playas are dry or ephemeral lakebeds that form in semi-arid to arid regions in closed evaporative basins and either receive surface-water flow and typically are nonsaline or receive groundwater discharge and typically are saline. The largest playa is in the Great Salt Lake Desert in the northeast part of the study area. This large playa forms a salt flat and is a remnant of ancient Lake Bonneville.

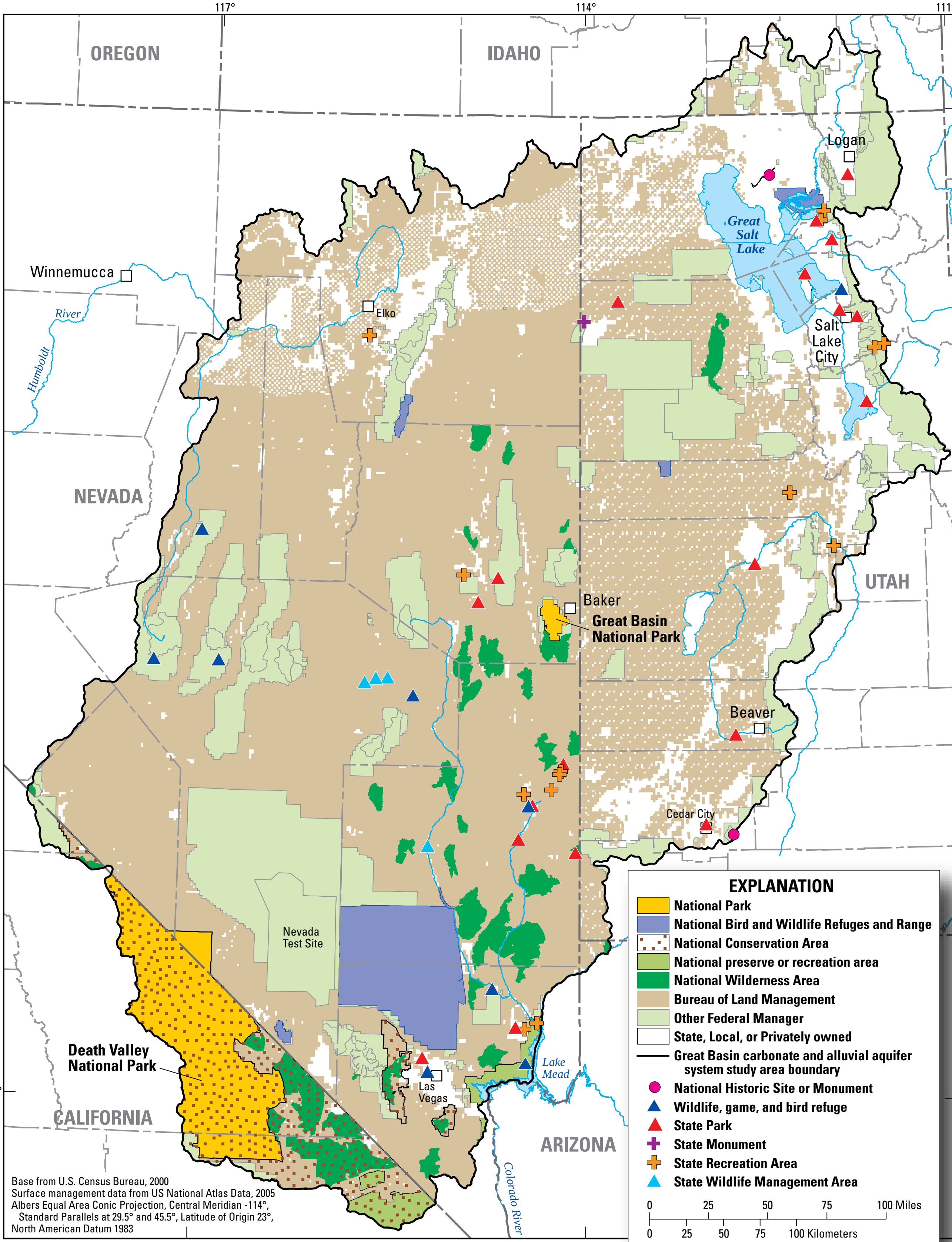

Figure A–3. Location of national and state parks, monuments, wilderness areas, and conservation areas in the Great Basin carbonate and alluvial aquifer system study area.

Summary

The Great Basin carbonate and alluvial aquifer system, located within the Basin and Range physiographic province, spans a large, topographically and climatologically diverse region that covers 110,000 mi^2. Altitudes range from below sea level in Death Valley to more than 14,000 ft in the mountains along the California border. Although most of the study area can be categorized as having a semi-arid or steppe climate, the extreme southwestern basins have an arid desert climate and the extreme northeastern mountains have an alpine/tundra climate. Annual precipitation ranges from 1.5 in. in southern Nevada and eastern California to 70 in. in northern Utah. Most of the precipitation falls during the winter as snowfall in the mountains at higher latitudes and is associated with storms originating in the Pacific Ocean, although substantial rainfall also can occur in late summer and early autumn, coincidental with monsoonal moisture that moves northward from the Gulf of Mexico and Gulf of California.

The GBCAAS study area has limited surface-water resources. The semi-arid setting, combined with rapid growth and high water use, has led to an increased dependence upon groundwater resources in many parts of the study area during the past 7 decades. The primary purpose of this report is to update and expand the conceptual model of this aquifer system that was initially developed during the RASA–GB study to evaluate regional groundwater availability. It also integrates newer subregional USGS studies such as the DVRFS and BARCAS into a comprehensive regional conceptual model. Particular objectives include (1) updating water budgets for the aquifer system (recharge and discharge components); (2) compiling current estimates and evaluating historic trends in groundwater use, storage, recharge, and discharge; and (3) updating the regional hydrogeologic framework. This updated and expanded conceptual model includes a more-detailed characterization of hydrogeologic units, the construction of a three-dimensional hydrogeologic framework, the evaluation of groundwater movement, depiction of groundwater levels in a potentiometric map, and the compilation of groundwater budgets.

References Cited

Allmendinger, R.W., Hauge, T.A., Hauser, E.C., Potter, C.J., Klemperer, S.L., Nelson, K.D., Knuepfer, P., and Oliver, J.E., 1987, Overview of the COCORP 40°N Transect, western United States: The fabric of an orogenic belt: Geological Society of America Bulletin, v. 98, p. 308–319.

Axen, G.J., Taylor, W.J., and Bartley, J.M., 1993, Space-time patterns and tectonic controls of Tertiary extension and magmatism in the Great Basin of the western United States: Geological Society of America Bulletin, v. 105, p. 56–76.

Belcher, W.R., ed., 2004, Death Valley regional ground-water flow system, Nevada and California—Hydrogeologic and transient ground-water flow model: U.S. Geological Survey Scientific Investigations Report 2004–5205, 408 p., 2 pls.

Belcher, W.R., Elliot, P.E., and Geldon, A.L., 2001, Hydraulic-property estimates for use with a transient ground-water flow model of the Death Valley regional ground-water flow system, Nevada and California: U.S. Geological Survey Water-Resources Investigations Report 01–4210, 28 p., 1 pl.

Bergquist, G., 1994, Per capita water use, *in* Strategic Assessment of Florida's Environment (SAFE): Florida Department of Environmental Protection, Tallahassee, Florida, p. 278–281.

Brenner, I.S., 1974, A surge of maritime tropical air—Gulf of California to southwestern United States: Monthly Weather Review, v. 102, p. 375–389.

Brooks, L.E., and Mason, J.L., 2005, Hydrology and simulation of ground-water flow in Cedar Valley, Iron County, Utah: U.S. Geological Survey Scientific Investigations Report 2005–5170, 114 p.

Burbey, T.J., 1997, Hydrogeology and potential for ground-water development, carbonate-rock aquifers, southern Nevada and southeastern California: U.S. Geological Survey Water-Resources Investigations Report 95–4168, 65 p., 1 pl. in pocket.

Cablk, M.E., and Kratt, C., 2007, A methodology for mapping shrub canopy cover in the Great Basin Desert using high spatial resolution satellite imagery: Desert Research Institute Publication No. 41236, 22 p.

Cardinalli, J.L., Roach, L.M., Rush, F.E., and Vasey, B.J., 1968, State of Nevada hydrographic areas, scale 1:500,000, *in* Rush, F.E., ed., Index of hydrographic areas: Nevada Division of Water Resources Information Report 6, 38 p.

Cederberg, J.R., Gardner, P.M., and Thiros, S.A., 2008, Hydrology of northern Utah Valley, Utah County, Utah, 1975–2005: U.S. Geological Survey Scientific Investigations Report 2008–5197, 97 p.

Daly, C., Gibson, W.P., Doggett, M., Smith, J., and Taylor, G., 2004, Up-to-date monthly climate maps for the conterminous United States, *in* Conference on Applied Climatology, 14th, American Meteorological Society 84th Annual Meeting, January 13–16, 2004, Seattle, Paper 5.1.

Daly, C., Halbleib, M., Smith, J.I., Gibson, W.P., Doggett, M.K., Taylor, G.H., Curtis, J., and Pasteris, P.A., 2008, Physiographically-sensitive mapping of temperature and precipitation across the conterminous United States: International Journal of Climatology, v. 6, no. 15, p. 2,031–2,064, doi: 10.1002/joc.1688, accessed March 6, 2008 at http://onlinelibrary.wiley.com/doi/10.1002/joc.1688/abstract.

Daly, C., Nielson, R.P., and Philips, D.L., 1994, A statistical-topographic model for mapping climatological precipitation over mountainous terrain: Journal of Applied Meteorology, v. 33, no. 2, p. 140–158, accessed June 11, 2007 at doi: 10.1175/1520-0450(1994)033<0140:ASTMFM>2.0.CO;2 link to the publication at http://journals.ametsoc.org/doi/pdf/10.1175/1520-0450%281994%29033%3C0140%3AASTMFM%3E2.0.CO%3B2.

Dettinger, M.D., 1989, Reconnaissance estimates of natural recharge to desert basins in Nevada, U.S.A., by using chloride-balance calculations: Journal of Hydrology, v. 106, p. 55–78.

Dettinger, M.D., Harrill, J.R., Schmidt, D.L., and Hess, J.W., 1995, Distribution of carbonate-rock aquifers and the potential for their development, southern Nevada and parts of Arizona, California, and Utah: U.S. Geological Survey Water-Resources Investigations Report 91–4146, 100 p., 2 pls. in pocket.

Dettinger, M.D., and Schaefer, D.H., 1996, Hydrogeology of structurally extended terrain in the eastern Great Basin of Nevada, Utah, and adjacent states, from geologic and geophysical models: U.S. Geological Survey Hydrologic Investigations Atlas HA–694-D, 1 sheet.

Epstein, B.J., 2004, Development and uncertainty analysis of empirical recharge prediction models for Nevada's desert basins, Reno, University of Nevada, M.S. Thesis, 131 p.

Faulds, J.E., and Stewart, J., eds., 1998, Accommodation zones and transfer zones—The regional segmentation of the Basin and Range: Geological Society of America Special Paper 323, 257 p.

Faunt, C.C., Sweetkind, D.S., and Belcher, W.R., 2004, Three-dimensional hydrogeologic framework model, Chap. E *of* Belcher, W.R., ed., 2004, Death Valley regional ground-water flow system, Nevada and California—Hydrogeologic framework and transient ground-water flow model: U.S. Geological Survey Scientific Investigations Report 2004–5205, p. 165–256.

Fenneman, N.M., 1931, Physiography of western United States: New York, McGraw-Hill Book Company, Inc., 534 p.

Flint, A.L., and Flint, L.E., 2007, Application of the basin characterization model to estimate in-place recharge and runoff potential in the Basin and Range carbonate-rock aquifer system, White Pine County, Nevada and adjacent areas in Nevada and Utah: U.S. Geological Survey Scientific Investigations Report 2007–5099, 20 p.

Gardner, P.M., 2009, Three-dimensional numerical model of ground-water flow in northern Utah Valley, Utah County, Utah: U.S. Geological Survey Scientific Investigations Report 2008–5049, 95 p.

Gates, J.S., 2004, Ground-water development in Utah and effects on ground-water levels and chemical quality *in* Spangler, L.E., ed., Groundwater in Utah: Resource, protection, and remediation: Utah Geological Association Publication 31, p. 3–26.

Gray, S.T., Betancourt, J.L., Fastie, C.L, and Jackson, S.T., 2003, Patterns and sources of multidecadal oscillations in drought-sensitive tree-ring records from the central and southern Rocky Mountains: Geophysical Research Letters v. 30, no. 6, p. 1,316, doi:10.1029/2002GS016154, accessed April 14, 2008 at http://www.agu.org/pubs/crossref/2003/2002GL016154.shtml.

Gray, S.T., Jackson, S.T., and Betancourt, J.L, 2004, Tree-ring based reconstructions of interannual to decadal scale precipitation variability for northeastern Utah since 1226 A.D.: Journal of the American Water Resources Association, Paper No. 03148, p. 947–960.

Hanks, T.C., Winograd, I.J., Anderson, R.E., Reilly, T.E., and Weeks, E.P., 1999, Yucca Mountain as a radioactive-waste repository: U.S. Geological Survey Circular C1184, 19 p.

Harrill, J.R., Gates, J.S., and Thomas, J.M., 1988, Major ground-water flow systems in the Great Basin region of Nevada, Utah, and adjacent states: U.S. Geological Survey Hydrologic Investigations Atlas HA–694-C, 2 sheets, scale 1:1,000,000.

Harrill, J.R., and Preissler, A.M., 1994, Ground-water flow and simulated response to several developmental scenarios in Stagecoach Valley—a small partly-drained basin in Lyon and Storey Counties, Nevada: U.S. Geological Survey Professional Paper 1409–H, 74 p.

Harrill, J.R., and Prudic, D.E., 1998, Aquifer systems in the Great Basin region of Nevada, Utah, and adjacent states—Summary Report: U.S. Geological Survey Professional Paper 1409–A, 66 p.

Hershey, R.L., Heilweil, V.M., Gardner, P.M., Lyles, B.F., Earman, S., Thomas, J.M., and Lundmark, K.W., 2007, Ground-water chemistry interpretations supporting the Basin and Range regional carbonate-rock aquifer system (BARCAS) study, eastern Nevada and western Utah: Desert Research Institute, Division of Hydrologic Sciences, Publication No. 41230, 86 p.

Hurlow, H.H., and Burk, N., 2008, Geology and ground-water chemistry, Curlew Valley, northwestern Utah and south-central Idaho—Implications for hydrogeology: Utah Geological Survey Special Study 126, 185 p., 2 pls.

Kirk, S.T., and Campana, M.E., 1990, A deuterium-calibrated groundwater flow model of a regional carbonate-alluvial system: Journal of Hydrology, v. 119, p. 357–388.

Laczniak, R.J., Cole, J.C., Sawyer, D.A., and Trudeau, D.A., 1996, Summary of hydrogeologic controls on groundwater flow at the Nevada Test Site, Nye County, Nevada: U.S. Geological Survey Water-Resources Investigations Report 96–4109, 59 p., 4 pls.

Lundmark, K.W., 2007, Regional water budget accounting and uncertainty analysis using a deuterium-calibrated discrete state compartment model: White Pine County, Nevada, and adjacent areas in Nevada and Utah: Reno, University of Nevada, Master's Thesis, 177 p.

Lundmark, K.W., Pohll, G.M., and Carroll, R.W.H., 2007, A steady-state water budget accounting model for the carbonate aquifer system in White Pine County, Nevada, and adjacent areas in Nevada and Utah: Desert Research Institute, Division of Hydrologic Sciences, Publication No. 41235, 56 p.

Mason, J.L., 1998, Ground-water hydrology and simulated effects of development in the Milford area, an arid basin in southwestern Utah: U.S. Geological Survey Professional Paper 1409–G, 69 p., 2 pls. in pocket.

Mizell, S.A., Russell, C.E., and Kluesner, T.L., 2007, Reconnaissance estimation of groundwater recharge to selected hydrographic basins of eastern Nevada and western Utah using the chloride mass-balance method: Desert Research Institute Publication No. 41232, 29 p.

Moreo, M.T., Laczniak, R.J., and Stannard, D.I., 2007, Evapotranspiration rate measurements of vegetation typical of ground-water discharge areas in the Basin and Range carbonate-rock aquifer system, White Pine County, Nevada, and adjacent areas in Nevada and Utah, September 2005–August 2006: U.S. Geological Survey Scientific Investigations Report 2007–5078, 36 p.

Nichols, W.D., 2000, Regional ground-water evapotranspiration and ground-water budgets, Great Basin, Nevada: U.S. Geological Survey Professional Paper 1628, 82 p., 4 pls. in pockets, optical disc in pocket.

Page, W.R., Dixon, G.L., Rowley, P.D., and Brickey, D.W., 2005, Geologic map of parts of the Colorado, White River, and Death Valley groundwater flow systems, Nevada, Utah, and Arizona: Nevada Bureau of Mines and Geology Map 150, 21 p., scale 1:250,000.

Page, W.R., Scheirer, D.S., and Langenheim, V.E., 2006, Geologic cross sections of parts of the Colorado, White River, and Death Valley regional ground-water flow systems, Nevada, Utah, and Arizona: U.S. Geological Survey Open-File Report 2006–1040, 23 p., 1 pl.

Pavelko, M.T., 2007, Spring database for the Basin and Range carbonate-rock aquifer system, White Pine County, Nevada, and adjacent areas in Nevada and Utah: U.S. Geological Survey Data Series 272, 10 p., with downloadable database, accessed November 29, 2010, from http://pubs.usgs.gov/ds/2007/272/.

Plume, R.W., and Carlton, S.M., 1988, Hydrogeology of the Great Basin region of Nevada, Utah, and adjacent states: U.S. Geological Survey Hydrologic Investigations Atlas HA 694–A, 1 sheet, scale 1:1,000,000.

Prudic, D.E., Harrill, J.R., and Burbey, T.J., 1995, Conceptual evaluation of regional ground-water flow in the Carbonate-Rock Province of the Great Basin, Nevada, Utah, and adjacent states: U.S. Geological Survey Professional Paper 1409–D, 102 p.

Prudic, D.E., and Herman, M.E., 1996, Ground-water hydrology and simulated effects of development in Paradise Valley, a basin tributary to the Humboldt River in Humboldt County, Nevada: U.S. Geological Survey Professional Paper 1409–F, 92 p.

Reilly, T.E., Dennehy, K.F., Alley, W.M., and Cunningham, W.L., 2008, Ground-water availability in the United States: U.S. Geological Survey Circular 1323, 70 p.

Rush, F.E., 1968, Index of hydrographic areas in Nevada: Nevada Division of Water Resources Information Report 6, 38 p.

Saltus, R.W., and Jachens, R.C., 1995, Gravity and basin-depth maps of the Basin and Range province, western United States: U.S. Geological Survey Geophysical Investigation Map GP–1012, 1 sheet, scale 1:2,500,000.

Smith, J.L., Laczniak, R.J., Moreo, M.T., and Welborn, T.L., 2007, Mapping evapotranspiration units in the Basin and Range carbonate-rock aquifer system, White Pine County, Nevada, and adjacent areas in Nevada and Utah: U.S. Geological Survey Scientific Investigations Report 2007–5087, 20 p., with downloadable video, accessed November 29, 2010, at http://pubs.usgs.gov/sir/2007/5087/.

Snow, J.K., and Wernicke, B., 2000, Cenozoic tectonism in the central Basin and Range; magnitude, rate, and distribution of upper crustal strain: American Journal of Science, v. 300, p. 659–719.

Stephens, D.W., and Arnow, T., 1987, Fluctuations of water level, water quality, and biota of Great Salt Lake, Utah, 1847–1986, *in* Cenozoic Geology of Western Utah—Sites for precious metal and hydrocarbon accumulations: Utah Geological Association Publication 16, p. 182–194.

Stolp, B.J., and Brooks, L.E., 2009, Hydrology and simulation of ground-water flow in the Tooele Valley ground-water basin, Tooele County, Utah: U.S. Geological Survey Scientific Investigations Report 2009–5154, 86 p., 3 appendixes, 1 pl., accessed December 3, 2010 at http://pubs.usgs.gov/sir/2009/5154/.

Strahler, A.N., 1989, Elements of Physical Geography, 4th edition: John Wiley and Sons, New York, 565 p.

Thomas, J.M., Calhoun, S.C., and Apambire, W.B., 2001, A deuterium mass-balance interpretation of groundwater sources and flows in southeastern Nevada: Desert Research Institute Publication no. 41169, p. 46.

Thomas, J.M., Mason, J.L., and Crabtree, J.D., 1986, Ground-water levels in the Great Basin region of Nevada, Utah, and adjacent states: U.S. Geological Survey Hydrologic Investigations Atlas HA–694–B, 2 sheets, scale 1:1,000,000.

Thomas, J.M., Welch, A.H., and Dettinger, M.D., 1996, Geochemistry and isotope hydrology of representative aquifers in the Great Basin region of Nevada, Utah, and adjacent states: U.S. Geological Survey Professional Paper 1409–C, 100 p., 2 pls. in pocket.

U.S. Census Bureau, 2005, Population projection program: U.S. Department of Commerce, accessed April 21, 2005 at http://www.census.gov/ipc/www/usinterimproj/.

U.S. Water News, June 2005, Utah searches for ways to satisfy thirst of a growing state, accessed July 7, 2005 at http://uswaternews.com/archives/arcsupply/5utahsear6.html.

Watson, P., Sinclair, P., and Waggoner, R., 1976, Quantitative evaluation of a method for estimating recharge to the desert basins of Nevada: Journal of Hydrology, v. 31, p. 335–357.

Welborn, T.L., and Moreo, M.T., 2007, Irrigated acreage within the Basin and Range carbonate-rock aquifer system, White Pine County, Nevada, and adjacent areas in Nevada and Utah: U.S. Geological Survey Data Series 273, 18 p., with downloadable geodatabase, accessed November 29, 2010, at http://pubs.usgs.gov/ds/2007/273/.

Welch, A.H., Bright, D.J., and Knochenmus, L.A., eds., 2007, Water resources of the Basin and Range carbonate-rock aquifer system, White Pine County, Nevada, and adjacent areas in Nevada and Utah: U.S. Geological Survey Scientific Investigations Report 2007–5261, 96 p., 4 pls., with downloadable appendix, accessed November 29, 2010, at http://pubs.usgs.gov/sir/2007/5261/.

Weng, C., and Jackson, S.T., 1999, Late glacial and Holocene vegetation history and paleoclimate of the Kaibab Plateau, Arizona: Paleogeography, Paleoclimatology, Paleoecology, v. 153, p. 179–201.

Wilson, J.W., 2007, Water-level surface maps of the carbonate-rock and basin-fill aquifers in the Basin and Range carbonate-rock aquifer system, White Pine County, Nevada, and adjacent areas in Nevada and Utah: U.S. Geological Survey Scientific Investigations Report 2007–5089, 10 p., with downloadable appendix, accessed November 29, 2010, at http://pubs.usgs.gov/sir/2007/5089/.

Workman, J.B., Menges, C.M., Page, W.R., Taylor, E.M., Ekren, E.B., Rowley, P.D., Dixon, G.L., Thompson, R.A., and Wright, L.A., 2002, Geologic map of the Death Valley ground-water model area, Nevada and California: U.S. Geological Survey Miscellaneous Field Studies Map MF–2381–A, 26 p., 2 sheets, scale 1:250,000.

Zhu, J., Young, M.H., and Cablk, M.E., 2007, Uncertainty analysis of estimates of ground-water discharge by evapotranspiration for the BARCAS study area: Desert Research Institute, Division of Hydrologic Sciences, Publication No. 41234, 28 p.

Chapter B: Hydrogeologic Framework

By Donald S. Sweetkind, Jay R. Cederberg, Melissa D. Masbruch, and Susan G. Buto

The geologic setting and history of the eastern Great Basin, inclusive of the Great Basin carbonate and alluvial aquifer system (GBCAAS) study area, is preserved in rocks and geologic structures that span more than a billion years (fig. B–1). This geology ranges from Late Proterozoic sedimentary rocks to widespread Quaternary alluvial deposits and active faults (Stewart and Poole, 1974; Speed and others, 1988; Dickinson, 2004; 2006). The geologic framework that has resulted from the geologic events during this protracted period profoundly affects groundwater flow. Thus, any water-resource assessment of the area must take into account the complex geologic history and consider the distribution of the diverse rock types and geologic environments.

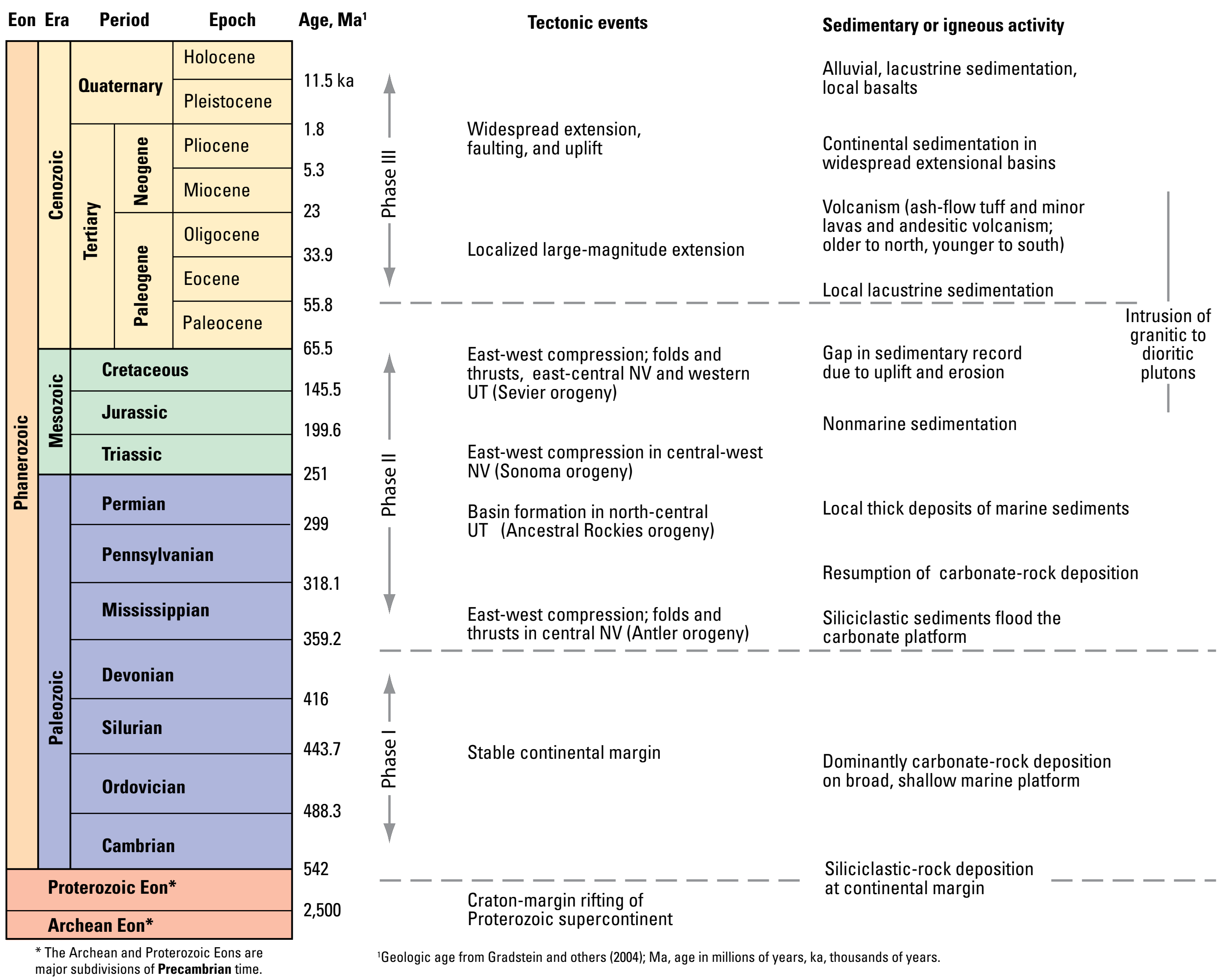

Figure B–1. Geologic time scale showing major geologic events in the Great Basin carbonate and alluvial aquifer system study area.

The geologic evolution of the GBCAAS study area since the end of Precambrian time may be subdivided into three general phases (Levy and Christie-Blick, 1989; Dickinson, 2006): (1) Late Proterozoic to Devonian marine sedimentation along a passive continental margin; (2) Late Devonian to Eocene compressional deformation, along with changes in sedimentation patterns related to the subduction of oceanic crust and accretion of exotic terrains along the western continental margin in western Nevada; and (3) mid- to late- Cenozoic extension, faulting, volcanism, and continental sedimentation (fig. B–1). Within the context of this three-phase evolution, numerous tectonic events and the accompanying changes in sedimentation patterns and igneous activity have occurred.

Hydrogeologic Units

The diverse sedimentary units of the GBCAAS study area are grouped into hydrogeologic units (HGUs) that are inferred to have reasonably distinct hydrologic properties due to their physical (geological and structural) characteristics. The definition of HGUs is important in conceptualizing the hydrogeologic system, construction of a geologic framework for describing the groundwater flow system, and use in numerical groundwater flow models. An HGU has considerable lateral extent and reasonably distinct physical characteristics that may be used to infer the capacity of a sediment or rock to transmit water. HGUs similar to those used in this study were first defined on the basis of geologic studies and hydrologic data for the pre-Cenozoic rocks in the vicinity of the Nevada Test Site (fig. A–1; Winograd and Thordarson, 1975). Most subsequent utilization of HGUs and groundwater flow models of the region (Laczniak and others, 1996; D'Agnese and others, 1997; Belcher, 2004) have honored these HGU subdivisions of the pre-Cenozoic sedimentary section. With modification for local stratigraphic variation and thickness changes, these units also can be used to represent the GBCAAS study area. In contrast, a variety of different approaches have been taken in subdividing the Cenozoic section into HGUs; past approaches have differed in the number of HGUs used within the GBCAAS study area and in the treatment of spatially variable material properties in the volcanic-rock units.

The consolidated pre-Cenozoic rocks, Cenozoic sediments, and igneous rocks of the GBCAAS study area are subdivided into nine HGUs: six of the units describe consolidated pre-Cenozoic rocks and the other three describe Cenozoic basin-fill and volcanic rocks (table B–1; fig. B–2). The HGUs for the GBCAAS study area include (1) a noncarbonate confining unit (NCCU) representing low-permeability Precambrian siliciclastic formations, (2) a lower carbonate aquifer unit (LCAU) representing high-permeability Cambrian through Devonian limestone and dolomite, (3) an upper siliciclastic confining unit (USCU) representing low-permeability Mississippian shale, (4) an upper carbonate aquifer unit (UCAU) representing high-permeability Pennsylvanian and Permian carbonate rocks, (5) a thrusted noncarbonate confining unit (TNCCU) representing low-permeability siliciclastic rocks incorporated in regional thrust faults, (6) a

Table B–1. Thickness and hydraulic properties of hydrogeologic units within the Great Basin carbonate and alluvial aquifer system study area.

[Modified from Belcher and others, 2001; 2002. >, greater than; NC, not calculated; LBFAU, lower basin-fill aquifer unit; UBFAU, upper basin-fill aquifer unit; VU, volcanic unit; UCAU, upper carbonate aquifer unit; USCU, upper siliciclastic confining unit; LCAU, lower carbonate aquifer unit; NCCU, noncarbonate confining unit]

Major hydrogeologic unit	Hydrogeologic unit abbreviation	Maximum unit thickness (feet)	Hydraulic conductivity (feet per day)				
			Arithmetic mean	Geometric mean	Minimum	Maximum	Count
Cenozoic basin-fill aquifer sediments	LBFAU and UBFAU[1]	36,000	31	4	0.0001	431	71
Cenozoic volcanic rock	VU	3,300 (>13,000 in calderas)	20	3	0.04	179	26
Upper Paleozoic carbonate rock	UCAU	24,000	62	0.4	0.0003	1,045	28
Upper Paleozoic siliciclastic confining rock	USCU	>5,000	0.4	0.06	0.0001	3	22
Lower Paleozoic carbonate rock	LCAU[2]	16,500	169	4	0.009	2,704	45
Noncarbonate confining rock	NCCU[3]	NC	0.8	0.008	0.00000009	15	26

[1]Includes both the upper basin-fill aquifer (UBFAU) and lower basin-fill aquifer (LBFAU) hydrogeologic units.

[2]Includes the thrusted lower carbonate aquifer (TLCAU) hydrogeologic unit.

[3]Includes the thrusted noncarbonate confining rock (TNCCU) hydrogeologic unit.

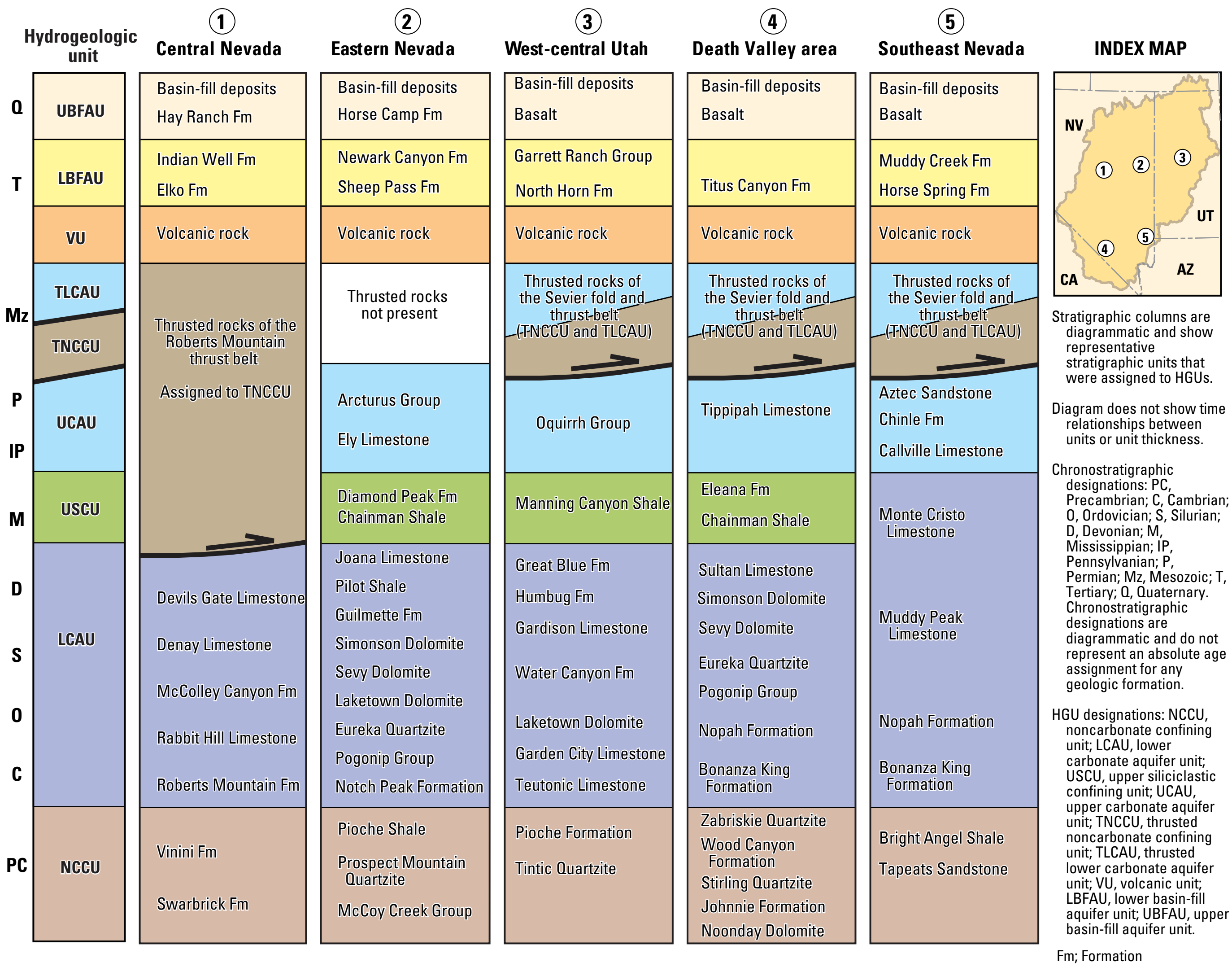

Figure B–2. Representative stratigraphic columns and designation of hydrogeologic units for the Great Basin carbonate and alluvial aquifer system study area.

thrusted lower carbonate aquifer unit (TLCAU) representing high-permeability limestone and dolomite incorporated in regional thrust faults, (7) a volcanic unit (VU) representing outcrop areas of volcanic rocks, (8) a lower basin-fill aquifer unit (LBFAU) representing the lower one-third of the Cenozoic basin fill, and (9) an upper basin-fill aquifer unit (UBFAU) representing the upper two-thirds of the Cenozoic basin fill. The surficial distribution of these hydrogeologic units across the study area is portrayed as a hydrogeologic map (fig. B–3).

The hydrogeologic units in the study area form three distinct aquifer systems composed of alternating more permeable and less permeable units. The three general types of aquifer materials are permeable portions of the UBFAU and LBFAU, some Cenozoic volcanic rocks within the VU—especially fractured welded tuff, and carbonate rocks of the LCAU and UCAU. Each of these units may include one or more water-bearing zones but are stratigraphically and structurally heterogeneous, resulting in a highly variable ability to store and transmit water. The aquifers within the consolidated pre-Cenozoic rocks are separated by the intervening low-permeability Mississippian shale of the USCU. Paleozoic carbonate rocks are underlain at depth by the lower permeability NCCU, which includes Cambrian and Precambrian siliciclastic formations. Volcanic rocks within the VU and the volcanic parts of LBFAU commonly display widely variable lithologic, physical, and hydraulic properties. The hydraulic properties of these deposits largely depend on the mode of eruption and cooling, the extent of primary and secondary fracturing, and the degree to which secondary alteration—such as zeolitic alteration—has affected primary permeability. Fractured rhyolite lava flows and moderately-to

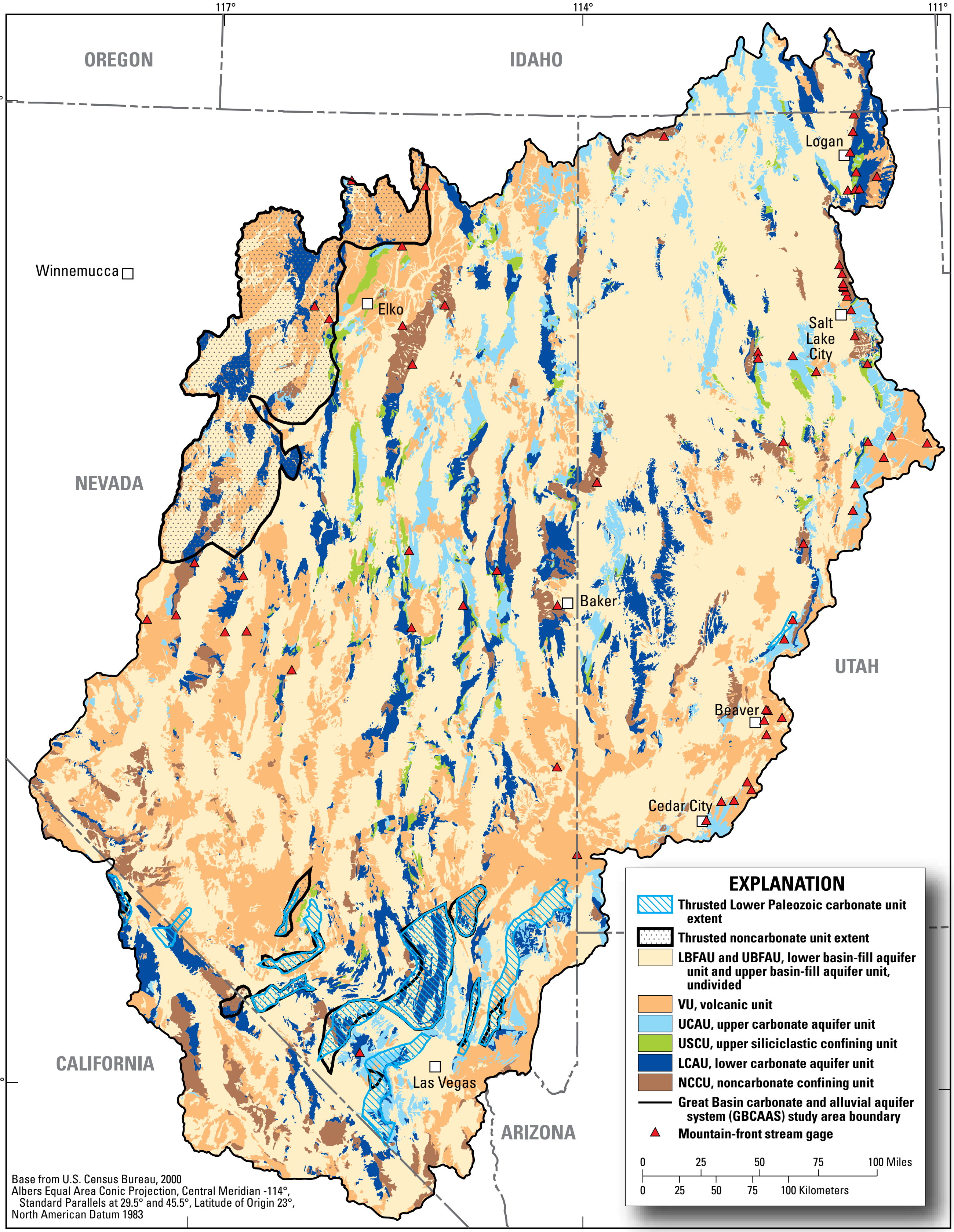

Figure B–3. Surficial hydrogeologic units of the Great Basin carbonate and alluvial aquifer system study area.

-densely welded ash-flow tuffs are the principal volcanic-rock aquifers. The confining units generally are nonwelded or partly welded tuff that have low fracture permeability and can be zeolitically altered in the older, deeper parts of the volcanic sections (Laczniak and others, 1996). The HGUs that correspond to the Cenozoic unconsolidated basin-fill aquifer units, LBFAU and UBFAU, include a wide variety of rock types and may have highly variable hydraulic properties. Relative differences in hydraulic properties were used to differentiate aquifers from confining or semiconfining HGUs in the study area. These evaluations primarily were based on relative differences in permeability determined from HGU material properties or on previous estimates of hydraulic conductivity—a quantitatively derived parameter that serves as a measure of permeability (Lohman, 1979; Todd, 1980).

Few aquifer tests have been completed in the study area, and, thus, estimates of hydraulic properties are sparse. Because of limited test data for the study area, estimates of hydraulic properties were compiled from aquifer tests in the Death Valley regional groundwater flow system (DVRFS) (Belcher and others, 2001; 2002). Hydraulic properties from the DVRFS area are considered to be representative of hydraulic properties over much of the GBCAAS study area because of similar rock types and HGUs (table B–1). Horizontal hydraulic conductivity (hereinafter referred to as hydraulic conductivity) values were selected from previous tabulations (Belcher and others, 2001; 2002) and grouped by HGU (table B–1).

For the study area, the hydraulic conductivity for an HGU can span three to nine orders of magnitude (Belcher and others, 2002). Statistical-probability distributions of hydraulic conductivity for specific hydrogeologic units in the DVRFS are presented in Belcher and others (2002) and generally are considered representative of the range of values in the GBCAAS study area. Carbonate and volcanic rocks are typically aquifers in the study area; in the absence of significant secondary porosity owing to fractures and dissolution, however, they are confining units. Grain size and sorting are important influences on hydraulic conductivity of the unconsolidated sediments (Belcher and others, 2001). Groundwater flow is affected by lower permeability rock units, such as consolidated siliciclastic rocks (NCCU and USCU) and low-permeability zones within the Cenozoic units. Matrix permeability, which defines the rock's primary permeability, is low for both the consolidated carbonate-rock aquifers (Winograd and Thordarson, 1975) and for the welded parts of the volcanic-rock aquifers (Blankennagel and Weir, 1973); as such, faults, shear zones, and fractures, which define the rock's secondary permeability, largely determine the water-transmitting properties of these consolidated rocks.

Each of these HGUs is stratigraphically and structurally heterogeneous, having highly variable hydraulic properties. The spatial variability of material properties is represented using a number of hydrogeologic zones for each HGU. Most zones were defined to represent geologic materials that likely have fairly uniform hydraulic properties. Properties of sediments or rocks within each HGU were derived from previously published geologic maps and reports and were used as indicators of primary and secondary permeability; examples of physical properties considered include grain size and sorting, degree of compaction, rock lithology and competency, degree of fracturing, and extent of solution caverns or karstification.

The hydrogeologic zonation presented for each HGU is intended as a geologically based starting point for further refinement of horizontal hydraulic conductivity of an HGU, perhaps by the use of groundwater flow modeling (D'Agnese and others, 1997, 2002; Belcher 2004). Many of the zones defined for each HGU do not have measurements of hydraulic conductivity from an aquifer test. In the absence of such tests, the relative differences in permeability are defined on the basis of other hydrogeologic information.

Non-Carbonate Confining Unit (NCCU)

In the GBCAAS study area, the oldest sedimentary rocks are Middle Proterozoic and Early Cambrian rocks (fig. B–2) that form a westward-thickening wedge of predominantly quartzite, siltstone, and metasedimentary rocks (Stewart, 1970; Stewart, 1972; Stewart and Poole, 1974). The NCCU includes these rocks, as well as all metamorphic and intrusive igneous rocks (Kistler, 1974; Barton, 1990; table B–1). Although only locally exposed in mountain ranges (fig. B–3), the unit is inferred to underlie most of the study area at great depth.

The permeability of the NCCU generally is low to moderate throughout the study area (Winograd and Thordarson, 1975; Plume, 1996; table B–2). Sandstones of the NCCU are often highly cemented, filling much of the original pore volume, and are overlain and underlain by a significant thickness of shale—all of which contribute to the low permeability of this HGU. Metasedimentary rocks of the NCCU that typically have schistose foliation lack a continuous fracture network. Intrusive igneous rocks act mostly as a confining unit, although small quantities of water may pass through these rocks where they are fractured or weathered; most commonly the fractures are poorly connected and these rocks generally impede groundwater flow (Winograd and Thordarson, 1975). As a result of these lithology-related controls on permeability, the NCCU has been subdivided into three hydrogeologic zones primarily on the basis of lithology (fig. B–4*A*; table B–2):

1. Siliciclastic sedimentary rocks, generally possessing a well-developed fracture network, especially along bedding planes. These rocks are Late Proterozoic to Early Cambrian in age (fig. B–1).
2. Metamorphic rocks including gneiss, schist, and slate associated with highly extended areas and metamorphic core complexes. Metamorphic rocks include Proterozoic rocks

Table B–2. Hydrogeologic zones for the noncarbonate confining unit (NCCU).

Zone code	Dominant lithology	Relative permeability	Permeability characteristics	Reference
1	Late Proterozoic siliciclastic rocks, such as the Prospect Mountain Quartzite in the northern part of the area and Wood Canyon Formation and Stirling Quartzite in the southern part of the area.	Moderate.	Generally well-developed fracture network, especially along bedding planes. Clay interbeds can inhibit connectivity; sandstones typically highly cemented.	Hintze and others (2000); Ludington and others (1996).
2	Foliated metamorphic rocks including gneiss, schist, slate associated with highly extended terranes and metamorphic core complexes.	Low.	Foliation prohibits development of well-connected fracture network, matrix is impermeable.	Raines and others (2003); Wernicke (1992).
3	Intrusive igneous rocks; inferred at depth from (a) projection of surface geology, (b) the assumption that plutons underlie calderas, and (c) published interpretation of magnetic and gravity data that portray plutons.	Low to moderate.	May support well-developed fracture networks where unit is at the surface or within 0.6 miles of the surface; deeper intrusives are probably less fractured. At depth, especially beneath calderas and volcanic centers, fracture permeability may be reduced by quartz veins filling fractures or by clay alteration along fracture walls.	Grauch (1996); Plume (1996); Glen and others (2004).

and those parts of the Paleozoic section affected by metamorphic events in Mesozoic and Tertiary time. Foliation in these rocks prohibits development of well-connected fracture networks; the rock matrix is considered impermeable. Spatial extent of metamorphic rocks was modified from maps of highly extended terrains (Wernicke, 1992; Raines and others, 2003).

3. Intrusive igneous rocks of all ages, predominantly Jurassic, Cretaceous, and Tertiary (fig. B–1). Spatial extent of intrusive igneous rocks was inferred at depth from projection of surface geology, geophysically based maps of inferred pluton extent (Grauch, 1996; Glen and others, 2004), and the assumption that plutons underlie calderas.

Lower Carbonate Aquifer Unit (LCAU)

The LCAU is a thick succession of predominantly carbonate rocks deposited throughout most of the eastern and central parts of the region during Middle Cambrian through Devonian time (fig. B–2). The LCAU represents a large volume of carbonate rock that is prominently exposed in the mountain ranges (fig. B–3) and is present beneath many of the valleys. The LCAU includes Cambrian through Devonian limestone and dolomite, with a few thin interbeds of siliciclastic rocks (fig. B–2).

In general, the carbonate rocks and calcareous shale of the LCAU form a westward-thickening carbonate-and-clastic rock section as much as 15,000 ft thick. The thickness of the unit may exceed 16,500 ft in central and southeastern Nevada, where it has been referred to as the “central carbonate corridor” (Dettinger and others, 1995). Where deposited in shallow-water continental shelf environments, such as eastern Nevada, west-central Utah, and the Death Valley area (columns 2–4, fig. B–2), carbonate rocks are thick-bedded and coarse-grained, as exemplified by units such as the Bonanza King Formation, the Notch Peak Formation, and the Laketown Dolomite. In central Nevada (column 1, fig. B–2), carbonate rocks such as the Roberts Mountain Formation were deposited in deeper water slope and deep basin environments and generally are thin-bedded and finer-grained, containing a high proportion of carbonate mud (Stewart and Poole, 1974; Poole and others, 1992; Cook and Corboy, 2004). Although thickness is not represented on figure B–2, Middle Cambrian through Devonian strata form a relatively thin (several hundreds of feet) cratonic sequence along the east side of the study area (column 5, fig. B–2; Hintze, 1988; Poole and others, 1992).

The carbonate rocks of the LCAU and UCAU form a major high-permeability, consolidated-rock aquifer system in the Great Basin (Winograd and Thordarson, 1975; Bedinger and others, 1989; Dettinger and others, 1995; Harrill and Prudic, 1998). Carbonate rocks of the LCAU and UCAU have three distinct types of permeability that influence the storage and movement of groundwater—primary or intergranular permeability; and two types of secondary permeability: fracture permeability and vug or solution permeability. Lower Paleozoic carbonate rocks in southern Nevada have relatively low primary permeability (Winograd and Thordarson, 1975). Studies of groundwater flow within the carbonate-rock province (Dettinger and others, 1995; Harrill and Prudic, 1998) and tabulations of hydraulic-property estimates for carbonate rocks (Dettinger and others, 1995; Belcher and others, 2001) emphasize the relation of faults and broad structural belts to zones of high permeability, presumably

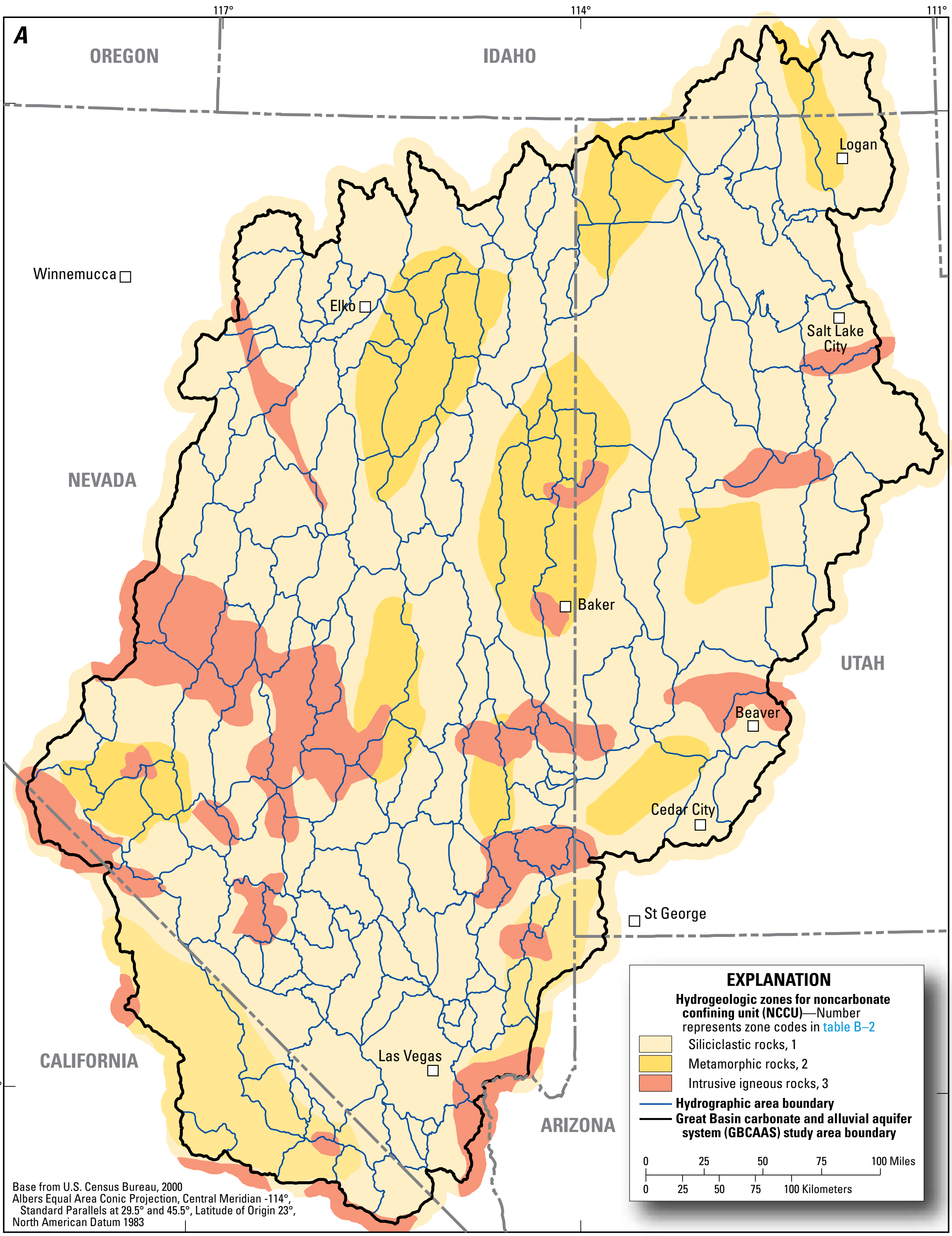

Figure B–4. Zones within some of the hydrogeologic units in the Great Basin carbonate and alluvial aquifer system study area: ***A***, noncarbonate confining unit (NCCU), ***B***, lower carbonate aquifer unit (LCAU), ***C***, upper carbonate aquifer unit (UCAU), ***D***, volcanic unit (VU), ***E***, lower basin-fill aquifer unit (LBFAU), and ***F***, upper basin-fill aquifer unit (UBFAU).

the result of the formation of fractures during deformation. Fracture permeability can be enhanced if vertical fractures intersect horizontal fractures, creating a well-connected network of openings through which water can move. Solution openings can create additional secondary permeability in carbonate rocks. For example, as a result of periodic declines in sea level during Paleozoic time, extensive areas of carbonate rock in east-central Nevada were exposed to subaerial weathering and subsequent erosion. These intervals of erosion are represented in the sedimentary record as unconformities (Cook and Corboy, 2004) —relatively long gaps in time when the carbonate platform was above sea level and conditions were favorable for erosion, dissolution, and development of solution caverns in the exposed carbonate rocks.

The LCAU has been subdivided into three hydrogeologic zones based on lithologic variability that potentially could affect permeability (fig. B–4*B*; table B–3). Lithology-based zones follow:

1. Carbonate rocks deposited in shallow waters. These rocks generally have high permeability as a result of coarse primary texture and frequent subaerial exposure and dissolution.
2. Shale of the Pilot basin. This zone, near the center of the GBCAAS study area, was the site of shale and other siliciclastic deposition in the Pilot basin (Poole and others, 1992) during Devonian to Mississippian time. The siliciclastic units are thin and their presence can result in a slight reduction of the overall permeability of the hydrogeologic unit.
3. Carbonate rocks deposited in deeper waters. These rocks along the western margin of the study area have lower permeability than shallow-water carbonate rocks to the east as a result of the dominance of carbonate mud within the rocks, thin bedding, and higher proportion of shale interbeds.

Upper Siliciclastic Confining Unit (USCU)

The USCU comprises Mississippian mudstone, siltstone, sandstone, and conglomerate that overlie the Lower Paleozoic carbonate rocks. Rocks in the USCU were formed as siliciclastic sediments that were shed eastward from a highland created by the Antler orogeny (fig. B–1), west of the study area. Sediments were deposited in a northeast-to-southwest-trending basin (Poole and Sandberg, 1977; Poole and others, 1992) and include an easterly thinning wedge of coarse clastic detritus, the Diamond Peak Formation (grading eastward into relatively low permeability argillites and shales), and the Chainman Shale (columns 2 and 4, fig. B–2). Siliciclastic rocks of similar age in western Utah include the Manning Canyon Shale (column 3, fig. B–2). This succession of sedimentary rocks is distributed widely across the study area and, where not thinned structurally, generally ranges in thickness from 2,500 ft to greater than 5,000 ft (Hose and others, 1976). The effects of the Antler orogeny did not extend to the southeastern part of the GBCAAS study area, and deposition of shelf-type carbonate rocks, such as the Monte Cristo Limestone, continued during Mississippian time (column 5, fig. B–2).

The shaly siliciclastic rocks of the USCU are fine grained and have low primary porosity and permeability (table B–1). Because of its low susceptibility to dissolution or fracturing, the USCU also lacks significant secondary permeability. The shaly rocks of the USCU yield in a ductile manner when deformed, and deformation does not result in significant fracture

Table B–3. Hydrogeologic zones for the lower carbonate aquifer unit (LCAU).

Zone code	Dominant lithology	Relative permeability	Permeability characteristics	Reference
1	Carbonate rocks deposited in shallow waters.	High.	Generally high permeability as a result of coarse primary texture and frequent subaerial exposure and dissolution.	Dettinger and others (1995); Plume (1996); Cook and Corboy (2004).
2	Shale and siliciclastic rocks of the Pilot basin.	Moderate to high.	Low-permeability shale and other higher permeability siliciclastic deposition in the Pilot basin during Devonian to Mississippian time. Unit is thin but may reduce LCAU permeability where repeated by faulting.	Poole and others (1992).
3	Carbonate rocks deposited in deeper waters.	Moderate.	Lower permeability than shallow-water carbonate rocks to the east as a result of the dominance of carbonate mud within the rocks, thin bedding, and higher proportion of shale interbeds.	Cook and Corboy (2004).

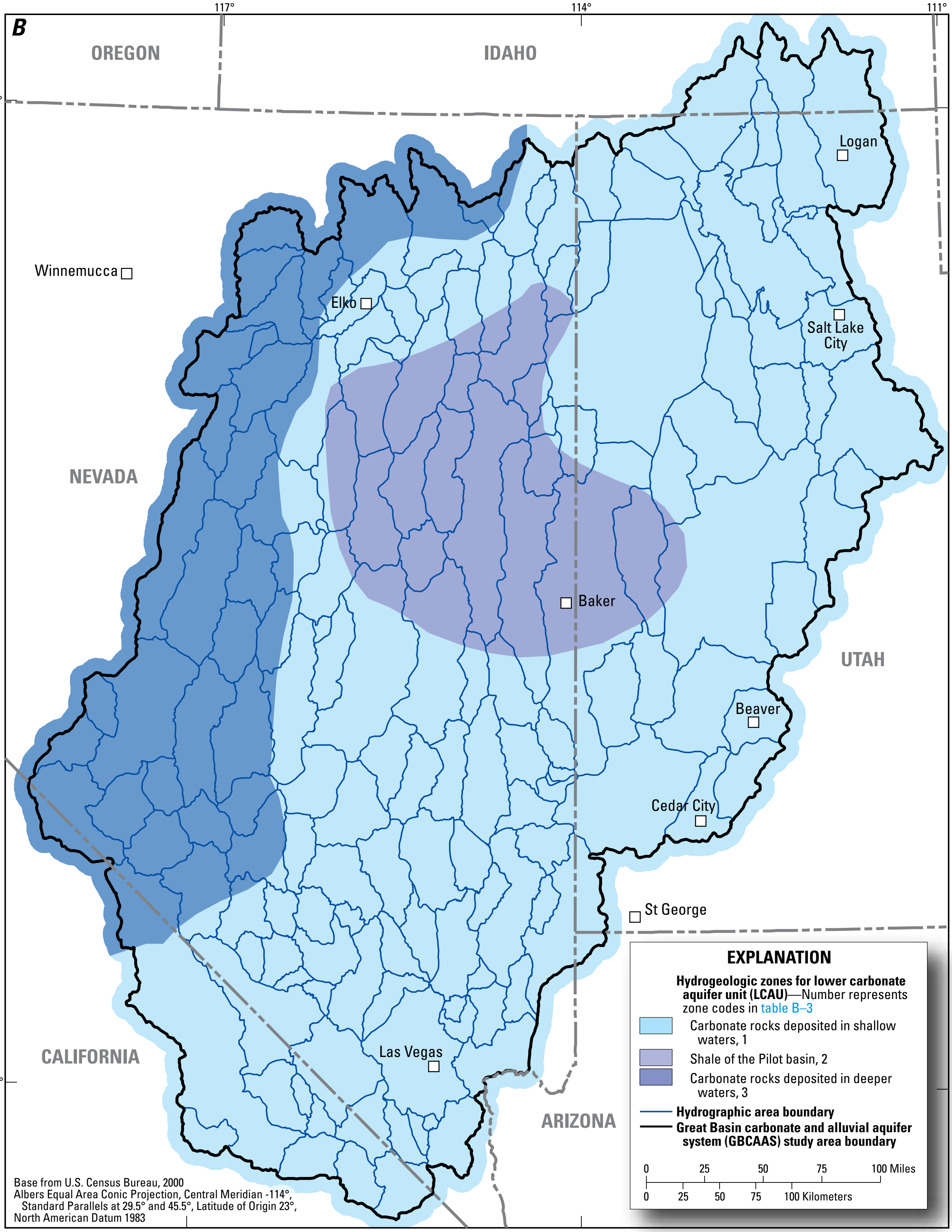

Figure B–4. Zones within some of the hydrogeologic units in the Great Basin carbonate and alluvial aquifer system study area: ***B***, lower carbonate aquifer unit (LCAU).—Continued openings through which water can flow. In southern Nevada, steep hydraulic gradients at the Nevada Test Site are attributed to the low permeability of the Mississippian siliciclastic rocks (Winograd and Thordarson, 1975; D'Agnese and others, 1997). The low porosity of the Chainman Shale in the study area has been documented (Plume, 1996) from data from oil and gas exploration wells.

Upper Carbonate Aquifer Unit (UCAU)

The UCAU primarily comprises thick, widespread Pennsylvanian and Permian rocks that overlie the Mississippian rocks of the USCU (table B–1); this unit generally represents the resumption of deposition of shallow-water marine carbonate sediments on the continental shelf (fig. B–1; Miller and others, 1992). The UCAU dominates outcrops in mountain ranges and at interbasin divides in the eastern parts of the study area (fig. B–3). In eastern Nevada, the unit is as much as 10,000 ft thick and includes the Ely Limestone, Arcturus Group limestone and silty limestone (Hose and others, 1976) (column 2, fig. B–2). In southern Nevada, the unit includes carbonate rocks such as the Tippipah Limestone (column 4, fig. B–2). In west-central Utah, the UCAU includes as much as 24,000 ft of Oquirrh Group marine limestone and sandstones that were deposited in localized basins in Utah as a result of the Ancestral Rocky Mountains orogenic event (fig. B–1; Burchfiel and others, 1992).

From the Late Triassic to Paleocene (early Tertiary) time, the entire width of the eastern Great Basin was compressed in a general west-to-east direction during the Sevier orogeny (fig. B–1). Uplift related to this tectonic event resulted in erosion or nondeposition of sediments in much of the study area; Mesozoic sedimentary rocks are either thin or entirely missing in most of the study area, except for in the extreme southeast (Stewart, 1980). To simplify the hydrogeologic map compilation and 3D-framework construction, outcrops of Mesozoic sedimentary rocks along the southeastern edge of the study area, such as the Chinle Formation and the Aztec Sandstone (column 5, fig. B–2), are also included in UCAU, as are local outcrops of prevolcanic Cenozoic sedimentary rocks in the Death Valley region.

The UCAU generally has high permeability throughout the study area (Winograd and Thordarson, 1975; Plume, 1996). The unit has similar secondary fracture and solution permeability to the LCAU (Winograd and Thordarson, 1975). Given the heterogeneous nature of this unit and the broad age span of the included rocks, the UCAU has been subdivided into five hydrogeologic zones on the basis of lithology and geologic age (fig. B–4*C*; table B–4):

1. Fractured carbonate rocks of Pennsylvanian-Permian age deposited in shallow water that occur throughout most of the study area (Miller and others, 1992).

Table B–4. Hydrogeologic zones for the upper carbonate aquifer unit (UCAU).

Zone code	Dominant lithology	Relative permeability	Permeability characteristics	Reference
1	Fractured carbonate rocks of Pennsylvanian-Permian age that were deposited in shallow water and occur throughout most of the study area. Predominantly limestone; Ely limestone and Arcturus Formation in central Nevada.	High.	Generally well-developed fracture network, in thick upper Paleozoic carbonate rocks.	Hintze and others (2000); Ludington and others (1996); Miller and others (1992).
2	Very thick silty carbonate rocks deposited in the Oquirrh Basin during Pennsylvanian time.	Moderate to high.	Generally well-developed fracture network, in thick upper Paleozoic carbonate rocks. Generally more silty than the shallow-water carbonates of zone 1, may somewhat reduce permeability.	Miller and others (1992); Hintze and others (2000).
3	Continental siliciclastic rocks and other Upper Paleozoic and Mesozoic rocks of the Colorado Plateau that occur along the eastern boundary of the study area.	Moderate.	Section is much thinner than in zones 1 and 2 and contains Triassic siliciclastic rocks, such as Chinle and Moenkopi Formations, that are shaly.	Hintze (1988); Ludington and others (1996).
4	Carbonate rocks deposited in deep water, generally thin-bedded, shaly Pennsylvanian-Permian rocks; exposed along western side of study area.	Low to moderate.	Thin bedded, shaly carbonate rocks deposited as turbidites. Thin bedding and fine-grained interbeds may preclude development of good fracture network and reduce overall permeability.	Miller and others (1992); Poole and others (1992).
5	Prevolcanic Cenozoic rocks of the Death Valley region.	Low to moderate.	Zone created for compatibility with the Death Valley three-dimensional hydrogeologic framework.	Faunt and others (2004).

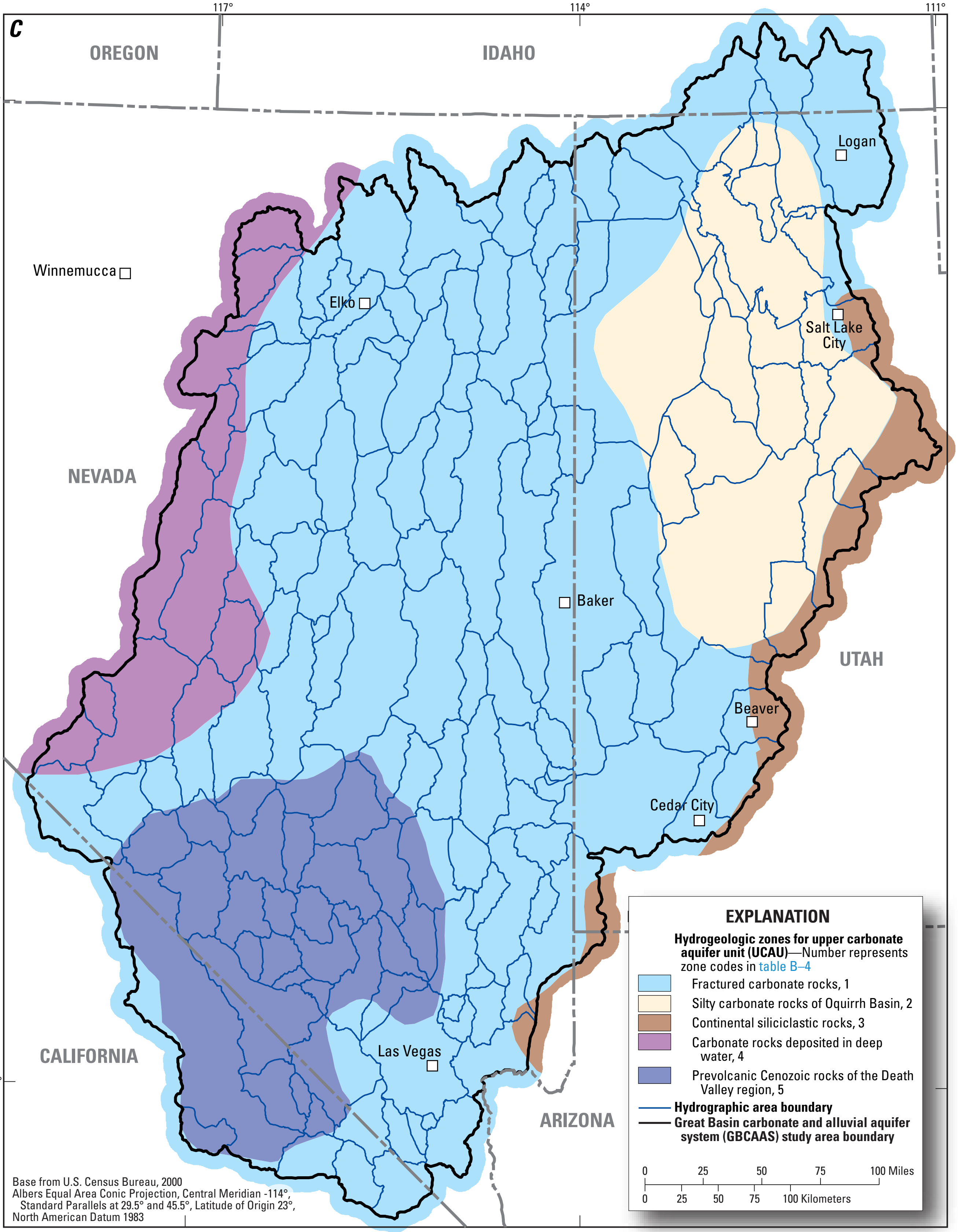

Figure B–4. Zones within some of the hydrogeologic units in the Great Basin carbonate and alluvial aquifer system study area: ***C***, upper carbonate aquifer unit (UCAU).—Continued

2. Silty carbonate rocks deposited in the Oquirrh Basin during Pennsylvanian time. These rocks generally are more silty than the shallow-water carbonates of zone 1, resulting in potentially lower permeability (Hintze, 1988).
3. Continental siliciclastic rocks and other Upper Paleozoic and Mesozoic rocks of the Colorado Plateau that occur along the eastern boundary of the study area.
4. Carbonate rocks of Pennsylvanian-Permian age deposited in deep water and that are generally thin-bedded, shaly, and exposed along the western side of study area.
5. Prevolcanic Cenozoic rocks of the Death Valley region. This zone was created to maintain consistency with the Death Valley three-dimensional hydrogeologic framework (Faunt and others, 2004).

Thrusted Non-Carbonate Confining Unit (TNCCU) and Thrusted Lower Carbonate Aquifer Unit (TLCAU)

Major thrust faults of the Roberts Mountain thrust belt and the Sevier fold-and-thrust belt (fig. B–5) resulted from the Antler and Sevier orogenies, respectively (fig. B–1). These thrust faults have stratigraphic offsets of several thousands of feet and horizontal displacements of several miles (Armstrong, 1968; Burchfiel and others, 1992; Allmendinger, 1992; DeCelles, 2004), resulting in stratigraphic repetition of HGUs. Because the HGUs must be represented as grids in the 3D-hydrogeologic framework, they cannot have multiple altitudes at a single location, as would be the case for repeated units. The repeated stratigraphy in thrusted areas was therefore treated as two additional HGUs, the TNCCU and the TLCAU. The TNCCU includes all Late Proterozoic siliciclastic rocks that are repeated by thrust faults within the Sevier fold-and-thrust belt (fig. B–5). For simplicity, the TNCCU also includes all thrusted rocks of the Roberts Mountain belt (fig. B–5), regardless of age or lithology. The TLCAU unit includes all thrusted Paleozoic rocks of the LCAU, USCU, and UCAU HGUs that lie within the Sevier fold-and-thrust belt (fig. B–5).To simplify construction of the 3D-hydrogeologic framework, thrusted rocks from three HGUs were assigned to the single thrusted HGU, TLCAU, regardless of age or lithology. This simplification is justified because most of the thrusted units are carbonate rocks. Not all thrusts within the study area are delineated as separate units; thrusted areas were selected for their size, offset, and potential hydrologic importance in juxtaposing carbonate and noncarbonate units. As such, relatively minor thrust repetition within the central Nevada thrust belt (fig. B–5) was not included.

A variety of potential changes to rock permeability are possible as a result of thrust faulting. Rocks involved in regional thrusting may be more highly fractured as a result of compressive deformation and transport as thrust sheets. Thrust faults often have sufficient offset to juxtapose higher permeability shallow-water facies against lower-permeability rocks deposited in deeper waters; such juxtaposition of different HGUs is considered the most important hydrologic effect of thrust faults.

Volcanic Unit (VU)

The VU includes large volumes of middle Tertiary (Eocene to middle Miocene) volcanic rocks that include welded and nonwelded tuff of rhyolite-to-andesite composition deposited during caldera-forming eruptions, as well as basalt, andesite, and rhyolite lava flows (McKee, 1971; Cross and Pilger, 1978; McKee and Noble, 1986; Best and others, 1989). Ash-flow tuffs erupted from multiple calderas as part of a general southward and westward sweep of volcanism across the study area in Oligocene and Miocene time (Best and others, 1989; McKee, 1996; Dickinson, 2002). The aggregate thickness of these eruptive deposits can exceed 3,000 ft; volcanic accumulations within the calderas can be up to 10,000 ft thick (Best and others, 1989; Sweetkind and du Bray, 2008). With the exception of Eocene andesitic volcanism to the north of Elko, Nevada, in the northwestern part of the study area (Ludington and others, 1996), the VU is relatively minor in the northern one-third of the study area (fig. B–3). As volcanism swept from north to south, eruption of many of the ash-flow tuffs in the central part of the study area occurred relatively early in the extensional history of the area (Best and Christiansen, 1991). As a consequence, regionally distributed ash-flow tuffs in the central part of the study area are preserved deep in the stratigraphy of the downfaulted basins and are often covered by thick intervals of younger sedimentary deposits. Continued sedimentation in the southern part of the study area resulted in the accumulation of considerable local thickness of sedimentary rocks that predate volcanic activity. In the southern parts of the study area, volcanic rocks are relatively young, occur high in the section, and form extensive outcrops.

Fractured Cenozoic volcanic rocks near the major volcanic fields are locally thick enough to be important subregional aquifers that interact with regional groundwater flow through the underlying Paleozoic carbonate rocks (Dettinger, 1989; Harrill and others, 1988). Volcanic-rock units commonly display widely variable lithology and degree of welding, both vertically and horizontally. The hydraulic properties of these deposits (table B–1) primarily depend on the mode of eruption and cooling, the extent of primary and secondary fracturing, and the degree to which secondary alteration (crystallization of volcanic glass and zeolitic alteration) has affected primary permeability. Fractured rhyolite-lava flows and moderately-to-densely welded ash-flow tuffs are the principal volcanic-rock aquifers. Rhyolite-lava flows and thick intracaldera welded tuff are relatively restricted to local areas areally, whereas outflow welded-tuff sheets are more regionally distributed and may provide lateral continuity for water to move through the regional flow system. Local confining units are generally formed by nonwelded or partly welded tuff that has low fracture permeability and can be zeolitically altered in the

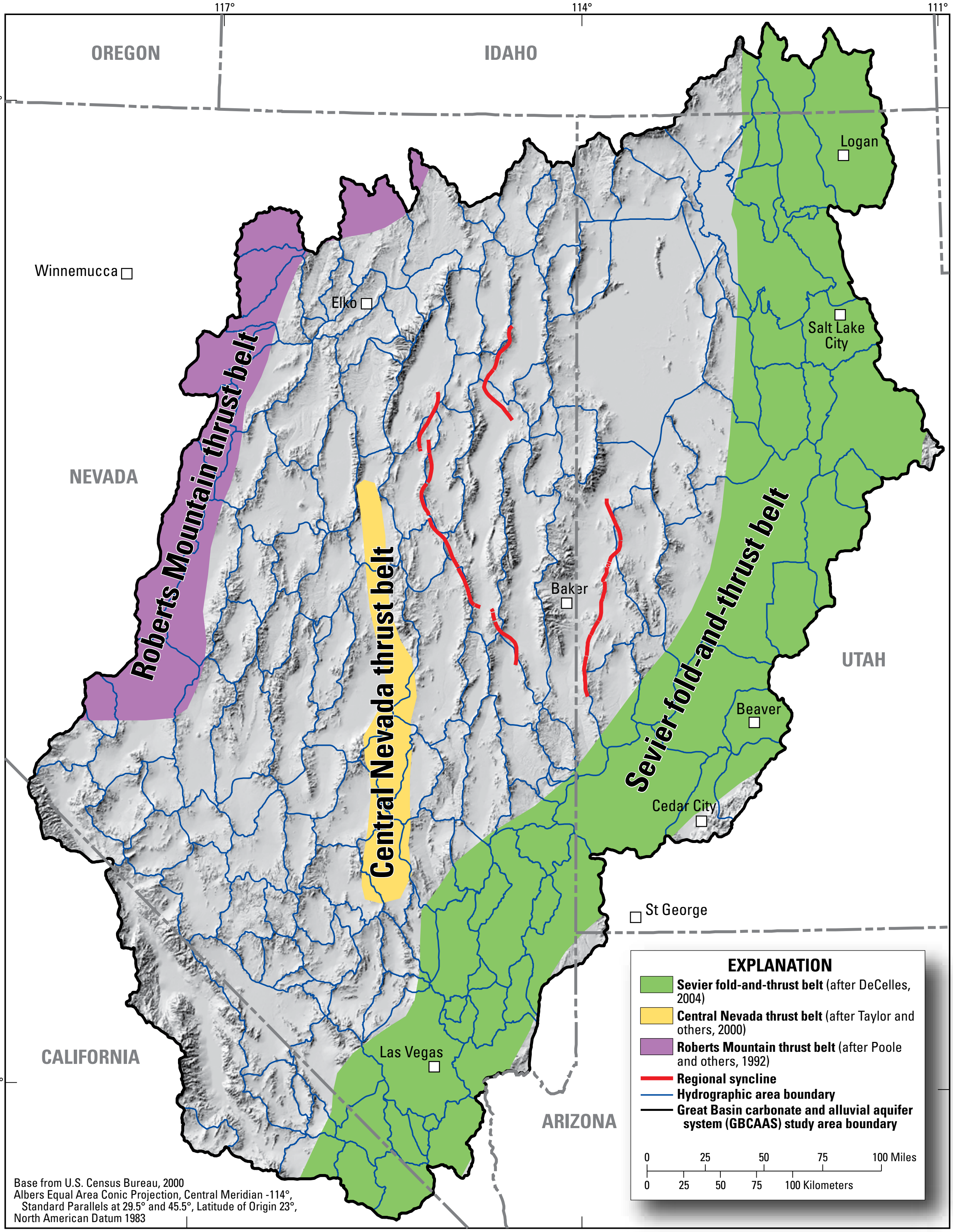

Figure B–5. Major Mesozoic structural belts of the Great Basin carbonate and alluvial aquifer system study area.

older, deeper parts of the volcanic sections (Laczniak and others, 1996). The hydraulic properties of volcanic rocks in the vicinity of the Nevada Test Site (fig. B–4*D*) were described by Blankennagel and Weir (1973) and Belcher and others (2001); these concepts likely apply throughout the GBCAAS study area.

The VU has been subdivided into seven hydrogeologic zones based on lithology and volcanic rock properties (fig. B–4*D*; table B–5). Because of the methodology used to construct the 3D-hydrogeologic framework, these zones primarily apply to surficial outcrops of VU; volcanic rock units buried within the basin fill are treated as part of the LBFAU. The zones of the VU are:

1. Welded ash-flow tuff. Generally in thick sequences and assumed to have a well-developed fracture network.
2. Local lava flows. Areas of rhyolite to andesite lava flows that form localized accumulations, not widespread sheets. These rocks can be highly fractured, but fracture pattern typically is disorganized and fractures are short.
3. Prevolcanic basins. Areas where significant amounts of sedimentary rocks may underlie outcrops of volcanic rocks.
4. Shallow basalt. Areas of outcropping or near-surface basalt flows. This zone was created to allow thin surficial basalt flows to stack correctly in the 3D framework.
5. Mesozoic and Cenozoic sedimentary rocks. Generally along the Wasatch Front and Colorado Plateau Basin and Range transition. This zone was created as a result of combination of some Mesozoic and Cenozoic sediments with VU.
6. Heterogeneous rocks in California. Includes tuff, rhyolite to basalt lava flows, and interbedded sedimentary rocks.
7. Intracaldera ash-flow tuff and other rocks related to caldera collapse.

Lower Basin-Fill Aquifer Unit (LBFAU)

Formations that fill Cenozoic basins were grouped into one of two HGUs based on the thickness of the basin-fill deposits: the LBFAU that comprises the deepest one-third of the basin fill and the UBFAU that comprises the shallowest two-thirds of the basin fill. The LBFAU consists of a wide variety of rock types, including volcanic rocks buried within the basin fill near the main volcanic centers, along with consolidated older Cenozoic basin-fill rocks that underlie the more recent basin-fill deposits (table B–6). The volcanic rocks include regionally distributed welded ash-flow tuffs and more local lava-flow deposits. The consolidated older Cenozoic basin-fill rocks are comprised of fluvial and lacustrine limestone, sandstone, siltstone, and local conglomerate, often with significant volcanic detritus. Permeability of the sedimentary part of the basin fill is affected by the original depositional environment, proximity to volcanic centers during sediment deposition, and depth of burial.

The lower unit (LBFAU) has been subdivided into five hydrogeologic zones based on lithology and volcanic rock properties (fig. B–4*E*; table B–6):

1. Welded ash-flow tuff. Thick sequences that fill the bottoms of Cenozoic basins within and surrounding volcanic fields; the spatial extent of buried volcanic rocks was guided by Cenozoic volcanic rocks (Best and others, 1989; Sweetkind and du Bray, 2008) and regional aeromagnetic maps (Raines and others, 2003; Glen and others, 2004).
2. Intracaldera ash-flow tuff and other rocks, where calderas extend from mountain ranges into intervening valleys.
3. Local lava flows. Areas of more localized lava flows, generally andesite or rhyolite, filling the bottoms of Cenozoic basins within and surrounding volcanic centers.
4. Prevolcanic Cenozoic sedimentary rocks. Generally lakebed and other fine-grained deposits (Fouch, 1979; Fouch and others, 1979), but can include some sandy or coarse-grained material.
5. Coarse-grained basin fill. Inferred to be early-to-mid Cenozoic sands and gravels, and may be intercalated with volcanic rocks or contain significant ash or volcanic detritus.

Upper Basin-Fill Aquifer Unit (UBFAU)

Modern Basin and Range topography began forming in Neogene time, resulting from extension along high-angle faults (fig. B–1). At this time, unconsolidated sediments began filling the broad, intermontane basins. Sedimentation in this period was largely postvolcanic, except for local basalts. Modern drainages were established during this period; low base levels along the Colorado River and Death Valley forced headward erosion along tributary drainages, resulting in downcutting and exposure of older sediments within the basins. In Pleistocene time, pluvial climates led to the creation of widespread shallow lakes throughout the region (Reheis, 1999). The drier Holocene climate led to the drying of these lakes and the abandonment or reduction in flow of numerous springs. This has resulted in the exposure of paleo-spring discharge deposits, common in many valleys in the southern part of the study area (Quade and others, 1995).

The UBFAU comprises the shallowest two-thirds of the basin fill and includes a wide variety of Quaternary and Tertiary basin-fill sediments younger than the VU and LBFAU (table B–1). Neogene sediments were deposited in lacustrine, fluvial, and alluvial environments and include unconsolidated alluvium and colluvium, along with local deposits of fresh water limestone, tuffaceous sandstone and siltstone, laminated clays, and water-lain tuffs and ash. Quaternary and Tertiary basalts, also included with this unit, are thin but locally cover significant areas. The distribution of Quaternary units and their hydrologic significance has been mapped in detail for Nevada (Maurer and others, 2004), but similar types of maps are lacking for other states in the GBCAAS study area. Unfortunately, the mapping by Maurer and others (2004) lacks

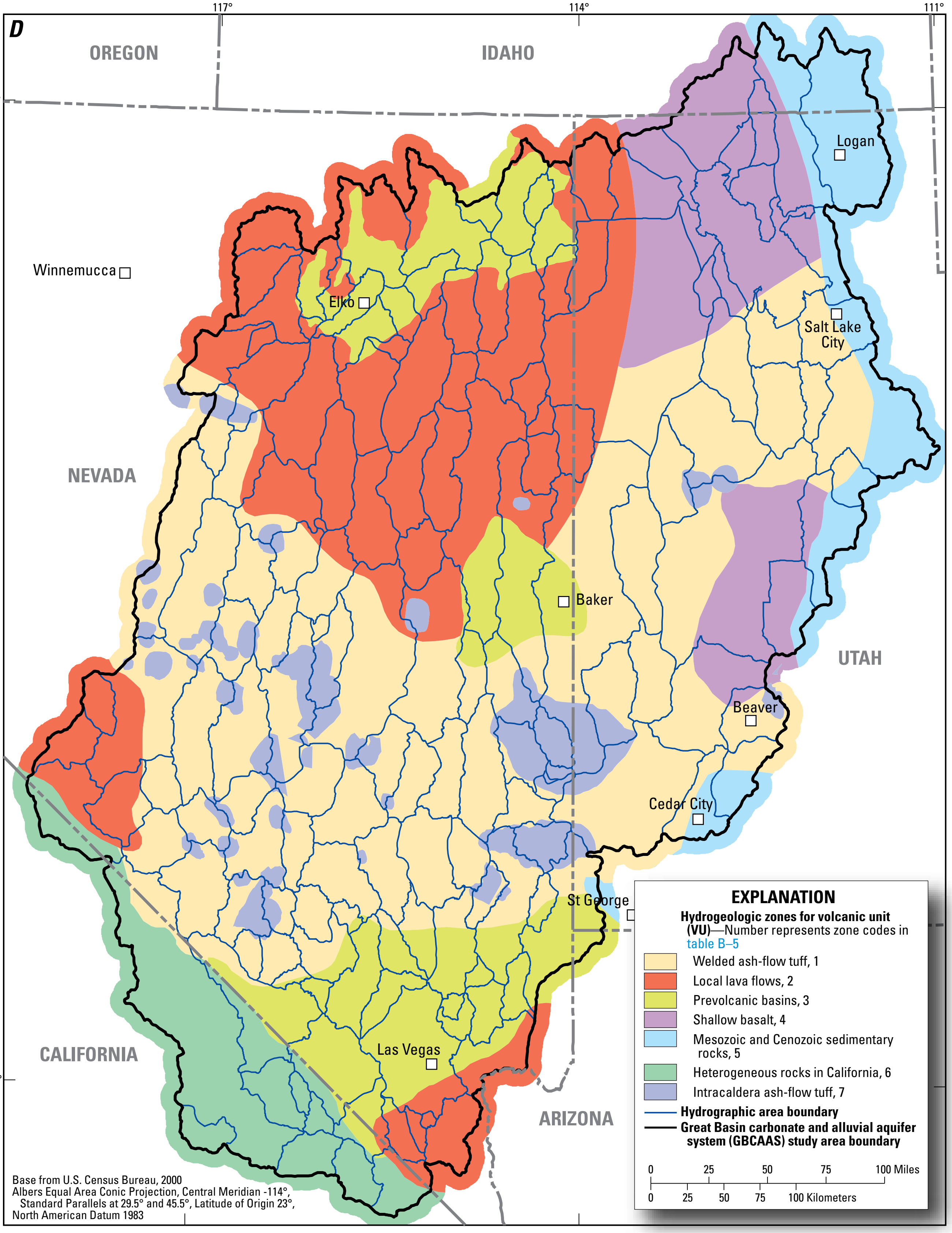

Figure B–4. Zones within some of the hydrogeologic units in the Great Basin carbonate and alluvial aquifer system study area: ***D***, volcanic unit (VU).—Continued

Table B–5. Hydrogeologic zones for the volcanic unit (VU).

Zone code	Dominant lithology	Relative permeability	Permeability characteristics	Reference
1	Welded ash-flow tuff; generally in thick sequences.	High.	Generally well-developed fracture network in sequences of welded ash-flow tuff. Permeability may be reduced somewhat inside calderas due to lithologic heterogeneity.	Laczniak and others (1996); Blankennagel and Weir (1973); Belcher and others (2001).
2	Local lava flows; areas of rhyolite to andesite lava flows that form localized accumulations, not widespread sheets.	Moderate to high.	Can be highly fractured, but fracture pattern is typically disorganized and fractures are short.	Laczniak and others (1996); Blankennagel and Weir (1973); Belcher and others (2001).
3	Prevolcanic basins; areas where significant amounts of sedimentary rocks may underlie outcrops of volcanic rocks.	Moderate.	Section consists of early Cenozoic lake beds and generally fine-grained deposits; can include some sandy or coarse-grained material. Zone created to account for areas where prevolcanic sedimentary rocks were combined with VU in the 3D hydrogeologic framework.	Hintze (1988); Ludington and others (1996).
4	Shallow basalt; areas of outcropping or near-surface basalt flows.	Moderate.	Zone was created to allow thin surficial basalt flows and underlying basin-fill sediments to stack correctly in the three-dimensional framework.	Hintze (1988); Ludington and others (1996).
5	Mesozoic and Cenozoic sedimentary rocks; generally along the Wasatch Front and Colorado Plateau-Basin and Range transition.	Low to moderate.	Zone created to revise hydrogeologic unit attribution from hydrogeologic map; several polygons of Mesozoic and Cenozoic sediments were included in VU.	Hintze (1988); Ludington and others (1996).
6	Heterogeneous rocks in California; includes tuff, rhyolite to basalt lava flows, and interbedded sedimentary rocks.	Low to moderate.	Zone created to revise hydrogeologic unit attribution that was inconsistent with Nevada and Utah hydrogeologic maps. Heterogeneous mixture of lithologies may tend to reduce overall permeability.	Hintze (1988); Ludington and others (1996).
7	Intracaldera ash-flow tuff and other rocks related to caldera collapse.	Moderate, variable.	Permeability of volcanic rocks may be reduced inside calderas due to extreme lithologic diversity and lack of organized fracture networks. Intracaldera volcanic rocks are thick sequences of highly heterogeneous volcanic rocks (including welded and nonwelded tuff, lava flows, volcanic breccias, and nonvolcanic megabreccia deposits) that are bounded by the caldera structures. This unit overlies intrusive rocks of the noncarbonate confining unit (NCCU) inferred to be present at depth with calderas; unit has potential to be hydrothermally altered.	Laczniak and others (1996); Blankennagel and Weir (1973); Belcher and others (2001).

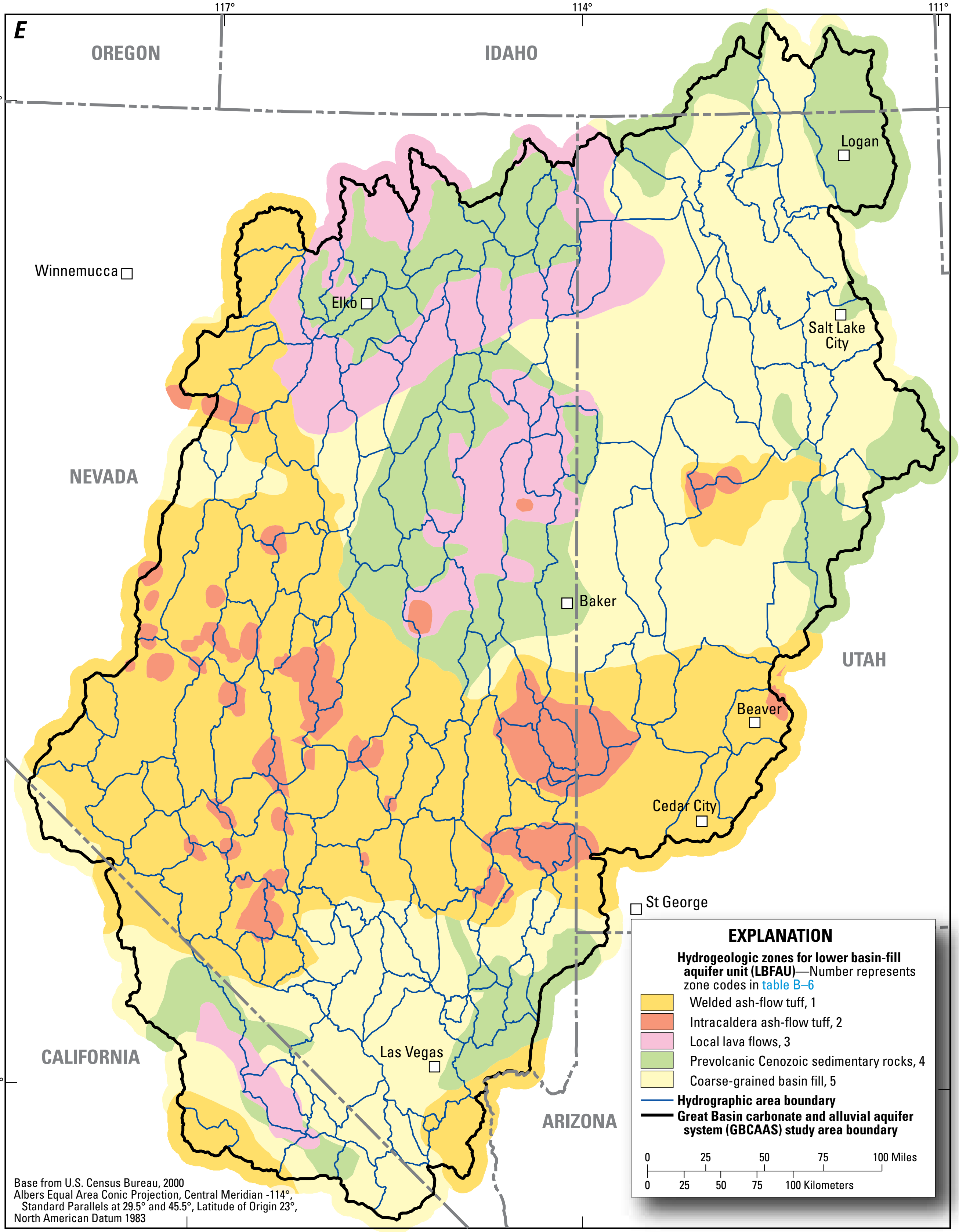

Figure B–4. Zones within some of the hydrogeologic units in the Great Basin carbonate and alluvial aquifer system study area: ***E***, lower basin-fill aquifer unit (LBFAU).—Continued

Table B–6. Hydrogeologic zones for the lower basin-fill aquifer unit (LBFAU).

Zone code	Dominant lithology	Relative permeability	Permeability characteristics	Reference
1	Welded ash-flow tuff; thick sequences that fill the bottoms of Cenozoic basins within and surrounding volcanic fields.	High.	Generally well-developed fracture network, in sequences of welded ash-flow tuff. Permeability may be reduced somewhat inside calderas due to lithologic heterogeneity.	Best and others (1989); Sweetkind and du Bray (2008); Raines and others (2003); Glen and others (2004).
2	Intracaldera ash-flow tuff and other rocks, where calderas extend from mountain ranges into intervening valleys.	Moderate, variable.	Permeability of volcanic rocks may be reduced inside calderas due to extreme lithologic diversity and lack of organized fracture networks. Intracaldera volcanic rocks are thick sequences of highly heterogeneous volcanic rocks (including welded and nonwelded tuff, lava flows, volcanic breccias, and nonvolcanic megabreccia deposits) that are bounded by the caldera structures. This unit overlies intrusive rocks of the noncarbonate confining unit (NCCU) inferred to be present at depth with calderas; unit has potential to be hydrothermally altered.	Best and others (1989); Sweetkind and du Bray (2008); Raines and others (2003); Glen and others (2004).
3	Local lava flows; areas of more localized lava flows, generally andesite or rhyolite, that fill the bottoms of Cenozoic basins within and surrounding volcanic centers.	Moderate to high.	Rhyolite to andesite lava flows form localized accumulations, not widespread sheets. Can be highly fractured, but fracture pattern is typically disorganized and fractures are short.	Best and others (1989); Sweetkind and du Bray (2008); Raines and others (2003); Glen and others (2004).
4	Prevolcanic Cenozoic sedimentary rocks; generally lake-bed and other fine-grained deposits, but can include some sandy or coarse-grained material. Includes the Sheep Pass, Horse Spring, Muddy Creek, and Elko Formations.	Moderate.	Section consists of early Cenozoic lake beds and generally fine-grained deposits; can include some sandy or coarse-grained material. Thin bedding and generally fine grain size reduce permeability.	Fouch (1979); Fouch and others (1979); Hintze (1988); Ludington and others (1996).
5	Generally coarse-grained basin fill.	Moderate.	Inferred to be early-to-mid Cenozoic sands and gravels; deep burial and cementation may reduce permeability.	Fouch (1979); Fouch and others (1979); Hintze (1988); Ludington and others (1996); Plume (1996).

a thickness component that would allow the mapped units to be used as an HGU within a geologic framework.

The UBFAU comprises gravel, sand, silt, clay, and fresh-water limestone and, thus. is expected to have a large range of permeability. Sediments of the UBFAU are not commonly cemented, but are semiconsolidated at depth. Where these deposits are coarse grained and well sorted, they are permeable and form local aquifers, particularly the alluvial fan and stream channel deposits (Belcher and others, 2001). However, in some areas, this unit contains intercalated, less permeable, finer grained sediments, or volcanic ash.

The UBFAU has been subdivided into four hydrogeologic zones based on lithology (fig. B–4*F*; table B–7):

1. Near-surface basalt flows. This zone was created to allow thin surficial basalt flows to stack correctly in the 3D framework.
2. Prevolcanic and synvolcanic sediments that are thick enough to be present within the shallowest two-thirds of the basin fill. Prevolcanic sections consist of early Cenozoic lake beds and generally fine-grained deposits. Zeolitic alteration of ash in synvolcanic sections that

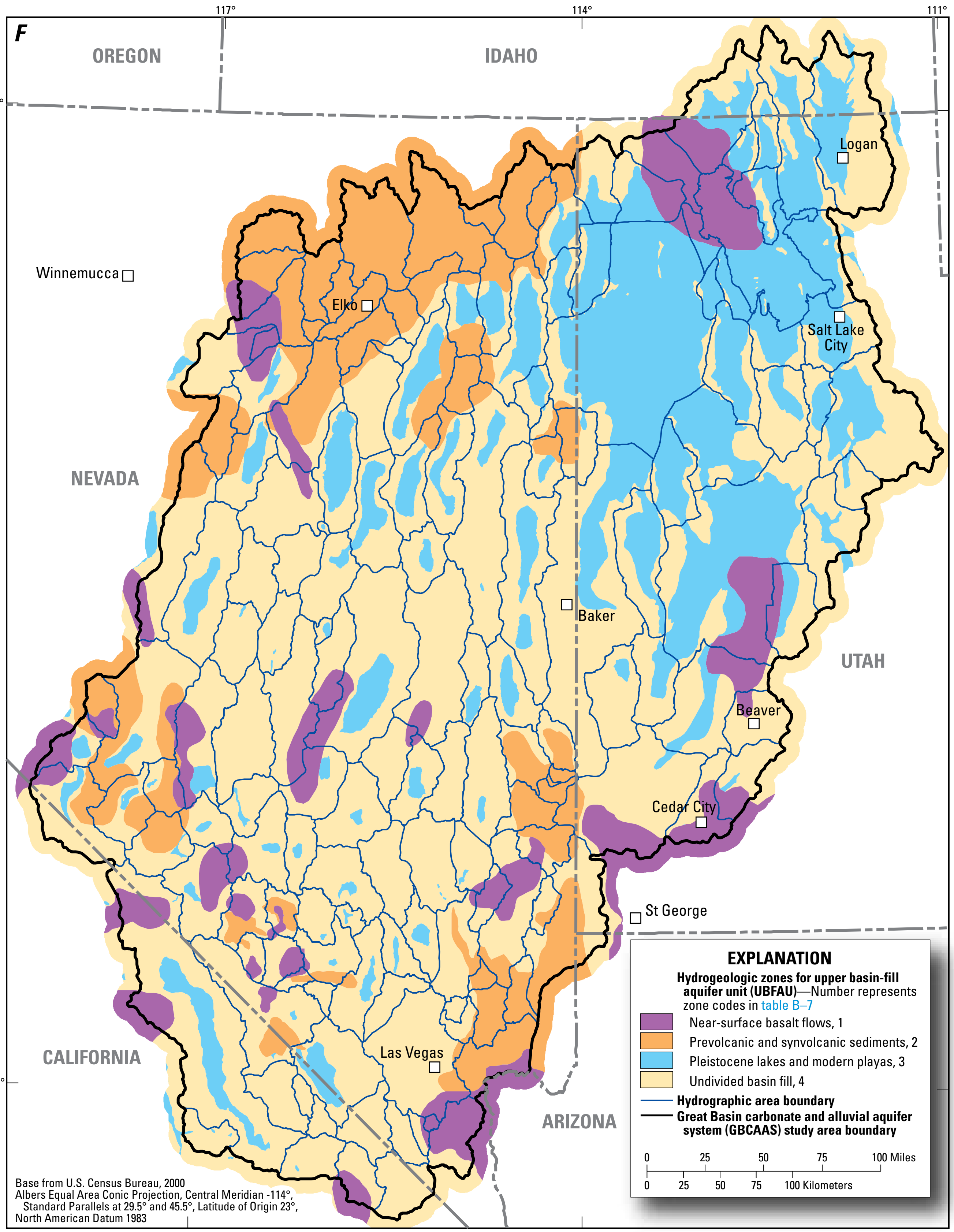

Figure B–4. Zones within some of the hydrogeologic units in the Great Basin carbonate and alluvial aquifer system study area: *F*, upper basin-fill aquifer unit (UBFAU).—Continued

Table B–7. Hydrogeologic zones for the upper basin-fill aquifer unit (UBFAU).

Zone code	Dominant lithology	Relative permeability	Permeability characteristics	Reference
1	Near-surface basalt flows.	Moderate.	Basalts are mostly thin flows either overlying or within coarse-grained basin fill. Basalts can have high fracture permeability and permeable zones at contacts between flows. Local alteration may reduce permeability.	Hintze (1988); Ludington and others (1996).
2	Prevolcanic and synvolcanic sediments that are thick enough to be present within the shallowest two-thirds of the basin fill.	Moderate-low.	Section consists of early Cenozoic lake beds and generally fine-grained deposits; synvolcanic basins that contain significant amount of volcanic ash may have lowered permeability due to zeolitic alteration of ash.	Fouch (1979); Fouch and others (1979); Hintze (1988); Ludington and others (1996).
3	Areas of Pleistocene lakes and modern playas consisting of fine-grained surficial sediments.	Moderate to low.	Fine-grained surficial units; considerable uncertainty as to how deep these units exist in the subsurface.	Hintze (1988); Ludington and others (1996); Reheis (1999).
4	Undivided basin fill.	Moderate.	Inferred to be late Cenozoic alluvial sands and gravels.	Hintze (1988); Ludington and others (1996); Plume (1996).

contain significant amounts of volcanic ash may lower permeability.

3. Areas of Pleistocene lakes and modern playas consisting of fine-grained surficial sediments. There is considerable uncertainty as to how deep these units extend in the subsurface.
4. Undivided basin fill. Areas of generally coarse-grained Late Cenozoic alluvial and colluvial sands and gravels.

Structural Geology

The structural geologic setting of the GBCAAS study area is complex, exhibiting several ages and styles of deformation. The study area is affected by two general phases of deformation: Late Devonian to Eocene compressional deformation characterized by regional folding and overthrusting, and a subsequent phase of Neogene extension characterized by regional-scale normal and strike-slip faulting (fig. B–1). Locally, Miocene calderas are an important structural element. HGUs are commonly disrupted by large-magnitude offset thrust, strike-slip, and normal faults, and locally affected by caldera formation, resulting in a complex distribution of rocks. Faults and caldera boundaries juxtapose HGUs with contrasting hydraulic properties and may divert groundwater flow paths and disrupt regional groundwater flow. Chapter C describes how these geologic controls affect groundwater flow.

Compressional Deformation

The oldest deformation of hydrologic significance in the GBCAAS study area was the Late Devonian to Late Mississippian east-west compression of the Antler orogeny (Poole and Sandberg, 1977; Speed and Sleep, 1982; Burchfiel and others, 1992; Poole and others, 1992; fig. B–1). This deformational event created the Roberts Mountain thrust belt, a stack of thrust sheets as much as 8,000 ft. thick along the northwestern margin of the study area (fig. B–5). The thrusts transported lower-permeability siliciclastic rocks (deposited in deeper water), all assigned to TNCCU, eastward onto the carbonate platform (fig. B–2). Although carbonate rocks extend some distance westward beneath the thrust sheet, in general, the eastern boundary of this thrust system forms the general western edge of the carbonate-rock section. Other compressive orogenic events occurred in western Nevada (Crafford, 2008) in Late Paleozoic time (fig. B–1), but had relatively little effect on the distribution of rocks in the study area.

The Paleozoic rocks throughout the region were affected by east-west compression related to the Sevier orogeny from Late Triassic to Paleocene time (fig. B–1). This deformational event resulted in the north-to-northeast-trending Sevier fold-and-thrust belt (fig. B–5) that extends along the eastern flank of the GBCAAS study area from near Las Vegas, Nevada, to southern Idaho (Armstrong, 1968; Allmendinger, 1992; Burchfiel and others, 1992; DeCelles, 2004). A second, smaller fold-and-thrust belt, the Central Nevada thrust belt (Speed, 1983; Taylor and others, 2000), is present as a generally north-south belt in east-central Nevada. These thrusts are discontinuous and more localized than the frontal thrusts of the Sevier thrust belt, but they can locally disrupt the continuity of the Paleozoic carbonate-rock section.

Associated with the Mesozoic regional thrusting are regional folds (fig. B–5). Regional synclines or downfolds have broadly sinuous but generally north-trending fold axes. These thrust-related synclines preserve Triassic rocks in their core and maintain a chiefly uninterrupted section of Paleozoic carbonate-rock section.

Cenozoic Extensional and Strike-Slip Deformation

Cenozoic deformation of the region is characterized by a variety of structural patterns that overlap in space and time and include (1) local extreme extension along detachment faults associated with the development of metamorphic core complexes and the development of greatly extended zones, (2) development of discrete strike-slip faults and transtensional basins within the Walker Lane belt (fig. B–6), (3) linear structural belts striking northwest-southeast or east-west that may represent reactivation of older crustal structures, (4) Basin and Range extension along steeply dipping faults, and (5) Cenozoic volcanism that preceded and was contemporaneous with regional extension, creating huge caldera complexes and depositing voluminous material into evolving basins.

A regional episode of extension occurred in Eocene-Oligocene time (fig. B–1) prior to the formation of much of the present Basin and Range physiography (Zoback and others, 1981). Large-magnitude extension occurred in localized highly deformed and extended areas (fig. B–6), creating metamorphic core complexes (Coney, 1980; Armstrong, 1982; Wernicke, 1992). These zones feature gentle-to-moderate dipping, large-offset extensional detachment faults that typically separate broadly domed, ductilely deformed metamorphic rocks of the NCCU in their lower plates from overlying unmetamorphosed rocks and brittlely deformed rocks of various HGUs that commonly are highly extended and tilted along a myriad of normal faults (Hamilton, 1988; Wernicke, 1992).

By Early Miocene time, the northwest-trending Walker Lane belt (fig. B–6) was established along the southwestern part of the GBCAAS study area (Stewart, 1988; Hardyman and Oldow, 1991; Stewart, 1998; Stewart and Crowell, 1992). The Walker Lane belt is a complex structural zone dominated by large right-lateral faults with northwest orientations, and it contains discontinuous east-northeast-trending left-lateral strike-slip faults and local normal faults (Stewart, 1988; Stewart and Crowell, 1992). Some of these faults are significant in that they are oriented transverse to the inferred direction of regional groundwater flow. The Walker Lane belt also includes the detachment faults and metamorphic core complexes near Death Valley that have accommodated large-magnitude northwest-directed horizontal extension (fig. B–6). These features are separated by major strike-slip faults that likely evolved coevally and are the result of northwest-directed extension (Wright, 1989).

Long, linear structures with northwest-southeast and east-west orientations (fig. B–6) have been proposed as being long-duration, crustal-scale features because of a variety of geologic, geophysical, and isotopic evidence. Mineral belts defined by the northwest-striking Carlin (Hofstra and Cline, 2000; Wallace and others, 2004; Cline and others, 2005; Emsbo and others, 2006) and Battle Mountain-Eureka trends (Crafford and Grauch, 2002) likely represent reactivated structural conduits of large-scale crustal geologic features; the Northern Nevada rift (Zoback and Thompson, 1978; Zoback and others., 1994; fig. B–6) may have similar origins. The existence of generally east-west-striking transverse zones (fig. B–6) in the central part of the study area has been proposed on the basis of changes in regional patterns of stratal dip direction (Stewart, 1998) and on alignments of plutons and volcanic vents, geophysical anomalies, and mineral deposits (Ekren and others, 1976; Rowley, 1998). These zones are not well expressed in surficial outcrops and the influence of such zones on modern groundwater flow patterns is largely unknown. Many zones are oriented, however, at a high angle to the valley axes of current basins and ranges and, as a result, may influence the rate or direction of groundwater flow parallel to valley axes.

In addition to the hydrologic effects of individual faults, rock deformation affecting broader areas may influence regional groundwater flow. Such subregional deformation might include widespread brecciation and fracturing, either of which could strongly influence the hydraulic conductivity of bedrock. Greatly extended regions (fig. B–7) are characterized by carbonate-rock aquifers that are disrupted by faulting and structural thinning (Dettinger and Schaefer, 1996; Wernicke, 1992). In contrast, less extended regions (fig. B–7) may be highly permeable as a result of preservation of primary texture and secondary dissolution features within relatively undeformed rock (Dettinger and others, 1995; Dettinger and Schaefer, 1996; Plume, 1996; Cook and Corboy, 2004). Zones of active seismicity (fig. B–7; Rogers and others, 1987; Bjarnason and Pechmann, 1989; Bennett and others, 1999) may be of special interest from a hydrologic standpoint. Active fault zones would be expected to have enhanced permeability in the rupture zone and enhanced fluid flow in fractured rock (Faunt, 1997; Potter and others, 2002). Certain areas within the Walker Lane and adjacent to the Las Vegas Valley shear zone have the potential for enhanced permeability as a result of rock deformation affecting broad areas not specifically associated with a single fault (fig. B–7; Carr, 1984; Potter and others, 2002). Such subregional deformation might include widespread brecciation and fracturing.

The southward sweep of volcanism across the eastern Great Basin during Oligocene through Miocene time (McKee, 1971; Cross and Pilger, 1978; McKee and Noble, 1986; Best and others, 1989) resulted in caldera-forming eruptions from several volcanic centers (fig. B–8). Calderas are structurally

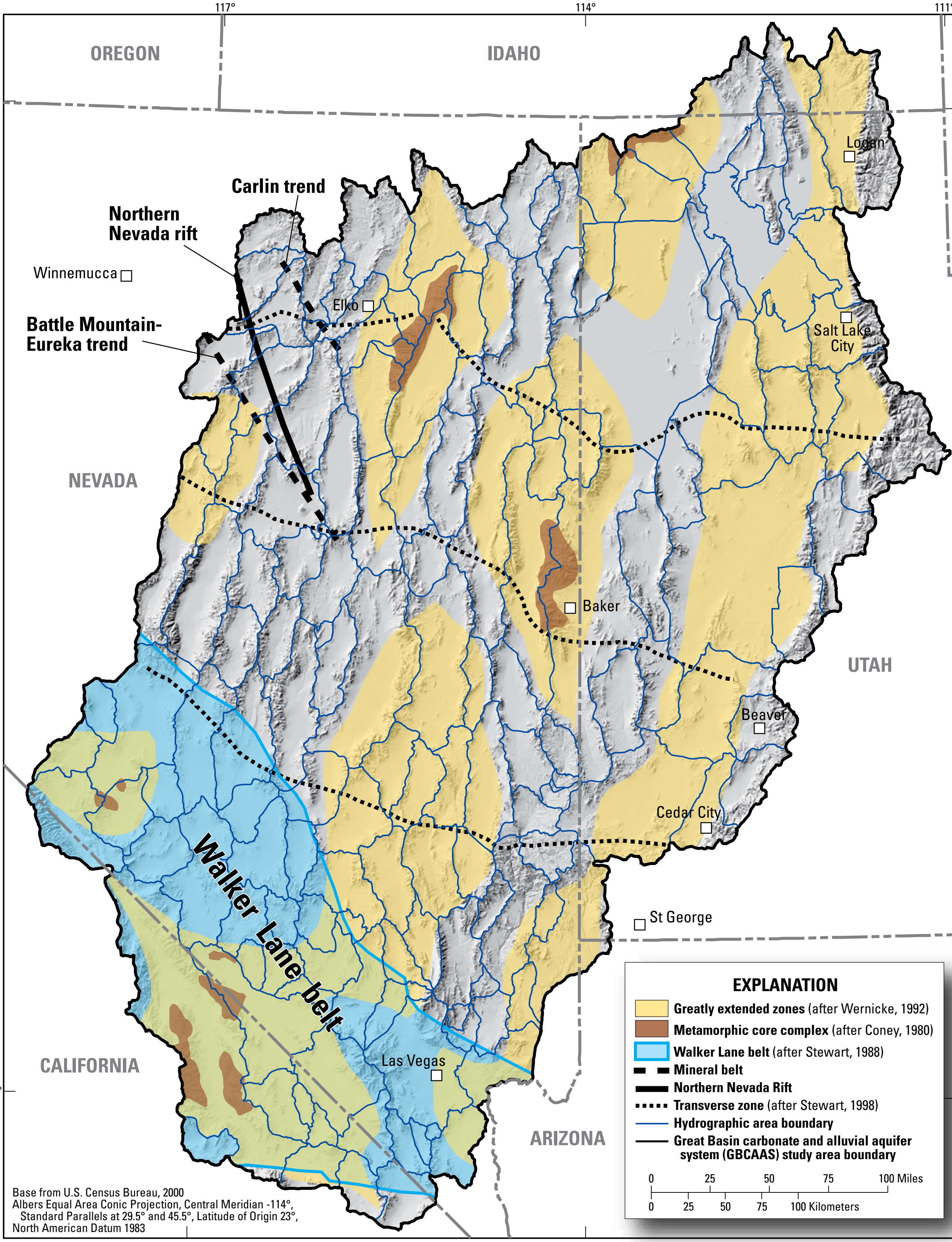

Figure B–6. Cenozoic tectonic provinces and structural belts of the Great Basin carbonate and alluvial aquifer system study area.

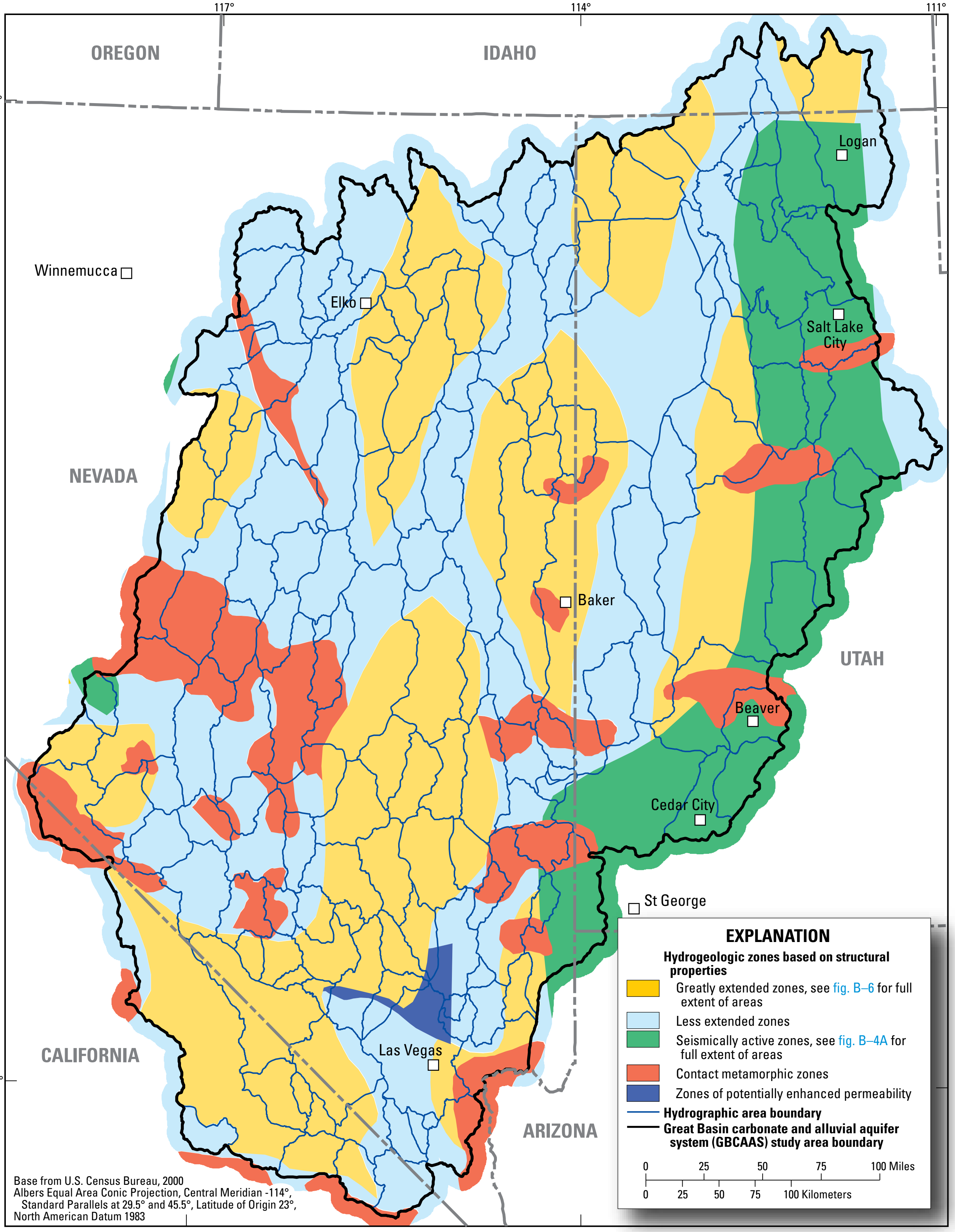

Figure B–7. Structural areas of potential hydrologic significance within the Great Basin carbonate and alluvial aquifer system study area.

complex depressions that can be as sizeable as 75 mi in diameter and are often bounded by structural and topographic margins (Smith and Bailey, 1968; Lipman, 1984). Subcaldera intrusions and other bodies of intrusive rocks within the study area (Grauch, 1996; Plume, 1996; Glen and others, 2004) can feature contact metamorphic zones around plutons (fig. B–7), especially in carbonate rock. Contact metamorphism may reduce carbonate-rock permeability through mineral growth and deposition in available pore space and recrystallization of rock matrix.

The present Basin and Range physiography across much of the GBCAAS study area generally is the result of Late Eocene through Holocene extension that created steeply dipping, range-bounding faults (fig. B–8) and intervening downfaulted basins (Zoback and others, 1981; Stewart, 1998). These faults produced elongated mountain ranges and controlled subsidence in the intervening Neogene basins. Moderately dipping, listric-to-planar extensional faults, with as much as 10,000 ft of displacement, separate basins from mountain ranges on one, or in some cases, both sides (Dohrenwend and others, 1996). Regional gravity investigations and models have played a critical role in defining major basin-bounding and intrabasin faults, delineating the thickness of Cenozoic geologic units, and inferring the subsurface 3D geometry of pre-Cenozoic rocks (fig. B–8; Saltus and Jachens, 1995; Blakely and Ponce, 2001; Watt and Ponce, 2007). Many of the basins have a characteristic half-graben structure with a dominant range-front fault on one side of the basin; this fault accommodates much of the extensional deformation and subsidence, producing a tilted, asymmetric basin (Stewart, 1998). Less commonly, basins have major faults bounding both sides of the basin, resulting in a symmetric graben located along the basin axis. A number of basins contain several subbasins that are separated by buried, structurally controlled intrabasin highs (fig. B–8).

Three-Dimensional Hydrogeologic Framework

A 3D-hydrogeologic framework was constructed from a variety of information sources, including geologic maps, cross-section data, drill-hole data, geophysical models representing the thickness of Cenozoic basin fill, and stratigraphic surfaces created for other 3D-hydrogeologic frameworks (Appendix 1). The 3D framework was constructed by standard subsurface mapping methods of creating structure contour and thickness maps for each of the HGUs; grids representing the top and base of each unit were then stacked in stratigraphic sequence. The 3D stacking was guided by rules that controlled stratigraphic onlap, truncation of units, and minimum thickness.

The 3D-hydrogeologic framework and component gridded surfaces were evaluated for accuracy by visual inspection and by mathematical manipulations. The extent and thickness of the HGUs were reviewed and compared to published geologic interpretations; in many cases, grids were reinterpreted to create more consistent isopach trends. For consistency, the elevations of HGUs were compared to a digital elevation model (DEM) and to each other. The 3D digital solid of the framework was clipped to the topographic surface by intersecting the solid volume with a DEM. The resulting upper surface of the 3D-hydrogeologic framework closely resembles the surficial hydrogeologic map (fig. B–3), and lends confidence to the subsurface interpretation. Vertical cross sections sampled from the digital 3D framework model along the trace of previously published geologic sections were compared to the published sections.

Geometric relations of the HGUs in the 3D-hydrogeologic framework were visualized by creating vertical slices through the 3D solid volume in several parts of the GBCAAS study area to portray cross-sectional views. Cross sections (figs. B–9 and B–10) were chosen to portray important hydrogeologic features. Several factors complicate the visual inspection of the vertical slices from the 3D-hydrogeologic framework, including (1) graphic artifacts related to the grid spacing (see Appendix 1), (2) abrupt truncation of HGUs as a result of gridding rules; and (3) the representation of faults as abrupt changes in unit elevation and thickness, rather than as discrete features. Although faults are shown on the vertical sections on figure B–10 as a visual aid, they are not modeled in the 3D solid as discrete digital surfaces.

Section *A–A′* (figs. B–9 and B–10*A*) in the northeast part of the GBCAAS study area portrays relatively thick subsurface sections of hydrogeologic units LCAU and USCU that are not readily apparent from exposures in isolated mountain blocks at the surface. The east-west section *C-C′* (figs. B–9 and B–10*A*) from east (near Salt Lake City, Utah) to west (near Elko, Nevada) portrays the following features: (1) uplifted NCCU in the Wasatch Range at the east end of the section, and in the Stansbury Mountains to the west of Tooele Valley; (2) an interpreted section of thick LCAU and UCAU beneath the Great Salt Lake Desert, including fault-bounded mountain blocks of predominantly UCAU between Goshute Valley and Ruby Valley; (3) uplifted NCCU in the Ruby Mountains, to the west of Ruby Valley; and (4) thrusted rocks of the Roberts Mountain thrust belt (fig. B–5), assigned to TNCCU that overlie LCAU near Pine Valley. Farther to the south, in section *D–D′* (figs. B–9 and B–10*A*), the NCCU generally is elevated where the section crosses more highly extended zones of the study area (fig. B–6). The Paleozoic carbonate section is preserved within the Butte syncline beneath Jakes Valley, and the Confusion Range syncline between Snake Valley and Tule Valley. Section *E–E′* in the western part of the study area (figs. B–9 and B–10*B*), portrays a thick, continuous section of LCAU that is mantled by VU; surface exposures are predominantly volcanic rocks of the LBFAU (fig. B–3). Section *F–F′* (figs. B–9 and B–10*B*), through the Indian Peak caldera complex, portrays the absence of carbonate rock within the caldera complex where granitic rocks of the NCCU are interpreted to be present in the subsurface. Thick LCAU is interpreted to exist to the west of the caldera complex beneath

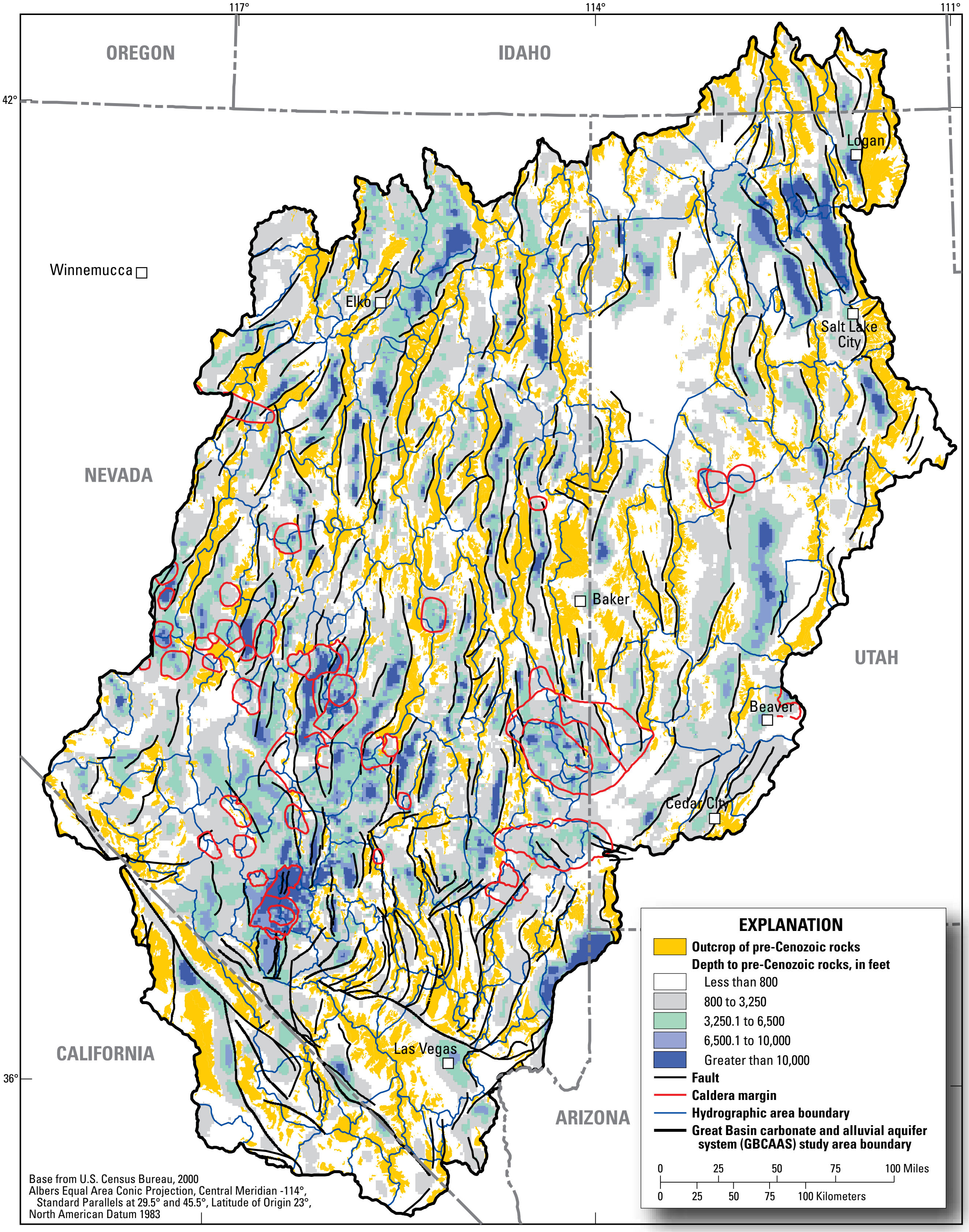

Figure B–8. Exposure of pre-Cenozoic rocks, depth to pre-Cenozoic rocks, and location of major fault zones and calderas in the Great Basin carbonate and alluvial aquifer system study area.

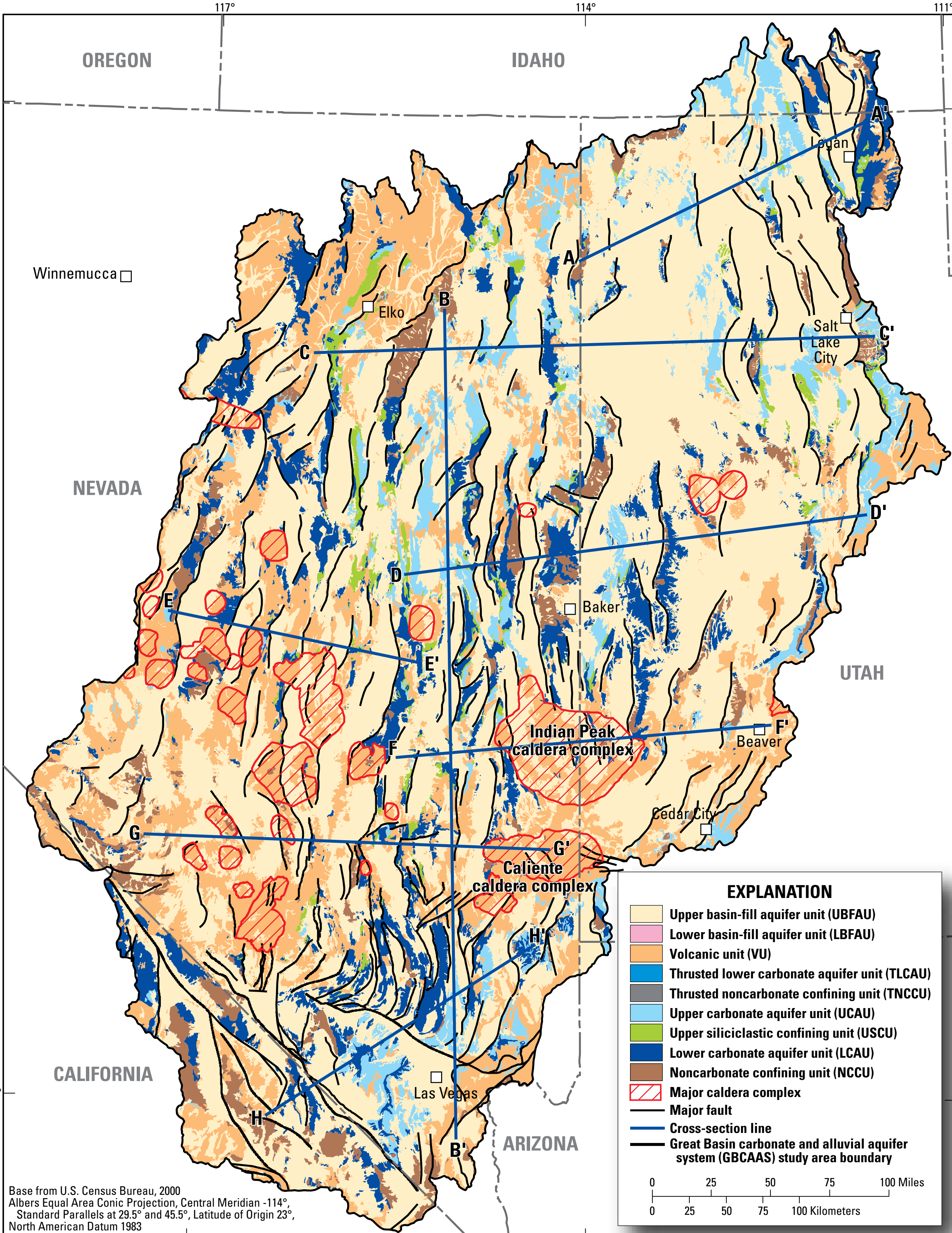

Figure B–9. Location of cross sections representing the three-dimensional hydrogeologic framework in the Great Basin carbonate and alluvial aquifer system study area.

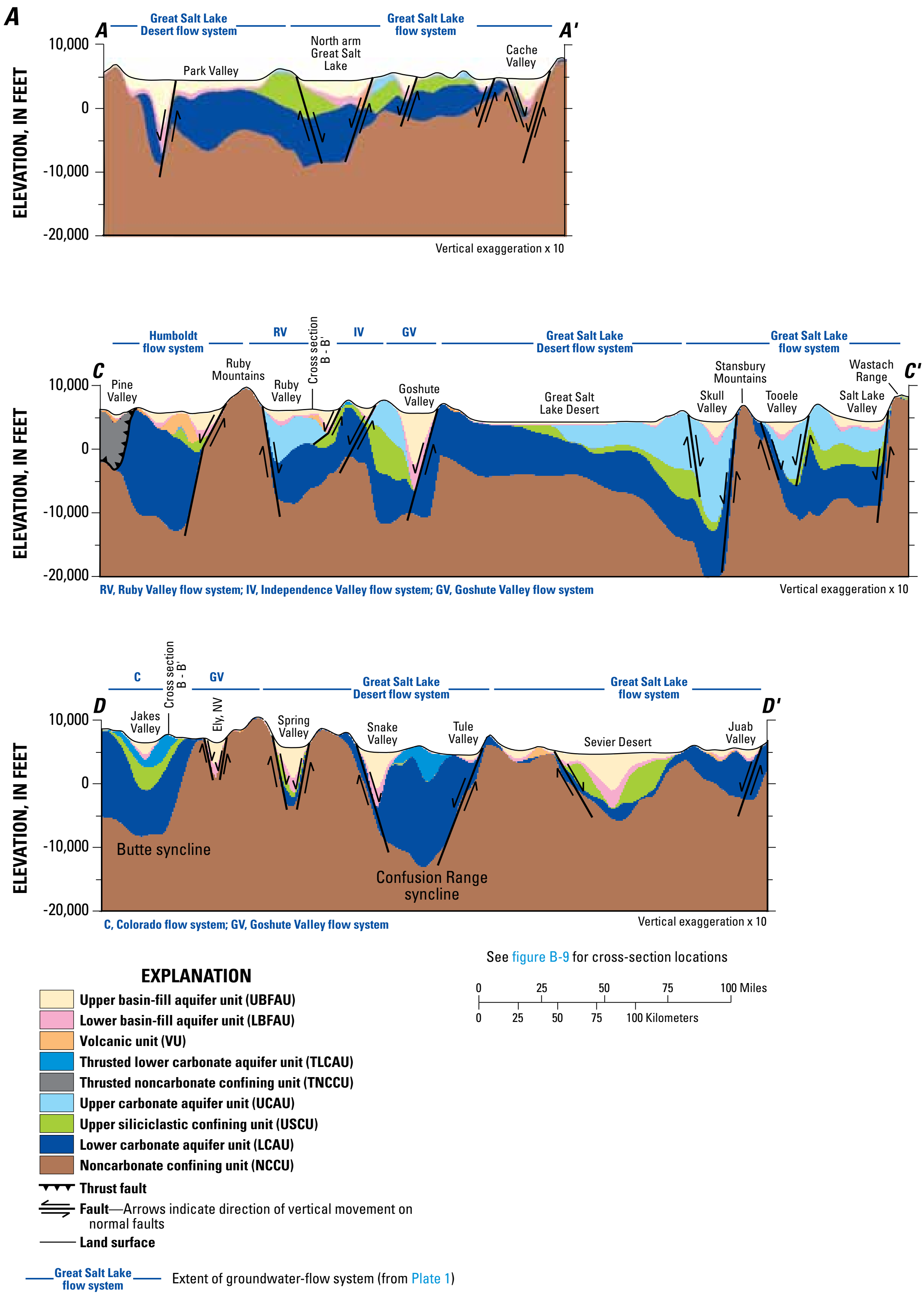

Figure B–10. Cross sections representing the three-dimensional hydrogeologic framework in the Great Basin carbonate and alluvial aquifer system study area. ***A***, Sections *A–A′*, *C–C′*, and *D–D′*; ***B***, Sections *B–B′*, *E–E′*, *F–F′*, *G–G′*, and *H–H′*.

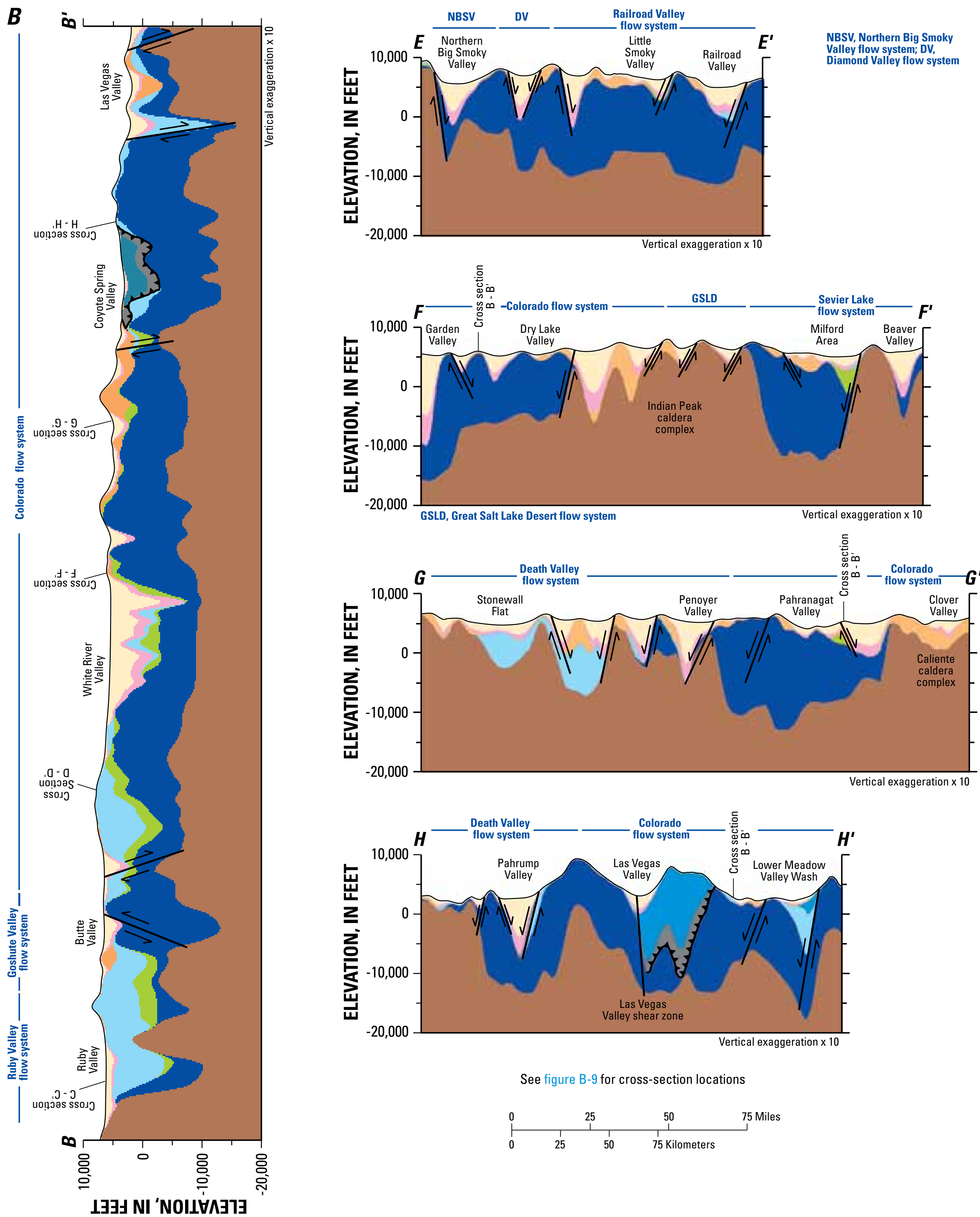

Figure B–10. Cross sections representing the three-dimensional hydrogeologic framework in the Great Basin carbonate and alluvial aquifer system study area. ***B***, Sections *B–B′*, *E–E′*, *F–F′*, *G–G′*, and *H–H′*.—Continued

Dry Lake Valley, and to the east beneath the Milford Area and Beaver Valley. The east-west section *G–G′* (figs. B–9 and B–10*B*) farther to the south portrays relatively little carbonate rock in the western part of the study area, with thick LCAU present along the main corridor of the Colorado groundwater flow system beneath Pahranagat Valley. The east end of section *G–G′* portrays relations within the Caliente caldera complex where VU overlies subcaldera intrusions of NCCU. The southernmost section, *H–H′* (figs. B–9 and B–10*B*) represents TLCAU of the Sevier fold-and-thrust belt overlying thick LCAU. The abrupt termination of the thrust sheet beneath Las Vegas Valley results from truncation against the Las Vegas Valley shear zone, a major strike-slip fault of the Walker Lane belt. In contrast to the generally disrupted nature of the LCAU as shown on east-west sections, section *B–B′* (figs. B–9 and B–10*B*), the lone north-south section, highlights the overall continuity of Paleozoic carbonate rocks when the cross section is parallel to the predominant north-south fault strike associated with Basin and Range extension and between mountain ranges. UCAU dominates section *B–B′* at the north end, whereas LCAU is predominant farther to the south. The TLCAU of the Sevier fold-and-thrust belt is apparent beneath Coyote Spring Valley on this section.

Perspective views of multiple vertical sections that cut through the solid-volume 3D-hydrogeologic framework model (fig. B–11*A*) emphasize the overall continuity of key HGUs between adjacent cross sections. Thrusted rocks (TNCCU) related to the Sevier fold-and-thrust belt are visible on several sections near the south end of the study area (fig. B–11*A*). Caldera complexes appear as tracts of thick volcanic rock (VU) underlain by NCCU. The Roberts Mountain thrust belt (TNCCU) is apparent along the northwest edge of the study area (fig. B–11*B*).

Summary

The GBCAAS study area contains numerous stratigraphic units that have been subjected to a variety of structural disruptions. The complex stratigraphy has been simplified to nine HGUs that differ in their ability to store and transmit water. HGU designations were based on lithologic, stratigraphic, and structural characteristics. Igneous, metamorphic, and siliciclastic rocks of the NCCU and Paleozoic siliciclastic rocks of the USCU typically form the least permeable HGUs within the consolidated, pre-Cenozoic rocks. Paleozoic carbonate rocks of the LCAU and the UCAU typically form the most permeable HGUs within the pre-Cenozoic consolidated rocks. Fractured Cenozoic volcanic rocks of the VU and permeable Cenozoic basin fill of the UBFAU and LBFAU are important local aquifers that interact with the underlying Paleozoic carbonate-rock aquifers. Most of these HGUs have been subdivided into a series of hydrogeologic zones that relate to differences in lithologic character or structural setting. These geologically defined zones provide a geologic basis for future refinement of horizontal hydraulic conductivity within each HGU.

Many of the HGUs are disrupted by large-magnitude offset thrust, strike-slip, and normal faults and calderas. Structural disruption has juxtaposed diverse rock types, ages, and deformational structures, creating variable and complex subsurface conditions. A 3D-hydrogeologic framework was constructed to represent the regional hydrogeology in digital form. The framework was constructed using numerous data sets including digital elevation, geologic and structural geologic maps, stratigraphic data from boreholes, cross sections, and gridded data from previously constructed geologic framework and geophysical models. The framework incorporates the spatial extent and thickness of each HGU and the geometry of major structures.

The 3D framework is useful for depicting the extent of the consolidated carbonate-rock aquifers LCAU and UCAU throughout the eastern and central parts of the GBCAAS study area. The carbonate-rock HGUs are segmented in a general east-west direction by numerous north-striking, Basin and Range faults that juxtapose carbonate rocks against other HGUs. In a north-south direction, parallel to the strike of these faults, these carbonate-rock HGUs are much more continuous. The 3D framework accurately represents areas where carbonate-rock HGUs have been thinned or disrupted as a result of large-magnitude extension and interrupted by regional thrust faults. Calderas represent a significant local impediment to any regional flow through carbonate rock HGUs because the aquifers have been removed locally as a consequence of caldera collapse, volcanism, and igneous intrusion. Thick sequences of young basin fill are present in all basins in the study area and constitute the shallow aquifer.

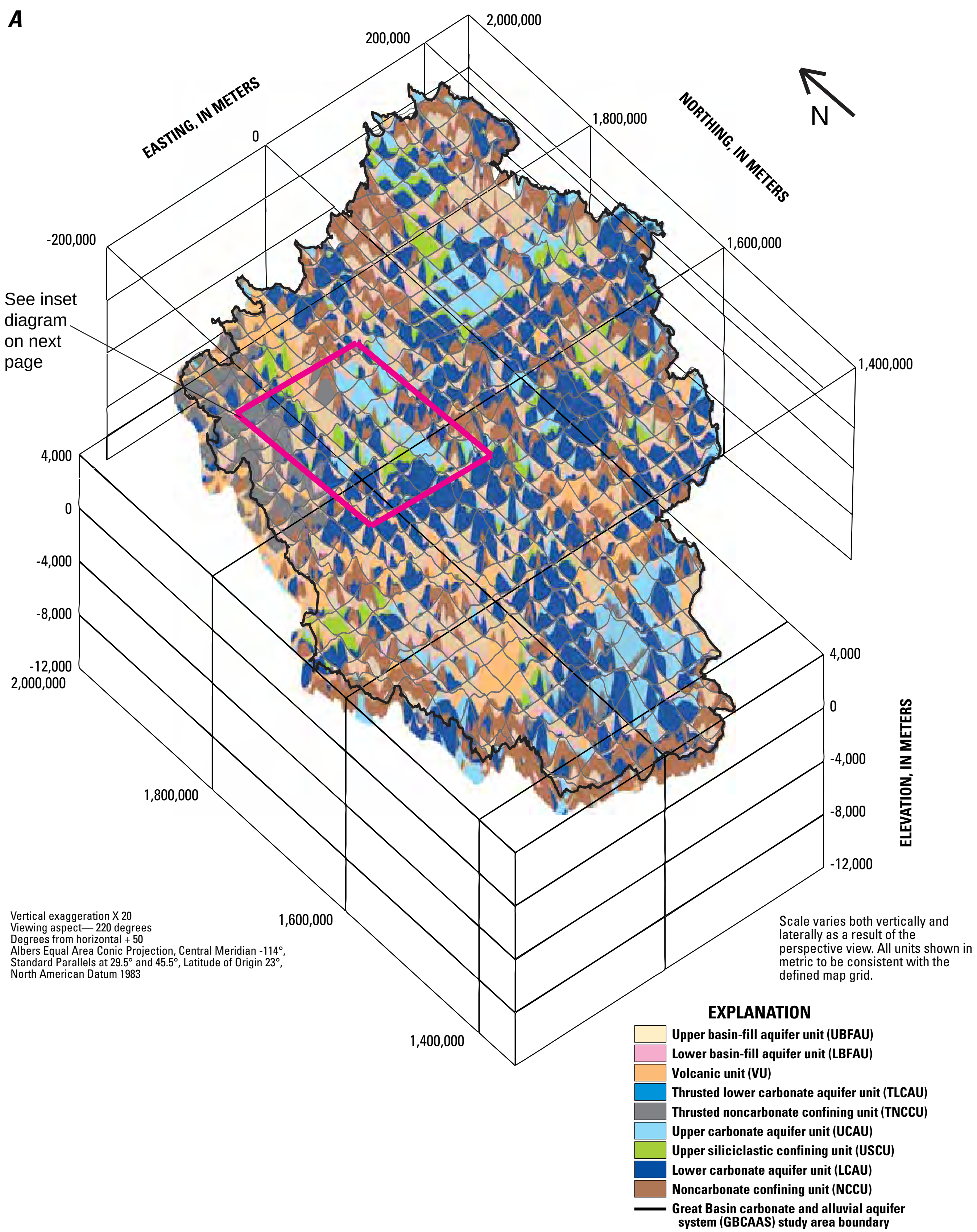

Figure B–11. Fence diagrams representing the three-dimensional hydrogeologic framework in the Great Basin carbonate and alluvial aquifer system study area. ***A***, the entire modeled hydrogeologic framework and ***B***, an inset portion of central Nevada.

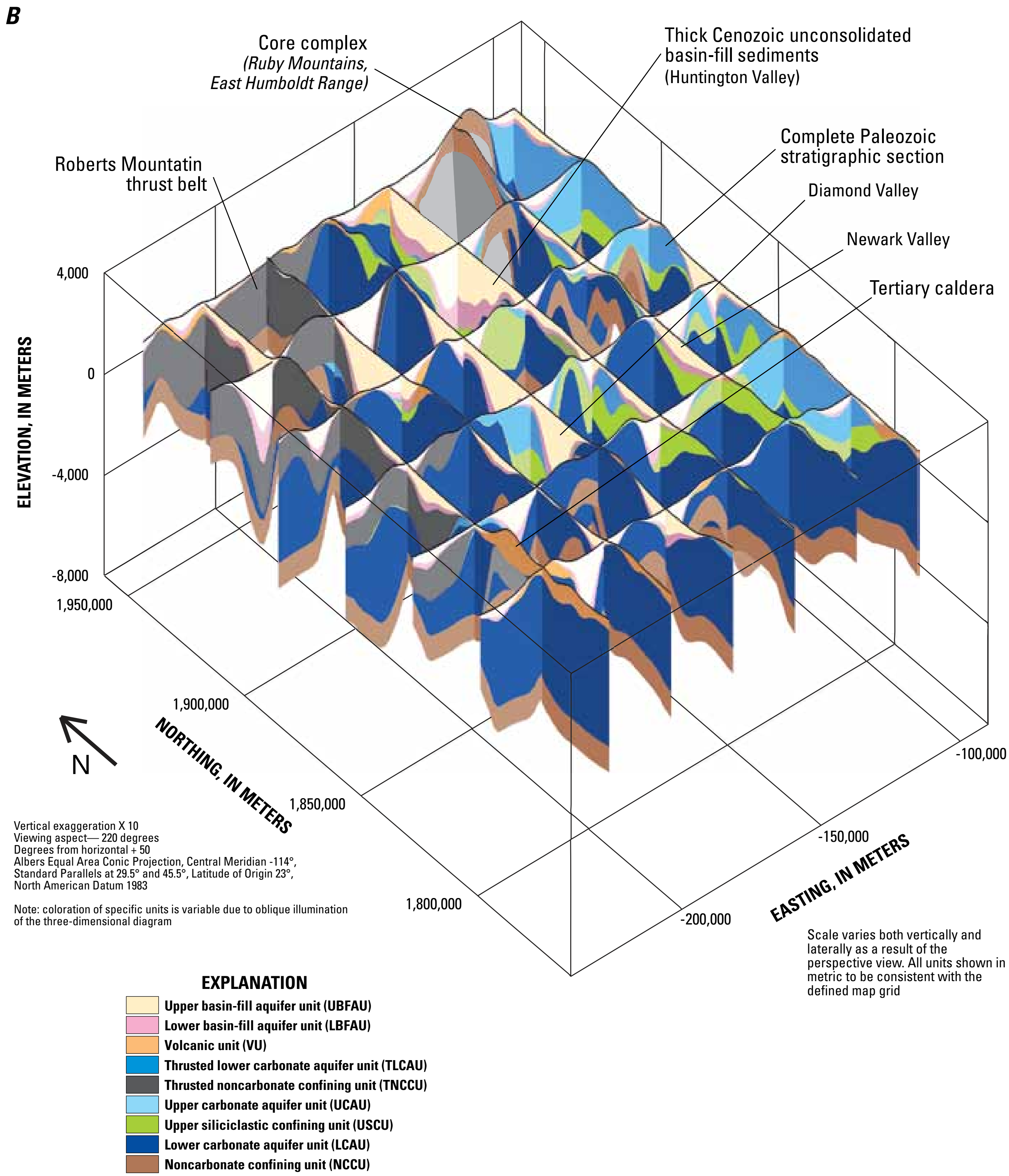

Figure B–11. Fence diagrams representing the three-dimensional hydrogeologic framework in the Great Basin carbonate and alluvial aquifer system study area. ***B***, an inset portion of central Nevada.—Continued

References Cited

Allmendinger, R.W., 1992, Fold and thrust tectonics of the western United States exclusive of the accreted terranes, *in* Burchfiel, B.C., Lipman, P.W., and Zoback, M.L., eds., The Cordilleran orogen: conterminous U.S.: Boulder, Colorado, Geological Society of America, Geology of North America, v. G–3, p. 583–607.

Armstrong, R.L., 1968, Sevier orogenic belt in Nevada and Utah: Geological Society of America Bulletin, v. 79, p. 429–458.

Armstrong, R.L., 1982, Cordilleran metamorphic core complexes—From Arizona to southern Canada: Annual Review of Earth and Planetary Sciences, v. 10, p. 129–154.

Barton, M.D., 1990, Cretaceous magmatism, mineralization and metamorphism in the east-central Great Basin, *in* Anderson, J. L., ed., The nature and origin of Cordilleran magmatism: Geological Society of America Memoir 174, p. 283–302.

Bedinger, M.S., Langer, W.H., and Reed, J.E., 1989, Ground-water hydrology, *in* Bedinger, M.S., Sargent, K.A., and Langer, W.H., eds., Studies of geology and hydrology in the Basin and Range Province, southwestern United States, for isolation of high-level radioactive waste—Characterization of the Death Valley region, Nevada and California: U.S. Geological Survey Professional Paper 1370–F, 49 p., 8 pls. in pocket.

Belcher, W.R., ed., 2004, Death Valley regional ground-water flow system, Nevada and California—Hydrogeologic framework and transient ground-water flow model: U.S. Geological Survey Scientific Investigations Report 2004–5205, 408 p.

Belcher, W.R., Elliot, P.E., and Geldon, A.L., 2001, Hydraulic-property estimates for use with a transient ground-water flow model of the Death Valley regional ground-water flow system, Nevada and California: U.S. Geological Survey Water-Resources Investigations Report 01–4210, 28 p.

Belcher, W.R., Sweetkind, D.S., and Elliott, P.E., 2002, Probability distributions of hydraulic conductivity for the hydrogeologic units of the Death Valley regional ground-water flow system, Nevada and California: U.S. Geological Survey Water-Resources Investigations Report 02–4212, 24 p.

Bennett, R.A., Davis, J.L., and Wernicke, B.P., 1999, Present-day pattern of Cordilleran deformation in the western United States: Geology, v. 27, p. 371–374.

Best, M.G., and Christiansen E.H., 1991, Limited extension during peak Tertiary volcanism, Great Basin of Nevada and Utah: Journal of Geophysical Research, v. 96, B8, p. 13,509–13,528.

Best, M.G., Christiansen, E.H., Deino, A.L., Gromme, C.S., McKee, E.H., and Noble, D.C., 1989, Excursion 3A—Eocene through Miocene volcanism in the Great Basin of the Western United States, *in* Chapin, C.E., and Zidek, Jiri, eds., Field excursions to volcanic terranes in the Western United States, v. II, Cascades and Intermountain West: New Mexico Bureau of Mines and Mineral Resources Memoir 47, p. 91–133.

Bjarnason, I.T., and Pechmann, J.C., 1989, Contemporary tectonics of the Wasatch Front region, Utah, from earthquake focal mechanisms: Bulletin of the Seismological Society of America, v. 79, p. 731–755.

Blakely, R.J., and Ponce, D.A., 2001, Map showing depth to pre-Cenozoic basement in the Death Valley ground-water model area, Nevada and California: U.S. Geological Survey Miscellaneous Field Studies Map MF–2381–E, 1 sheet, scale 1:250,000, with pamphlet.

Blankennagel, R.K., and Weir, J.E., Jr., 1973, Geohydrology of the eastern part of Pahute Mesa, Nevada Test Site, Nye County, Nevada: U.S. Geological Survey Professional Paper 712–B, 35 p.

Burchfiel, B.C., Cowan, D.S., and Davis, G.A., 1992, Tectonic overview of the Cordilleran orogen in the western United States, *in* Burchfiel, B.C., Lipman, P.W., and Zoback, M.L., eds., The Cordilleran orogen: conterminous U.S.: Boulder, Colorado, Geological Society of America, Geology of North America, v. G–3, p. 407–480.

Carr, W.J., 1984, Regional structural setting of Yucca Mountain, southeastern Nevada, and late Cenozoic rates of tectonic activity in part of the southwestern Great Basin, Nevada and California: U.S. Geological Survey Open-File Report 1984–854, 98 p.

Cline, J.S., Hofstra, A.H., Muntean, J.L., Tosdal, R.M., and Hickey, K. A., 2005, Carlin-type characteristics and viable models: Economic Geology, 100th anniversary volume, p. 1,905–2,005.

Coney, P.J., 1980, Cordilleran metamorphic core complexes, *in* Crittenden, M.D., Coney, P.J., and Davis, G.H., eds., Cordilleran metamorphic core complexes: Geological Society of America Memoir 153, p. 7–34.

Cook, H.E., and Corboy, J.J., 2004, Great Basin Paleozoic carbonate platform: facies, facies transitions, depositional models, platform architecture, sequence stratigraphy and predictive mineral host models—Field trip guidebook: U.S. Geological Survey Open–File Report 2004–1078, 129 p.

Crafford, A.E.J., 2008, Paleozoic tectonic domains of Nevada—An interpretive discussion to accompany the geologic map of Nevada: Geosphere, v. 4, p. 260–291; doi: 10.1130/GES00108.1, accessed January 19, 2009 at http://geosphere.gsapubs.org/content/4/1/260.

Crafford, A.E.J., and Grauch, V.J.S., 2002, Geologic and geophysical evidence for the influence of deep crustal structures on Paleozoic tectonics and the alignment of world-class gold deposits, north-central Nevada, USA: Ore Geology Reviews, v. 21 p. 157–184.

Cross, T.A., and Pilger, R.H., 1978, Constraints on absolute motion and plate interaction inferred from Cenozoic igneous activity in the western United States: American Journal of Science, v. 278, p. 865–902.

D'Agnese, F.A., Faunt, C.C, Turner, A.K., and Hill, M.C., 1997, Hydrogeologic evaluation and numerical simulation of the Death Valley regional ground-water flow system, Nevada, and California: U.S. Geological Survey Water-Resources Investigations Report 96–4300, 124 p.

D'Agnese, F.A., O'Brien, G.M., Faunt, C.C., Belcher, W.R., and San Juan, C., 2002, A three-dimensional numerical model of predevelopment conditions in the Death Valley regional ground-water flow system, Nevada and California: U.S. Geological Survey Water-Resources Investigations Report 02–4102, 114 p.

DeCelles, P.G., 2004, Late Jurassic to Eocene evolution of the Cordilleran thrust belt and foreland basin system, western USA: American Journal of Science, v. 304, p. 105–168.

Dettinger, M.D., 1989, Distribution of carbonate-rock aquifers in southern Nevada and the potential for their development—Summary of findings, 1985–88: Carson City, State of Nevada, Program for the Study and Testing of Carbonate-Rock Aquifers in Eastern and Southern Nevada, Summary Report no. 1, 37 p.

Dettinger, M.D., Harrill, J.R., Schmidt, D.L., and Hess, J.W., 1995, Distribution of carbonate-rock aquifers and the potential for their development, southern Nevada and parts of Arizona, California, and Utah: U.S. Geological Survey Water-Resources Investigations Report 91–4146, 100 p.

Dettinger, M.D., and Schaefer, D.H., 1996, Hydrogeology of extended terrains in the eastern Great Basin from geologic and geophysical models: U.S. Geological Survey Hydrologic Investigations Atlas HA–694–D, 1 sheet.

Dickinson, W.R., 2002, The Basin and Range province as a composite extensional domain: International Geology Review, v. 44, p. 1–38.

Dickinson, W.R., 2004, Evolution of the North American Cordillera: Annual Review of Earth and Planetary Sciences, v. 32, p. 13–44.

Dickinson, W.R., 2006, Geotectonic evolution of the Great Basin: Geosphere, v. 2, no. 7, p. 353–368, doi: 10.1130/GES00054.1, accessed February 11, 2008 at http://geosphere.geoscienceworld.org/cgi/content/full/2/7/353.

Dohrenwend, J.C., Jachens, R.C., Moring, C.M., and Schruben, P.C., 1996, Indicators of subsurface basin geometry, chap. 8 *of* Singer, D.A., ed., An analysis of Nevada's metal-bearing mineral resources: Nevada Bureau of Mines and Geology Open-File Report 96–2, 8 p.

Ekren, E.B., Bucknam, R.C., Carr, W.J., Dixon, G.L., and Quinlivan, W.D., 1976, East-trending structural lineaments in central Nevada: U.S. Geological Survey Professional Paper 986, 16 p., 1 pl. in pocket.

Emsbo, Poul, Groves D.I., Hofstra A.H., and Bierlein, F.P., 2006, The giant Carlin gold province—A protracted interplay of orogenic, basinal, and hydrothermal processes above a lithospheric boundary: Mineralium Deposita, v. 41, p. 517–525.

Faunt, C.C., 1997, Effect of faulting on ground-water movement in the Death Valley region, Nevada and California: U.S. Geological Survey Water-Resources Investigations Report 95–4132, 42 p., 1 pl. in pocket.

Faunt, C.C., Sweetkind, D.S., and Belcher, W.R., 2004, Three-dimensional hydrogeologic framework model, chap. E *of* Belcher, W.R., ed., 2004, Death Valley regional ground-water flow system, Nevada and California—Hydrogeologic framework and transient ground-water flow model: U.S. Geological Survey Scientific Investigations Report 2004–5205, p. 165–256.

Fouch, T.D., 1979, Character and paleogeographic distribution of upper Cretaceous(?) and Paleogene nonmarine sedimentary rocks in east-central Nevada, *in* Armentrout, J.M., Cole, M.R., and TerBest, H., Jr., eds., Cenozoic paleogeography of the western United States: Society of Economic Paleontologists and Mineralogists, Pacific Section, Pacific Coast Paleogeography Symposium 3, p. 97–111.

Fouch, T.D., Hanley, J.H., and Forester, R.M., 1979, Preliminary correlation of Cretaceous and Paleogene lacustrine and related nonmarine sedimentary and volcanic rocks in parts of the Great Basin of Nevada and Utah, *in* Newman, G.W., and Goode, H.D., eds., Basin and Range symposium and Great Basin field conference: Rocky Mountain Association of Petroleum Geologists and Utah Geological Association, p. 305–312.

Glen, J.M.G., McKee, E.H., Ludington, S.D., Ponce, D.A., Hildenbrand, T.G., and Hopkins, M.J., 2004, Geophysical terranes of the Great Basin and parts of surrounding provinces: U.S. Geological Survey Open-File Report 2004–1008, 303 p.

Gradstein, F.M., Ogg, J.G., and Smith, A.G., eds., 2004, A geologic timescale 2004: Cambridge, United Kingdom, Cambridge University Press, 589 p., 1 pl.

Grauch, V.J.S., 1996, Magnetically interpreted, granitoid plutonic bodies in Nevada, *in* Singer, D., ed., An analysis of Nevada's metal-bearing mineral resources: Nevada Bureau of Mines and Geology Open-File Report 96–2, p. 7–1 through 7–16, 1 pl., scale 1:1,000,000.

Hamilton, W.B., 1988, Detachment faulting in the Death Valley region, California and Nevada, *in* Carr, M.D., and Yount, J.C., eds., Geologic and hydrologic investigations of a potential nuclear waste disposal site at Yucca Mountain, southern Nevada: U.S. Geological Survey Bulletin 1790, p. 51–85.

Hardyman, R.F., and Oldow, J.S., 1991, Tertiary tectonic framework and Cenozoic history of the central Walker Lane, Nevada, *in* Raines, G.L., Lisle, R.E., Schafer, R.W., and Wilkinson, W.H., eds., Geology and ore deposits of the Great Basin: Geological Society of Nevada Symposium Proceedings, v. 1, p. 279–301.

Harrill, J.R., Gates, J.S., and Thomas, J.M., 1988, Major ground-water flow systems in the Great Basin region of Nevada, Utah, and adjacent States: U.S. Geological Survey Hydrologic Investigations Atlas HA–694–C, 2 sheets, scale 1:1,000,000.

Harrill, J.R., and Prudic, D.E., 1998, Aquifer systems in the Great Basin region of Nevada, Utah, and adjacent States—Summary report: U.S. Geological Survey Professional Paper 1409–A, 66 p.

Hintze, L.F., 1988, Geologic history of Utah: Brigham Young University Geology Studies Special Publication 7, 202 p.

Hintze, L.F., Willis, G.C., Laes, D.Y.M., Sprinkel, D.A., and Brown, K.D., 2000, Digital geologic map of Utah: Utah Geological Survey Map 179DM, CD-ROM, scale 1:500,000.

Hofstra, A.H., and Cline, J.S., 2000, Characteristics and models for Carlin-type gold deposits: Reviews in Economic Geology, v. 13, p. 163–220.

Hose, R.K., Blake, M.C., Jr., and Smith, R.M., 1976, Geology and mineral resources of White Pine County, Nevada: Nevada Bureau of Mines and Geology Bulletin 85, 105 p.

Kistler, R.W., 1974, Phanerozoic batholiths in western North America—Summary of some recent work on variations in time, space, chemistry, and isotopic compositions: Annual Review of Earth and Planetary Sciences, v. 2, p. 403–418.

Laczniak, R.J., Cole, J.C., Sawyer, D.A., and Trudeau, D.A., 1996, Summary of hydrogeologic controls on ground-water flow at the Nevada Test Site, Nye County, Nevada: U.S. Geological Survey Water-Resources Investigations Report 96–4109, 59 p.

Levy, Marjorie, and Christie-Blick, Nicholas, 1989, Pre-Mesozoic palinspastic reconstruction of the eastern Great Basin (Western United States): Science, v. 245, p. 1,454–1,462.

Lipman, P.W., 1984, The roots of ash flow calderas in western North America—Windows into the tops of granitic batholiths: Journal of Geophysical Research, v. 89, p. 8,801–8,841.

Lohman, S.W., 1979, Ground-water hydraulics: U.S. Geological Survey Professional Paper 708, 70 p.

Ludington, Steve, Cox, D.P., Leonard, K.R., and Moring, B.C., 1996, Cenozoic volcanic geology of Nevada, chap. 5 *of* Singer, D.A., ed., An analysis of Nevada's metal-bearing mineral resources: Nevada Bureau of Mines and Geology Open-File Report 96–2, 10 p.

Maurer, D.K., Lopes, T.J., Medina, R.L., and Smith, J.L., 2004, Hydrogeology and hydrologic landscape regions of Nevada: U.S. Geological Survey Scientific Investigations Report 2004–5131, 35 p., 4 pls., with supplemental GIS data.

McKee, E.H., 1971, Tertiary igneous chronology of the Great Basin of western United States—Implications for tectonic models: Geological Society of America Bulletin, v. 82, p. 3,497–3,502.

McKee, E.H., 1996, Cenozoic magmatism and mineralization in Nevada, *in* Coyner, A.R. and Fahey, P.L., eds., Geology and ore deposits of the American Cordillera: Geological Society of Nevada Symposium Proceedings, Reno-Sparks, Nevada, April 1995, p. 581–588.

McKee, E.H., and Noble, D.C., 1986, Tectonic and magmatic development of the Great Basin of western United States during late Cenozoic time: Modern Geology, v. 10, p. 39–49.

Miller, D.M., Nilsen, T.H., and Bilodeau, W.L., 1992, Late Cretaceous to early Eocene geologic evolution of the U.S. Cordillera, *in* Burchfiel, B.C., Lipman, P.W., and Zoback, M.L., eds., The Cordilleran orogen: conterminous U.S.: Boulder, Colorado, Geological Society of America, Geology of North America, v. G–3, p. 205–260.

Plume, R.W., 1996, Hydrogeologic framework of the Great Basin region of Nevada, Utah, and adjacent States: U.S. Geological Survey Professional Paper 1409–B, 64 p.

Poole, F.G., and Sandberg, C.A., 1977, Mississippian paleogeography and tectonics of the western United States, *in* Stewart, J.H., Stevens, C.H., and Fritsche, A.E., eds., Paleozoic paleogeography of the western United States, Pacific Coast Paleogeography Symposium 1: Society of Economic Paleontologists and Mineralogists, p. 67–85.

Poole, F.G., Stewart, J.H., Palmer, A.R., Sandberg, C.A., Madrid, R.J., Ross, R.J., Jr., Hintze, L.F., Miller, M.M., and Wrucke, C.T., 1992, Latest Precambrian to latest Devonian time; development of a continental margin, in Burchfiel, B.C., Lipman, P.W., and Zoback, M.L., eds., The Cordilleran orogen: conterminous U.S.: Boulder, Colorado, Geological Society of America, The Geology of North America, v. G–3, p. 9–56.

Potter, C.J., Sweetkind, D.S., Dickerson, R.P. and Killgore, M.L., 2002, Hydrostructural map of the Death Valley ground-water basin, Nevada and California: U.S. Geological Survey Miscellaneous Field Studies Map MF–2372, 2 sheets, scale 1:350,000, with pamphlet.

Quade, Jay, Mifflin, M.D., Pratt, W.L., McCoy, W., and Burckle, Lloyd, 1995, Fossil spring deposits in the southern Great Basin and their implications for changes in water-table levels near Yucca Mountain, Nevada, during Quaternary time: Geological Society of America Bulletin, v. 107, p. 213–230.

Raines, G.L., Connors, K.A., Moyer, L.A., and Miller, R.J., 2003, Spatial digital database for the geologic map of Nevada: U.S. Geological Survey Open-File Report 03–66, 33 p. with digital database (version 3.0).

Reheis, Marith, 1999, Extent of Pleistocene lakes in the western Great Basin: U.S. Geological Survey Miscellaneous Field Studies Map MF–2323, 1 sheet, scale 1:800,000.

Rogers, A.M., Harmsen, S.C., and Meremonte, M.E., 1987, Evaluation of the seismicity of the southern Great Basin and its relationship to the tectonic framework of the region: U.S. Geological Survey Open-File Report 87–408, 196 p., 1 pl. in pocket.

Rowley, P.D., 1998, Cenozoic transverse zones and igneous belts in the Great Basin, western United States—Their tectonic and economic implications, *in* Faulds, J.E., and Stewart, J.H., eds., Accommodation zones and transfer zones; The regional segmentation of the Basin and Range province: Geological Society of America Special Paper 323, p. 195–228.

Saltus, R.W., and Jachens, R.C., 1995, Gravity and basin-depth maps of the Basin and Range province, Western United States: U.S. Geological Survey Geophysical Investigation Map GP–1012, 1 sheet, scale 1:2,500,000.

Smith, R.L., and Bailey, R.A., 1968, Resurgent calderas: Geological Society of America Memoir 116, p. 613–662.

Speed, R.C., 1983, Evolution of the sialic margin in the central-western United States, *in* Watkins, J.S., and Drake, C.L., eds., Studies in continental margin geology: American Association of Petroleum Geologists Memoir 34 (Hedberg series), p. 457–468.

Speed, R.C., Elison, M.W., and Heck, F.R., 1988, Phanerozoic tectonic evolution of the Great Basin, *in* Ernst, W.G., ed., Metamorphism and crustal evolution of the western United States, Rubey v. 7: Englewood Cliffs, New Jersey, Prentice-Hall, p. 572–605.

Speed, R.C. and Sleep, N.H., 1982, Antler orogeny and foreland basin—A model: Geological Society of America Bulletin, v. 93, p. 815–828.

Stewart, J.H., 1970, Upper Precambrian and Lower Cambrian strata in the southern Great Basin, California and Nevada: U.S. Geological Survey Professional Paper 620, 206 p.

Stewart, J.H., 1972, Initial deposits in the Cordilleran geosyncline; evidence of a late Precambrian (~850 m.y.) continental separation: Geological Society of America Bulletin, v. 83, p. 1,345–1,360.

Stewart, J.H., 1980, Geology of Nevada, a discussion to accompany the geologic map of Nevada: Nevada Bureau of Mines and Geology Special Publication 4, 136 p.

Stewart, J.H., 1988, Tectonics of the Walker Lane belt, western Great Basin Mesozoic and Cenozoic deformation in a zone of shear, *in* Ernst, W.G., ed., Metamorphism and crustal evolution of the western United States (Rubey v. 7): Englewood Cliffs, New Jersey, Prentice-Hall, p. 683–713.

Stewart, J.H., 1998, Regional characteristics, tilt domains, and extensional history of the later Cenozoic Basin and Range province, western North America, *in* Faulds, J.E., and Stewart, J.H., eds., Accommodation zones and transfer zones, the regional segmentation of the Basin and Range Province: Geological Society of America Special Paper 323, p. 47–74.

Stewart, J.H., and Crowell, J.C., 1992, Strike-slip tectonics in the Cordilleran region, western United States, *in* Burchfiel, B.C., Lipman, P.W., and Zoback, M.L., eds., The Cordilleran Orogen—Conterminous U.S.: Boulder, Colorado, Geological Society of America, Geology of North America, v. H–3, p. 609–628.

Stewart, J.H., and Poole, F.G., 1974, Lower Paleozoic and uppermost Precambrian Cordilleran miogeocline, Great Basin, western United States, *in* Dickinson, W.R., ed., Tectonics and Sedimentation: Tulsa, Oklahoma, Society of Economic Petrologists and Mineralogists, p. 27–57.

Sweetkind, D.S. and du Bray, E.A., 2008, Compilation of stratigraphic thicknesses caldera-related Tertiary volcanic rocks, east-central Nevada and west-central Utah: U.S. Geological Survey Digital Data Series DS–271, 40 p., with GIS data.

Taylor, W.J., Bartley, J.M., Martin, M.W., Geissman, J.W., Walker, J.D., Armstrong, P.A., and Fryxell, J.E., 2000, Relations between hinterland and foreland shortening, Sevier Orogeny, central North American Cordillera: Tectonics, v. 19, p. 1,124–1,143.

Todd, D.K., 1980, Groundwater hydrology: New York, John Wiley and Sons, 535 p.

Wallace, A.R., Ludington, Steve, Mihalasky, M.J., Peters, S.G., Theodore, T.G., Ponce, D.A., John, D.A., Berger, B.R., Zientek, M.L., Sidder, G.B., and Zierenberg, R.A, 2004, Assessment of metallic resources in the Humboldt River basin, northern Nevada, *with a section on* platinum-group-elements (PGE) potential of the Humboldt mafic complex: U.S. Geological Survey Bulletin 2218, 312 p., with 1 disc.

Watt, J.T., and Ponce, D.A., 2007, Geophysical framework investigations influencing ground-water resources in east-central Nevada and west-central Utah, *with a section on* geologic and geophysical basin-by-basin descriptions by Wallace, A.R., Watt, J.T., and Ponce, D.A.: U.S. Geological Survey Open-File Report 2007–1163, 40 p., 2 pls., scale 1:750,000.

Wernicke, B.P., 1992, Cenozoic extensional tectonics of the U.S. Cordillera, *in* Burchfiel, B.C., Lipman, P.W., and Zoback, M.L., eds., The Cordilleran Orogen—Conterminous U.S.: Boulder, Colorado, Geological Society of America, Geology of North America, v. G–3, p. 553–581.

Winograd, I.J., and Thordarson, W., 1975, Hydrogeologic and hydrochemical framework, south-central Great Basin, Nevada-California, with special reference to the Nevada Test Site: U.S. Geological Survey Professional Paper 712–C, 126 p.

Wright, L.A., 1989, Overview of the role of strike-slip and normal faulting in the Neogene history of the region northeast of Death Valley, California-Nevada, *in* Ellis, M.A., ed., Late Cenozoic evolution of the southern Great Basin: Nevada Bureau of Mines and Geology Open-File Report 89–1, Selected papers from a workshop at University of Nevada, Reno, November 10–13, 1987, p. 1–11.

Zoback, M.L., Anderson, R.E., and Thompson, G.A., 1981, Cainozoic evolution of the state of stress and style of tectonism of the Basin and Range province of the western United States: Philosophical transactions of the Royal Society of London, Series A, Mathematical and Physical Sciences, v. 300, p. 407–434.

Zoback, M.L., McKee, E.H., Blakely, R.J., and Thompson, G.A., 1994, The northern Nevada rift—Regional tectono-magmatic relations and middle Miocene stress direction: Geological Society of America Bulletin, v. 106, p. 371–382.

Zoback, M.L., and Thompson, G.A., 1978, Basin and Range rifting in northern Nevada: Clues from a mid-Miocene rift and its subsequent offsets: Geology, v. 6, p. 111–116.

Chapter C: Groundwater Flow

By Donald S. Sweetkind, Melissa D. Masbruch, Victor M. Heilweil, Susan G. Buto

The Great Basin carbonate and alluvial aquifer system (GBCAAS) study area includes a vast climatologically and geologically diverse part of the western United States. This chapter further develops the conceptual understanding of groundwater flow in the GBCAAS by (1) subdividing the study area into smaller regions of hydrographic areas (HAs) and groundwater flow systems, (2) presenting a regional potentiometric-surface map that can be used to determine generalized groundwater flow directions, (3) integrating geologic constraints along the boundaries of the HAs in the regional potentiometric-surface map, and (4) further interpreting geologic controls on the flow of groundwater. Because of the large size of the study area and sparsity of water-level data in many areas, the potentiometric-surface map depicts a simplified representation of groundwater conditions best suited for evaluating groundwater flow in a regional context.

Hydrographic Areas and Regional Groundwater Flow Systems

The GBCAAS study area comprises 165 individual HAs (pl. 1). HAs in Nevada were delineated systematically by the U.S. Geological Survey (USGS) and Nevada Division of Water Resources (NDWR) in the late 1960s (Cardinalli and others, 1968; Rush, 1968) for scientific and administrative purposes. The same system was extended into Utah, Idaho, and California during the USGS Great Basin Regional Aquifer Systems Analysis (RASA) study (Harrill and others, 1988). Generally, HA boundaries coincide with topographic basin divides; however, some divisions are arbitrary, without topographic basis (Welch and others, 2007). Most HAs represent a single watershed, including both basin fill and adjacent mountain blocks up to the topographic divide (Harrill and Prudic, 1998).

This study utilizes the naming and numbering convention for HAs used by Harrill and others (1988). While this naming and numbering convention is generally the same as the system developed by Cardinalli and others (1968), the following eight differences are noteworthy:

1. Snake Valley (HA 254 in the current study) was originally divided into three valleys by Cardinalli and others (1968): Hamlin Valley (HA196), Pleasant Valley (HA 194), and Snake Valley (HA 195).
2. Death Valley (HA 243 in the current study) is extended slightly to the southwest from the original RASA boundary to match the Death Valley regional flow system (DVRFS) study area boundary (Belcher, 2004); it is divided into two valleys by Cardinalli and others (1968): Grapevine Canyon (HA 231) and Oriental Wash (HA 232).
3. Beryl-Enterprise Area (HA 280) is referred to by Cardinalli and others (1968) as the Escalante Desert (HA 197).
4. Tenmile Creek Area (HA 48 in the current study) is referred to by Cardinalli and others (1968) as Dixie Creek-Tenmile Creek area (HA 48).
5. Great Salt Lake Desert West Part (HA 261A in the current study) is referred to by Cardinalli and others (1968) as Great Salt Lake Desert (HA 192).
6. Pilot Valley (HA 252 in the current study) is included by Cardinalli and others (1968) as part of the Great Salt Lake Desert (HA 192).
7. Grouse Creek Valley (HA 251 in the current study) is referred to by Cardinalli and others (1968) as Grouse Creek Valley (HA 190) and has a significantly different southwestern boundary.
8. Deep Creek Valley (HA 253 in the current study) is referred to by Cardinalli and others (1968) as Deep Creek Valley (HA 193).

Descriptive information for the 165 HAs is given in Appendix 2. HAs range in size from 12 mi^2 for Rose Valley (HA 199) to 4,648 mi^2 for the Great Salt Lake Desert West Part (HA 261A). The mean altitude, including both the valley and mountain blocks (up to the surface-water divide) of individual HAs ranges from 2,025 ft at Lower Moapa (HA 220) to 7,788 ft at Monitor Valley Southern Part (HA 140B). Mean annual precipitation ranges from 5 in. for Amargosa Desert, Death Valley, and Valjean Valley (HAs 230, 243, 244, respectively) to 26 in. for Cache Valley (HA 272) (PRISM, 2007).

The HAs in the GBCAAS study area were grouped previously by the Great Basin RASA study into 18 regional groundwater flow systems (Harrill and others, 1988; Harrill and Prudic, 1998). These regional groundwater flow systems primarily were based on the direction of groundwater flow across HA boundaries, the permeability of the bedrock in the mountain blocks separating the HAs, and the location of major recharge and terminal discharge areas (Harrill and Prudic, 1998). Harrill and others (1988, sheet 1) state

> *Boundaries between systems are only generally defined; some may represent physical barriers to flow such as masses of intrusive rocks and others represent ground-water divides or divisions where an area of parallel flow ultimately diverges downgradient. Again, adequate hydrologic data are needed to precisely define flow-system boundaries. For much of the Great Basin, these data are not yet available.*

Since this earlier study, one small groundwater flow system (Penoyer) was incorporated into the Death Valley System in the DVRFS study (Belcher, 2004). The current study uses the same convention as the DVRFS study and groups the HAs within the study area into 17 regional groundwater flow systems (pl. 1). The groundwater flow systems are associated with flow-system numbers that appear in parentheses after the flow-system name. The Humboldt groundwater flow system (7) within the GBCAAS is only a portion of the Humboldt groundwater flow system defined in the RASA study. Because previous studies (Harrill and others, 1988; Harrill and Prudic, 1998) show only a small amount of subsurface outflow mainly along the Humboldt River from this portion of the Humboldt groundwater flow system (7), the portion of the flow system within the GBCAAS study area is assumed to be separate from the remaining flow system that is outside the GBCAAS study area. Groundwater flow systems range in size from 282 mi^2 for the Monte Cristo Valley (23) to 18,849 mi^2 for the Great Salt Lake Desert (37) groundwater flow systems (Appendix 2).

To ensure consistency with earlier studies, the groundwater flow system boundaries defined in this study coincide with HA boundaries, though in some cases these boundaries may not define actual groundwater flow boundaries. For example, recent three-dimensional numerical modeling of groundwater flow in coupled mountain/basin terrain indicates that in moderately steep topographic settings with recharge controlled water-table altitudes (such as the eastern Great Basin), groundwater divides (a type of no-flow groundwater flow boundary) may be quite different from surface-water divides (Gleeson and Manning, 2008). Previous investigations within the study area, in fact, suggest there is substantial movement of groundwater flow across these groundwater flow system boundaries (Winograd and Pearson, 1976; Harrill and others, 1988; Belcher, 2004; Welch and others, 2007; Belcher and others, 2009). These previous findings are based on groundwater budget, geologic structure, hydraulic gradient, and geochemical mass balance evaluations.

Groundwater Movement

Groundwater movement within the study area typically occurs from higher altitude bedrock of mountains receiving recharge toward lower altitude discharge areas. Groundwater movement in mountainous terrains, such as the GBCAAS study area, occurs at local, intermediate, and interbasin scales (Toth, 1963; fig. C–1). At the local scale, groundwater moves along shallow and short flow paths, such as (1) from a high altitude area in the mountains to a nearby mountain stream or spring, or, (2) from a losing stream or canal along the alluvial fan near the edge of the basin to a lower altitude spring or evapotranspiration area. At the intermediate scale, some of the groundwater recharge originating in the mountains flows along paths of intermediate length and depth to discharge areas in the adjacent valley. Because of the relatively high permeability of many consolidated rocks within the study area, some mountain recharge also moves at the interbasin scale along deeper and longer flow paths that may cross HA boundaries to more distant discharge areas. Interbasin flow paths define groundwater basins that are larger than surface-water basins (defined by topography). Significant interbasin groundwater flow may occur through intervening mountains, particularly where recharge in the mountain block does not cause a substantial groundwater mound directly beneath the mountain block. Interbasin flow is well documented in certain conceptual models (Toth, 1963; Gleeson and Manning, 2008) and numerous field studies (Tiedeman and others, 1998; Thyne and others, 1999). Within the GBCAAS study area, interbasin flow has been suggested on the basis of (1) groundwater-budget imbalances and (or) the absence of groundwater discharge in some HAs (Stephens, 1974; Gates and Kruer, 1981; Harrill and Prudic, 1998; Welch and others, 2007), (2) isotopic studies (Winograd and Pearson, 1976; Coplen and others, 1994; Kirk and Campana, 1990; Thomas and others, 2001; Lundmark, 2007), (3) combined potentiometric gradient/geologic structure data (Belcher and others, 2009), and (4) numerical modeling (Prudic and others, 1995; Belcher, 2004).

In the GBCAAS study area, much of the recharge occurs in mountainous areas on consolidated rock, and most of the discharge occurs as evapotranspiration from basin fill. Consolidated rock and basin-fill aquifers typically are well connected hydraulically. Within the GBCAAS study area, most groundwater flow occurs in the upper basin-fill aquifer (UBFAU), upper carbonate aquifer (UCAU), and lower carbonate aquifer (LCAU) hydrogeologic units (HGUs; Chapter B of this report). Other HGUs may be local aquifers, but typically have lower permeability and more heterogeneous properties and do not transmit significant regional groundwater flow.

Groundwater movement between two locations requires both a permeable medium (aquifer) and a hydraulic gradient—a difference in hydraulic head between the two locations. The amount of groundwater flow (Q) is defined by Darcy's Law (Freeze and Cherry, 1979) as follows:

$$Q = KIA \qquad \text{(C–1)}$$

where

K is the hydraulic conductivity of the aquifer,
I is the hydraulic gradient, and
A is the cross-sectional area of the aquifer.

Cross-sectional area (A) is defined as the product of aquifer thickness (b) and aquifer width (w). The degree to which an

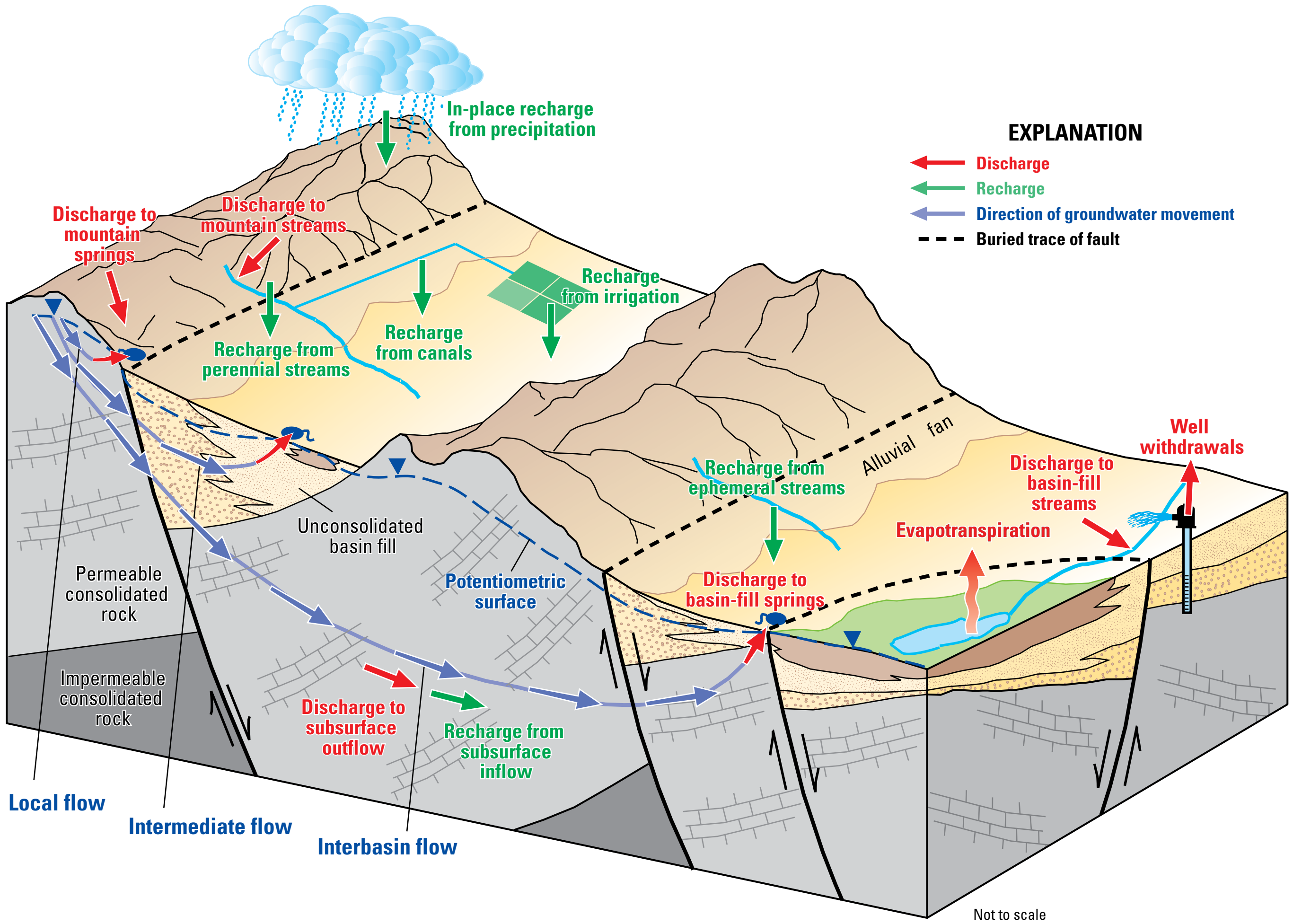

Figure C–1. Schematic diagram showing conceptualized groundwater flow in the Great Basin carbonate and alluvial aquifer system study area.

aquifer or other hydrogeologic unit is able to transmit water is often discussed in terms of its transmissivity. Transmissivity is defined as the product of the aquifer thickness and its hydraulic conductivity. Darcy's Law states that the hydraulic gradient (*I*) alone does not control groundwater flow; flow also depends on the hydraulic conductivity (*K*) and cross-sectional area (*A*).

Potentiometric-Surface Map

A potentiometric-surface map showing contours of equal groundwater-level altitude (pl. 2) was developed to show generalized hydraulic gradients affecting both intrabasin and interbasin groundwater flow throughout the study area. Because of the large size of the GBCAAS study area, the sparsity of hydrologic data in many of the HAs and hydrogeologic units (HGUs), and the 109-year time span (1900–2009) of the available water-level measurements, it was not within the scope of the current study to evaluate and present detailed hydraulic gradients pertaining to groundwater flow within each HA or HGU at one particular point in time. Alternatively, the groundwater conditions depicted on plate 2 are best suited for evaluating groundwater flow in a regional context, rather than addressing specific localized or transient groundwater conditions. In general, the majority of HAs within the study area have not undergone enough groundwater development to affect the potentiometric contours.

Groundwater generally follows topography and flows from areas of high land-surface altitude to areas of lower land-surface altitude, creating a general pattern of flow from mountainous areas to the Great Salt Lake Desert, the Humboldt River, the Colorado River, and Death Valley. Specifically, groundwater flows from higher to lower groundwater-level altitudes perpendicular to the potentiometric-surface contours. While not shown on the regional potentiometric-surface map of the GBCAAS study area, it is assumed that downward vertical gradients typically exist beneath recharge areas in the mountain block or along the valley margins and that upward vertical gradients exist in valley-bottom discharge areas.

The potentiometric-surface map illustrates groundwater mounding in high-precipitation and (or) less permeable mountain-block areas. Within the study area, estimated saturated hydraulic conductivity for alluvial basin-fill material is generally much higher (4.5–13 ft/d, except for mud/salt flats and playas) than consolidated bedrock (0.00016–2.6 ft/d; table A3–1). Mounding beneath the mountains is based on supporting data within the GBCAAS study area that include well water levels, along with perennial stream and spring altitudes. The concept of such mounding is consistent with earlier work. Fetter (1980) states

> *In arid regions, many rivers are fed by overland flow, interflow, and baseflow at high altitudes. As they wind their way to lower elevation, the local precipitation amounts decrease; consequently, there is less infiltration and a lower water table. There may also be a dramatic change in the depth to groundwater when a stream draining a high-altitude basin of lower permeability material flows out onto coarse alluvial materials.*

A recent modeling study of groundwater flow in mountainous terrain (Gleeson and Manning, 2008) states

> *In crystalline and other lower permeability regions, existing data suggest that water tables are often relatively close to land surface, even below high ridges. High-relief and high-water table elevations suggest that significant gravity-driven regional flow could be present in mountainous terrain.*

Data and Construction of Potentiometric-Surface Map

The potentiometric contours are based on water-level data for wells and springs compiled from the U.S. Geological Survey's National Water Information System (NWIS; Mathey, 1998) and water-level altitudes in gaged perennial mountain streams from the U.S. Geological Survey's National Hydrography Dataset (U.S. Geological Survey, 1999) for stream reaches assumed to be in hydraulic connection with recharge in the mountain block. The water-level altitudes for each well that were used as a control point for the potentiometric-surface map were averaged over the period of record for that well. Generally, the control points are coincident with the well locations, except in areas where well density is high (HAs 153, 159, 162, 212, 230, 262, 265, 266, 267, 268, 272, 273, 278, 280, 281, 282, 283, 284, 286, 287). For these HAs with high well densities, the basin fill was discretized into a grid of 2-mi^2 cells. The temporally averaged water levels for all wells within a cell were then averaged together and this water level was assigned to a single point at the center of the cell. Only nonpumping (static) water levels from wells were used to compute an average water-level altitude. Some wells were excluded from the dataset, including (1) shallow wells in mountain terrains typically less than 50 ft deep and possibly perched; (2) wells with an incorrect location in NWIS, as determined by the local name not matching the map location; (3) wells with incorrect altitude in NWIS, as determined by altitudes not matching the National Elevation Dataset (NED) altitude within the vertical accuracy of the NED (average of ± 23 ft); and (4) wells with water levels that were considered outliers when compared to other nearby control points and that may represent perched or pumping conditions. Additional exclusions were made by comparing water levels to those compiled in an unpublished database for the DVRFS study (C. Faunt, U.S. Geological Survey, written commun., 2008). If all of the water levels for a specific well were flagged in the DVRFS database with "insufficient data," "suspect," or "non-static level," these wells were not used as control points in the current study. Of the original 14,182 wells compiled from the NWIS database having water-level measurements, 387 were not used as control points, and only selected water-level measurements were used in 95 additional wells (Auxiliary 5). The majority of these omissions fall within the Death Valley groundwater flow system, on the basis of detailed analyses related to recent studies in this area (Belcher, 2004; Fenelon and others, 2010). A total of 13,795 wells with water-level measurements were used in constructing the potentiometric surface map (Auxiliary 6).

The potentiometric surface shown on plate 2 was generated by manually contouring the control-point data without consideration for either the depth of well penetration or the geologic formations (or HGUs) penetrated by the wells. Thus, the derived potentiometric surface emphasizes horizontal groundwater movement from recharge to discharge areas and does not depict vertical hydraulic gradients, such as localized downward vertical gradients assumed to occur in recharge areas and upward vertical gradients in discharge areas. Previous studies have published separate carbonate aquifer and basin-fill potentiometric-surface maps (Thomas and others, 1986, pls. 1 and 2; Wilson, 2007, pls. 1 and 2). The water levels in these previously published carbonate aquifer potentiometric-surface maps, however, largely were based on wells screened in the basin fill, in part owing to the scarcity of wells penetrating the deeper bedrock aquifers. The potentiometric-surface map developed for the current study, in contrast, does not distinguish wells screened within the basin fill from wells screened within the bedrock. This simplifying assumption is consistent with previous subregional potentiometric-surface maps of portions of the study area in which water levels in the shallow alluvium were assumed to be in hydraulic connection with the underlying permeable bedrock (Belcher, 2004; Wilson, 2007). The assumption is supported by groundwater altitudes from nested piezometers in Snake Valley (HA 254) that show little to no vertical gradient between basin-fill and carbonate-rock aquifers (Hugh Hurlow, Utah Geological Survey, written commun., 2008). In other areas of higher permeability bedrock overlain by basin-fill deposits, vertical nested water-level data generally are not available to confirm this assumption. In areas of low-permeability volcanic rock, such as Yucca Mountain (C. Faunt, U.S. Geological Survey, unpublished data, 2008) and Rainier Mesa (Fenelon and others, 2010), large vertical hydraulic gradients are known to exist. These steep vertical gradients may be representative of other areas with low-permeability bedrock within the GBCAAS study area, however vertically nested water-level data are not available elsewhere to confirm this.

The spring and stream altitudes used as control points for the potentiometric-surface map were considered especially important in the mountain blocks where well data are sparse. For the spring data, water-level altitudes were assumed to be equal to the spring altitude. Only single springs or groups of smaller springs (typically within 1 mi of each other), with discharge greater than 300 gal/min (about 500 acre-ft/yr), were included as control points; springs with discharge less than 300 gal/min were assumed to represent localized, perched aquifers. Stream altitudes of perennial gaining streams located within the mountain block having a baseflow of at least 300 gal/min (with a few exceptions to include streams with slightly less baseflow) were used as control points. A median altitude was calculated for each perennial mountain stream reach and used as a control point in the potentiometric-surface map. This assumes that the reach of the stream below the median altitude typically gains from groundwater discharge and is in hydraulic connection with the regional aquifer. In areas with multiple stream reaches, these median perennial stream altitudes were averaged over a 1-mi^2 grid cell and the median altitude is represented as a point at the center of the cell for the potentiometric-surface map.

The use of mountain stream altitudes as control points for the potentiometric-surface map assumes that a hydraulic connection exists between mountain-block bedrock and the rest of the groundwater system. This assumption also implies that perennial mountain-block streams are maintained by baseflow derived from discharging groundwater in the mountain block, such that the stream acts as a drain for the mountain-block aquifer. Most perennial streams occur in higher altitude mountain-block areas with higher precipitation and lower permeability bedrock. This is consistent with findings in the northern half of Great Basin National Park (Elliot and others, 2006). In such areas, groundwater mounding can be relatively steep, resulting in high-altitude water tables and local flow paths (fig. C–1) ending in discharge as baseflow to mountain streams and springs. Mounding is a function of both recharge and hydraulic conductivity. High-altitude water tables in areas such as the volcanic rocks of Rainier Mesa between Fortymile Canyon-Buckboard Mesa (HA 227B) and Yucca Flat (HA 159), and in the southern part of the San Francisco Mountains between Wah Wah Valley (HA 256) and Milford Area (HA 284), illustrate that groundwater mounding can occur in areas having low recharge rates and low hydraulic conductivity.

By use of the control points (6,444 water levels based on measurements from 13,795 wells (Auxiliary 6), 395 spring altitudes, and 2,135 gaged perennial mountain stream altitudes), as well as the characterization of groundwater flow potential across HA boundaries on the basis geologic structure and the possible presence of recharge mounds, potentiometric contours were drawn for the entire study area at 500-ft contour intervals (pl. 2). These contours represent approximate water-level altitudes that have assumed uncertainties of at least ± 50 ft. A link to the geospatial dataset containing the control points and potentiometric contours is given in Appendix 6.

The potentiometric contours were then compared to land-surface altitudes using the U.S. Geological Survey's National Elevation Dataset (NED; U.S. Geological Survey EROS Data Center, 1999). Throughout most of the Great Basin, aquifers are generally unconfined and have water-level altitudes that are lower than land-surface altitudes. If a potentiometric altitude was greater than 100 ft above the NED altitude in areas without water-level control points, the location of the contour was adjusted until it was less than 100 ft above the NED altitude. This maximum tolerance of 100 ft above the NED altitude was chosen because of error in vertical accuracy of the NED (average of ± 23 ft) and errors associated with the computation of the control point altitudes (including both spatial and temporal averaging), which are assumed to be ± 50 ft.

Five shaded areas depicted on plate 2 represent valley areas and adjacent mountain blocks where potentiometric-surface contours are considered less certain because of the lack of water-level data. These five areas are located in (1) the northern part of the Colorado groundwater flow system centered on Jakes Valley (HA 174); (2) the western part of the Railroad Valley (30), the eastern part of the South-Central Marshes (24), and the northwestern part of the Death Valley groundwater flow systems; (3) the northeastern part of the Death Valley groundwater flow system (28); (4) the south-central part of the Colorado groundwater flow system (34) centered on Kane Springs Valley (HA 206); and (5) the southern end of the Great Salt Lake Desert groundwater flow system (37) centered on the southern parts of Snake Valley (HA 254) and Pine Valley (HA 255). While potentiometric-surface contours are drawn through these areas, the locations of these contours are less certain than in other parts of the GBCAAS study area.

Because the water-level altitudes for each well were averaged over the period of record, the potentiometric-surface map does not portray conditions during a particular season or year, but rather portrays an approximate average based on water levels spanning a period of more than 70 years. This temporal averaging approach is considered appropriate for the scope and scale of this study, with the objective of providing an overview of regional-scale groundwater flow. There are inherent uncertainties, however, in using a temporally mixed (averages computed for different periods of record) water-level data set for the development of the regional potentiometric-surface map. The majority of water-level hydrographs from the study area show no long-term monotonic trends (declining or rising water levels), but do show responses to both seasonal precipitation patterns and multiyear cycles of drought and wet periods. The use of one particular water-level measurement from a well with multiple measurement dates was not considered as representative as a temporal average, particularly for wells in fractured bedrock or along valley margins where seasonal variations can approach 100 ft. This is consistent with water-level data from wells in alpine watersheds, where seasonal water-level fluctuations approach 170 ft (Manning and Caine, 2007) and numerical modeling shows that high relief, high water-table elevations in mountainous terrain can cause significant gravity-driven regional groundwater flow (Gleeson and Manning, 2008). The maximum historical change in water level at any particular well is generally less than 100 ft. The error associated with the use of temporally averaged water levels for these wells is assumed to be consistent with, and of similar magnitude to, other simplifications and sources of inaccuracy regarding the water-level control points used to constrain the potentiometric-surface map (pl. 2).

Analysis of Potentiometric-Surface Map

Within the GBCAAS, groundwater levels and horizontal hydraulic gradients (pl. 2) typically follow topographic gradients, but with a dampened amplitude. Areas with locally steep hydraulic gradients (higher density of potentiometric contours) may indicate a decrease in transmissivity (either thinning of the more permeable zones within the aquifer or reduction in the hydraulic conductivity) and (or) relatively high groundwater flow. At the interbasin scale, groundwater flow between HAs or groundwater flow systems may occur only where a gradient exists and the intervening mountains comprise permeable rocks. The potentiometric-surface map indicates the potential for water to move in directions perpendicular to the contours. Figure C–2 conceptually illustrates three types of groundwater flow conditions at HA boundaries: (1) no-flow divides, such as beneath the Ruby and Stansbury mountains, where the modeled hydrogeologic framework indicates a low likelihood of hydraulic connection (see “Likelihood of Hydraulic Connection Across Hydrographic Area Boundaries” section below); (2) no-flow divides, such as beneath the Oquirrh Mountains, where the geology indicates a high likelihood of hydraulic connection, but groundwater mounding forms a hydraulic divide; and (3) flow across HA boundaries, such as beneath the Pequop Mountains, where the geology indicates a high likelihood of hydraulic connection and there is likely insufficient mounding to cause a hydraulic divide.

The potentiometric-surface map developed for the GBCAAS study area (pl. 2) shows that groundwater has the potential to flow across the previously defined groundwater flow system boundaries at many locations. The following list gives those locations and also gives references to previous reports indicating similar flowpaths:

1. The Grass Valley groundwater flow system (25) north to the Humboldt groundwater flow system (7);

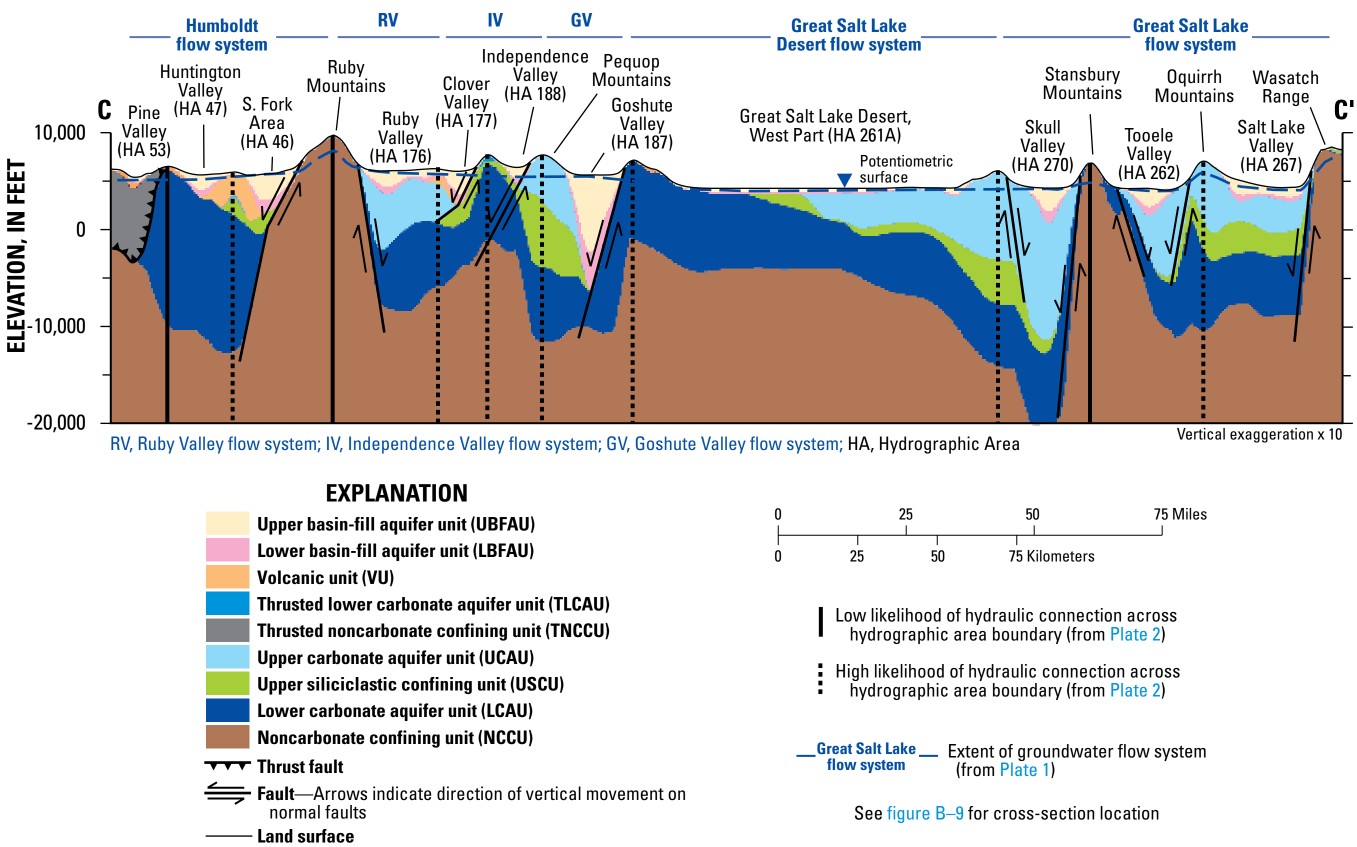

Figure C–2. Cross section showing the modeled hydrogeologic framework, potentiometric surface, and likelihood of hydraulic connections across hydrographic area boundaries and groundwater flow systems in the Great Basin carbonate and alluvial aquifer system study area.

2. The Ruby Valley groundwater flow system (33) northwest to the Humboldt groundwater flow system (7) (fig. C–2; Thomas and others, 1986, sheet 2);
3. The Ruby Valley groundwater flow system (33) northeast through the Independence Valley groundwater flow system (32) and northern portion of the Goshute Valley groundwater flow system (35) toward the Great Salt Lake Desert groundwater flow system (37; fig. C–2) (Thomas and others, 1986, sheet 2);
4. The Diamond Valley (27) and Newark Valley (29) groundwater flow systems north to the Humboldt groundwater flow system (7);
5. The Diamond Valley (27) and Newark Valley (29) groundwater flow systems south to the South-Central Marshes (24) and Railroad Valley (30) groundwater flow systems (Thomas and others, 1986, sheet 2; Wilson, 2007, pl. 1);
6. The Monte Cristo Valley (23), South-Central Marshes (24), and Railroad Valley (30) groundwater flow systems toward the Death Valley groundwater flow system (28) (Belcher, 2004, pl. 1);
7. The Independence groundwater flow system (32) north toward the Great Salt Lake Desert groundwater flow system (37);
8. The Independence groundwater flow system (32) west through the Goshute Valley groundwater flow system (35) toward the Great Salt Lake Desert groundwater flow system (37) (fig. C–2; Thomas and others, 1986, sheet 2);
9. The northern part of the Goshute Valley groundwater flow system (35) toward the Great Salt Lake Desert groundwater flow system (37) (fig. C–2; Thomas and others, 1986, sheet 2; Wilson, 2007, pl. 1); and
10. The Great Salt Lake Desert (37), Great Salt Lake (38), and Sevier Lake (39) groundwater flow systems in eastern Nevada and western Utah toward the Great Salt Lake Desert playa and the Great Salt Lake (Thomas and others, 1986, sheet 2).

Comparisons were made between the potentiometric-surface map developed in the current study and regional potentiometric-surface maps developed for the Great Basin RASA study (Thomas and others, 1986, pls. 1 and 2), the DVRFS study (Belcher, 2004, pl. 1), and the Basin and Range carbonate-rock aquifer system (BARCAS) study (Wilson, 2007, pls. 1 and 2). In general, water-level altitudes are consistent between the maps. The main differences between the current study map and these previous regional potentiometric-surface maps are (1) the inclusion of control point altitudes of springs and gaged perennial streams thought to represent recharge mounds beneath mountain blocks and (2) having contours intersect HA boundaries perpendicularly in areas where groundwater flow between HAs is improbable because of a low likelihood of hydraulic connection on the basis of subsurface geology. In areas having high mountain-block recharge and (or) categorized as low likelihood of hydraulic connection across HA boundaries (pl. 2), flow will tend to be diverted around the mountains (instead of beneath them). For example, the existence of perennial streams within the Snake range between Spring Valley (HA 184) and Snake Valley (HA 254) in east-central Nevada and west-central Utah, and the presence of high estimated in-place recharge rates, as well as water-level altitudes of wells and large springs in and near the mountain block, suggest that a recharge mound likely exists beneath the range, as is shown in the current study potentiometric-surface map (pl. 2).

One particular difference between the current study's potentiometric-surface map and that of the RASA study (Harrill and others, 1988) is an area of high water-level altitude having a flat gradient south of Elko in the Ruby Valley (33), Newark Valley (29), and Diamond Valley (27) groundwater flow systems; the area also includes Long Valley (HA 175) of the Colorado groundwater flow system (34). The current study's potentiometric-surface map presents a new interpretation of hydraulic gradients in this area, with the potential for groundwater to flow toward four other groundwater flow systems: the Humboldt (7), Death Valley (28), Colorado (34), and Great Salt Lake Desert (37). Separating the region into four larger groundwater flow systems differs from the previous interpretation, which invoked multiple, small groundwater flow systems. In particular, Long Valley (HA 175) does not necessarily form the start of an elongated Colorado River groundwater flow system. Instead, Long Valley has the potential to receive groundwater flow from the east and contribute groundwater flow to the north and west.

Geologic Controls Affecting Groundwater Flow

Groundwater flow is affected by geology through a number of factors, including: HGU thickness, geologic structures and structural zones, fault juxtaposition of HGUs with contrasting hydrologic properties, caldera formation, and regional crustal extension. Several of the areas with low hydraulic gradients on the potentiometric-surface map (pl. 2) occur in areas with large thicknesses (figs. A1–4, A1–8, and A1–9) of the most permeable HGUs (UBFAU, UCAU, and LCAU). These areas include southeast of Baker, Nevada, and west of Cedar City, Utah; the high flat area in the Ruby Valley (33), Newark Valley (29), and Diamond Valley (27) groundwater flow systems south of Elko, Nevada, that is the divide for water flowing north and south; and the flat areas in Sarcobatus Flat (HA 146), Frenchman Flat (HA 160), Penoyer Valley (HA 170), Railroad Valley-Southern Part (HA 173A), and Amargosa Desert (HA 230). Not all areas of low hydraulic gradient can be attributed to thick permeable materials. For instance, the flat area in the Great Salt Lake Desert, west of Salt Lake City, is caused by a combination of a large evapotranspiration area, flat land-surface topography, homogenous aquifer material, and little recharge.

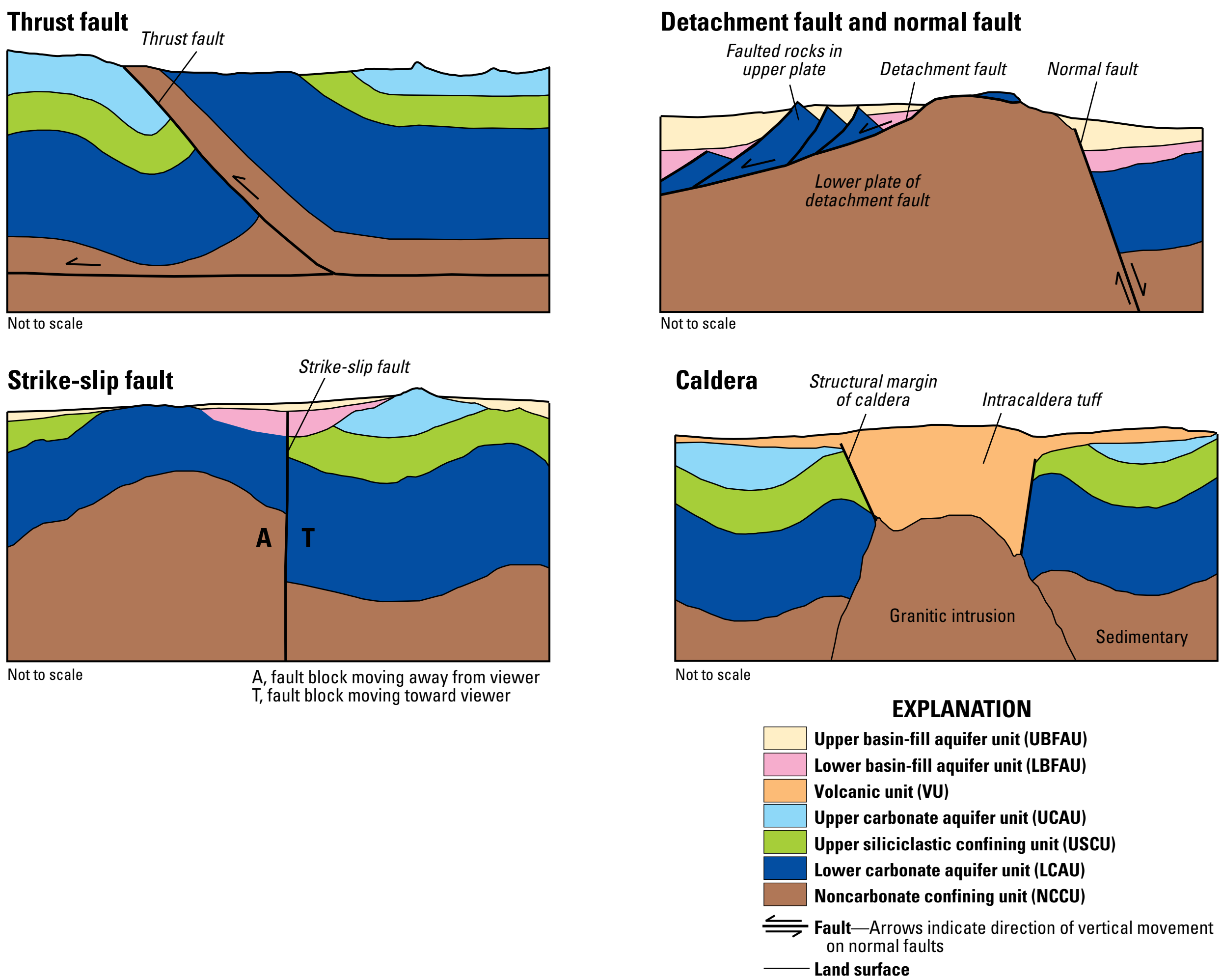

Figure C–3. Schematic diagram showing conceptualized juxtaposition of hydrogeologic units (HGUs) by different types of structures.

Given the complex geologic history of the GBCAAS study area, HGUs often are disrupted by large-magnitude offset thrust, strike-slip, and normal faults. These geologic structures disrupt bedrock continuity (figs. C–2 and C–3) and result in a complex distribution of rocks that affect the direction and rate of interbasin groundwater flow by altering flow paths. The juxtaposition of thick, low-permeability siliciclastic-rock strata against higher permeability carbonate-rock aquifers, caused by faulting, commonly forms barriers to groundwater flow and greatly influences the shape of the potentiometric surface (Winograd and Thordarson, 1975; McKee and others, 1998; Thomas and others, 1986). Examples of this are hydraulic flow barriers ("low likelihood of hydraulic connection across an HA boundary") on the east and west sides of Northern Big Smoky Valley (HA 137B) and along the northwest edge of the Ruby Valley groundwater flow system (33) (pl. 2 and fig. C–2). Physical characteristics of fault zones may cause specific parts of the fault zone to act either as conduits or barriers to flow (Caine and others, 1996).

Structural Belts, Transverse Zones, and Mineral Belts

Thrust faults place Late Proterozoic siliciclastic rocks of the noncarbonate confining unit (NCCU) over lower Paleozoic carbonate rocks of the LCAU. In these cases, the NCCU in regional thrusts may serve to divide groundwater flow systems or divert interbasin flow. For example, thrusted NCCU on the boundary between Pine Valley (HA 53) and Huntington Valley (HA 47) locally divide groundwater flow between these HAs (pls.1 and 2). This division of flow is shown on the west end of cross section *C–C′* (fig. C–2) as the juxtaposition of thrusted noncarbonate confining unit (TNCCU) to the west and LCAU to the east; it is also shown on plate 2 as a "low likelihood of hydraulic connection." Thrust faults along the southeastern edge of the Sevier fold-and-thrust belt place lower Paleozoic carbonate rocks of the LCAU over cratonic clastic sedimentary rocks of Triassic through Cretaceous age (Armstrong, 1968; Burchfiel and others, 1992; Allmendinger, 1992; DeCelles, 2004); these rocks have been included within the UCAU (east end of section *H–H′* beneath Lower Meadow Valley Wash on fig. B–10*B*). In these cases, such as in the Muddy, Clover, and Meadow Valley mountains (pl. 1), lower permeability rocks beneath the thrust may impede downward groundwater flow from the carbonate rocks of the thrust sheet, or even force groundwater to the surface. Low-permeability siliciclastic rock in the upper plate of some thrust faults have been interpreted to cause significant diversions of groundwater flow or steep hydraulic gradients in the Death Valley region (Winograd and Thordarson, 1975; D'Agnese and others, 1997; Potter and others, 2002).

Major strike-slip faults of the Walker Lane belt (fig. B–6) occupy broad valleys in the southwestern part of the study area; these large-offset, strike-slip faults are oriented northwest and, in many cases, juxtapose different HGUs on opposite sides of the fault (fig. B–9). Detailed geologic and hydrologic studies of two of these faults, the Las Vegas Valley shear zone northwest of Las Vegas (fig. B–9; Winograd and Thordarson, 1975) and the Stateline fault system, along the Nevada-California border (fig. B–9; Sweetkind and others, 2004), interpreted these faults as barriers to groundwater flow on the basis of the presence of local steep hydraulic gradients, the location of springs, and the location of the fault with respect to predominant northeast-to-southwest groundwater flow in the region. For example, there is a steep hydraulic gradient and a low likelihood of hydraulic connection along the boundary between Amargosa Desert (HA 230) and Death Valley (HA 243) (pl. 2). Geophysical investigations of strike-slip faults of the Walker Lane belt (Blakely and others, 1998; Langenheim and others, 2001) portray a structurally complex pre-Cenozoic surface adjacent to these faults that comprise steep-sided local depressions and ridges that juxtapose HGUs in complex ways. The occurrence of springs in Pahranagat Valley (HA 209) in the Colorado groundwater flow system (34), and the southward gradient of the potentiometric surface in this vicinity (pl. 2) may be associated with northeast-striking strike-slip faults of the Pahranagat shear zone (northeast-striking faults to the south of section *G–G′*, fig. B–9).

Regional-scale transverse zones (Ekren and others, 1976; Rowley, 1998; Stewart, 1998; fig. B–6) are not well expressed in surficial outcrops, and the influence of such zones on groundwater flow patterns is largely unknown and is not readily apparent on the potentiometric-surface map. Many of the proposed zones are oriented nearly perpendicular to the long axes of current basins and ranges, however, and, as a result, may influence the rate or direction of groundwater flowing parallel to valley axes. Northwest-striking structural zones associated with major mineral belts in north-central Nevada appear to have localized mineralizing fluids periodically over geologic time (Hofstra and Cline, 2000; Emsbo and others, 2006), though the effect of this process on groundwater flow is unclear.

Calderas

The juxtaposition of contrasting lithologies at the margins of calderas affects local and regional groundwater hydrology. Structural collapse, the hallmark of caldera-forming eruptions, occurs along a generally circular system of normal faults that constitute the caldera's structural margin (fig. B–8). The lithologic discontinuity across the steeply inclined structural margin can extend to depths of several thousands of feet. Where calderas form within the carbonate rock terrain, little or no carbonate aquifer would be expected at depth beneath the caldera structure; these rocks are presumably removed during explosive caldera eruptions and intruded by subcaldera granitic rocks (fig. C–3). The structural and topographic margins of calderas juxtapose intracaldera and outflow-facies volcanic rocks. The intracaldera environment is usually filled by several thousands of feet of ash-flow tuff and interleaved landslide materials (Smith and Bailey, 1968; Lipman, 1984). Intracaldera rocks differ in their geometry and material properties from equivalent outflow rocks in that they have greater thicknesses of welded material and more complex welding zonation, greater lithologic diversity (including megabreccia and thick lava accumulations), and a greater degree of alteration. Fracture patterns in intracaldera rocks tend to be more irregular than those of outflow tuffs (Blankennagel and Weir, 1973), leading to a smaller number of connected flow paths. Outflow tuff sheets, although thinner than intracaldera tuff accumulations, have better connected fracture networks and less likelihood of significant alteration (Blankennagel and Weir, 1973). In addition to juxtaposition at the caldera margins, calderas typically are underlain by large subvolcanic granitic intrusions, which are deep, and presumably of low permeability. These intrusions may further lower permeability of rocks surrounding calderas through contact metamorphism, hydrothermal alteration, and the replacement of precaldera rocks deposited throughout the area. This is evident on plate 2 by a steep hydraulic gradient and low likelihood of hydraulic connection between Kawich Valley (HA 157) to the northwest and Emigrant Valley-Groom Lake Valley (HA 158A) to the southeast.

Extension

Regions within the GBCAAS study area where the NCCU is structurally high often are associated with Eocene-Oligocene extension and major detachment faults (fig. B–6) that juxtapose lower plate, midcrustal, medium- and high-grade metamorphic rocks of the NCCU against unmetamorphosed upper plate rocks from various HGUs (Hamilton, 1988; fig. C–3). Examples of mountain ranges with uplifted, metamorphosed NCCU include the Ruby Mountains and East Humboldt Range, the northern Snake Range, and the ranges bounding Death Valley, including the Panamint, Funeral, and Black Mountains (pl. 1). These regions are of hydrologic significance because the major detachment faults typically bring large amounts of low-permeability rocks to the surface, usually forming the highest topography in the region (Coney, 1980), and are represented as HA boundaries with a low likelihood of hydraulic connection. The low likelihood of hydraulic connection along the HA boundary between Spring Valley (HA 184) and Snake Valley (HA 254) is one such example.

Previous regional studies noted that some steep hydraulic gradients are coincident spatially with NCCU in the lower plates of major extensional detachments (Thomas and others, 1986). Previous studies of the Death Valley groundwater flow system linked exposures of relatively low-permeability NCCU with a steep hydraulic gradient along the east side of Death Valley (D'Agnese and others, 1997; Bedinger and Harrill, 2004). Large springs in Death Valley (HA 243) are located only on the flanks of the northern part of the Grapevine Mountains and the southern part of the Funeral Mountains (Steinkampf and Werrell, 2001), where relatively permeable Paleozoic carbonate rocks of LCAU are conducive to groundwater flow; large springs are absent in areas where low-permeability NCCU units are exposed by the detachment faults.

The direction and intensity of late Eocene through Holocene extension have varied both geographically and chronologically across the GBCAAS study area, creating domains of differential extension, with highly extended domains alternating with less extended domains (Gans and Miller, 1983; Wernicke and others, 1984; Smith and others, 1991; Wernicke, 1992). Figure B–6 depicts these greatly extended zones (tan shading) separated by less extended zones (grey shading). Less extended domains preserve the entire thickness of the LCAU and UCAU within regional-scale synclines formed during Cretaceous and early Tertiary Sevier thrusting. The LCAU and UCAU within the greatly extended domains are typically complexly faulted and thinned as a result of structural disruption (Gans and Miller, 1983). Highly extended domains often have low-permeability (siliciclastic rocks or metamorphic rocks) of the NCCU at or near the surface (Dettinger and Schaefer, 1996). Many of these highly extended domains appear to be separated by lateral faults, which form boundaries and transfer extensional strain between differentially extended domains.

Dettinger and Schaefer (1996) compared the structural setting and distribution of rocks within various extensional domains to the location of regional groundwater flow systems within the carbonate-rock province. They concluded that regional groundwater movement in the eastern Great Basin is dominated by flow through thick sections of consolidated carbonate rock within portions of the study area that had been extended only slightly, whereas regions affected by large-magnitude crustal extension were found to be characterized by smaller, local flow systems. Portions of the Great Salt Lake Desert groundwater flow system (HAs 254, 255, 257, 258; pl. 1) fit this conceptualization, where less extended zones within LCAU (figs. B–4B and B–6) underlie those parts of the groundwater flow system that connect upgradient, recharge-dominated parts of the system with distal discharge areas (pl. 2). The region south of the Muddy River Springs (HA 219) is an example of an area where regional extension (fig. B–6) has reduced permeability. The lower permeability in the greatly extended terrains forces water to the surface at the springs instead of allowing water to continue flowing south for eventual discharge to the Virgin River or Lake Mead (pl. 1). This is also expressed in the shape of the potentiometric contours in this area, showing a coalescing of groundwater that discharges at Muddy River Springs (pls. 1 and 2). In contrast, parts of the Colorado groundwater flow system (HA 207, HA 208; pl. 1) and the Death Valley groundwater flow system (HA 160, HA 161; pl. 1), known to be underlain by thick sections of consolidated carbonate rock, fall within greatly extended zones (fig. B–6). In these cases, lack of correspondence between extensional domain and the location of regional groundwater flow systems is, in part, a result of differences in the mapped extent of greatly extended regions used by Dettinger and Schaeffer (1996) and those shown in figure B–6. The lack of correspondence may result from the effects of other geologic factors, such as the inferred enhanced permeability north of the Las Vegas Valley shear zone (fig. B–7).

High-angle normal faults associated with younger basin-and-range style extension can have sufficiently large stratigraphic offset such that HGUs with contrasting hydrologic properties are juxtaposed across the fault. These faults disrupt aquifer continuity (fig. C–3) and may alter groundwater flow paths. Interbasin southwest-flowing groundwater in consolidated carbonate rocks is forced to the surface at Ash Meadows, in the eastern Amargosa Desert (HA 230; pl. 1), likely because the LCAU here is juxtaposed against low-permeability basin-fill materials of the lower basin-fill aquifer unit (LBFAU) and UBFAU across a normal fault (Winograd and Thordarson, 1975); Dudley and Larsen, 1976). Winograd and Thordarson (1975) interpreted a distinct gradient across this fault on their detailed potentiometric surface; at the regional scale, however, the gradient across the fault is not apparent, (pl. 2).

Faults as Hydrogeologic Features

Many brittle fault zones contain a narrow core of fine-grained, relatively low-permeability gouge that is the locus of fault displacement (Caine and others, 1996). The core zone can be flanked by damage zones, a network of subsidiary small faults and fractures that enhance secondary permeability (Caine and others, 1996; Caine and Forster, 1999). In many cases, the core zone reduces permeability relative to that of the original rock or the surrounding damage zone as a result of progressive grain-size reduction, formation of clay minerals, and mineral precipitation during fault motion. Low-permeability fault cores potentially restrict fluid flow across the fault, whereas the damage zone may conduct groundwater flow parallel to the fault zone. The width of the low-permeability core zone is commonly 1.8 to 3.3 ft for high-angle normal faults in volcanic rocks at Yucca Mountain (pl. 1) and in carbonate rocks near the Nevada Test Site (fig. A–1). For these normal faults, the surrounding more permeable damage zones vary in width from about 30 to 300 ft. Dettinger (1989) reported enhanced transmissivities in normal-faulted carbonate rocks, as measured in wells drilled for the U.S. Air Force's MX missile-siting program in Coyote Spring Valley, Nevada (HA 210; pl. 1); these transmissivities are 20–40 times those measured in relatively undeformed carbonates near the Nevada Test Site (fig. A–1), and likely occur in a broad fault-related damage zone. Certain springs, such as those in central White River Valley (HA 207; pl. 1), are associated with faults, but the faults are aligned with the inferred direction of groundwater flow. It is possible, in these cases, that permeable damage zones along the fault could enhance flow.

Strike-slip faults within the GBCAAS study area are typically buried beneath alluvial cover, obscuring any direct observations of the fault core zone within these structures. In other areas where well-exposed, large-displacement, strike-slip faults have been studied, they have been characterized by a continuous, low-permeability core zone (Chester and Logan, 1986). Flow barriers along strike-slip faults, though effective locally, may be regionally discontinuous. Chester and Logan (1986), for example, noted considerable variations in the thickness of the core zone (about 0.2 to 3 ft) along an inactive strand of the San Andreas Fault. Thus, it seems likely that core zones could become irregular and discontinuous locally, resulting in a discontinuous groundwater flow barrier.

The hydrologic influence of regional fault zones has been shown numerically to be governed, at least in part, by the relative hydraulic conductivities of the mountain block, valley-fill, and fault zone, and illustrates the control exerted by regional faults in basin-and-range settings with overlying alluvium (Folch and Mas-Pla, 2008). The hydrologic influence of large-offset normal faults appears to be variable in the GBCAAS study area. In some cases, large-offset normal faults correspond to the locations of substantial groundwater discharge, and the faults may be interpreted to affect groundwater flow by impeding lateral flow and enhancing upward flow. Elsewhere, groundwater flow appears to pass directly across normal faults. Differences in water levels and water chemistry across faults in the Yucca Mountain area (pl. 1) provide evidence that some normal faults in volcanic rocks impede cross-fault flow (Luckey and others, 1996), acting as barriers and compartmentalizing the groundwater flow system. In contrast, interbasin groundwater flow has been suggested on the basis of potentiometric contours (Harrill, 1982) that pass unaffected directly across a normal fault bounding the eastern side of the Nopah Range to the west of Pahrump Valley (HA 162; pl. 1). Few data are available, however, to define the gradient to the west of the Nopah Range. Springs in Pahrump Valley discharge where LCAU is juxtaposed against LBFAU and UBFAU, even though no fault has been defined in the area. Similarly, several studies have inferred interbasin groundwater flow to the south of the Snake Range (HA 184 and 254, pl. 1) on the basis of water-budget considerations (Harrill and others, 1988; Welch and others, 2007). In this case, generally west-to-east flow must cross discontinuous north-striking normal faults bounding each side of the uplifted carbonate rocks of the Limestone Hills at the south end of the range, suggesting that these faults do little to impede interbasin flow. From data presented in Chapter D of this report, water-budget considerations based on new recharge estimates do not require interbasin flow in this area, although the potential does exist (pl. 2).

Aquifer Storage Volumes

Estimating groundwater storage is helpful for evaluating regional groundwater resources. Groundwater within the GBCAAS study area is stored within the saturated pore spaces (including both primary and fracture porosity) of both unconsolidated and consolidated hydrogeologic units. This stored groundwater is the initial source of water to a pumped well, which is later replaced by water from other sources after a new equilibrium is established within the aquifer. For a given withdrawal rate, a relatively large amount of available storage in the vicinity of the aquifer will result in less substantial drawdown effects (declining water levels, aquifer compaction, and land subsidence) and a longer lag time before re-equilibration to this stress is established, and capture of natural discharge or recharge sources occurs. The magnitude of water-level decline and (or) recovery is dependent upon aquifer storage properties: specific yield under water-table conditions and storage coefficient under confined conditions. Specific yield is typically less than the porosity of saturated sediments because some of this water is tightly bound in the pore spaces and cannot be removed under gravity drainage. A recently published groundwater resources evaluation within the study area (Welch and others, 2007) estimated groundwater storage volumes assuming a constant 100-ft decline throughout both basin-fill and adjacent consolidated rock. Within the larger GBCAAS study area, both the extent and magnitude of future water-level declines, and whether such declines would occur under confined or unconfined conditions, are unknown. Also, the storage properties of the carbonate HGUs are assumed to be much smaller and less certain than those of volcanic and basin-fill HGUs because fewer modeling studies and multiple-well aquifer tests have been done. The approach used in the current study was to estimate the total quantity of water stored in only the volcanic and basin-fill deposits. The following estimates represent the total volume of groundwater that could potentially be removed from volcanic and basin-fill units within the GBCAAS study area under unconfined conditions. These stored volumes should not be considered usable storage since it is highly unlikely that any volcanic or basin-fill HGU would undergo such complete drainage. Furthermore, the storage volumes presented here should not be considered analogous to groundwater availability within the GBCAAS study area.

Groundwater availability, in contrast, is generally considered in the context of groundwater sustainability, defined by Alley and Leake (2004):

> *as the development and use of ground water resources in a manner that can be maintained for an indefinite time without causing unacceptable environmental, economic, or social consequences.*

The estimated total storage volumes presented here, therefore, are only useful for illustrating differences in stored volumes of groundwater between HGUs in the 17 individual groundwater flow systems.

To calculate storage quantities, the aquifer volumes (below the water table) of each Cenozoic HGU (volcanic unit [VU], LBFAU, and UBFAU) were first calculated. Volumes were not determined for the older LCAU, UCAU, upper siliciclastic confining unit (USCU) and NCCU HGUs. The volumes of Cenozoic sediments were calculated on the basis of thicknesses of these units in the three-dimensional hydrogeologic framework (Chapter B of this report). The altitude used to calculate the volumes is the top of the surficial unit, or the altitude of the potentiometric surface (pl. 2) if the potentiometric surface is below land surface. Unlike the BARCAS study (Welch and others, 2007), playa deposits were not mapped separately from other basin-fill deposits and, therefore, were not subtracted from total basin-fill volumes. The estimated aquifer volumes are 1.06 x 10^{15} ft^3, 1.32 x 10^{15} ft^3, and 2.36 x 10^{15} ft^3 for VU, LBFAU, and UBFAU, respectively, within the GBCAAS study area.

The estimated total volume of water stored in these three Cenozoic aquifers was calculated by multiplying their respective aquifer volumes by ranges of previously published specific-yield values for Cenozoic deposits within the study area. These calculated volumes are hypothetical and should be used only for comparing groundwater storage volumes across the 17 groundwater flow systems; these volumes are much larger than could potentially be recovered. Specific-yield values (representing unconfined conditions) were used, rather than confined specific-storage values, because the estimates are for total volume of water stored. Specific storage would be applicable only for calculating groundwater extraction under confined conditions, not accounting for actual drainage of soil pores (Freeze and Cherry, 1979, p. 61).

A median specific-yield value of 0.03 was used for calculating water storage in the VU. This was based on reported values from multiple-well aquifer tests (table C–1), including an arithmetic mean of 0.03 from 10 aquifer tests conducted in a variety of tertiary volcanic rocks in and around the Nevada Test Site of the Death Valley (28) groundwater flow system, a value of 0.04 from an aquifer test conducted in fractured welded tuffs at the J–12WW Area 25 well in Fortymile Canyon-Jackass Flats (HA 227A) on the Nevada Test Site, and a value of 0.01 from an aquifer test conducted in volcanic rocks at the Tahoe-Reno Industrial Center in Storey County, Nevada. Although the latter test was outside of the GBCAAS study area, it is considered representative of the less fractured volcanic rocks that are present in many parts of the study area, such as zone 2 of the VU shown in figure B–4D.

Table C–1. Previously reported estimates of specific yield for Cenozoic hydrogeologic units within the Great Basin carbonate and alluvial aquifer system study area.

[HGU, hydrogeologic unit; HA, hydrographic area; VU, volcanic unit; LBFAU, lower basin-fill aquifer unit; UBFAU, upper basin-fill aquifer unit; <, less than; >, greater than; ft, feet]

Area name	Specific yield	Type of material	Pertinent HGU	Analysis type	Report	Comment
Fortymile Canyon-Jackass Flats (HA 227A)	0.04	Fractured welded tuffs	VU	Aquifer testing	http://nevada.usgs.gov/water/AquiferTests/j12ww.cfm?studyname=j12ww, accessed on 01/28/2010	J-12WW Area 25 well on the Nevada Test Site.
Nevada Test Site area of Death Valley groundwater flow system (28)	0.03	Tertiary volcanic rocks	VU	Aquifer testing	Belcher and others, 2001	Reported arithmetic mean of 0.03 based on 10 aquifer tests with values ranging from 0.001 to 0.20.
Tahoe-Reno Industrial Center (outside study area)	0.01	Less-fractured volcanic rocks	VU	Aquifer testing	http://nevada.usgs.gov/water/AquiferTests/tracy_W36-Center.cfm?studyname=tracy_W36-Center, accessed on 01/28/2010	
Frenchman Flat (HA 160)	0.21	Unconsolidated basin-fill sediments	LBFAU, UBFAU	Aquifer testing	http://nevada.usgs.gov/water/AquiferTests/rnm-2s.cfm?studyname=rnm-2s, accessed on 01/28/2010	Well RNM-2S.
Snake Valley (HA 254)	0.15	Unconsolidated basin-fill sediments	LBFAU, UBFAU	Aquifer testing	http://nevada.usgs.gov/water/AquiferTests/snake_valley_n.cfm?studyname=snake_valley_n, accessed on 01/28/2010	Reported range of 0.12 to 0.18 for well (C-20-19)19dcd-1.

Table C–1. Previously reported estimates of specific yield for Cenozoic hydrogeologic units within the Great Basin carbonate and alluvial aquifer system study area.—Continued

[HGU, hydrogeologic unit; HA, hydrographic area; VU, volcanic unit; LBFAU, lower basin-fill aquifer unit; UBFAU, upper basin-fill aquifer unit; <, less than; >, greater than; NC, not calculated; ft, feet]

Area name	Specific yield	Type of material	Pertinent HGU	Analysis type	Report	Comment
Cedar City Valley (HA 282)	0.20	Gravel	LBFAU, UBFAU	Aquifer testing	Bjorklund and others, 1978	Estimated on the basis of recovery of pumped well (C-35-10)18cca-1 (Bjorklund and others, 1978, table 4).
Milford Area (HA 284)	0.20	Coarser sediments	LBFAU, UBFAU	Aquifer testing	Mower and Cordova, 1974	Minimum value; could be as high as 0.40 for fine-grained materials.
Southern Utah and Goshen Valleys (HA 265)	0.06	Cemented sediments, gravel, sand, silt, clay	LBFAU, UBFAU	Field and lab studies	Cordova, 1970; Brooks and Stolp, 1995	Weight-based mean calculated by Brooks and Stolp of six classes (0.25, 0.05, 0.25, 0.05, 0.03, 0.01) listed in Cordova p. 56.
Deep Creek Valley (HA 253)	0.10	Sand and gravel intercalated with clay	LBFAU, UBFAU	Estimated from coarseness correlation	Hood and Waddell, 1969	On the basis of specific yield of 0.2 to 0.3 for permeable layers, which only comprise 20 percent of saturated section.
Ogden Valley (HA 268)	0.10	Unconsolidated basin-fill sediments	LBFAU, UBFAU	Estimated from coarseness correlation	Avery, 1994	
Juab Valley (HA 266)	0.15	Unconsolidated basin-fill sediments	LBFAU, UBFAU	Numerical model	Thiros and others, 1996	Area-based mean from three zones of calibrated numerical model (0.05 for fine-grained, 0.10 for medium-grained, and 0.20 for coarse-grained sediments).
Salt Lake Valley (HA 267)	0.15	Unconsolidated basin-fill sediments	LBFAU, UBFAU	Numerical model	Lambert, 1995	On the basis of calibrated specific yield for model layers 1 and 2.
Cache Valley (HA 272)	0.20	Unconsolidated basin-fill sediments	LBFAU, UBFAU	Numerical model	Kariya and others, 1994	On the basis of visual weighting of five zones from 0.01 to 0.30
Beryl-Enterprise Area (HA 280)	0.17	Fine-to-coarse unconsolidated sediments	LBFAU, UBFAU	Numerical model	Mower, 1982	On the basis of visual weighting of five zones from <0.05 to > 0.20
Cedar City Valley (HA 282)	0.05	Unconsolidated basin-fill sediments	LBFAU, UBFAU	Numerical model	Brooks and Mason, 2005	Area-based mean from two zones of calibrated numerical model (0.04 for finer-grained and 0.07 for coarser-grained deposits)
Pavant Valley (HA 286)	0.25	Finer grained silt and clay below 4,800 ft	LBFAU, UBFAU	Numerical model	Holmes and Thiros, 1990	Median of 0.20 used for finer grained silt and clay below 4,800 ft and 0.30 used for coarser-grained sand and gravel above 4,800 ft

A specific-yield value of 0.15 was used for calculating water storage in the LBFAU and UBFAU. This value is a median value derived from 13 previously reported studies having values that ranged from 0.05 to 0.25 for unconsolidated basin-fill deposits (table C–1). These studies included aquifer testing, field and lab studies, coarseness correlations, and calibrated numerical groundwater flow models. Previously reported estimates of specific yield include 0.20 to 0.25 from aquifer testing, 0.06 from field and lab studies, 0.10 from coarseness correlations, and 0.05 to 0.25 from calibrated numerical models. The median specific-yield value of 0.15 used in the current study is the same as the specific-yield value of 0.15 used for unconfined basin-fill deposits in the BARCAS study (Welch and others, 2007).

Multiplying these estimated values of specific yield of 0.03 for VU and 0.15 for LBFAU and UBFAU by their respective aquifer volumes, the estimated volumes of water stored within the Cenozoic aquifer units within the GBCAAS are 7.3 x 10^8 acre-ft, 4.5 x 10^9 acre-ft, and 8.1 x 10^9 acre-ft for VU, LBFAU, and UBFAU, respectively. Storage volumes in each of the Cenozoic HGUs for each groundwater flow system are shown on figure C–4. Estimated quantities of water stored in the VU range from 1.2 x 10^3 acre-ft to 2.2 x 10^8 acre-ft. Estimated water storage for LBFAU ranges from 1.0 x 10^7 acre-ft to 7.2 x 10^8 acre-ft. Estimated quantities of water stored in the UBFAU range from 2.0 x 10^7 acre-ft to 1.2 x 10^9 acre-ft. The smallest storage volumes are located in the Mesquite Valley groundwater flow system (36), while the largest storage volumes are located in the Death Valley groundwater flow system (28).

Likelihood of Hydraulic Connection Across Hydrographic Area Boundaries

The distribution of aquifers and confining units along HA boundaries is a principal control on interbasin groundwater flow in the study area. The occurrence and juxtaposition of aquifers and confining units in these areas must be understood to assess the geologic controls on the relative potential for groundwater flow across these boundaries. Significant groundwater flow across HA boundaries is possible only where the rocks connecting the hydrographic areas have sufficient permeability.

To assess the geologic controls on the likelihood of hydraulic connections across HA boundaries, the regional stratigraphic and structural features described previously were summarized into 14 general subsurface geologic configurations that result in differing likelihoods of hydraulic connection across HA boundaries (table C–2). Each of the

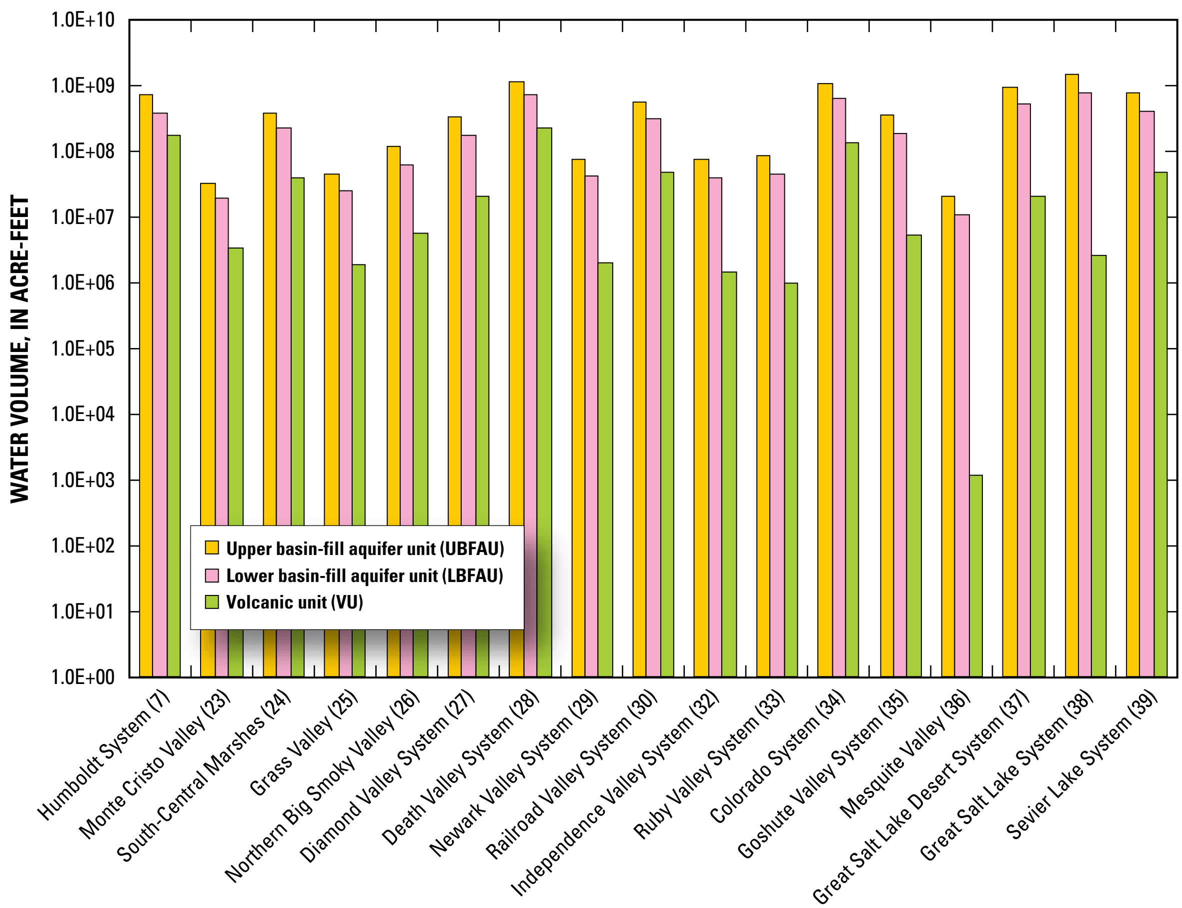

Figure C–4. Estimated volume of water stored within Cenozoic hydrogeologic units in the 17 groundwater flow systems of the Great Basin carbonate and alluvial aquifer system study area.

Table C–2. Likelihood of hydraulic connection across hydrographic area boundaries within the Great Basin carbonate and alluvial aquifer system study area.

[HGUs, hydrogeologic units; NCCU, noncarbonate confining unit; USCU, upper siliciclastic confining unit; TNCCU, thrusted noncarbonate confining unit; UCAU, upper carbonate aquifer unit; LCAU, lower carbonate aquifer unit; VU, volcanic unit; LBFAU, lower basin-fill aquifer unit; UBFAU, upper basin-fill aquifer unit; ft, feet; 3-D, three-dimensional; HA, hydrographic area; NV, Nevada; CA, California; UT, Utah ; >, greater than]

Likelihood of hydraulic connection across HA boundary	HGUs primarily responsible for geologic condition at boundary	Geologic rationale for classification
Low	NCCU	NCCU near (within about 300 ft) or at land surface, on the basis of 3-D framework. Unit assumed to project to great depths below any outcrop exposure. Included NCCU exposures from surface geologic map in places where 3-D framework did not exactly replicate the geologic map. Ignored small inliers of permeable units surrounded by NCCU.
Low	USCU	USCU near (within about 250 ft) or at land surface and unit greater than about 800 ft thick, on the basis of 3-D framework. Included selected USCU exposures from geologic map in places where unit thickness was less than about 800 ft where dip of the unit increases the cross-sectional area of the unit at the HA boundary so that unit could still function as a geologic barrier.
Low	TNCCU	HA boundaries that are parallel to thrust faults and TNCCU, such that water in Paleozoic rocks would not be expected to cross the thrust fault. For the purposes of potentiometric surface interpretation, included thrust faults from the central Nevada thrust belt and the Sevier thrust belt that were not explicitly included in the 3-D framework.
Low	Not related to a specific HGU	HA boundaries within structurally disrupted areas where local extreme extension thins or disrupts Paleozoic carbonate rocks, such that a continuous carbonate aquifer is unlikely. Includes portions of the Grant Range, northern part of the Snake Range, Egan Range, and Mormon Mountains.
Low	TNCCU	Presence of thrusted deep-water assemblages in the upper plate of the Roberts Mountain allocthon. Includes siliceous chert and limestone assemblages of the Vinini and Valmy Formations in the vicinity of Elko and Battle Mountain, NV. These units are attributed as TNCCU in the 3-D framework and are expected to be generally low-permeability rocks.
High	LCAU and UCAU	LCAU or UCAU near (within about 150 ft) or at land surface and unit greater than about 800 ft thick, on the basis of 3-D framework. Included narrow basin-fill valleys that were flanked by carbonate-rock mountain ranges where carbonate bedrock could reasonably be inferred at depth beneath valley.
High	VU	Thick (>250 ft) ash-flow tuffs overlying permeable carbonate bedrock. Ash-flow tuffs expected to support well-developed fracture networks and be moderately permeable local to subregional aquifers.
High	LBFAU and UBFAU	Areas of Cenozoic basin fill where the LBFAU is interpreted to be either ash-flow tuff or prevolcanic sedimentary rock, and the UBFAU is interpreted to be either coarse-grained younger sediment or exposures of prevolcanic sedimentary rocks that exist in the shallow part of the basin.
Uncertain	VU	Intracaldera volcanic rocks. Thick sequences of highly heterogeneous volcanic rocks (including welded and nonwelded tuff, lava flows, volcanic breccias, and nonvolcanic megabreccia deposits) that are bounded by the caldera structures. This unit overlies intrusive rocks of the NCCU inferred to be present at depth within calderas; unit has potential to be hydrothermally altered.
Uncertain	VU	Volcanic rocks, mainly ash-flow tuffs, of variable thickness that overlie impermeable bedrock. Common in Esmeralda County, NV, near Lake Mead in the southern part of Clark County, NV, and in San Bernardino County, CA.
Uncertain	VU	Highly variable volcanic rock overlying bedrock that has variable or uncertain permeability. Examples include local accumulations of rhyolite lava flow, such as at the southern end of Butte Valley, NV, or intervals of thin welded ash-flow tuff interbedded with nonwelded tuff.

Table C–2. Likelihood of hydraulic connection across hydrographic area boundaries within the Great Basin carbonate and alluvial aquifer system study area.—Continued

[HGUs, hydrogeologic units; NCCU, noncarbonate confining unit; USCU, upper siliciclastic confining unit; TNCCU, thrusted noncarbonate confining unit; UCAU, upper carbonate aquifer unit; LCAU, lower carbonate aquifer unit; VU, volcanic unit; LBFAU, lower basin-fill aquifer unit; UBFAU, upper basin-fill aquifer unit; ft, feet; 3-D, three-dimensional; HA, hydrographic area; NV, Nevada; CA, California; UT, Utah]

Likelihood of hydraulic connection across HA boundary	HGUs primarily responsible for geologic condition at boundary	Geologic rationale for classification
Uncertain	Modification of VU, LCAU, or UCAU	Mineral deposits that are associated with hydrothermal alteration and mineralization at a scale large enough to potentially disrupt the regional aquifer systems. Mainly associated with copper porphyry systems and epithermal and hot-spring precious-metal systems. Deemed important where mineralizing system intruded otherwise permeable carbonate rocks, such as at Bingham Canyon, UT, or Battle Mountain, NV. Where the mineralizing system overprints lower-permeability rocks, such as at Tintic, UT, HA boundaries were not modified from their original classification based on rock type.
Uncertain	LBFAU and UBFAU	Areas where the LBFAU, the UBFAU, or both units were fine-grained or had a large volcanic ash component.
Uncertain	NCCU	Areas where zones of closely spaced normal faults may enhance permeability of otherwise low-permeability rocks. Examples include seismogenically active faults cutting granites of the Slate Range near Lida Valley and Clayton Valley, Esmeralda County, NV.

14 subsurface geologic configurations is determined by the permeability and cross-sectional area of the HGUs and (or) geologic structures at an HA boundary. The subsurface geology at HA boundaries was interpreted primarily by evaluating vertical, irregularly bending cross-section views of the three-dimensional hydrogeologic framework model (described in Chapter B and Appendix 1) for altitude, thickness, and relative juxtaposition of specific HGUs.

Interpretation of the subsurface geology relative to the likelihood of hydraulic connection across HA boundaries primarily was based on the presence of specific HGUs or juxtaposition of HGUs with contrasting hydraulic conductivity. The degree of structural disruption at the boundary is considered an important, but secondary, control. Structural disruption may be considered as a boundary condition where closely spaced high-angle normal faults disrupt a relatively broad region and where carbonate-rock aquifers (UCAU and LCAU) are highly faulted and disrupted in the upper plates of low-angle normal faults. Because data are lacking, however, the likelihood of hydraulic connection across HA boundaries (table C–2) does not incorporate the effects of individual faults as distinct hydrologic entities. For example, the analysis omits potential effects of low-permeability, clay-rich fault core zones, fractured and potentially more permeable zones that might be located adjacent to the fault core, or strata-bound fractured intervals in volcanic or carbonate rocks.

For each of the 14 general subsurface geologic configurations (table C–2), the likelihood of hydraulic connection across HA boundaries was summarized by assigning portions of HA boundaries to one of three likelihoods (low, high, or uncertain) of hydraulic connection across the boundary (pl. 2): (1) low—relatively impermeable consolidated rock occurs at depth that inhibits groundwater flow (solid lines on plate 2), (2) high—permeable consolidated rock or basin fill occurs at depth that permits groundwater flow (dashed lines on plate 2), or (3) uncertain—the permeability of the consolidated rock or basin fill is highly variable, such that the groundwater flow potential across HA boundaries is uncertain (double lines on plate 2).

The likelihood of hydraulic connections across HA boundaries varies throughout the study area (pl. 2). HA boundaries with low likelihood of hydraulic connection (table C–2) include (1) exposures of NCCU associated with metamorphic core complexes and with other large-offset normal faults (HAs 176 and 230; pl. 1); (2) areas of thick USCU, such as thick sections of Diamond Peak Formation and Chainman Shale in north-central parts of Nevada (HAs 174 and 175; pl. 1) and at the Nevada Test Site (HA 159; pl. 1); (3) local areas where thrusted Late Proterozoic siliciclastic rocks of unit TNCCU are extensive (HA 162; pl. 1); and (4) regions of low-permeability rocks associated with the Roberts Mountains thrust belt (HAs 137B and 138; pl. 1) in the northwestern part of the study area (fig. B–5). HA boundaries with high likelihood of hydraulic connection include (1) those underlain by thick sequences of consolidated carbonate rock HGUs LCAU and UCAU (HAs 160, 161, 168, 208, 209, and 210; pl. 1), generally corresponding to the central carbonate corridor described by Dettinger and others (1995); (2) those underlain by welded ash-flow tuffs overlying permeable bedrock, typically associated with outflow tuffs that surround the major caldera complexes (HAs, 146, 150, 156, 227A, and 228; pl. 1); and (3) those underlain by permeable basin fill, especially in the Humboldt River drainage (HAs 43, 45, and 48; pl. 1) in the northwestern part of the study area (fig. A–1). HA boundaries with an uncertain likelihood of hydraulic connection include (1) accumulations of volcanic rocks (VU) that are heterogeneous (HAs 204 and 221; pl. 1) or that overlie impermeable bedrock (HAs 144 and 147; pl. 1); (2) areas where permeability may be modified as the result of hydrothermal alteration and mineralization (HA 267; pl. 1) or by the presence of structures; and (3) areas where the lower or upper basin fill (LBFAU or UBFAU) have variable properties.

Limitations

The following are several limitations that should be considered when utilizing the information presented in Chapter C:

- The objective of the potentiometric-surface contours depicted on plate 2 is to illustrate the general directions of horizontal groundwater flow within the GBCAAS study area. Because of its large regional extent and the 500-ft contour intervals, this map is not suitable for evaluating detailed flow conditions at the sub-HA level.
- Plate 2 was developed without consideration for vertical flow between HGUs because of a general lack of water-level data to accurately quantify vertical hydraulic gradients in most of the GBCAAS study area. While not displayed on plate 2, there is the possibility that significant vertical gradients between HGUs exist in parts of the study area, typically in lower permeability bedrock. Detailed water-level data from volcanic aquifers, such as those at Rainier Mesa and the Nevada Test Site (Fenelon and others, 2010), show that hydrogeologic complexities and large vertical hydraulic gradients can exist within lower permeability rocks within the GBCAAS study area.
- There is the possibility that some areas with high-altitude water-level mounding (shown on plate 2 and figure C–2) beneath mountain blocks may represent perched water levels, rather than the regional potentiometric surface, particularly in areas having low-permeability bedrock that may impede vertical flow. Water levels known to represent perched conditions were not used to develop the potentiometric surface. In contrast, mounding likely occurs beneath other mountain-block areas that are not shown on plate 2 because of the lack of water-level control points (deep wells, springs, perennial streams) to constrain water-table altitudes in these areas. Additional water-level data from deep wells are needed to confirm the extent of regional mounding beneath mountain blocks shown on plate 2.
- While plate 2 delineates five larger shaded areas where potentiometric contours are less certain due to sparsity of water-level data, other smaller areas without water-level data are not delineated, including many mountain blocks without water-level control points that could have groundwater mounding. Water-level mounding in mountain blocks is only shown where there is direct hydrologic evidence (well water levels, spring altitudes, perennial stream altitudes). Water-level mounding likely occurs beneath other mountain blocks within the GBCAAS area and is dependent on recharge and hydraulic conductivity. There is the possibility, therefore, of groundwater mounds not shown on the plate that would divert groundwater flow.
- The estimated total storage volumes of the VU, LBFAU, and UBFAU HGUs are given only for comparison between groundwater flow systems and should not be considered analogous to groundwater availability within the GBCAAS study area.

Summary

The GBCAAS study area has been subdivided into 165 individual HAs and 17 regional groundwater flow systems by previous studies (Harrill and Prudic, 1998, Belcher, 2004). The HAs primarily were based on surface-water divides and range in size from 12 to 4,648 mi^2. The groundwater flow systems were based on directions of interbasin groundwater flow and the location of major discharge areas, and range in size from 282 to 18,849 mi^2. Groundwater flow systems primarily follow surface-water divides.

Groundwater movement in the GBCAAS study area occurs at local, intermediate, and interbasin scales. Within each HA, groundwater typically moves along shallow, short (local scale) or medium (intermediate scale) flow paths, typically from higher altitude areas in the mountains or upper part of the alluvial fan to a nearby stream, spring, or evapotranspiration area. At the interbasin scale, groundwater flows along deeper and longer flow paths between HAs from high-altitude mountains to distant discharge points, often through or around one or more mountain blocks. This interbasin flow typically occurs in areas with hydraulically connected permeable bedrock and where recharge rates in the intervening mountains are relatively small (minimal groundwater mounding). Within the GBCAAS study area, interbasin flow previously had been suggested on the basis of groundwater-budget imbalances (including lack of discharge from some basins), geochemical and isotopic mass-balance studies, and numerical modeling.

A potentiometric-surface map of the GBCAAS study area was constructed for evaluating regional groundwater flow by using water-level data for wells and water-level altitudes for springs and perennial mountain streams. The map illustrates that within each HA, groundwater levels and hydraulic gradients typically follow topographic gradients, but to a lesser degree. Areas with locally steep hydraulic gradients may indicate a decrease in transmissivity or relatively high recharge. At the interbasin scale, groundwater flow between HAs or groundwater flow systems may occur where a gradient exists, higher permeability rocks that permit groundwater flow comprise the intervening mountains, and substantial groundwater mounding from recharge in the intervening mountains does not occur. The potentiometric-surface map developed for the current study shows water from the central part of Nevada flowing north to the Humboldt River groundwater flow system, northwest to the Great Salt Lake Desert groundwater flow system, or south toward the Death Valley and Colorado River groundwater flow systems. Groundwater from eastern Nevada and western Utah flows east, north, and south towards the Great Salt Lake Desert and Great Salt Lake. Because of averaging of decades of water-level measurements at many wells, the potentiometric-surface map represents an approximate long-term average rather than any specific season or year. This approach is considered appropriate for evaluating regional groundwater flow.

Aquifer geometry and geologic structural features are integral to groundwater flow in the GBCAAS study area. HGUs within the GBCAAS study area often are disrupted by extension; by large-magnitude offset thrust, strike-slip, and normal faults; and by caldera formation; resulting in a complex distribution of rocks. Juxtaposition of thick, low-permeability rock with higher permeability carbonate-rock aquifers by faulting or caldera emplacement commonly forms barriers to groundwater flow and is an important influence on the potentiometric surface. Fault zones themselves may contain low-permeability cores flanked by higher permeability damage zones. These low-permeability fault cores potentially restrict fluid flow across the fault, while the damage zone may conduct groundwater flow parallel to the fault zone.

Regional stratigraphic and structural features within the GBCAAS study area are organized into 14 general subsurface geologic configurations that result in differing likelihoods of hydraulic connection across HA boundaries. For each of these subsurface boundary conditions, the subsurface geologic controls influencing the likelihood of hydraulic connection at HA boundaries were further simplified as (1) low—where low-permeability rocks likely exist at depth and hydraulic connection is unlikely, (2) high—where permeable rocks likely exist at depth and hydraulic connection is permitted by the geologic conditions, or (3) uncertain—where the subsurface geology beneath the boundary or divide is not well constrained and the geologic controls on hydraulic connection are uncertain.

References Cited

Alley, W.M., and Leake, S.A., 2004, The journey from safe yield to sustainability: Ground Water, v. 42 (no. 1), p. 12–16.

Allmendinger, R.W., 1992, Fold and thrust tectonics of the western United States exclusive of the accreted terranes, *in* Burchfiel, B.C., Lipman, P.W., and Zoback, M.L., eds., The Cordilleran orogen, the Conterminous U.S.: Boulder, Colorado, Geological Society of America, the Geology of North America, v. G–3, p. 583–607.

Armstrong, R.L., 1968, Sevier orogenic belt in Nevada and Utah: Geological Society of America Bulletin, v. 79, p. 429–458.

Avery, Charles, 1994, Ground-water hydrology of Ogden Valley and surrounding area, eastern Weber County, Utah, and simulation of ground-water flow in the valley-fill aquifer system: Utah Department of Natural Resources Technical Publication 99, 84 p.

Bedinger, M.S., and Harrill, J.R., 2004, Regional potential for interbasin flow of ground water, Appendix 1, in Belcher, W.R., ed., Death Valley regional ground-water flow system, Nevada and California—Hydrogeologic framework and transient ground-water flow model: U.S. Geological Survey Scientific Investigations Report 2004–5205, p. 355–374.

Belcher, W.R., ed., 2004, Death Valley regional ground-water flow system, Nevada and California—Hydrogeologic framework and transient ground-water flow model: U.S. Geological Survey Scientific Investigations Report 2004–5205, 408 p.

Belcher, W.R., Bedinger, M.S., Back, J.T., and Sweetkind, D.S., 2009, Interbasin flow in the Great Basin with special reference to the southern Funeral Mountains and the source of Furnace Creek springs, Death Valley, California, U.S.: Journal of Hydrology, v. 369, p. 30–43.

Belcher, W.R., Elliot, P.E., and Geldon, A.L., 2001, Hydraulic-property estimates for use with a transient ground-water flow model of the Death Valley regional ground-water flow system, Nevada and California: U.S. Geological Survey Water-Resources Investigations Report 2001–4210, 28 p.

Bjorklund, L.J., Sumsion, C.T., and Sandberg, G.W., 1978, Ground-water resources of the Parowan-Cedar City drainage basin, Iron County, Utah: State of Utah Department of Natural Resources Technical Publication 60, 93 p.

Blakely, R.J., Morin, R.L., McKee, E.H., Schmidt, K.M., Langenheim, V.E., and Dixon, G.L., 1998, Three-dimensional model of pre-Cenozoic basement beneath Amargosa Desert and Pahrump Valley, California and Nevada—Implications for tectonic evolution and water resources: U.S. Geological Survey Open-File Report 98–496, 29 p.

Blankennagel, R.K., and Weir, J.E., Jr., 1973, Geohydrology of the eastern part of Pahute Mesa, Nevada Test Site, Nye County, Nevada: U.S. Geological Survey Professional Paper 712–B, 35 p.

Brooks, L.E., and Mason, J.L., 2005, Hydrology and simulation of ground-water flow in Cedar Valley, Iron County, Utah: U.S. Geological Survey Scientific Investigations Report 2005–5170, 127 p.

Brooks, L.E., and Stolp, B.J., 1995, Hydrology and simulation of ground-water flow in southern Utah and Goshen Valleys, Utah, Utah Department of Natural Resources Technical Publication 111, 96 p.

Burchfiel, B.C., Cowan, D.S., and Davis, G.A., 1992, Tectonic overview of the Cordilleran orogen in the western United States, *in* Burchfiel, B.C., Lipman, P.W., and Zoback, M.L., eds., The Cordilleran orogen, conterminous U.S.: Boulder, Colorado, Geological Society of America, Geology of North America, v. G–3, p. 407–480.

Caine, J.S., Evans, J.P., and Forster, C.B., 1996, Fault zone architecture and permeability structure: Geology, v. 24, p. 1,025–1,028.

Caine, J.S., and Forster, C.B., 1999, Fault zone architecture and fluid flow—Insights from field data and numerical modeling, *in* Haneberg, W.C., Mozley, P.S., Moore, J.C., and Goodwin, L.B., eds., Faults and subsurface fluid flow in the shallow crust: American Geophysical Union Monograph 113, p. 101–127.

Cardinalli, J.L., Roach, L.M., Rush, F.E., and Vasey, B.J., 1968, State of Nevada hydrographic areas, scale 1:500,000, *in* Rush, F.E., ed., Index of hydrographic areas: Nevada Division of Water Resources Information Report 6, 38 p.

Chester, F.M., and Logan, J.M., 1986, Implications for mechanical properties of brittle faults from observations of the Punchbowl fault zones, California: Pure and Applied Geophysics (PAGEOPH), v. 124, p. 79–106.

Coney, P.J., 1980, Cordilleran metamorphic core complexes, *in* Crittenden, M.D., Coney, P.J., and Davis, G.H., eds., Cordilleran metamorphic core complexes: Geological Society of America Memoir 153, Geological Society of America, Boulder, Colorado, p. 7–34.

Coplen, T.B., Winograd, I.J., Landwehr, J.M., and Riggs, A.C., 1994, 500,000-year stable carbon isotopic record from Devils Hole, Nevada: Science, v. 263, p. 361–365.

Cordova, R.M., 1970, Ground-water conditions in southern Utah Valley and Goshen Valley, Utah: Utah Department of Natural Resources Technical Publication 28, 79 p.

D'Agnese, F.A., Faunt, C.C., Turner, A.K., and Hill, M.C., 1997, Hydrogeologic evaluation and numerical simulation of the Death Valley regional ground-water flow system, Nevada, and California: U.S. Geological Survey Water-Resources Investigations Report 1996–4300, 124 p.

DeCelles, P.G., 2004, Late Jurassic to Eocene evolution of the Cordilleran thrust belt and foreland basin system, western USA: American Journal of Science, v. 304, p. 105–168.

Dettinger, M.D., 1989, Distribution of carbonate-rock aquifers in southern Nevada and the potential for their development—Summary of findings, 1985–88: Carson City, Nev., State of Nevada, Program for the Study and Testing of Carbonate-Rock Aquifers in Eastern and Southern Nevada, Summary Report no. 1, 37 p.

Dettinger, M.D., Harrill, J.R., Schmidt, D.L., and Hess, J.W., 1995, Distribution of carbonate-rock aquifers and the potential for their development, southern Nevada and parts of Arizona, California, and Utah: U.S. Geological Survey Water–Resources Investigations Report 91–4146, 100 p.

Dettinger, M.D., and Schaefer, D.H., 1996, Hydrogeology of structurally extended terrain in the eastern Great Basin of Nevada, Utah, and adjacent states, from geologic and geophysical models: U.S. Geological Survey Hydrologic Investigations Atlas HA–694–D, 1 sheet, scale 1:15,000,000.

Dudley, W.W., Jr., and Larsen, J.D., 1976, Effect of irrigation pumping on desert pupfish habitats in Ash Meadows, Nye County, Nevada: U.S. Geological Survey Professional Paper 927, p. 1–52.

Ekren, E.B., Bucknam, R.C., Carr, W.J., Dixon, G.L., and Quinlivan, W.D., 1976, East-trending structural lineaments in central Nevada: U.S. Geological Survey Professional Paper 986, 16 p., 1 pl. in pocket.

Elliot, P.E., Beck, D.A., and Prudic, D.E., 2006, Characterization of surface-water resources in the Great Basin National Park area and their susceptibility to ground-water withdrawals in adjacent valleys, White Pine County, Nevada: U.S. Geological Survey Scientific Investigations Report 2006–5099, 156 p.

Emsbo, Poul, Groves D.I., Hofstra A.H., and Bierlein, F.P., 2006, The giant Carlin gold province – A protracted interplay of orogenic, basinal, and hydrothermal processes above a lithospheric boundary: Mineralium Deposita, v. 41, p. 517–525.

Fenelon, J.M., Sweetkind, D.S., and Laczniak, R.J., 2010, Groundwater flow systems at the Nevada Test Site, Nevada: A synthesis of potentiometric contours, hydrostratigraphy, and geologic structures: U.S. Geological Survey Professional Paper 1771, 54 p., 6 pls.

Fetter, C.W., 1980, Applied hydrogeology: Charles E. Merrill Publishing Company, Columbus, Ohio, 488 p.

Folch, Albert, and Mas-Pla, Josep, 2008, Hydrogeological interactions between fault zones and alluvial aquifers in regional flow systems: Hydrological Processes v. 22, p. 3,476–3,487.

Freeze, R.A., and Cherry, J.A., 1979, Groundwater: Englewood Cliffs, New Jersey, Prentice-Hall, 604 p.

Gans, P.B., and Miller, E.L., 1983, Styles of mid-Tertiary extension in east-central Nevada, *in* Gurgel, K.D., ed., Geologic excursions in the overthrust belt and metamorphic core complexes of the intermountain region, Nevada: Utah Geological and Mineral Survey Special Studies 59, p. 107–160.

Gates, J.S., and Kruer, S.A., 1981, Hydrologic reconnaissance of the southern Great Salt Lake Desert and summary of the hydrology of west-central Utah: State of Utah Department of Natural Resources Technical Publication 71, 55 p.

Gleeson, Tom, and Manning, A.H., 2008, Regional groundwater flow in mountainous terrain: Three-dimensional simulations of topographic and hydrogeologic controls: Water Resources Research, v. 44, 16 p.W10403, doi:10.1029/2008WR006848, accessed December 22, 2008 at http://www.agu.org/pubs/crossref/2008/2008WR006848.shtml.

Hamilton, W.B., 1988, Detachment faulting in the Death Valley region, California and Nevada, *in* Carr, M.D., and Yount, J.C., eds., Geologic and hydrologic investigations of a potential nuclear waste disposal site at Yucca Mountain, southern Nevada: U.S. Geological Survey Bulletin 1790, p. 51–85.

Harrill, J.R., 1982, Ground-water storage depletion in Pahrump Valley, Nevada-California, 1962–75: U.S. Geological Survey Water-Supply Paper 2279, 53 p.

Harrill, J.R., Gates, J.S., and Thomas, J.M., 1988, Major ground-water flow systems in the Great Basin region of Nevada, Utah, and adjacent states: U.S. Geological Survey Hydrologic Investigations Atlas HA–694–C, 2 sheets, scale 1:1,000,000.

Harrill, J.R. and Prudic, D.E., 1998, Aquifer systems in the Great Basin region of Nevada, Utah, and adjacent states—Summary report: U.S. Geological Survey Professional Paper 1409–A, 66 p.

Holmes, W.F., and Thiros, S.A., 1990, Ground-water hydrology of the Pahvant Valley and adjacent areas, Utah: Utah Department of Natural Resources Technical Publication 98, 64 p.

Hofstra, A.H., and Cline, J.S., 2000, Characteristics and models for Carlin-type gold deposits: Reviews in Economic Geology, v. 13, p. 163–220.

Hood, J.W., and Waddell, K.M., 1969, Hydrologic reconnaissance of Deep Creek Valley, Tooele and Juab Counties, Utah and Elko and White Pine Counties, Nevada: State of Utah Department of Natural Resources Technical Publication 24, 54 p.

Kariya, K.A., Roark, D.M., Hanson, K.M., 1994, Hydrology of Cache Valley, Cache County, Utah, and adjacent part of Idaho, with emphasis on simulation of ground-water flow, Utah Department of Natural Resources Technical Publication 108, 120 p.

Kirk, S.T., and Campana, M.E., 1990, A deuterium-calibrated groundwater flow model of a regional carbonate-alluvial system: Journal of Hydrology, v. 119, p. 357–388.

Lambert, P.M., 1995, Numerical simulation of ground-water flow in basin-fill material in Salt Lake Valley, Utah: Utah Department of Natural Resources Technical Publication 110–B, 58 p.

Langenheim, V.E., Grow, J.A., Jachens, R.C., Dixon, G.L., and Miller, J.J., 2001, Geophysical constraints on the location and geometry of the Las Vegas Valley shear zone, Nevada: Tectonics, v. 20, p. 189–209.

Lipman, P.W., 1984, The roots of ash flow calderas in western North America—windows into the tops of granitic batholiths: Journal of Geophysical Research, v. 89, p. 8,801–8,841.

Luckey, R.R., Tucci, Patrick, Faunt, C.C., Ervin, E.M., Steinkampf, W.C., D’Agnese, F.A., and Patterson, G.L., 1996, Status of understanding of the saturated-zone ground-water flow system at Yucca Mountain, Nevada, as of 1995: U.S. Geological Survey Water-Resources Investigations Report 96–4077, 71 p.

Lundmark, K.W., 2007, Regional water budget accounting and uncertainty analysis model using a deuterium-calibrated discrete state compartment model: White Pine County, Nevada and adjacent areas in Nevada and Utah: Reno, University of Nevada, M.S. thesis, 177 p.

Manning, A.H., and Caine, J.S., 2007, Groundwater noble gas, age, and temperature signatures in an alpine watershed: Valuable tools in conceptual model development: Water Resources Research, v. 43, W04404, 16 p., doi:10.1029/2006WR005349, accessed November 6, 2008 at http://www.agu.org/pubs/crossref/2007/2006WR005349.shtml.

Mathey, Sharon B., ed., 1998, National Water Information System (NWIS): U.S. Geological Survey Fact Sheet 027–98, 2 p., accessed January 14, 2009 at http://pubs.usgs.gov/fs/FS-027-98/fs-027-98.pdf.

McKee, E.H., Wickham, T.A., and Wheeler, K.L., 1998, Evaluation of faults and their effect on ground-water flow southwest of Frenchman Flat, Nye and Clark Counties, Nevada—A digital database: U.S. Geological Survey Open-File Report 98–580, 16 p., 4 plates.

Mower, R.W., 1982, Hydrology of the Beryl-Enterprise Area, Escalante Desert, Utah, with emphasis on ground water: Utah Department of Natural Resources Technical Publication 73, 66 p.

Mower, R.W., and Cordova, R.M., 1974, Water resources of the Milford area, Utah, with emphasis on ground water: Utah Department of Natural Resources Technical Publication 43, 106 p.

Potter, C.J., Sweetkind, D.S., Dickerson, R.P., and Killgore, M.L., 2002, Hydrostructural maps of the Death Valley regional flow system, Nevada and California, version 1.0: U.S. Geological Survey Miscellaneous Field Studies Map MF–2372, 2 sheets, scale 1:350,000, with pamphlet.

PRISM Climate Group, Oregon State University, 2007, Digital climate data, accessed May 2, 2007, at http://www.ocs.oregonstate.edu/prism/index.phtml.

Prudic, D.E., Harrill, J.R., and Burbey, T.J., 1995, Conceptual evaluation of regional ground-water flow in the Carbonate-Rock Province of the Great Basin, Nevada, Utah, and adjacent states: U.S. Geological Survey Professional Paper 1409–D, 102 p.

Rowley, P.D., 1998, Cenozoic transverse zones and igneous belts in the Great Basin, western United States—Their tectonic and economic implications, *in* Faulds, J.E., and Stewart, J.H., eds., Accommodation zones and transfer zones; The regional segmentation of the Basin and Range province: Geological Society of America Special Paper 323, p. 195–228.

Rush, F.E., 1968, Index of hydrographic areas in Nevada: Nevada Division of Water Resources Information Report 6, 38 p.

Smith, D.L., Gans, P.B., and Miller, E.L., 1991, Palinspastic restoration of Cenozoic extension in the central and eastern Basin and Range province at latitude 39–40 degrees N, *in* Geology and ore deposits of the Great Basin, Reno NV: Geological Society of Nevada Symposium Proceedings, p. 75–86.

Smith, R.L., and Bailey, R.A., 1968, Resurgent calderas: Geological Society of America Memoir 116, p. 613–662.

Steinkampf, W.C., and Werrell, W.L., 2001, Ground-water flow to Death Valley as inferred from the chemistry and geohydrology of selected springs in Death Valley National Park, California and Nevada: U.S. Geological Survey Water-Resources Investigations Report 98–4114, 37 p.

Stephens, J.C., 1974, Hydrologic reconnaissance of the northern Great Salt Lake Desert and summary hydrologic reconnaissance of northwestern Utah: State of Utah Department of Natural Resources Technical Publication 42, 55 p.

Stewart, J.H., 1998, Regional characteristics, tilt domains, and extensional history of the later Cenozoic Basin and Range province, western North America, *in* Faulds, J.E., and Stewart, J.H., eds., Accommodation zones and transfer zones, the regional segmentation of the Basin and Range Province: Geological Society of America Special Paper 323, p. 47–74.

Sweetkind, D.S., Belcher, W.R., Faunt, C.C., and Potter, C.J., 2004, Geology and hydrogeology, Chap. B of Belcher, W.R., ed., 2004, Death Valley regional ground-water flow system, Nevada and California—Hydrogeologic framework and transient ground-water flow model: U.S. Geological Survey Scientific Investigations Series Report 1171, p. 21–98.

Thiros, S.A., Stolp, B.J., Hadley, H.K., and Steiger, J.I., 1996, Hydrology and simulation of ground-water flow in Juab Valley, Juab County, Utah: Utah Department of Natural Resources Technical Publication 114, 100 p.

Thomas, J.M., Calhoun, S.C., and Apambire, W.B., 2001, A deuterium mass-balance interpretation of groundwater sources and flows in southeastern Nevada: Desert Research Institute Publication no. 41169, p. 46.

Thomas, J.M., Mason, J.L., and Crabtree, J.D., 1986, Ground-water levels in the Great Basin region of Nevada, Utah, and adjacent states: U.S. Geological Survey Hydrologic Investigations Atlas HA–694–B, 2 sheets.

Thyne, G.D., Gillespie, J.M., and Ostdick, J.R, 1999, Evidence for interbasin flow through bedrock in the southeastern Sierra Nevada: Geological Society of America Bulletin, v. 111, p. 1,600–1,616.

Tiedeman, C.R., Goode, D.J., and Hseih, P.A., 1998, Characterizing a ground water basin in a New England mountain and valley terrain: Ground Water, v. 36, no. 4, p. 611–620.

Toth, Jozsef, 1963, A theoretical analysis of groundwater flow in small drainage basins: Journal of Geophysical Research, v. 68, no. 8, p. 2,354–2,356, doi:10.1029/JZ068i008p02354, accessed October 31, 2008 at http://www.agu.org/journals/jz/v068/i008/JZ068i008p02354/.

U.S. Geological Survey EROS Data Center, 1999, 1 arc-second (30-meter) National Elevation Dataset: U.S. Geological Survey dataset, accessed September 15, 2008 at http://ned.usgs.gov/.

U.S. Geological Survey, 1999, National Hydrography Dataset: U.S. Geological Survey Fact Sheet 106–99, accessed March 2007 at http://erg.usgs.gov/isb/pubs/factsheets/fs10699.html.

Welch, A.H., Bright, D.J., and Knochenmus, L.A., eds., 2007, Water resources of the Basin and Range carbonate-rock aquifer system, White Pine County, Nevada, and adjacent areas in Nevada and Utah: U.S. Geological Survey Scientific Investigations Report 2007–5261, 96 p.

Wernicke, B.P., 1992, Cenozoic extensional tectonics of the U.S. Cordillera, *in* Burchfiel, B.C., Lipman, P.W., and Zoback, M.L., eds., The Cordilleran orogen, conterminous U.S.: Boulder, Colorado, Geological Society of America, Geology of North America, v. G–3, p. 553–581.

Wernicke, B.P., Guth, P.L., and Axen, G.J., 1984, Tertiary extensional tectonics in the Sevier thrust belt of southern Nevada, *in* Lintz, J.P., ed., Western geological excursions: Mackay School of Mines, Reno, University of Nevada, Geological Society of America, Cordilleran Section, Field Trip Guidebook, p. 473–510.

Wilson, J.W., 2007, Water-level surface maps of the carbonate-rock and basin-fill aquifers in the Basin and Range carbonate-rock aquifer system, White Pine County, Nevada, and adjacent areas in Nevada and Utah: U.S. Geological Survey Scientific Investigations Report 2007–5089, 10 p., 2 pls.

Winograd, I.J., and Pearson, F.J., 1976, Major carbon 14 anomaly in a regional carbonate aquifer: possible evidence for megascale channeling, south central Great Basin: Water Resources Research, v. 12, p. 1,125–1,143.

Winograd, I.J., and Thordarson, W., 1975, Hydrogeologic and hydrochemical framework, south-central Great Basin, Nevada-California, with special reference to the Nevada Test Site: U.S. Geological Survey Professional Paper 712–C, 126 p.

Chapter D: Estimated Groundwater Budgets

By Melissa D. Masbruch, Victor M. Heilweil, Susan G. Buto, Lynette E. Brooks, David D. Susong, Alan L. Flint, Lorraine E. Flint, and Philip M. Gardner

An important component of the Great Basin carbonate and alluvial aquifer system (GBCAAS) conceptual model is the quantification of groundwater fluxes moving through the region. The groundwater budgets presented in this report provide an estimate of recharge and discharge within the GBCAAS study area.

Detailed budgets are presented for average annual conditions prior to substantial groundwater development that began in the 1940s, as well as for the year 2000. In addition, annual well withdrawals are estimated for 1940–2006. In most hydrographic areas (HAs), current conditions are assumed to be representative of predevelopment conditions because groundwater development has been minimal. Predevelopment recharge estimates, however, do include the effects of surface-water development, including imported water in irrigated areas. Much of this surface-water development occurred from the 1850s to 1940; data and reports prior to 1940 are sparse. This lack of data precludes analysis of hydrologic conditions prior to surface-water development. Prior to the 1940s, recharge from irrigation with surface water was a significant part of the budget only in the Great Salt Lake groundwater flow system (38) (specifically in Utah Valley Area, HA 265; Salt Lake Valley, HA 267; East Shore Area, HA 268; Cache Valley, HA 272; and Malad-Lower Bear River Area, HA 273). Groundwater development since the 1940s has led to increased recharge, generally as groundwater irrigation return flow. In addition, surface-water development from the Colorado River and Lake Mead since the early 1940s has led to increased groundwater recharge in Las Vegas Valley (HA 212).

Because significant groundwater development in the GBCAAS study area began in the 1940s, conditions prior to 1940 represent the predevelopment budgets presented in this report. The primary objectives of this chapter are to present estimates of (1) groundwater recharge- and discharge-budgets for predevelopment conditions, and (2) the effects of groundwater development (well withdrawals) during 1940–2006 on groundwater budgets.

The current study presents an alternative groundwater-budget conceptualization to previous groundwater studies regarding groundwater recharge and discharge in the mountain block. Beginning with groundwater studies in the 1940s, recharge estimates were based on a percentage of precipitation in the mountains calibrated to groundwater discharge in the adjacent basin-fill aquifer (Maxey and Eakin, 1949). These early studies did not consider groundwater discharge in the mountain block and, therefore, they provide an estimate of "net" recharge. More recent spatially distributed water-balance recharge methods estimate "total" recharge in the mountains, a fraction of which becomes groundwater discharge to mountain streams and springs and is removed from the groundwater system. If groundwater discharge in the mountain block is not removed from the groundwater budget, estimates of groundwater discharge from an HA as subsurface outflow may be overestimated. The earlier "net" recharge estimates have typically been used by regulatory agencies for developing HA-based estimates of safe or perennial yield for allocating water rights. The newer spatially distributed "total" recharge estimates are typically higher, and should not be used for managing water resources without also considering losses associated with groundwater discharge in the mountain block.

Organization of Groundwater Budgets

The GBCAAS study area comprises 165 HAs, which typically define a topographic basin including the surrounding mountains (pl. 1). Most of the previous groundwater-budget estimates are for individual or groups of HAs. Because these previous estimates usually apply to individual HAs and because socio-political, water-related decisions often are based on HA boundaries, an HA-level approach was used to compile previous estimates and to compare previous estimates with current study estimates. For most HAs, previous groundwater-budget estimates were developed only for the basin part of an HA and did not include the surrounding mountains (except as a source of recharge to the basin). This study estimates groundwater budgets for entire HAs and, therefore, the current study estimates are not directly comparable to the previous studies' estimates for partial HAs.

The preparation of the groundwater budgets for each HA and groundwater flow system included compiling all previously published estimates (Auxiliary 2) and developing current study estimates for each budget component, except subsurface inflow and outflow. The budget component data are presented in tables by HA and groundwater flow system in the Auxiliary 3 files. Appendix 4 presents current study recharge estimates for predevelopment conditions and ranges of previously reported total recharge estimates by HA. Appendix 5 presents current study discharge estimates for predevelopment conditions and ranges of previously reported total discharge estimates by HA. More recent (year 2000) groundwater-budget estimates for each HA are presented in Appendix 7.

The HA-based groundwater-budget estimates in Appendixes 4, 5, and 7 were then used to develop budgets for each of the 17 groundwater flow systems of the GBCAAS study area, defined in Chapter C of this report (pl. 1). To determine the groundwater budgets for these groundwater flow systems, recharge and discharge components for each HA within the groundwater flow system were summed. The predevelopment groundwater flow system recharge and discharge budgets are presented in tables D–1 and D–2, respectively, along with ranges of previously reported recharge and discharge. Subsurface flow between groundwater flow systems was not estimated for the current study. For comparison purposes, the previously reported recharge and discharge estimates, therefore, were adjusted to also exclude subsurface flow. Previously reported estimates of subsurface inflow are listed by HA and groundwater flow system in Auxiliaries 3E and 3F, respectively. Previously reported estimates of subsurface outflow are listed by HA and groundwater flow system in Auxiliaries 3M and 3N, respectively. Recent (2000) groundwater flow system budgets are presented in table D–3.

Predevelopment Groundwater Recharge

Groundwater Recharge Processes

Precipitation within the GBCAAS study area is the primary source of groundwater recharge. The majority of precipitation comes as winter snowfall on the mountain ranges, with lesser amounts falling as rain. Infiltration of precipitation and snowmelt within the mountain block provides (1) discharge to mountain springs and baseflow to mountain streams; (2) inflow to the adjacent basin fill, also referred to as mountain-block recharge (Wilson and Guan, 2004); and (3) recharge to consolidated bedrock aquifers, which typically follows deeper and longer flow paths to regional discharge locations, including large springs and areas of evapotranspiration (fig. C–1). The majority of groundwater recharge within the study area is assumed to occur in the higher altitude mountain ranges as direct infiltration of precipitation (in-place recharge), which, in part, is controlled by bedrock permeability in the

Table D–1. Current study annual groundwater-recharge estimates for predevelopment conditions and ranges of previously reported estimates of annual groundwater recharge for each of the 17 groundwater flow systems within the Great Basin carbonate and alluvial aquifer system study area.

[All values (except Flow system area and In-place recharge rate) are in acre-feet per year rounded to two significant figures. Estimated error in all values is ±50 percent. Groundwater flow system name: number in parentheses following name is groundwater flow system number. Flow system area: mi², square miles. In-place recharge rate: ft/yr, feet per year. Subsurface inflow: groundwater recharge by subsurface inflow between groundwater flow systems considered possible, likely, or unlikely based on information given on plate 2. Previously reported total groundwater recharge minimum and maximum: totals adjusted to exclude reported recharge by subsurface inflow (see Auxiliary 3F). Abbreviations: N/A, Not Applicable; —, no estimate]

Groundwater flow system name	Flow system area (mi²)	Current study groundwater recharge estimates							Previously reported estimates	
		In-place recharge rate (ft/yr)	In-place recharge	Runoff	Mountain stream baseflow	Imported surface water	Subsurface inflow	Total groundwater recharge	Total groundwater recharge (minimum)	Total groundwater recharge (maximum)
Humboldt System (7)	10,375	0.04	240,000	120,000	4,400	20,000	Possible	380,000	310,000	840,000
Monte Cristo Valley (23)	282	1.33	1,200	63	0	—	Possible	1,300	400	3,300
South-Central Marshes (24)	5,790	0.06	50,000	4,700	5	—	Possible	55,000	27,000	120,000
Grass Valley (25)	598	0.63	16,000	1,400	0	—	Possible	17,000	9,100	31,000
Northern Big Smoky Valley (26)	1,313	0.29	58,000	28,000	1,400	—	Possible	87,000	52,000	78,000
Diamond Valley System (27)	3,156	0.12	94,000	15,000	390	—	Unlikely	110,000	42,000	180,000
Death Valley System (28)[1]	17,362	0.02	100,000	4,000	28	—	Possible	100,000	50,000	190,000
Newark Valley System (29)	1,446	0.26	33,000	1,500	0	—	Possible	34,000	16,000	72,000
Railroad Valley System (30)	4,120	0.09	65,000	2,900	60	—	Likely	68,000	49,000	140,000
Independence Valley System (32)	1,040	0.36	26,000	2,500	0	—	Possible	28,000	30,000	110,000
Ruby Valley System (33)	1,300	0.29	64,000	14,000	750	—	Possible	79,000	60,000	170,000
Colorado System (34)	16,508	0.02	240,000	9,600	370	—	Possible	250,000	100,000	540,000
Goshute Valley System (35)	3,658	0.10	120,000	5,500	360	—	Possible	130,000	69,000	230,000
Mesquite Valley (36)	457	0.82	1,900	14	0	—	Possible	1,900	1,000	5,500
Great Salt Lake Desert System (37)	18,849	0.02	440,000	31,000	640	—	Possible	470,000	330,000	480,000
Great Salt Lake System (38)	13,823	0.03	1,000,000	260,000	110,000	960,000	Unlikely	2,300,000	1,700,000	1,900,000
Sevier Lake System (39)	10,475	0.04	310,000	71,000	11,000	12,000	Unlikely	400,000	320,000	320,000
Study area total			**2,900,000**	**570,000**	**130,000**	**990,000**	**N/A**	**4,500,000**	**3,200,000**	**5,400,000**

[1]Penoyer Valley, which Harrill and others (1988) defined as a separate groundwater flow system, is included in the Death Valley System in this report.

mountain blocks. This assumption is supported by analysis of environmental tracers and coupled flow/thermal modeling as part of a detailed groundwater study in Salt Lake Valley (HA 267) (Manning and Solomon, 2003; 2005).

Previous groundwater studies in the eastern Great Basin, beginning with Maxey and Eakin (1949), generally developed groundwater budgets focused on the basin-fill (valley) portion of each HA, where groundwater was being developed as a resource. In recent years, groundwater development, targeting permeable consolidated rock beneath the unconsolidated basin-fill deposits and in the surrounding mountains, has increased. Also, a new class of spatially distributed recharge estimation techniques utilizing water-balance methods has been developed that provides estimates for "total" recharge of precipitation in a watershed or HA (Flint and Flint, 2007a; 2007c; Hevesi and others, 2003; Leavesley and others, 1983; Markstrom and others, 2008). This is in contrast to the earlier estimation techniques, which were typically calibrated to groundwater discharge in the valleys, and provided estimates of "net" recharge to the unconsolidated basin-fill aquifer. These earlier methods did not consider groundwater discharge within the mountain block as stream baseflow and spring discharge, nor the subsequent recharge of a portion of this water as infiltration of runoff to unconsolidated basin-fill deposits. The current GBCAAS study considers all forms of recharge to and discharge from the groundwater system, including the surrounding mountains. This can be illustrated by considering the fate of recharge from direct infiltration of mountain precipitation and subsurface inflow from adjacent HAs to permeable consolidated rock of the mountain block (R1 and R4 of fig. D–1). Part of this recharge moves directly through the subsurface from the mountain block into the adjacent unconsolidated basin fill (fig. D–1). Another part of this recharge becomes groundwater discharge to mountain streams and springs (D1 of fig. D–1). A fraction of this mountain-block groundwater discharge is consumptively

Table D–2. Current study annual groundwater-discharge estimates for predevelopment conditions and ranges of previously reported estimates of annual groundwater discharge for each of the 17 groundwater flow systems within the Great Basin carbonate and alluvial aquifer system study area.

[All values (except flow system area) are in acre-feet per year rounded to two significant figures. Estimated error in all values is ±30 percent. Groundwater flow system name: number in parentheses following name is groundwater flow system number. Flow system area: mi², square miles. Subsurface outflow: groundwater discharge to subsurface groundwater outflow between groundwater flow systems that is considered possible, likely, or unlikely based on information given on plate 2. Previously reported total groundwater discharge minimum and maximum: totals adjusted to exclude groundwater discharge by subsurface outflow (see Auxiliary 3N). Abbreviations: ETg, groundwater evapotranspiration; N/A, Not Applicable; —, no estimate]

Groundwater flow system name	Flow system area (mi²)	Current study groundwater discharge estimates							Previously reported estimates	
		ETg	Mountain streams	Basin-fill streams/ lakes/ reservoirs	Springs	Sub-surface outflow	Adjustment to natural discharge for well withdrawals	Total groundwater discharge	Total groundwater discharge (minimum)	Total groundwater discharge (maximum)
Humboldt System (7)	10,375	240,000	15,000	14,000	28,000	Possible	600	300,000	[2]120,000	[2]170,000
Monte Cristo Valley (23)	282	400	0	0	0	Likely	0	400	400	400
South-Central Marshes (24)	5,790	58,000	46	0	4,800	Possible	0	63,000	63,000	63,000
Grass Valley (25)	598	7,500	0	0	1,500	Likely	0	9,000	—	—
Northern Big Smoky Valley (26)	1,313	62,000	4,700	0	2,300	Possible	0	69,000	64,000	77,000
Diamond Valley System (27)	3,156	44,000	1,500	0	12,000	Likely	0	58,000	53,000	60,000
Death Valley System (28)[1]	17,362	66,000	280	61	35,000	Possible	0	100,000	86,000	110,000
Newark Valley System (29)	1,446	22,000	0	0	9,700	Possible	0	32,000	[3]20,000	[3]72,000
Railroad Valley System (30)	4,120	65,000	600	300	32,000	Possible	0	98,000	95,000	100,000
Independence Valley System (32)	1,040	26,000	0	0	3,300	Possible	0	29,000	[3]28,000	[3]130,000
Ruby Valley System (33)	1,300	64,000	2,500	0	12,000	Possible	0	78,000	[3]76,000	[3]180,000
Colorado System (34)	16,508	62,000	3,700	39,000	130,000	Possible	0	230,000	160,000	210,000
Goshute Valley System (35)	3,658	83,000	3,600	0	45,000	Possible	0	130,000	120,000	180,000
Mesquite Valley (36)	457	2,200	0	0	0	Unlikely	0	2,200	2,200	2,200
Great Salt Lake Desert System (37)	18,849	330,000	4,500	0	110,000	Possible	1,600	450,000	370,000	450,000
Great Salt Lake System (38)	13,823	430,000	370,000	570,000	520,000	Possible	260,000	2,200,000	1,800,000	2,000,000
Sevier Lake System (39)	10,475	210,000	40,000	37,000	47,000	Possible	71,000	400,000	[2]350,000	[2]350,000
Study area total		**1,800,000**	**450,000**	**660,000**	**990,000**	**N/A**	**330,000**	**4,200,000**	**3,400,000**	**4,200,000**

[1]Penoyer Valley, which Harrill and others (1988) defined as a separate groundwater flow system, is included in the Death Valley System in this report.

[2]Previously reported estimates are lower than current study estimates because there were no previously reported total groundwater-budget estimates for all of the HAs within this flow system.

[3]Previously reported estimates include those by Nichols (2000), which are suspected to be too high (did not use Nichols (2000) in calculations of current study estimates; see text for explanation).

lost as evapotranspiration, both in the mountains and as this water enters the valley in streams and canals. A fraction of the remaining mountain-block groundwater discharge, combined with surface-water runoff from precipitation in the mountains, becomes recharge to the unconsolidated basin fill (R2 and R3 of fig. D–1). This water ultimately discharges naturally in the valley lowlands as evapotranspiration and basin-fill springs and streams (D2 and D3 of fig. D–1), well withdrawals (D4 of fig. D–1), or subsurface outflow (D5 of fig. D–1). To include the partial loss of in-place recharge as groundwater discharge in the mountains to streams and springs, the newer spatially distributed recharge methods often yield higher "total" recharge estimates for an HA than the previous Maxey-Eakin type of "net" basin-fill recharge estimates. The Nevada State Engineer bases water rights appropriations by HA on perennial yield quantities that have typically been based on the earlier Maxey-Eakin type of recharge estimates. The Nevada Division of Water Resources (2010) definition of perennial yield is

> *The amount of usable water from a groundwater aquifer that can be economically withdrawn and consumed each year for an indefinite period of time. It cannot exceed the natural recharge to the aquifer and ultimately is limited to maximum amount of discharge that can be utilized for beneficial use.*

The newer spatially distributed recharge estimates may cause over-appropriations if the consumptive losses of groundwater discharge in the mountains are not also considered.

The spatial distribution of average annual 1940–2006 precipitation shown on figure D–2 is used for estimating both predevelopment and recent (2000) recharge for the study area (see "Basin Characterization Model" section below). The precipitation data were based on the PRISM (Parameter-elevation Regressions on Independent Slopes Model) 4,000-m grid (Daly and others, 1994, 2008) resampled to a 270-m grid as

Table D–3. Predevelopment and recent (2000) groundwater-budget estimates for each of the 17 groundwater flow systems within the Great Basin carbonate and alluvial aquifer system study area.

[All values (except flow system area) are in acre-feet per year rounded to two significant figures. Estimated error in recharge values is ±50 percent. Estimated error in discharge values is ± 30 percent. Values in blue are for predevelopment conditions. Values in red are for recent (2000) conditions. Groundwater flow system name: number in parantheses following name is groundwater flow system number. Flow system area: mi², square miles; Abbreviations —, no estimate]

Groundwater flow system name	Flow system area (mi²)	Groundwater recharge for pre-development conditions	Recharge from unconsumed irrigation and public supply water from well withdrawals (2000)	Groundwater recharge for recent (2000) conditions	Groundwater discharge for pre-development conditions	Well withdrawals (2000)	Decrease in natural discharge and/or storage (net well withdrawals) (2000)	Minimum decrease in groundwater storage (2000)	Groundwater discharge for recent (2000) conditions
Humboldt System (7)	10,375	380,000	[2]25,000	400,000	300,000	200,000	180,000	—	320,000
Monte Cristo Valley (23)	282	1,300	6	1,300	400	20	14	—	410
South-Central Marshes (24)	5,790	55,000	16,000	71,000	63,000	52,000	36,000	—	79,000
Grass Valley (25)	598	17,000	3	17,000	9,000	10	7	—	9,000
Northern Big Smoky Valley (26)	1,313	87,000	[2]270	87,000	69,000	5,900	5,600	—	69,000
Diamond Valley System (27)	3,156	110,000	22,000	130,000	58,000	74,000	52,000	24,000	100,000
Death Valley System (28)[1]	17,362	100,000	16,000	120,000	100,000	55,000	38,000	9,300	130,000
Newark Valley System (29)	1,446	34,000	2,000	36,000	32,000	6,700	4,700	—	34,000
Railroad Valley System (30)	4,120	68,000	760	69,000	98,000	2,500	1,700	—	99,000
Independence Valley System (32)	1,040	28,000	2,800	31,000	29,000	9,400	6,600	—	32,000
Ruby Valley System (33)	1,300	79,000	1,800	81,000	78,000	5,900	4,100	—	80,000
Colorado System (34)	16,508	250,000	[3]120,000	370,000	230,000	170,000	48,000	—	350,000
Goshute Valley System (35)	3,658	130,000	3,400	130,000	130,000	12,000	8,100	—	130,000
Mesquite Valley (36)	457	1,900	3,900	5,800	2,200	13,000	9,100	—	6,100
Great Salt Lake Desert System (37)	18,849	470,000	7,900	480,000	450,000	26,000	19,000	—	460,000
Great Salt Lake System (38)	13,823	2,300,000	160,000	2,500,000	2,200,000	520,000	360,000	—	2,400,000
Sevier Lake System (39)	10,475	400,000	93,000	490,000	400,000	310,000	220,000	34,000	520,000
Study area total		**4,500,000**	**[3]470,000**	**5,000,000**	**4,200,000**	**[4]1,500,000**	**990,000**	**67,000**	**4,800,000**

[1]Penoyer Valley, which Harrill and others (1988) defined as a separate groundwater flow system, is included in the Death Valley System in this report.

[2]Adjusted to exclude well withdrawals for mining operations, which are assumed not to be applied as irrigation and therefore do not contribute to groundwater recharge.

[3]Amount includes an additional 30,000 acre-ft of recharge from injected Colorado River water [Nevada Division of Water Resources (NDWR), Water Rights Section, pumpage inventory] and 41,000 acre-ft of recharge from imported Colorado River Water (calculated as 10 percent of total imported Colorado water (440,000 acre-ft reported in NDWR pumpage inventory) minus amount injected (30,000 acre-ft)) in HA 212; imported surface water was included in this category because HA 212 is the only HA with postdevelopment surface-water importation.

[4]Includes 3,130 acre-ft of well withdrawals that were not accounted for in total study area well withdrawals in Auxiliary 4; totals do not match as this extra amount causes rounding of total in this table to increase by 100,000 acre-ft.

Groundwater budget = R1 - D1 + R2 + R3 + R4 - D2 - D3 - D4 - D5

R1 = In-place recharge from precipitation
R2 = Recharge from perennial and ephemeral streams (includes mountain stream baseflow, runoff, recharge from canals, and recharge from irrigation)
R3 = Recharge from imported surface water (includes recharge from canals, and recharge from irrigation)
R4 = Recharge from subsurface inflow from an upgradient hydrographic area

D1 = Discharge to mountain streams and mountain springs
D2 = Discharge to evapotranspiration
D3 = Discharge to basin-fill springs and basin-fill streams/lakes/reservoirs
D4 = Discharge to well withdrawals
D5 = Discharge to subsurface outflow to a downgradient hydrographic area

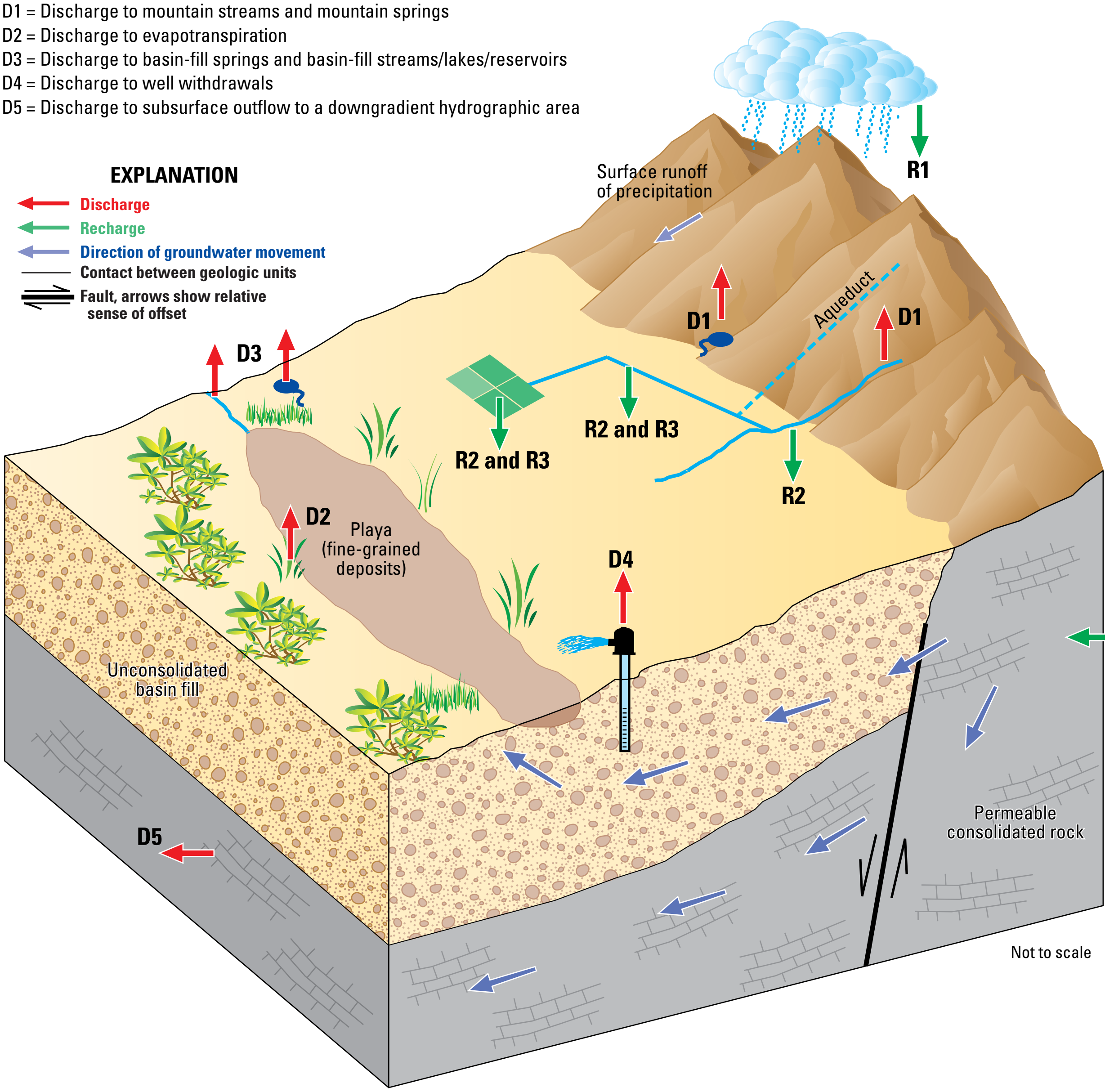

Figure D–1. Schematic diagram showing conceptualization of groundwater budget components and budget calculation for the Great Basin carbonate and alluvial aquifer system study area.

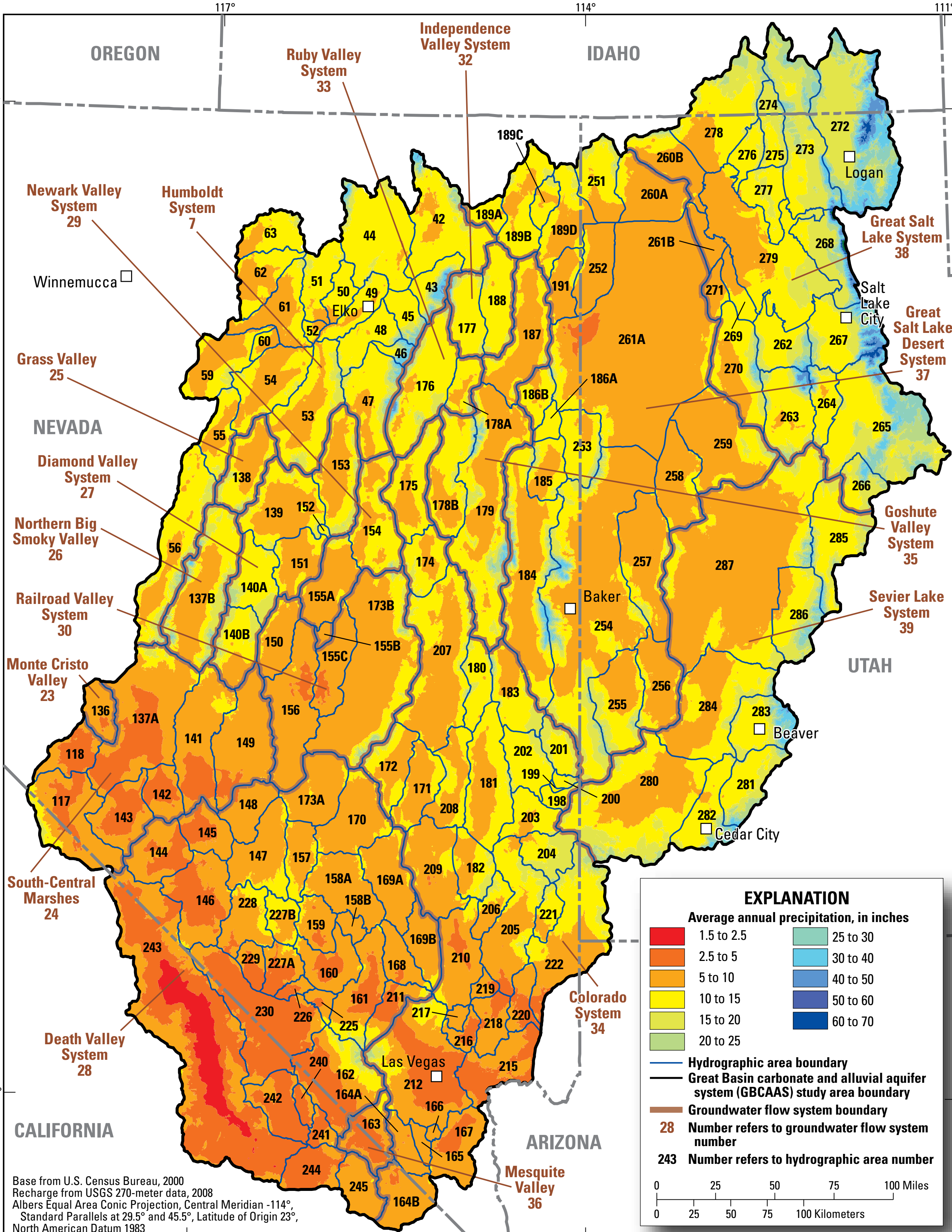

Figure D–2. Distribution of 1940–2006 average annual precipitation used as input for the Basin Characterization Model for the Great Basin carbonate and alluvial aquifer system study area.

described in Appendix 3. This 67-year period was selected for estimating predevelopment recharge because there is limited climatic data available prior to the 1940s. The highest amounts of precipitation (as much as 70 in/yr) are concentrated over the higher altitude mountains within the study area. These high precipitation areas primarily occur along the northern Wasatch Front in the Great Salt Lake groundwater flow system (38) and also in various other isolated mountain ranges throughout the study area. The driest areas are in the southwestern part of the study area in the Death Valley groundwater flow system (28), including portions of the Amargosa Desert (HA 230), Death Valley (HA 243), and Valjean Valley (HA 244), which only receive about 5 in/yr of precipitation (Appendix 2).

Estimated annual average precipitation for the study area was quite variable between 1940 and 2006, ranging from 6.7 in/yr (1953) to 16.7 in/yr (2005) with a mean of 10.7 ± 4.8 in/yr (2σ) for the 67-year period (fig. D–3). The driest periods (less than 8 in/yr) occurred in 1953, 1959–60, 1966, 1974, and 2002. The wettest periods (greater than 14 in/yr) occurred in 1941, 1980, 1982–84, 1995, 1998, and 2005. The 1980s and 1990s were abnormally wet decades, having five of the eight wettest years and none of the driest years in the 67-year period.

Precipitation that does not infiltrate into the subsurface or is not consumed by evapotranspiration and sublimation in the mountain block becomes runoff. The majority of runoff generated in the mountains flows into adjacent basins. A portion of this runoff recharges the unconsolidated deposits as infiltration beneath stream channels, irrigation canals, and irrigated fields (fig. D–1). Recharge from runoff occurs predominantly through coarser deposits along the margins of each basin.

In addition to runoff from precipitation, streamflow at the mountain front also includes baseflow. This water enters the groundwater system as in-place recharge from precipitation in the mountains and then discharges to mountain streams. A portion of this baseflow subsequently recharges basin-fill deposits as infiltration beneath the stream channel, canals, or irrigated fields.

Recharge from irrigation return flow of imported surface water originating from outside an HA also occurs in some parts of the GBCAAS study area. This water includes natural streamflow (such as rivers and streams flowing from upgradient HAs or from areas outside of the study area) and (or) imported surface water associated with engineered transbasin diversions that originate outside the HA or study area. The analysis of groundwater recharge, therefore, includes recharge from this imported surface water along streams, canals, and from irrigation.

Groundwater recharge to each HA also may include subsurface inflow (figs. C–1 and D–1). Recharge from subsurface inflow (or interbasin flow) is derived from groundwater that originates in upgradient areas and subsequently flows into downgradient areas through the subsurface in basin fill or consolidated rock. The amount of subsurface inflow depends on the hydraulic gradient across the HA or groundwater flow system boundary and the hydraulic conductivity and cross sectional area of the intervening bedrock and alluvium.

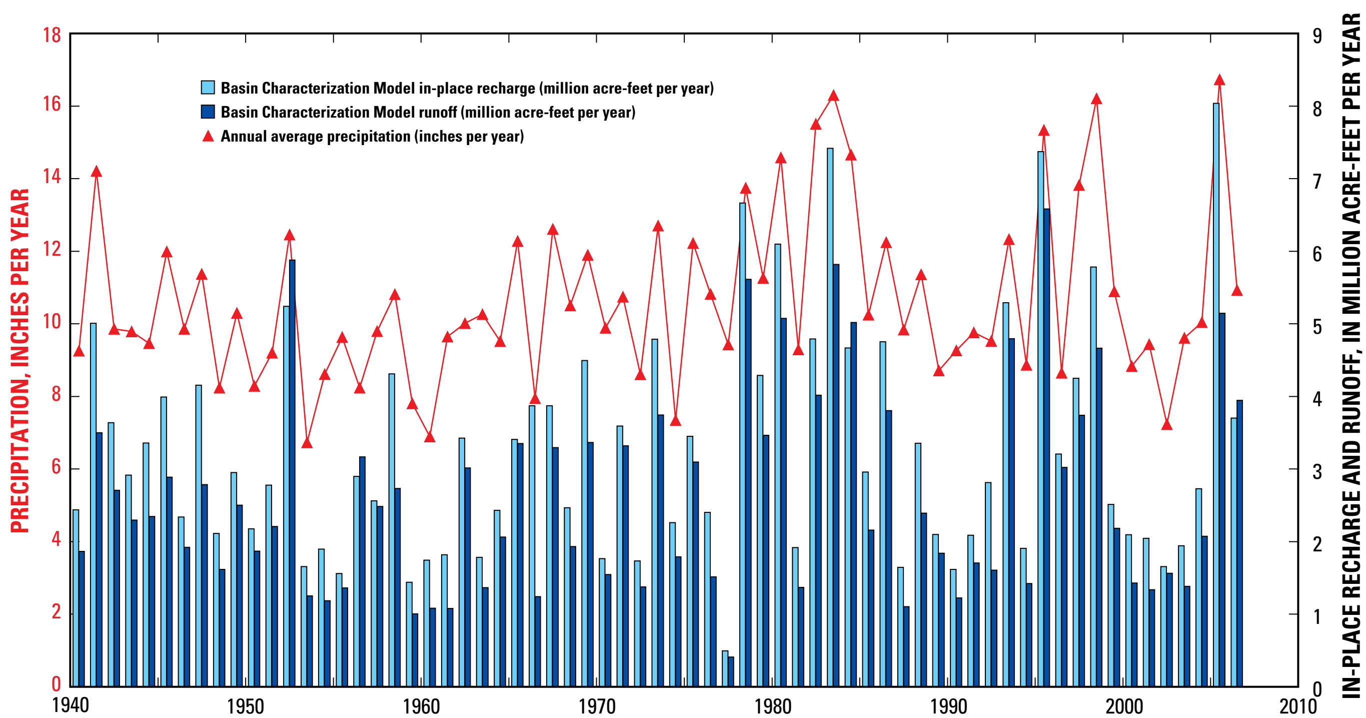

Figure D–3. Annual average precipitation and Basin Characterization Model in-place recharge and runoff for the Great Basin carbonate and alluvial aquifer system study area, water years 1940–2006.

Recharge from Precipitation

To provide estimates of annual recharge from direct infiltration of precipitation (in-place recharge) and runoff in a consistent manner across the large and climatically diverse GBCAAS study area, a regional-scale water balance method, known as the Basin Characterization Model (BCM; Flint and Flint, 2007a), was applied.

Basin Characterization Model

The BCM is a distributed-parameter water-balance accounting model used to identify areas having climatic and geologic conditions that allow for precipitation to become potential runoff or potential in-place recharge, and to estimate the amount of each. For this study, BCM calculations were made on a 270-m grid. In-place recharge is calculated as the volume of water per time that percolates through the soil zone past the root zone and becomes net infiltration to consolidated rock or unconsolidated deposits. Runoff is the volume of water per time that runs off the surface. Runoff may infiltrate the subsurface, undergo evapotranspiration further downslope, or become streamflow. The BCM does not track or route this streamflow runoff. Total groundwater recharge from precipitation is the sum of in-place recharge and the runoff that infiltrates into the subsurface (a percentage of total BCM runoff). An advantage of using a distributed-parameter water-balance model, such as BCM, is that the model identifies likely locations of the generation of runoff and in-place recharge accounting for the temporal and spatial distribution of precipitation, snowmelt, sublimation, evapotranspiration, soil-storage capacity, and saturated hydraulic conductivity.

Input data utilized by BCM is organized into (1) spatial data, including topography, soil porosity and coarseness for estimating soil-water storage, and saturated hydraulic conductivity for partitioning water between in-place recharge and runoff; and (2) time-series data, including precipitation and air temperature (Flint and Flint, 2007c) (Appendix 3). Other time-series input data, calculated separately, include (1) potential evapotranspiration, determined by calculations of solar radiation using topographic shading, cloudiness, and vegetation density data; and (2) snowpack accumulation and melting, modeled using precipitation and air-temperature data. A schematic illustrating the relation among the various BCM components of the model, along with specific model inputs and instructions for running the model, are given in Appendix 3.

A water-balance equation for each grid cell was developed using monthly estimates of precipitation, maximum and minimum air temperature, and potential evapotranspiration to calculate the monthly volume of runoff and in-place recharge for each grid cell. The volume of available water (AW) per unit area for soil-water storage, runoff, and in-place recharge is computed monthly for each cell in the 270-m grid on the basis of the following equation:

$$AW = P + S_m - PET - S_a + S_s \qquad \text{(D–1)}$$

where

P is the estimated precipitation for the grid cell,
S_m is the estimated snowmelt,
PET is potential evapotranspiration,
S_a is the estimated snow accumulation, and
S_s is the stored soil water from the previous month.

Energy and mass balance calculations for snow accumulation and sublimation were adapted by Lundquist and Flint (2006), as described in Appendix 3. Sublimation is controlled by radiant and turbulent fluxes and will vary from site to site. Unfortunately, sublimation rates within the study area are not well known. An initial estimate of about 0.2 in/month (5 mm/month) was applied on the basis of unpublished data from the Spring Mountains in the southwestern part of the GBCAAS study area (pl. 1); however, rates of about 0.5 in/month (12 mm/month) have been reported east of the study area in Colorado (Molotch and others, 2006). Snow accumulation that does not melt or sublimate during the month is carried over into the following month. This carry over is particularly important when temperatures are cold enough for precipitation to form snow. Because snow may persist for several months prior to melting, large volumes of water will become available for runoff and in-place recharge in the monthly time step in which melting occurs. Any remaining water in the soil zone above field capacity at the end of the month is added to soil-water storage (S_s) at the beginning of the next month. The form and amount of precipitation, the factors affecting evapotranspiration, and the mechanisms controlling drainage from the soil zone all dictate the locations where both in-place recharge and runoff occur within an HA.

Potential Evapotranspiration

Potential evapotranspiration (PET) is dependent on vegetation type and density, topography, and atmospheric conditions. Vegetation density and the percentage of bare-soil surfaces were both determined using the National Gap Analysis Program; (http://gapanalysis.nbii.gov/portal/server.pt). Daily PET values were calculated using the Priestley-Taylor Equation (Priestley and Taylor, 1972) and a detailed solar radiation model (Flint and Childs, 1987). The solar radiation model uses topographic shading, which is particularly important in mountainous terrain, and a correction for cloudiness (Flint and Flint, 2007b). PET is partitioned on the basis of vegetation cover to represent both bare-soil evaporation and transpiration due to vegetation. These results are averaged into monthly values for use in equation D–1. PET is highest during the warm summer months, which decreases the amount of water stored in the soil zone, and is lowest during the cooler winter months, which allows for increased water storage from precipitation and snowmelt. The average annual PET was approximately 55 in/yr for the study area and ranged from approximately 16 in/yr in the higher altitude mountain ranges along the Wasatch Front in Utah and in east-central Nevada to 95 in/yr on the basin floor of Death Valley (HA 243).

Soil-Water Storage

Where soils are present, thickness of the soil zone, porosity, and drainage characteristics determine how much water is stored in the soil zone. Soil properties (thickness, porosity, and particle-size distributions) used by BCM were obtained from U.S. Department of Agriculture Natural Resource Conservation Service's State Soil Geographic Database (STATSGO) and are discussed in Appendix 3. Drainage below the root zone occurs when sufficient water is available to exceed the soil-water storage capacity of the soil (or rock), and only then does the net infiltration have the potential to become groundwater recharge.

The soil-water storage in thin soils underlain by bedrock will quickly approach saturation during and (or) after a precipitation event if the saturated hydraulic conductivity of the bedrock is low. If the soil becomes saturated, runoff will occur. In locations with thick soil, a greater volume of water is needed to exceed the soil-water storage capacity of the root zone, and saturation and runoff are less likely. If the saturated hydraulic conductivity of the underlying consolidated rocks or basin-fill deposits is low, then gravity drainage occurs slowly and evapotranspiration has more time to remove stored water between infiltration events. If the saturated hydraulic conductivity of the underlying consolidated rocks or basin-fill deposits is high, more recharge can occur during and after an infiltration event. Also, if the soil-water storage capacity is high and the saturated hydraulic conductivity of the soil zone is low (for example, for finer grained silts and clays) then drainage through the root zone occurs slowly and evapotranspiration processes can remove more stored water between infiltration events.

Geology

One factor controlling in-place recharge in BCM is the saturated hydraulic conductivity of consolidated rocks in the mountains or basin-fill deposits on the alluvial fans and basin floor. When moisture in the soil zone exceeds field capacity, the rate of infiltration (in-place recharge) is set equal to the saturated hydraulic conductivity of the underlying consolidated rocks or basin-fill deposits, assuming a unit vertical hydraulic gradient. To account for spatial differences in saturated hydraulic conductivity, the geology of the GBCAAS study area was categorized into 57 geologic units for estimating saturated hydraulic conductivity (Appendix 3, table A3–1). These geologic units primarily are based on differences in permeability (rock and soil type) rather than geologic age. Estimates of saturated hydraulic conductivity values were based on a calibration of BCM runoff to gaged mountain stream discharge (Appendix 3, table A3–2). For an equal amount of available water (eq. D–1), areas with low saturated hydraulic conductivity will generate a higher percent of runoff relative to in-place recharge; areas with high saturated hydraulic conductivity will generate a smaller percent of runoff relative to in-place recharge.

Estimated saturated hydraulic-conductivity values used in BCM for the study area range from about 0.00016 ft/d for quartzite to about 13 ft/d for eolian sand (Appendix 3, table A3–1 and fig. D–4). These extremes, however, occur at the surface in only small portions of the study area. For the portion of the study area where in-place recharge is significant (0.1 ft/yr or greater; fig. D–5), the primary surficial geologic units are limestone (estimated saturated hydraulic conductivity of 0.03 ft/d) and volcanic nonwelded and undifferentiated ash-flow tuffs (estimated saturated hydraulic conductivity of 0.02 and 0.007 ft/d, respectively). These two types of consolidated rock each cover about 28 percent of these higher recharge areas. Other exposed rocks in high-recharge areas include dolomite (estimated saturated hydraulic conductivity of 0.2 ft/d, covering about 10 percent of the study area) and volcanic flow and breccia andesite (estimated saturated hydraulic conductivity of 0.02 ft/d, covering about 5 percent of the study area).

Basin Characterization Model Calculations of In-Place Recharge and Runoff

Excess water is calculated in the BCM as the summed values of average monthly precipitation and snowmelt, minus average monthly PET. This excess water is the amount available to replenish soil-water storage, provide in-place recharge, or result in runoff. Runoff is calculated as the available water minus the total soil-water storage capacity (soil porosity multiplied by soil depth). In-place recharge is the available water remaining after runoff, minus the field capacity of the soil (the water content at which drainage becomes negligible). Depending on the soil-water storage capacity and the saturated hydraulic conductivity of the underlying consolidated rock or basin-fill deposits, excess water is partitioned in BCM as either in-place recharge or as runoff that can potentially become groundwater recharge from infiltration losses further downstream in the mountains, alluvial fans, or basin fill. Mountain stream baseflow is derived from in-place recharge that subsequently discharges to streams in the mountain block. Manning and Caine (2007) provide compelling environmental tracer evidence of such mountain block recharge and groundwater flow paths at the Handcart Gulch study site in the Colorado Rockies.

Basin Characterization Model In-Place Recharge

Direct infiltration of precipitation (BCM in-place recharge) is by far the most important form of recharge in the GBCAAS study area. Average annual in-place recharge rates calculated by BCM range from 0 to 3.1 ft/yr (fig. D–5). The highest in-place recharge rates are generally located in the areas of highest precipitation in the mountains of the Great Salt Lake (38) and Sevier Lake (39) groundwater flow systems in Utah, and in the mountains of the Goshute Valley (35), Great Salt Lake Desert (37), Humboldt (7), and Ruby Valley (33) groundwater flow systems of northern and eastern Nevada. However, the effects of saturated hydraulic conductivity used by BCM are readily apparent. An example is the Ruby

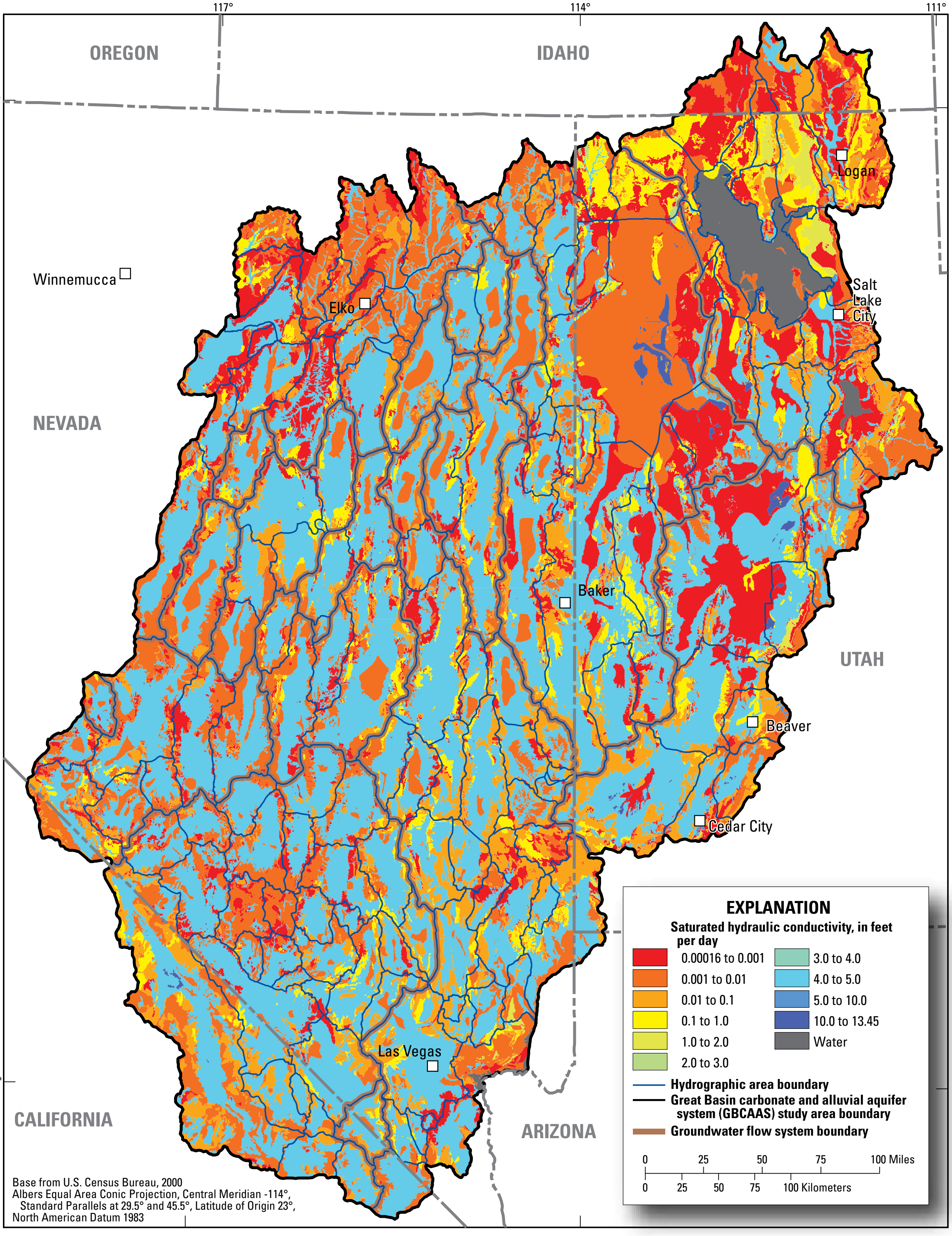

Figure D–4. Distribution of values of saturated hydraulic conductivity of bedrock and unconsolidated sediments used as input for the Basin Characterization Model for the Great Basin carbonate and alluvial aquifer system study area.

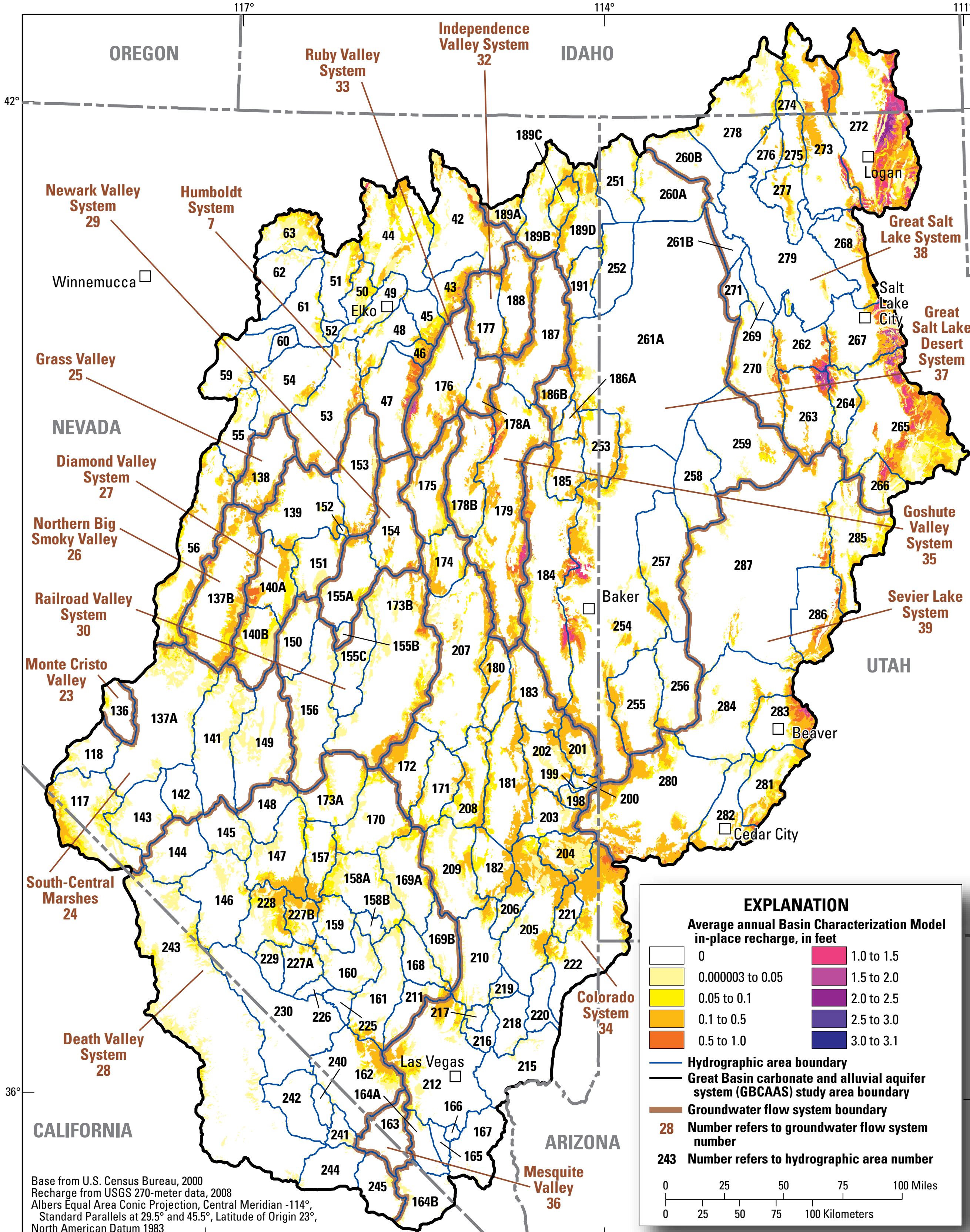

Figure D–5. Distribution of average annual 1940–2006 Basin Characterization Model (BCM) in-place recharge for the Great Basin carbonate and alluvial aquifer system study area.

Mountains, along the western boundary of the Ruby Valley groundwater flow system (33) and the eastern boundary of the Humboldt groundwater flow system (7). Although the Ruby Mountains have a relatively uniform average annual precipitation of about 25–50 in/yr (fig. D–2), the southern portion is dominated by carbonate rocks (fig. B–3) having an estimated saturated hydraulic conductivity of about 0.1 ft/d (fig. D–4) and a BCM in-place recharge rate of about 2 ft/yr. In contrast, the northern portion of the Ruby Mountains is dominated by noncarbonate rocks with an estimated saturated hydraulic conductivity of about 0.002 ft/d (fig. D–4) and a BCM in-place recharge rate of about 0.1–0.2 ft/yr.

In-place recharge computed using BCM for the GBCAAS study area varies substantially from year to year (fig. D–3). Between 1940 and 2006, BCM in-place recharge ranged from a minimum amount of about 0.5 million acre-ft in water year 1977 to a maximum amount of 8 million acre-ft in water year 2005. Compared to precipitation, in-place recharge has larger annual variations—higher during very wet years and greatly diminished during very dry years (Gates, 2007). This is mainly because of evapotranspiration in the recharge areas (mountains). During wet periods more water is available than is needed by vegetation, and during dry periods vegetation tries to maintain its rate of evapotranspiration. As a result, the groundwater recharge is greater during wet periods and lesser during dry periods than would be estimated from the ratio of annual average precipitation to average annual 1940–2006 precipitation. As an example, the largest year-to-year change in annual average precipitation was between 1952 and 1953, when precipitation declined by 54 percent from 12.5 to 6.7 inches. During this period, estimated BCM in-place recharge declined by 67 percent, from 5.2 to 1.7 million acre-ft. Conversely, when average annual precipitation increased by 46 percent between 1977 and 1978 (from 9.4 to 13.7 in.), BCM in-place recharge increased by 1,240 percent, from 0.5 million to 6.7 million acre-ft.

The comparison of average precipitation to BCM in-place recharge for water year 1977 (fig. D–3) shows the importance of using monthly data for BCM. Although average precipitation for 1977 (9.5 in) was only slightly below the average annual 1940–2006 precipitation (10.7 in/yr), nearly all of this precipitation occurred in May, August, and September as rain rather than winter snow. During these 3 months, evapotranspiration was at or near peak rates and effectively used all of this moisture. Winter precipitation, beginning in October 1976, was well below normal and likely resulted in little snowmelt runoff, soil-water storage, and in-place recharge. The monthly data, therefore, explain the anomalously low BCM in-place recharge for 1977 of only 0.5 million acre-ft.

Basin Characterization Model Runoff

In addition to computing in-place recharge, BCM computes the amount of runoff that is generated from each 270-m grid cell. Figure D–6 shows the spatial distribution of average annual BCM runoff. It is important to note that the figure shows the amount and area where runoff originates and not where or how much recharge occurs. The BCM neither routes surface water, nor distinguishes where or how much runoff may subsequently infiltrate and become groundwater recharge. Some portion of BCM-generated runoff will contribute recharge to the basin fill, either as focused infiltration along streams and canals or as diffuse infiltration of unconsumed irrigation water.

Average annual runoff rates calculated by BCM range from 0 ft/yr in valley bottoms to 4.5 ft/yr in the higher altitude mountains. Similar to BCM in-place recharge, the largest runoff rates are generally located in the areas of highest precipitation, including the mountains along the eastern side of the Great Salt Lake (38) and Sevier Lake (39) groundwater flow systems in Utah, as well as mountains in the Goshute Valley (35), Great Salt Lake Desert (37), Humboldt (7), and Ruby Valley (33) groundwater flow systems of northern and eastern Nevada. Saturated hydraulic conductivity, which is a function of rock type, also affects locations and amounts of runoff. Although the Malad Range, between Cache Valley (HA 272) and Malad–Lower Bear River Area (HA 273) of the Great Salt Lake groundwater flow system (38) in southern Idaho, receives average annual precipitation of about 30 in/yr (fig. D–2), it has an average annual BCM runoff rate of only about 0.01–0.05 ft/yr (fig. D–6). This mountain range comprises carbonate rocks (fig. B–3) with an estimated saturated hydraulic conductivity of about 0.03 ft/d (fig. D–4). In contrast, the Toquima Range, between Northern Big Smoky Valley (HA 137B) and Monitor Valley–Northern and Southern Parts (HAs 140A and 140B) in the Northern Big Smoky Valley (26) and Diamond Valley (27) groundwater flow systems of central Nevada, receives about the same amount of precipitation as the Malad Range, but has an average annual BCM runoff rate of about 1 ft/yr (fig. D–6); this mountain range is dominated by noncarbonate rocks with a lower estimated saturated hydraulic conductivity of about 0.002 ft/d (fig. D–4).

Similar to in-place recharge, BCM-generated runoff for the GBCAAS study area varies substantially from year to year (fig. D–3). Between water years 1940 and 2006, BCM runoff ranged from a minimum of about 0.4 million acre-ft in 1977 to a maximum of 6.6 million acre-ft in 1995. Like in-place recharge, yearly runoff varies much more than precipitation. Runoff is greatly amplified during very wet years and greatly diminished during very dry years. For example, compared to the 54 percent decline in average precipitation between 1952 and 1953, BCM runoff declined by 80 percent from 5.9 to 1.3 million acre-ft. Conversely, the 46 percent increase in average precipitation between 1977 and 1978 resulted in an increase in BCM runoff by 1,300 percent, from 0.4 million to 5.6 million acre-ft.

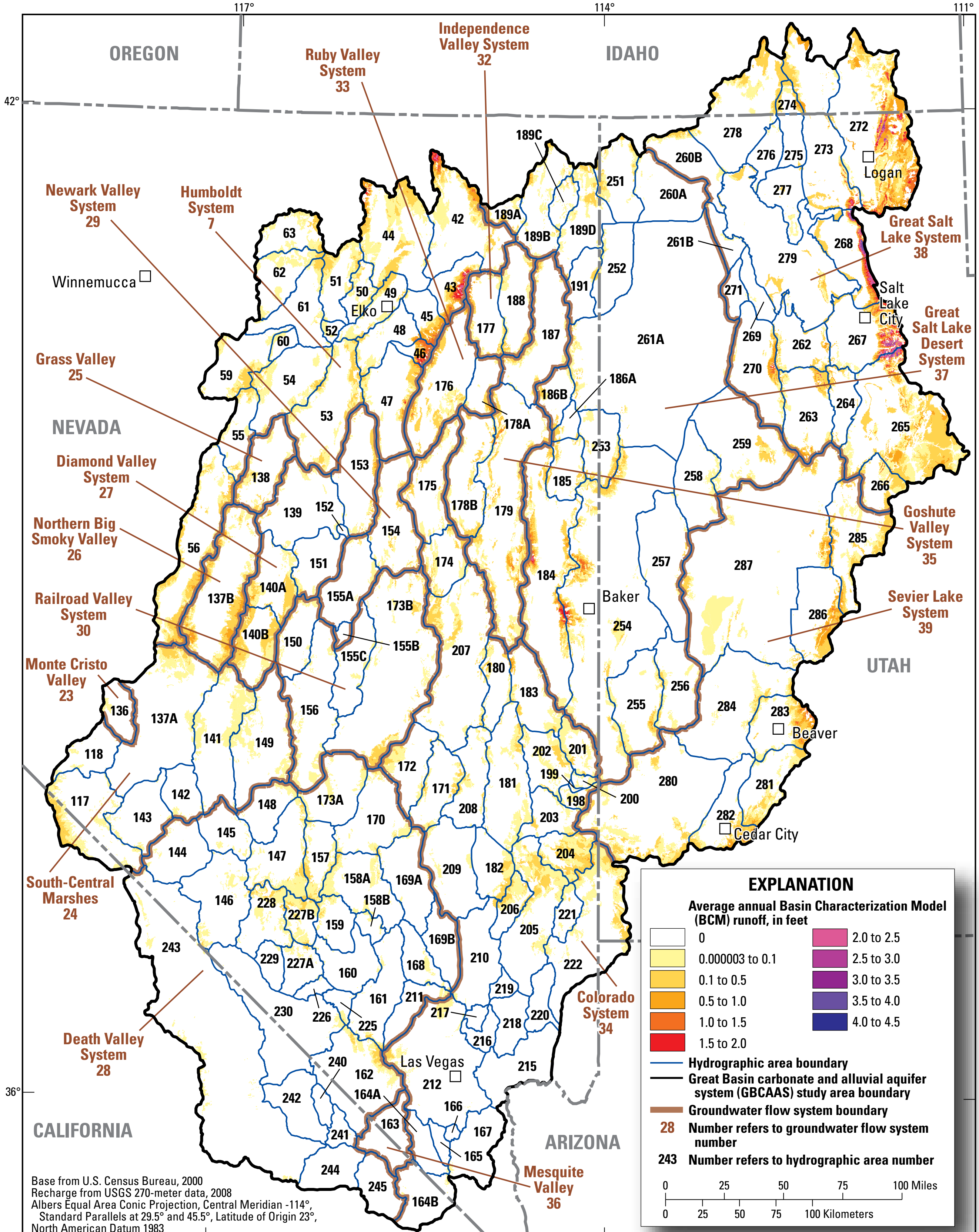

Figure D–6. Distribution of average annual 1940–2006 Basin Characterization Model (BCM) runoff for the Great Basin carbonate and alluvial aquifer system study area.

Recharge from Basin Characterization Model Runoff

The majority of runoff generated in the mountains flows into adjacent basins, some portion of which recharges the unconsolidated deposits as infiltration beneath stream channels, irrigation canals, and irrigated fields. Because BCM does not estimate how much of the runoff becomes recharge, estimates were made by assigning a percentage of runoff that becomes recharge. The predevelopment budget presented in this report includes groundwater recharge from irrigation with surface water; surface water was developed before most hydrologic studies were done. Irrigation with surface water is assumed to increase recharge because the water is removed from armored natural stream channels and spread into canals and onto fields. Areas highly irrigated with surface water were compared to areas not highly irrigated with surface water to determine how irrigation affects the amount of runoff that becomes recharge. In the Death Valley Regional Flow System (DVRFS) study, an area that is not highly irrigated with surface water, about 18,000 acre-ft/yr (25 ft^3/s) of recharge from runoff was estimated, compared to a total estimated runoff of about 180,000 acre-ft/yr (250 ft^3/s; Hevesi and others, 2003, p. 3; Belcher and others, 2004, p. 9; San Juan and others, 2004, p. 115–118). This yields a percentage of runoff that becomes recharge of about 10 percent. In comparison, the percentage of runoff that becomes recharge in 13 HAs that are highly irrigated with surface water within the Humboldt (7), Great Salt Lake (38), and Sevier Lake (39) groundwater flow systems ranges from about 10 to 50 percent, with an average of about 30 percent (Auxiliary 3C). This percentage was calculated by dividing the previously reported estimates of recharge from runoff/streams/canals and unconsumed irrigation water by the reported total available water from runoff, imported water, and groundwater withdrawals for irrigation (Auxiliaries 3B and 3C). On the basis of the above analyses, the fraction of runoff that is assumed to become recharge is 10 percent for HAs that are not highly irrigated with surface water and 30 percent for those that are highly irrigated with surface water.

To determine which percentage of runoff to use for estimating recharge from runoff in the current study, all 165 HAs within the study area were categorized as either “highly irrigated with surface water” or “not highly irrigated with surface water” on the basis of the available surface-water resources. This is centered on the assumption that in HAs where surface-water resources are plentiful, these resources would most likely be developed for irrigation, resulting in substantial irrigation return flow (infiltration of unconsumed irrigation) and a higher percentage of recharge than for nonirrigated HAs. The spreading of irrigation water on permeable surficial basin-fill deposits increases the area for surface water to infiltrate and recharge the underlying aquifer. This designation was obtained through the calculation of the “stream density” for each HA. Stream density was determined by dividing the sum of the mean discharge (period of record) for all gaged streams originating within the mountain block in each HA, by the area of the HA (Auxiliary 3D). HAs with stream densities greater than, or equal to, 0.01 ft/yr were categorized as HAs highly irrigated with surface water, while HAs with stream densities less than 0.01 ft/yr were categorized as not highly irrigated with surface water. Because stream densities were not determined for HAs with ungaged streams, HAs with no gaged streamflow (not listed in Auxiliary 3D) were assumed to be not highly irrigated with surface water and were categorized as such. Because of this assumption, the stream-density estimates and the number of highly irrigated HAs are considered a minimum. Of the 165 HAs within the study area, 30 are designated as highly irrigated with surface water, and 135 are designated as not highly irrigated with surface water (fig. D–7). Most of the HAs categorized as highly irrigated with surface water are located along the Wasatch Front in the Great Salt Lake (38) and Sevier Lake (39) groundwater flow systems of Utah, and in, or near, the Humboldt groundwater flow system (7) of Nevada.

Analysis and Adjustment of Basin Characterization Model Results

Recharge from precipitation includes in-place recharge and recharge from runoff. The amount of recharge from precipitation estimated for the current study is based on BCM results, but has been adjusted by applying a multiplication factor to BCM in-place recharge and runoff in some areas to better match estimates of predevelopment groundwater discharge (Auxiliary 3A). The process for estimating recharge from precipitation for the current study included (1) comparing the recharge from precipitation calculated by BCM to local and regional discharge estimates, and (2) determining whether significant subsurface flow was possible and could account for differences between estimated BCM recharge from precipitation and discharge. Comparison of current study predevelopment discharge estimates (see “Groundwater Discharge” section) to recharge calculated using BCM results shows very large differences for parts, or all, of some groundwater flow systems. Spatially, these differences do not appear to be randomly distributed. A few of the groundwater flow systems, particularly Death Valley (28) and the southern portion of the Colorado (34) groundwater flow systems, have BCM-computed recharge that is 130 percent or more of discharge. The Colorado groundwater flow system has the largest difference between BCM-computed recharge and estimated discharge in both percent and amount. Recharge from precipitation, calculated using the unadjusted BCM results of in-place recharge and recharge from runoff in the Colorado groundwater flow system (34), is estimated to be 490,000 acre-ft/yr (Auxiliary 3A); this is more than 200 percent of the current study predevelopment discharge estimate of 230,000 acre-ft/yr (table D–2).

A sensitivity analysis of BCM in-place recharge for water year 1996, in which soil thickness, monthly minimum and maximum air temperature, monthly precipitation, and sublimation as a percentage of PET were varied within the range of their respective uncertainties, showed that recharge and runoff estimates are very sensitive to small changes in these input parameters. The estimated uncertainty in BCM

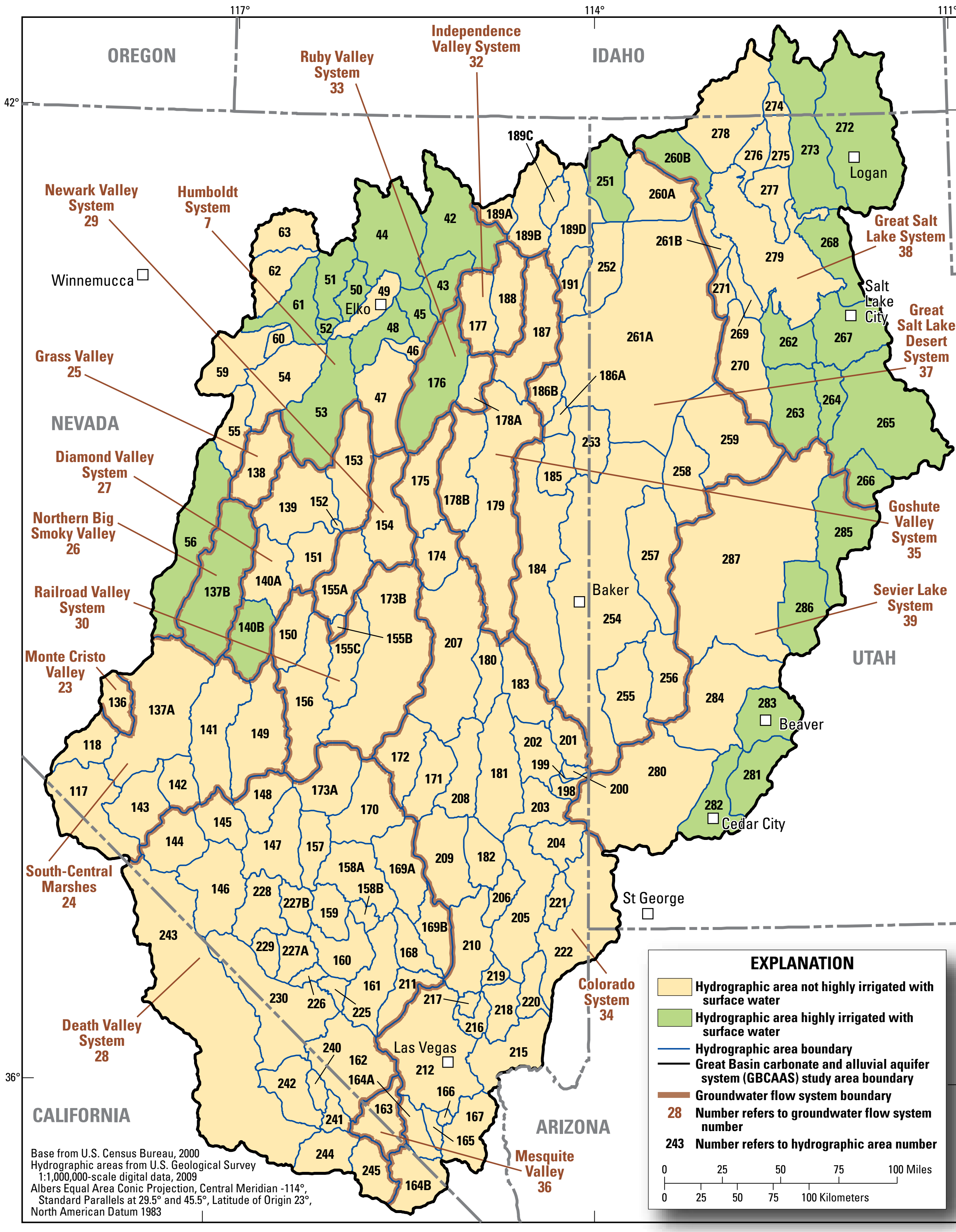

Figure D–7. Distribution of hydrographic areas highly irrigated with surface water and hydrographic areas not highly irrigated with surface water in the Great Basin carbonate and alluvial aquifer system study area.

in-place recharge was ±50 percent (Appendix 3). However, this sensitivity analysis did not include all parameters (such as saturated hydraulic conductivity), which may increase the uncertainty. Much of the input data used in BCM have been interpolated over large (coarse) grid cell sizes, and this tends to smooth factors related to heterogeneity and introduce additional uncertainty. Therefore, the ±50 percent uncertainty is a conservative estimate. Because of its smaller percentage of overall recharge, no sensitivity analysis was performed for BCM runoff calculations.

Other possible causes for the large discrepancy between BCM results and predevelopment discharge in the Death Valley (28) and Colorado (34) groundwater flow systems may be that the saturated hydraulic conductivity used in BCM is weakly constrained in these areas because of the lack of gaged mountain streams for calibrating modeled runoff. Because recharge from runoff is estimated to be only 10 or 30 percent of runoff for the GBCAAS study area (versus 100 percent for in-place recharge), a change in the partitioning of water within BCM from in-place recharge to runoff would result in a substantial decline in estimated recharge. An alternative explanation is that BCM improperly accounts for differences in water- and energy-balance processes in the southern part of the GBCAAS study area. Unlike the northern part of the study area, there is little accumulation of snow in the southern mountains, and a larger percent of precipitation occurs during summer and early autumn when evapotranspiration rates are high. These differences could mean that less water is actually available for either in-place recharge or runoff than is being estimated. A more detailed uncertainty analysis of BCM is discussed in Appendix 3.

Because there is no evidence that input data to BCM are biased, no systematic changes could be made to BCM to reduce in-place recharge and runoff in these groundwater flow systems with excess BCM-computed recharge without introducing an unacceptable decrease in recharge for the other groundwater flow systems that had smaller discrepancies between BCM-computed recharge and estimated discharge. The following paragraphs describe how estimates of recharge from precipitation for each of the 17 groundwater flow systems were determined for this study. If combined predevelopment recharge from precipitation calculated using BCM results, recharge from mountain stream baseflow, and recharge from imported water was within 30 percent of estimated discharge in individual or selected contiguous groups of groundwater flow systems likely having interconnected subsurface flow, BCM in-place recharge and runoff were not adjusted. The ±30 percent criterion is based on the assumed 30-percent composite uncertainty in discharge estimates (discussed below).

Humboldt and Grass Valley Groundwater Flow Systems

Sources of predevelopment recharge to the Humboldt groundwater flow system (7) in the current study include recharge from precipitation, mountain stream baseflow, and imported water. Combined predevelopment recharge calculated using BCM results (Auxiliary 3A), along with recharge from mountain stream baseflow and from imported water (table D-1) exceeds estimated predevelopment groundwater discharge (table D–2) by less than 30 percent. It is possible that discharge is underestimated in the Humboldt groundwater flow system (7) because (1) groundwater discharge to the Humboldt River is poorly defined, (2) subsurface outflow to areas west of the study area is possible, and (3) more springs may exist than those that have been measured and inventoried in National Water Information System (NWIS). The only source of predevelopment recharge to the Grass Valley groundwater flow system (25) estimated in the current study is from precipitation. Predevelopment recharge to the Grass Valley groundwater flow system (25) calculated using BCM results (Auxiliary 3A) exceeds the estimated predevelopment groundwater discharge (table D–2) by more than 30 percent. However, the occurrence of subsurface flow from the Grass Valley groundwater flow system (25) to Crescent Valley (HA 54) in the Humboldt groundwater flow system (7) is possible on the basis of potentiometric contours and the uncertain likelihood of a hydraulic connection (pl. 2). The combined recharge from precipitation calculated using BCM results (Auxiliary 3A), along with recharge from mountain stream baseflow and from imported surface water (table D–1) for these two groundwater flow systems, is about 400,000 acre-ft/yr. This is about 28 percent higher than the estimated predevelopment groundwater discharge of about 310,000 acre-ft/yr (table D–2). The BCM results for these two groundwater flow systems, therefore, are used as the estimated recharge from precipitation for the current study (Auxiliary 3A); a multiplication factor of 1.00 (no adjustment) is shown in figure D–8.

Monte Cristo Valley and South-Central Marshes Groundwater Flow Systems

Sources of predevelopment recharge to the Monte Cristo Valley (23) and South-Central Marshes (24) groundwater flow systems in the current study include recharge from precipitation and mountain stream baseflow. Recharge calculated using BCM results in the Monte Cristo Valley groundwater flow system exceeds the estimated predevelopment groundwater discharge (table D–2) by 225 percent. However, subsurface flow to the surrounding South-Central Marshes groundwater flow system is possible on the basis of potentiometric contours and the high likelihood of a hydraulic connection at the HA boundary between Monte Cristo Valley (HA 136) and Big Smoky Valley-Tonopah Flat Valley (HA 137A) in the South-Central Marshes groundwater flow system (24) (pl. 2). Recharge calculated using BCM results (Auxiliary 3A) and recharge from mountain stream baseflow (table D–1) in the South-Central Marshes groundwater flow system (24) is within 30 percent of estimated predevelopment groundwater discharge (table D–2). The combined recharge calculated using BCM results and recharge from mountain stream baseflow for these two groundwater flow systems is about 56,000 acre-ft/yr (Auxiliary 3A and table D–1), which is about 11 percent lower than the estimated predevelopment groundwater discharge of about 63,000 acre-ft/yr (table D–2). The BCM results, therefore, are used to estimate recharge from precipitation for these two

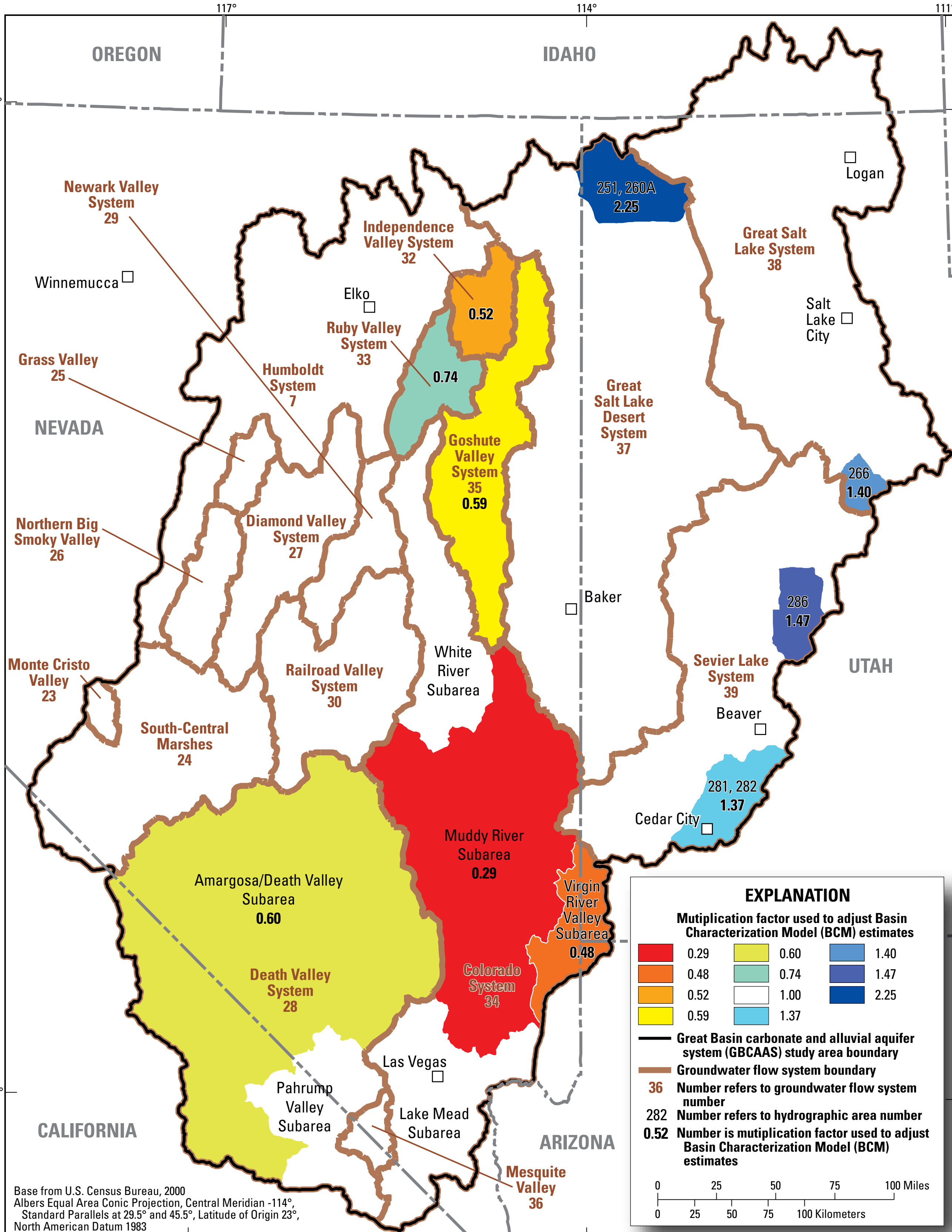

Figure D–8. Multiplication factors used for adjusting Basin Characterization Model (BCM) in-place recharge and runoff for the Great Basin carbonate and alluvial aquifer system study area.

groundwater flow systems for the current study (multiplication factor of 1.00; Auxiliary 3A; fig. D–8).

Northern Big Smoky Valley Groundwater Flow System

Sources of predevelopment recharge to the Northern Big Smoky groundwater flow system (26) in the current study include recharge from precipitation and mountain stream baseflow. Combined predevelopment recharge calculated using BCM results (Auxiliary 3A) and recharge from mountain stream baseflow (table D–1) is 87,000 acre-ft/yr, within 30 percent of the estimated predevelopment groundwater discharge of 69,000 acre-ft/yr (table D–2). The BCM results, therefore, are used to calculate recharge from precipitation for this groundwater flow system in the current study (multiplication factor of 1.00; Auxiliary 3A; fig. D–8).

Diamond Valley, Newark Valley, and Railroad Valley Groundwater Flow Systems

Sources of predevelopment recharge to the Diamond Valley (27), Newark Valley (29), and Railroad Valley (30) groundwater flow systems in the current study include recharge from precipitation and mountain stream baseflow. Recharge in the Diamond Valley groundwater flow system (27) exceeds discharge by more than 30 percent; discharge in the Railroad Valley groundwater flow system (30) exceeds recharge by more than 30 percent; and recharge in the Newark Valley groundwater flow system (29) is within 30 percent of discharge (tables D–1 and D–2). Hydraulic gradients derived from the potentiometric-surface map and the high likelihood of hydraulic connections across groundwater flow system boundaries (pl. 2) indicate the potential for groundwater flow from the Diamond Valley (27) and Newark Valley (29) groundwater flow systems to the Railroad Valley groundwater flow system (30). This flow was also indicated by the Great Basin regional aquifer-system analysis (RASA) groundwater flow model (Prudic and others, 1995, fig. 24). Combined recharge calculated using BCM results (Auxiliary 3A) and recharge from mountain stream baseflow (table D–1) for these three groundwater flow systems is about 210,000 acre-ft/yr. This is about 13 percent higher than the estimated predevelopment groundwater discharge of about 190,000 acre-ft/yr (table D–2). The BCM results, therefore, are used to calculate recharge from precipitation for these groundwater flow systems in the current study (multiplication factor of 1.00; Auxiliary 3A; fig. D–8).

Death Valley Groundwater Flow System

Sources of predevelopment recharge to the Death Valley groundwater flow system (28) in the current study include recharge from precipitation and mountain stream baseflow. Combined predevelopment recharge calculated using BCM results (Auxiliary 3A) and recharge from mountain stream baseflow (table D–1) is 170,000 acre-ft/yr. This is 70 percent higher than the estimated groundwater discharge of 100,000 acre-ft/yr (table D–2). Because the Death Valley groundwater flow system (28) is at the downgradient end of a regional discharge area, it is unlikely that there is significant subsurface outflow, and recharge must balance discharge within uncertainty limits. The BCM results for the Death Valley groundwater flow system (28) suggest that recharge from precipitation can sufficiently provide for all of the estimated predevelopment groundwater discharge and that subsurface inflow may not be needed. This is in contrast to previous studies, which suggested the occurrence of subsurface inflow to the Death Valley groundwater flow system (28).

Recharge calculated using BCM results was compared to discharge for each HA in the Death Valley groundwater flow system (28) to determine whether the computed recharge estimates were reasonable and whether any imbalances between BCM computed recharge and the discharge could be balanced by subsurface flow. On the basis of hydraulic gradients, the high likelihood of hydraulic connections across HA boundaries (pl. 2), and the location of major discharge areas, the Death Valley groundwater flow system (28) can be considered as two separate subareas. These subareas are defined in the current study as the Armargosa/Death Valley subarea and Pahrump Valley subareas (fig. D–8, Appendixes 4 and 5). In the Amargosa/Death Valley subarea, recharge calculated using BCM results is 140,000 acre-ft/yr (Auxiliary 3A), which is about 170 percent of the estimated predevelopment discharge of 81,000 acre-ft/yr (Appendix 5). In this subarea, therefore, BCM in-place recharge and runoff are multiplied by 0.6 for the current study estimate of recharge from precipitation (Auxiliary 3A; fig. D–8). In the Pahrump Valley subarea, the recharge calculated using BCM results of 23,000 acre-ft/yr (Auxiliary 3A) is within 30 percent of the estimated predevelopment groundwater discharge of 20,000 acre-ft/yr (Appendix 5). The BCM results, therefore, are used to calculate recharge from precipitation in the Pahrump Valley subarea in the current study (multiplication factor of 1.00; Auxiliary 3A; fig. D–8).

Independence Valley, Ruby Valley, and Goshute Valley Groundwater Flow Systems

Sources of predevelopment recharge to the Independence Valley (32), Ruby Valley (33), and Goshute Valley (35) groundwater flow systems in the current study include recharge from precipitation and mountain stream baseflow. On the basis of hydraulic gradients and the high likelihood of hydraulic connections across flow system boundaries (pl. 2), the budgets in these three groundwater flow systems can be considered together. Combined predevelopment recharge calculated using BCM results (Auxiliary 3A) and recharge from mountain stream baseflow (table D–1) for the Independence Valley (32), Ruby Valley (33), and Goshute Valley (35) groundwater flow systems is 380,000 acre-ft/yr. This is about 58 percent higher than the estimated predevelopment groundwater discharge of 240,000 acre-ft/yr (table D–2). It is possible, however, that discharge is underestimated in these three groundwater flow systems. Pavelko (2007) presents a database of numerous springs in Steptoe Valley (HA 179) in the Goshute Valley groundwater flow system (35), but very few have discharge estimates.

Some of these springs in the mountains may intercept a portion of the in-place recharge in the mountain block and prevent it from infiltrating to deeper layers and becoming part of a longer flow path discharging to the basin fill. On the basis of hydraulic gradients and the high likelihood of hydraulic connections across HA boundaries (pl. 2), it is possible that subsurface outflow from the Independence Valley (32), Ruby Valley (33), and Goshute Valley (35) groundwater flow systems occurs to the Great Salt Lake Desert groundwater flow system (37), along with lesser potential for flow to the Humboldt (7) and Colorado (34) groundwater flow systems. These possible subsurface outflows, however, are not quantified in the current study because of inherent water-budget uncertainties. The Basin and Range carbonate-rock aquifer system (BARCAS) study (Welch and others, 2007) required subsurface outflow from the Goshute Valley groundwater flow system (35) of 77,000 acre-ft/yr to the Ruby Valley (33), Colorado (34), and Great Salt Lake Desert (37) groundwater flow systems in order to balance the budget. The definition of the BARCAS study area was based, in part, on political boundaries rather than complete groundwater flow systems. The current study evaluated groundwater budgets for entire groundwater flow systems, and it was determined that the groundwater flow systems surrounding the Independence Valley (32), Ruby Valley (33), and Goshute Valley (35) groundwater flow systems do not require subsurface outflow to balance estimated predevelopment discharge. In order to balance the water budgets for these three groundwater flow systems in the current study, BCM in-place recharge and runoff were decreased using multiplication factors of 0.52, 0.74, and 0.59, for the Independence Valley (32), Ruby Valley (33), and Goshute Valley (35) groundwater flow systems, respectively (Auxiliary 3A and fig. D–8).

Colorado Groundwater Flow System

Sources of predevelopment recharge to the Colorado groundwater flow system (34) in the current study include recharge from precipitation and mountain stream baseflow. Combined predevelopment recharge calculated using BCM results (Auxiliary 3A) and recharge from mountain stream baseflow (table D–1) of 490,000 acre-ft/yr is 213 percent higher than the estimated predevelopment groundwater discharge of 230,000 acre-ft/yr (table D–2). Recharge calculated using BCM results was compared to discharge estimated for each HA in the Colorado groundwater flow system (34) to determine whether the computed recharge estimates were reasonable, and whether any imbalances between BCM computed recharge and the discharge could be balanced by subsurface flow. Based upon hydraulic gradients, the high likelihood of hydraulic connections across HA boundaries (pl. 2), and the location of major discharge areas, the Colorado groundwater flow system (34) can be divided into four separate regions, defined in the current study as the Lake Mead, Muddy River, White River, and Virgin River subareas (fig. D–8, Appendixes 4 and 5).

Recharge calculated using BCM results is much larger than estimated predevelopment groundwater discharge in the Muddy River and Virgin River Valley subareas (fig. D–8). In the Muddy River and Virgin River Valley subareas, recharge calculated using BCM results is 360,000 acre-ft/yr (Auxiliary 3A). This is about 300 percent higher than the estimated predevelopment discharge of 120,000 acre-ft/yr (Appendix 5). The high recharge portions of these subareas are dominated by volcanic nonwelded ash-flow tuffs; one possible explanation for the budget discrepancy is that BCM overestimates saturated hydraulic conductivity of this rock type. Estimates of saturated hydraulic-conductivity values were based on a calibration of BCM runoff to gaged mountain stream discharge (Appendix 3) for watersheds dominated by different geologic formations. Volcanic nonwelded ash-flow tuffs were the predominant geology in eight gaged watersheds. The comparison of BCM runoff to gaged runoff (total streamflow less baseflow) for each of these eight gages shows that BCM overestimates runoff by an average of only 10 percent. Two of these stream gages are located in the Muddy River and Virgin River Valley subareas: Site 9413900 on Beaver Dam Wash near Enterprise, Utah, and Site 9417500 on Meadow Valley Wash at Eagle Canyon near Ursine, Nevada. Estimated BCM runoff for these two watersheds was 95 and 74 percent of gaged runoff, respectively (table A3–2). While this potential underestimation of BCM runoff would indicate a reciprocal overestimation of BCM in-place recharge, it is not nearly enough to explain the 300 percent discrepancy between recharge and discharge for these two subareas. Regardless of whether or not BCM may be overestimating recharge, BCM results for the Muddy River subarea suggest that recharge from precipitation within the subarea can sufficiently provide for all of the estimated predevelopment groundwater discharge, which occurs mostly in Pahranagat Valley (HA 209), Muddy River Springs Area (HA 219), and Lower Moapa Valley (HA 220). Thus, the Muddy River and Virgin River Valley subareas do not require additional recharge as subsurface inflow from the northern part of the Colorado groundwater flow system (34). This is in contrast to previous studies (Maxey and Eakin, 1949; Welch and others, 2007), which suggest that subsurface inflow to this part of the Colorado groundwater flow system (34) from upgradient White River Valley (HA 207) was required to balance discharge. Because the southern part of the Colorado groundwater flow system is at the downgradient end of regional discharge areas, it is unlikely that there is significant subsurface outflow, and recharge should balance discharge within uncertainty limits. In order to balance the water budgets for this groundwater flow system in the current study, BCM in-place recharge and runoff were decreased in the Muddy River and Virgin River Valley subareas by using multiplication factors of 0.29 and 0.48, respectively (Auxiliary 3A and fig. D–8).

Other subareas within the Colorado groundwater flow system (34) do not have significant groundwater-budget imbalances. The recharge estimates calculated using BCM results for the Lake Mead and White River Valley subareas were within 30 percent of the predevelopment groundwater-discharge estimates. The BCM results, therefore, are used to calculate recharge from precipitation for these subareas for the current study (multiplication factor of 1.00; Auxiliary 3A; fig. D–8).

Mesquite Valley Groundwater Flow System

The only source of predevelopment recharge to the Mesquite Valley groundwater flow system (36) in the current study is recharge from precipitation. Recharge calculated using BCM results for the Mesquite Valley groundwater flow system (36) is 1,900 acre-ft/yr (Auxiliary 3A). This is within 30 percent of the estimated predevelopment groundwater discharge of 2,200 acre-ft/yr for this small flow system (table D–2). The BCM results, therefore, are used to calculate recharge from precipitation for the current study (multiplication factor of 1.00; Auxiliary 3A; fig. D–8).

Great Salt Lake Desert, Great Salt Lake, and Sevier Lake Groundwater Flow Systems

In the current study, sources of predevelopment recharge to the Great Salt Lake Desert (37), Great Salt Lake (38), and Sevier Lake (39) groundwater flow systems include recharge from precipitation, mountain stream baseflow, and imported water. Based upon hydraulic gradients and the high likelihood of a hydraulic connection across flow system boundaries (pl. 2), the budgets in these three groundwater flow systems can be considered together. Combined predevelopment recharge calculated using BCM results (Auxiliary 3A) and recharge from mountain stream baseflow and imported surface water (table D–1) is 3,200,000 acre-ft/yr. This is within 30 percent of the estimated predevelopment groundwater discharge of 3,000,000 acre-ft/yr (table D–2). The BCM results, therefore, generally are used to calculate recharge from precipitation for the current study estimate (multiplication factor of 1.00). The recharge calculated using BCM results, however, is less than 70 percent of the estimated predevelopment groundwater discharge for six HAs (Grouse Creek Valley, HA 251; Park Valley-West Park Valley, HA 260A; Northern Juab Valley, HA 266; Parowan Valley, HA 281; Cedar City Valley, HA 282; and Pavant Valley, HA 286), located at the upgradient ends of these groundwater flow systems that likely do not receive subsurface inflow (fig. D–8). In order to estimate recharge for these HAs, BCM in-place recharge and runoff were multiplied by factors ranging from 1.37 to 2.25 (Auxiliary 3A and fig. D–8).

Current Study Estimates of Recharge from Precipitation

Estimated in-place recharge from precipitation for the current study, 2,900,000 acre-ft/yr, accounts for about 62 percent of the total estimated groundwater recharge for predevelopment conditions (table D–1). The highest long-term (1940–2006) average annual amounts of in-place recharge occur in the Great Salt Lake (38), Great Salt Lake Desert (37), Sevier Lake (39), Humboldt (7), and Colorado (34) groundwater flow systems (table D–1). Estimates of long-term (1940–2006) average annual in-place recharge by HA are given in Appendix 4 and Auxiliary 3A. Because of the large range in groundwater flow system areas (282–18,849 mi^2), the mean annual in-place recharge rate (total volume of in-place recharge divided by flow system area) for each groundwater flow system also is given in table D–1. The mean rates are useful for comparing in-place recharge between the 17 groundwater flow systems within the study area.

Estimated recharge from runoff for the current study, 570,000 acre-ft/yr, accounts for about 13 percent of the total estimated groundwater recharge for predevelopment conditions (table D–1). The highest amounts of recharge from runoff occur in the Great Salt Lake (38) and Humboldt (7) groundwater flow systems (table D–1). Particularly in the Great Salt Lake groundwater flow system (38), many HAs are highly developed and have large networks of canals and diversions for irrigation purposes. Current study estimates of annual recharge from runoff by HA are given in Appendix 4 and Auxiliary 3A.

Recharge from Mountain Stream Baseflow

Estimates of recharge from mountain stream baseflow are not included in the estimates of recharge from runoff discussed above. The same percentages (30 percent for HAs highly irrigated with surface water; 10 percent for HAs not highly irrigated with surface water) are used for estimating recharge from mountain stream baseflow. Estimated recharge from mountain stream baseflow for the current study, 130,000 acre-ft/yr, accounts only for about 3 percent of total estimated groundwater recharge under predevelopment conditions (table D–1). Most of this recharge (85 percent) is concentrated within the Great Salt Lake groundwater flow system (38). Estimates of annual recharge from mountain stream baseflow by HA are given in Appendix 4. Estimates could not be made for HAs without gaged mountain streams and are made only for HAs with records of gaged perennial mountain streams.

Recharge from Imported Surface Water

Recharge from irrigation return flow of imported surface water is a major component of the groundwater-recharge budget, but it is concentrated almost exclusively within the Great Salt Lake groundwater flow system (38). Amounts of naturally imported surface water (such as rivers and streams flowing from upgradient HAs or outside of the study area) were calculated from streamgage data; amounts of water imported in association with engineered transbasin diversions that originate outside the HA or study area were either compiled from previous reports or calculated from diversion records (Auxiliary 3C). Estimated recharge from imported surface water for the current study, 990,000 acre-ft/yr, accounts for 22 percent of total estimated groundwater recharge under predevelopment conditions (table D–1). Recharge from imported surface water accounts for 42 percent of the total recharge for the Great Salt Lake groundwater flow system (38), and it includes naturally imported water from the Bear, Ogden, Weber, Jordan, and Provo rivers (fig. A–1), as well as imported water from engineered transbasin diversions east of the study area.

HAs that receive natural surface-water inflow from upgradient areas (Appendix 4 and Auxiliary 3C) include Tenmile Creek Area (HA 48) within the Humboldt groundwater flow system (7); and Utah Valley Area (HA 265), East Shore Area (HA 268), Cache Valley (HA 272), and Malad-Lower Bear River Area (HA 273) within the Great Salt Lake groundwater flow system (38). HAs that receive imported surface water from transbasin diversions include Utah Valley Area (HA 265), Salt Lake Valley (HA 267), and East Shore Area (HA 268) within the Great Salt Lake groundwater flow system (38), and Pavant Valley (HA 286) within the Sevier Lake groundwater flow system (39). Estimates of groundwater recharge from imported surface water for each HA were calculated using the same percentages that were used to determine the recharge from runoff estimates. Based on this convention, in HAs highly irrigated with surface water (fig. D–7), 30 percent of the imported water is estimated to recharge the groundwater flow system (Auxiliary 3C).

Recharge from Subsurface Groundwater Inflow

Previous estimates of both subsurface inflow and outflow within the GBCAAS study area typically have been based upon (1) water-balance methods, where subsurface inflow is determined as the residual of total discharge and the sum of all other forms of recharge; (2) Darcy flux calculations, which are based on the hydraulic gradient, hydraulic conductivity, and aquifer cross-sectional area between HAs; or (3) geochemical approaches, such as the deuterium mass-balance method (Thomas and others, 2001; Lundmark and others, 2007). Previous estimates of subsurface inflow were compiled by HA (Auxiliary 3E) and by groundwater flow system (Auxiliary 3F); the estimates compiled by groundwater flow system account for subsurface inflow that originates outside of the groundwater flow system and do not account for subsurface inflow between HAs within the groundwater flow system.

Recharge from subsurface inflow was not estimated for the current study, however, because of (1) the large uncertainty in groundwater-budget components (such as an estimated ±50 percent uncertainty in recharge from precipitation) for use in water-balance methods; (2) the sparse information on hydraulic gradients, hydraulic properties, and aquifer geometry at HA boundaries for use in Darcy flux methods; and (3) the application of geochemical approaches, such as the deuterium mass-balance method for all 165 HAs within the GBCAAS study area, was not within the scope of the current study. Subsurface flow estimates between HAs based on groundwater-balance methods are further complicated in the GBCAAS study area by conditions of subsurface outflow from one HA moving into several downgradient HAs within and between groundwater flow systems; partitioning this subsurface outflow cannot be resolved with the water-balance approach. An example of this is in eastern Nevada, where the BARCAS study (Welch and others, 2007) used a deuterium mass-balance method to help constrain subsurface outflow from Steptoe Valley (HA 179) in the Goshute Valley groundwater flow system (35) that becomes subsurface inflow to (1) Goshute Valley (HA 187) in the Goshute Valley groundwater flow system (35); (2) Jakes Valley (HA 174), White River Valley (HA 207), and Lake Valley (HA 183) in the Colorado groundwater flow system (34); and (3) Spring Valley (HA 184) in the Great Salt Lake Desert groundwater flow system (37).

Previous estimates of subsurface inflow to HAs and groundwater flow systems could not be used in the current study because, in many of these studies, balancing groundwater budgets in adjacent HAs or groundwater flow systems was not considered. For example, Maxey and Eakin (1949), Scott and others (1971), Harrill and others (1988), and Welch and others (2007) indicate subsurface inflow to HAs south of White River Valley (HA 207) in the Colorado groundwater flow system (34) ranging from 18,000 to 40,000 acre-ft/yr. These studies, however, did not necessarily consider the consequences of routing this subsurface flux southward. In the current study, the White River subarea (fig. D–8), within the Colorado groundwater flow system (34), is assumed to have a balance between groundwater recharge and discharge within ± 30 percent (see “Colorado Groundwater flow System” section under “Analysis and Adjustment of BCM Results”). Furthermore, the downgradient Muddy River subarea does not require any additional recharge from subsurface inflow; this additional flux would cause a groundwater-budget imbalance.

The current study recognizes that all groundwater-budget components have errors and that estimates of subsurface inflow as a budget residual of the recharge and discharge estimates are highly uncertain; it was assumed for most groundwater flow systems that the amounts of subsurface inflow fall within the range of these uncertainties (Auxiliary 3F). Figure D–9 shows groundwater-budget imbalances and indicates with arrows where the potentiometric contours and the likelihood of a hydraulic connection across the HA boundary (pl. 2) suggest possible groundwater subsurface flow between groundwater flow systems (table D–1). Groundwater flow-system- and subarea-budget imbalances imply that although there may be a potential for subsurface flow, this flow may not be needed to balance budgets. With the exception of South-Central Marshes (24), Railroad Valley (30), and Mesquite Valley (36) groundwater flow systems, none of the groundwater flow systems shown as possibly receiving subsurface inflow in figure D–9 and table D–1 need this flux to balance predevelopment estimates

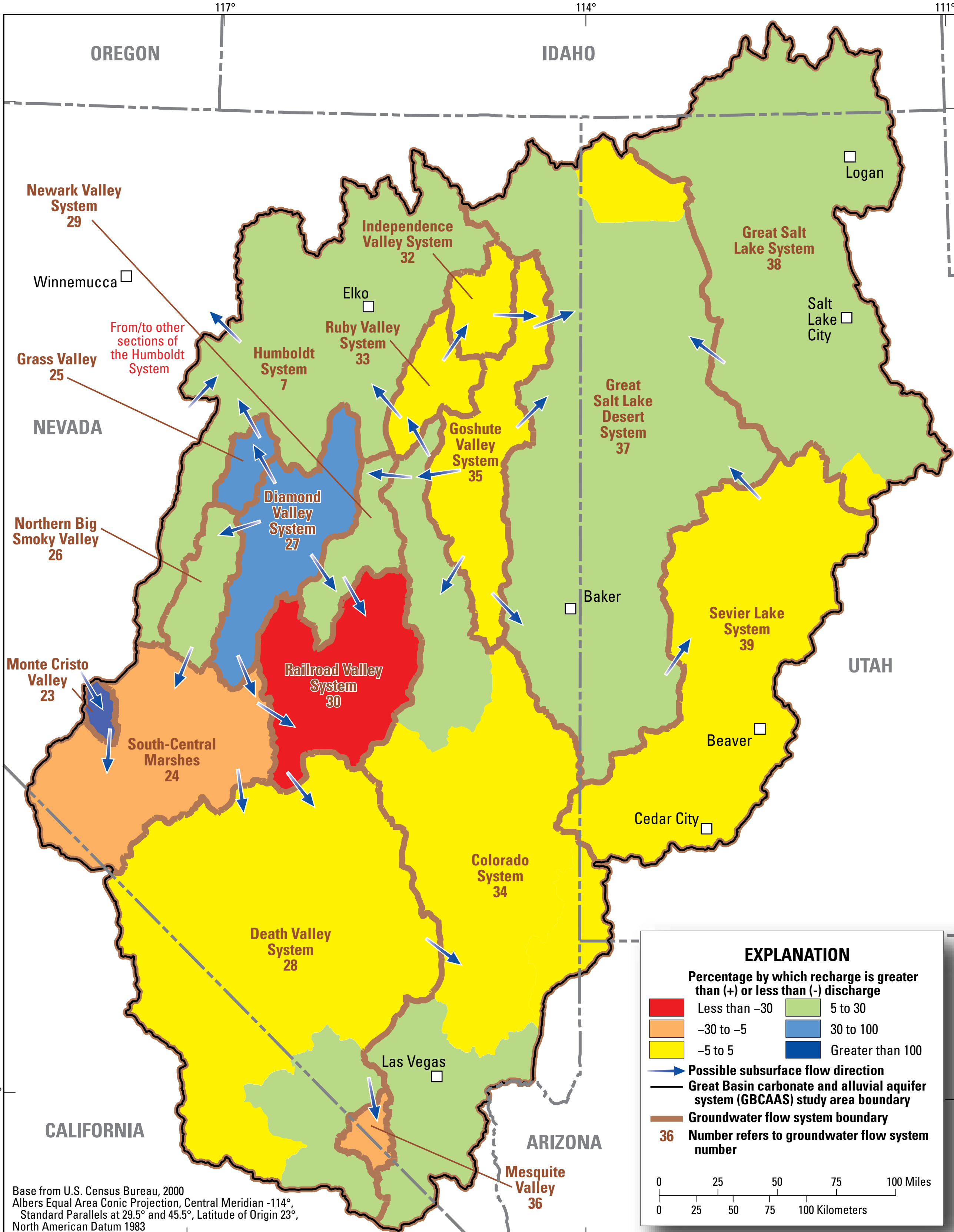

Figure D–9. Possible subsurface flow between groundwater flow systems and groundwater-budget imbalances in groundwater flow systems and subareas in the Great Basin carbonate and alluvial aquifer system study area.

of discharge within the groundwater flow system. In the South-Central Marshes (24) and Mesquite Valley (36) groundwater flow systems, however, recharge and discharge balance within a 30-percent uncertainty without subsurface inflow. Only the Railroad Valley groundwater flow system (30) has an imbalance where estimated predevelopment groundwater discharge exceeds current study recharge estimates by more than 30 percent (see “Analysis and Adjustment of BCM Results”). Therefore, using the criteria adopted for this study, Railroad Valley (30) is the only groundwater flow system within the GBCAAS study area where substantial subsurface inflow originating from inside the GBCAAS is likely.

Subsurface inflow originating from outside the study area may provide recharge to the Humboldt (7) and Monte Cristo Valley (23) groundwater flow systems on the western side of the study area (fig. D–9). This assumption is based on water levels outside the study area, hydraulic gradients within these flow systems, and the likelihood of a hydraulic connection across the study area boundary. These fluxes, however, are not required to balance predevelopment groundwater budgets in these two groundwater flow systems. The Humboldt groundwater flow system (7) is the only partial flow system in the study area, and this potential subsurface inflow toward the northeast is from sections of the flow system outside the GBCAAS study area.

Previously Published Estimates of Groundwater Recharge

Previously reported recharge estimates from HA-based groundwater studies were compiled for comparison to current study groundwater-recharge estimates. Current study estimates are for predevelopment groundwater conditions, yet estimates from previous studies are for periods from the 1940s through the 2000s. Although most HAs in the study area arguably still are in a predevelopment state, some HAs have undergone extensive groundwater development during this period. The only recharge budget components affected by groundwater development, however, are recharge from irrigation and public supply using groundwater. Recharge from irrigation with groundwater is estimated to be only a small percentage of total groundwater recharge (discussed in the “Recharge of Unconsumed Irrigation Water from Well Withdrawals” section). In Las Vegas Valley (HA 212), recharge from water imported from Lake Mead, starting in the late 1980s, needs to also be considered for recent groundwater conditions.

Previous studies in Nevada include U.S. Geological Survey/state cooperative studies beginning in the 1940s (published as Nevada Water Resources Bulletins and Nevada Water Resources Reconnaissance Reports). Recharge estimates from these studies are summarized by Harrill and others (1988). Although similar groundwater studies by the U.S. Geological Survey (USGS) in Utah also began in the 1940s (published as State of Utah Technical Publications or USGS reports), these reports were not quantitative with respect to groundwater-budget components. Previously reported recharge estimates for Utah used in this study, therefore, were from HA-based studies beginning in the 1960s. These individual reported estimates are given in Auxiliary 3G.

Beginning in the late 1940s, hydrologists working in the GBCAAS study area developed empirical techniques using precipitation zones for estimating groundwater recharge (Auxiliary 3G) that were calibrated to HA-based discharge estimates (including evapotranspiration, spring discharge, and subsurface outflow). Although subsurface flow was not quantified explicitly for each HA, some amount of inflow or outflow may have been included in the water budgets upon which these empirical techniques were based. This approach was first published by Maxey and Eakin (1949) for 13 HAs along the White River within the Colorado groundwater flow system (34), using an annual precipitation map for the State of Nevada (Hardman, 1936) for assigning the following recharge percentages for specified ranges of precipitation: 0 percent for 0–8 in. of precipitation, 3 percent for 8–12 in., 7 percent for 12–15 in., 15 percent for 15–20 in., and 25 percent for more than 20 in. of precipitation. Many of the subsequent studies published in cooperation with the states of Nevada and Utah used this Maxey-Eakin approach to estimate recharge. The use of precipitation zones for estimating groundwater recharge also was utilized by Watson and others (1976), in which Maxey-Eakin recharge estimates were revised on the basis of simple-linear and multiple-linear regression models. Harrill and Prudic (1998, p. 23–25) used the Maxey-Eakin method for estimating recharge in many of the Great Basin HAs and developed an equation for determining recharge from precipitation.

Nichols (2000) published recharge estimates based on regression modeling for selected HAs in the eastern Great Basin (Auxiliary 3G) using updated precipitation zones from PRISM mapping (Daly and others, 1994). Similar to the Maxey-Eakin approach of equating recharge estimates to discharge estimates, Nichols’ (2000) empirical relations are based on discharge via evapotranspiration (ET). Because these estimates do not account for the contribution of annual precipitation to ET, they may overestimate recharge. Epstein (2004) calculated Maxey-Eakin recharge for the majority of HAs within the GBCAAS study area and developed another empirical method known as the Bootstrap Brute-Force Recharge Model for estimating recharge by utilizing coefficients applied to spatially distributed precipitation; this study was the first to evaluate uncertainty in these empirical estimates. Although each of these empirical methods indirectly accounts for subsurface inflow from, and outflow to, adjacent basins (HA reconnaissance studies include varying estimates of inflow and outflow in their estimated discharge amounts), these methods do not explicitly factor in these inflow/outflow amounts.

In addition to recharge estimates based on empirically derived formulas, estimates of HA-based recharge have been developed using other methods such as the chloride mass-balance and deuterium mass-balance methods, (Auxiliary 3G). Using the chloride mass-balance method, Dettinger (1989) provided estimates of natural recharge for 16 HAs in the Great Basin, 10 of which are in the GBCAAS study area. Kirk and Campana (1990) developed a deuterium-based mixing cell flow model of the White River Valley subarea of the Colorado flow system (34) for estimating both recharge and interbasin groundwater fluxes. Similarly, Thomas and others (2001) developed a groundwater deuterium-calibrated mass-balance model of the White River Valley, Muddy River, and Lake Mead subareas of the Colorado groundwater flow system (34). More recently, groundwater-budget components, including recharge for the 12 HAs within the BARCAS study area of east-central Nevada and west-central Utah, were quantified using a deuterium-calibrated discrete-state compartment (DSC) model, coupled with shuffled complex evolution (SCE) optimization calibrated to groundwater deuterium values and groundwater-evapotranspiration estimates (Lundmark and others, 2007; Welch and others, 2007).

Previously reported minimum and maximum annual recharge estimates by HA (Appendix 4) are compiled by groundwater flow system and shown in table D–1. Total previously reported annual recharge for the entire study area ranges from 3,200,000 to 5,400,000 acre-ft/yr.

Summary of Recharge Components for Predevelopment Conditions

Total recharge for predevelopment conditions to the GBCAAS study area is estimated to be 4,500,000 acre-ft/yr (table D–1). In-place recharge from precipitation is the largest component of recharge and accounts for 64 percent of total recharge (figs. D–10 and D–11), followed by recharge from imported water (22 percent), runoff (13 percent), and mountain stream baseflow (3 percent). The Great Salt Lake groundwater flow system (38) receives 51 percent of the recharge within the entire study area, and more than four times as much as the Great Salt Lake Desert (37) and Sevier Lake (39) groundwater flow systems, which rank second and third, respectively. In-place recharge from precipitation is the dominant form of recharge for all 17 groundwater flow systems and accounts for 43–100 percent of the total recharge for each flow system (figs. D–10 and D–11). Recharge from imported water is significant only for the Great Salt Lake groundwater flow system (38), where it ranks second in importance and accounts for nearly 42 percent of the total recharge for the flow system. With the exception of the Great

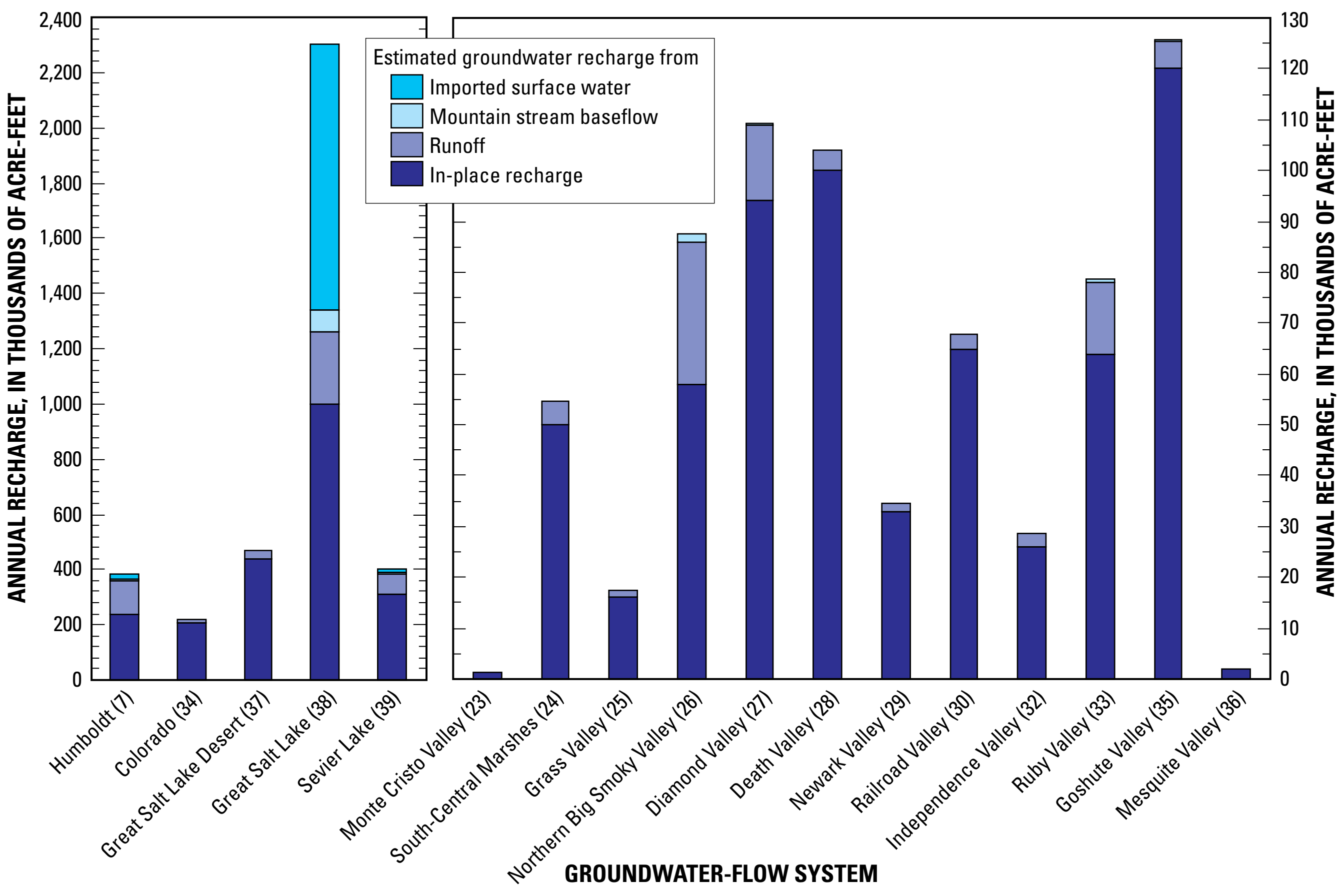

Figure D–10. Estimates of recharge components for predevelopment conditions for the 17 groundwater flow systems of the Great Basin carbonate and alluvial aquifer system study area.

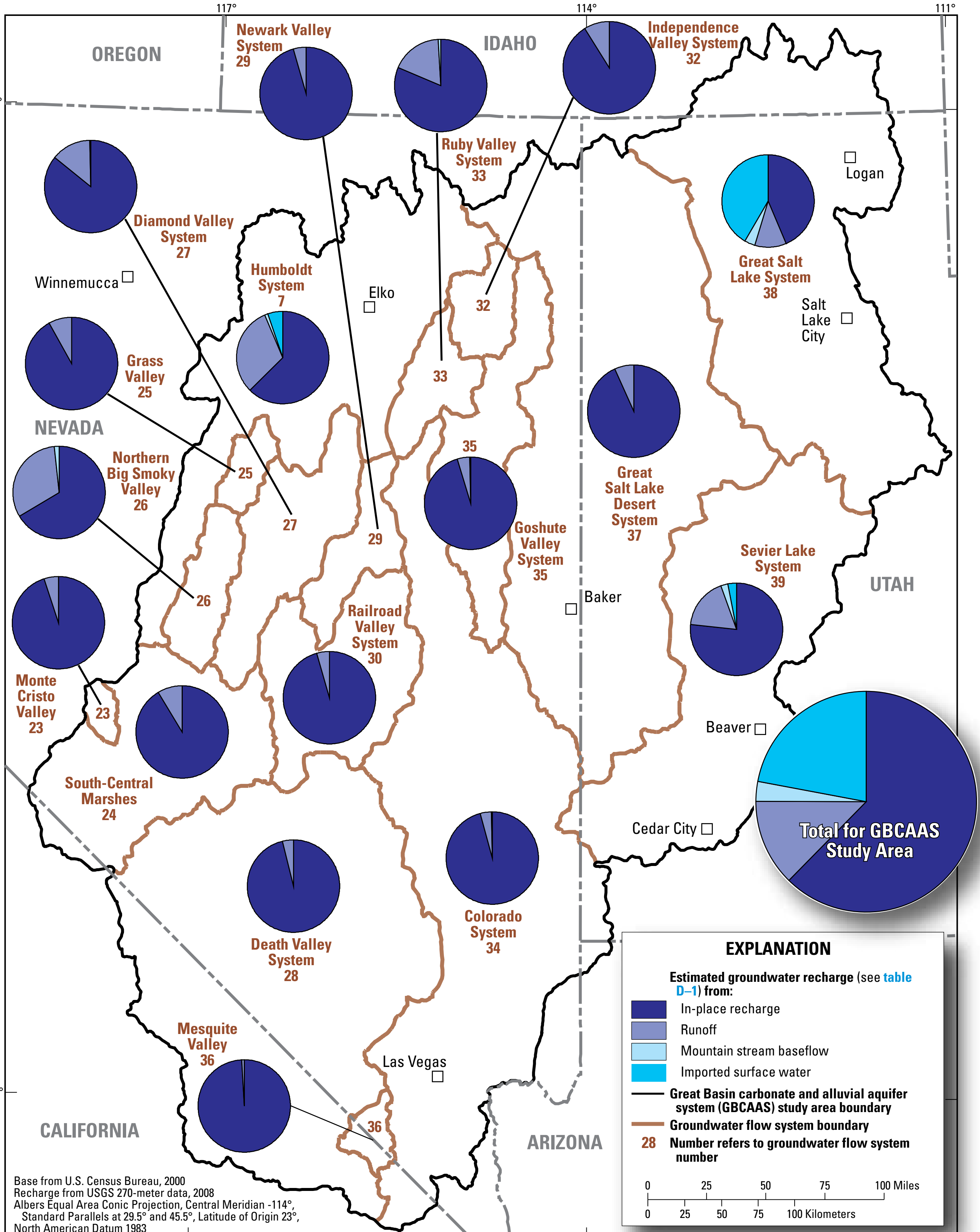

Figure D–11. Groundwater recharge components for predevelopment conditions for the 17 groundwater flow systems of the Great Basin carbonate and alluvial aquifer system study area.

Salt Lake groundwater flow system (38), recharge from runoff generally ranks second in importance.

Total recharge estimated for each groundwater flow system in the current study generally falls within the range of compiled previous estimates (table D–1). Current recharge estimates for the Northern Big Smoky Valley (26), Great Salt Lake (38), and Sevier Lake (39) groundwater flow systems, however, exceed the compiled maximum of previous estimates by 12, 21, and 25 percent, respectively. One possible reason for this discrepancy is that the previous estimates largely were based on the Maxey-Eakin method, which uses a maximum of 25 percent precipitation becoming recharge. In contrast, BCM in-place recharge exceeds 25 percent of precipitation at the highest altitudes in the Northern Big Smoky Valley (26), Great Salt Lake (38), and Sevier Lake (39) groundwater flow systems (figs. D–2 and D–5). The current recharge estimate for the Independence Valley groundwater flow system (32) is slightly less (7 percent) than the compiled minimum of previous estimates.

Predevelopment Groundwater Discharge

Groundwater Discharge Processes

Groundwater evapotranspiration (ETg) is the primary form of discharge within the GBCAAS study area (figs. C–1 and D–1). Total evapotranspiration (ET) is the process by which water is transferred from the land surface to the atmosphere and includes transpiration by plants and evaporation from bare soils and free water surfaces. ETg is the component of ET that is derived from groundwater, and it usually occurs in areas where groundwater levels are shallow or near land surface. Topographically, areas of ETg generally are found in the low areas near the center of a basin. In these areas, groundwater is discharged by springs, by diffuse seepage upward through basin-fill aquifers, by evaporation from soils and water bodies, and by evapotranspiration by plants. The amount of ETg is dependent upon the vegetation type, vegetation density, groundwater levels, soil characteristics, and micro climate.

Moreo and others (2007), Smith and others (2007), and Welch and others (2007) describe Great Basin phreatophytic vegetation types; delineate ET units based on vegetation type, density, and distribution; and provide a summary of the range of measured ET rates for various ET units. These rates range from average values of 0.71 ft/yr for dry playa areas to 5.1 ft/yr for open water. The volume of water exchanged to the atmosphere by ET is estimated as the product of the area of ET vegetation units and the rates determined from point measurements of ET. Annual ETg generally is estimated as the difference between the estimated annual ET and the annual precipitation (Laczniak and others, 1999; Laczniak and others, 2001; Moreo and others, 2007; Welch and others, 2007). The assumption is that in areas with phreatophytic vegetation, all local precipitation is consumed by plants and any remaining plant water requirements are met by groundwater utilization. Because of the combination of controlling factors, it is difficult to estimate ETg, and the estimates may have large uncertainties.

Groundwater seepage to surface water bodies is another form of groundwater discharge within the GBCAAS study area (figs. C–1 and D–1). This includes discharge to mountain streams, basin-fill streams, basin-fill lakes, and basin-fill reservoirs. Evidence for discharge to mountain streams is provided by the gaining perennial stream reaches often observed in the lower parts of the mountain ranges. Gaining reaches in the Bear, Humboldt, Jordan, and Sevier Rivers (fig. A–1), and other smaller streams, indicate groundwater discharge to perennial streams flowing through the basin fill. Groundwater discharge to lakes and reservoirs located within the basin-fill deposits occurs to the Great Salt Lake, Lake Mead, Utah Lake (fig. A–1) and various other smaller reservoirs.

Groundwater discharge to springs occurs throughout the study area, both in small amounts to local springs, as well as larger amounts to regional springs (figs. C–1 and D–1, pl. 1). The smaller springs located in mountains may represent discharge from perched aquifers not in direct hydraulic connection with the regional water table. Some of the largest regional springs may discharge water that enters the HA as subsurface inflow from adjacent HAs. It is probable that some flow paths to large regional springs incorporate groundwater from several upgradient HAs (Winograd and Thordarson, 1975; Winograd and Pearson, 1976; Thomas and others, 2003).

Groundwater discharge also may include subsurface outflow to downgradient HAs and groundwater flow systems (figs. C–1 and D–1). Discharge as subsurface outflow is derived from groundwater that originates in upgradient areas and subsequently flows into downgradient areas through the subsurface in basin fill or consolidated rock. The amount of subsurface outflow depends on the hydraulic gradient between the HAs or groundwater flow systems, the hydraulic conductivity of the intervening bedrock and alluvium, and the cross-sectional area between the HAs or groundwater flow systems (for example, equation C–1).

Discharge to Evapotranspiration

Current study estimates of groundwater discharge to ETg were derived by compiling and re-evaluating data from more than 100 previous studies, including USGS reports, Nevada Department of Natural Resources (DNR) reconnaissance reports, Utah DNR technical publications, and journal articles (Auxiliary 2). ETg estimates from previous studies were examined closely to determine whether they represented predevelopment conditions or incorporated the effects of significant groundwater withdrawals. For ETg estimates from previous studies that were conducted during significant groundwater development, an adjustment was made to the natural discharge to account for well withdrawals (see “Adjustment to natural discharge for well withdrawals” section in this chapter); this was necessary to establish a predevelopment groundwater budget because these well withdrawals may capture water that would otherwise discharge naturally. It should be noted, however, that the adjusted ETg estimates likely represent maximum values because well withdrawals may have captured some groundwater from groundwater storage instead of from natural discharge.

Groundwater Evapotranspiration Areas

Data delineating areas of ETg were compiled from a number of previous reports and mapped for the study area (fig. D–12; Appendix 6). Most of the data used to map the ETg area boundaries are digital data from four regional-scale studies: BARCAS (Laczniak and others, 2007), DVRFS (Laczniak and Smith, 2001), eastern Nevada (Smith and others, 2000), and the Great Basin Regional Aquifer-Systems Analysis (RASA–GB; Medina, 2005). The boundaries of the ETg areas delineated in these studies define the outer extent of phreatophyte areas (including playas) where groundwater may be consumed by ET. The BARCAS, DVRFS, and eastern Nevada studies used a combination of satellite and aerial photographic imagery, as well as field studies and verification to identify areas within the HAs where ETg may occur (Smith and others, 2000; Laczniak and others, 2001; Smith and others, 2007). The ETg areas defined in the RASA study are a compilation of the data from earlier reconnaissance studies in Nevada and Utah (Harrill and others, 1988), in which ETg areas were delineated using field mapping techniques. In the current study, data from the BARCAS and DVRFS studies were used preferentially to map ETg areas because these studies are most recent and involved extensive detailed mapping of phreatophyte areas. In areas outside the BARCAS and DVRFS study areas, data from the eastern Nevada (Smith and others, 2000) and RASA–GB studies (Medina, 2005) were used, with the eastern Nevada study (Smith and others, 2000) data preferentially used because it is most recent and was derived from more detailed mapping of ETg areas.

Additional ETg areas were mapped in six HAs using information from four smaller-scale (HA-scale) studies (Rush, 1964, fig. 2; Rush, 1968, pl. 1; Bolke and Price, 1972, pl. 1; Thiros and others, 1996, pl. 1). The ETg areas delineated in these studies were manually added to the digital data set of ETg areas for HAs in which either (1) there was a previously reported ETg estimate, but no ETg area was formerly delineated in the regional-scale digital data sets; or (2) the ETg area defined in the report differed significantly from the ETg areas delineated in the regional-scale digital data sets (discussed above).

Groundwater Evapotranspiration Estimates

Current study estimates of groundwater discharge to ETg for each HA and groundwater flow system were determined by compiling data from previously published studies (Auxiliary 3H). The published reports used to derive the current study estimates can be divided into three types: (1) full-HA reports, where ETg estimates for the entire ETg area within a single HA are reported; (2) partial-HA reports, where the ETg estimates are reported only for a section of the ETg area within a single HA; and (3) multi-HA reports, where ETg estimates from two or more HAs are summed together into a single reported ETg estimate. All but seven of the HAs with mapped ETg areas had at least one previously reported ETg estimate.

For the majority of HAs within the study area, ETg estimates were taken directly from the previous reports. The ETg estimates from more recent studies were used preferentially as the current study estimates, especially in the cases of the BARCAS (12 HAs, fig. A–2), DVRFS (31 HAs, fig. A–2), and Wasatch Front studies (Tooele Valley, HA 262; Utah Valley Area (Southern section and Goshen Valley), HA 265; Northern Juab Valley, HA 266; Cedar City Valley, HA 282). ETg estimates from the BARCAS and DVRFS studies included more extensive, detailed mapping of vegetation units and detailed point measurements of ET rates. The Wasatch Front studies took advantage of information on more recently published ETg rates and included more detailed information about whether precipitation and spring discharge were included in the reported ETg than previous reports in these areas. If an HA had multiple ETg estimates from different sources, an average of these estimates was calculated and used as the current study estimate when there was no definitive reason for selecting one estimate over another. ETg estimates from partial-HA reports were used only if (1) there were no full-HA ETg estimates for the HA, or (2) the total ETg area within the HA was represented by multiple partial-HA ETg estimates.

Generally, ETg estimates from multi-HA reports were used only if there were no full-HA ETg estimates for the HA. If a multi-HA report contained an estimate for HAs that have no full-HA ETg estimates, the multi-HA ETg estimate was divided among the HAs by the fraction of the total ETg area located within each HA (Auxiliary 3I—Case 1). In some cases, a previously published ETg estimate for multiple HAs included both an HA for which no other ETg estimates existed and an HA for which there was a separately reported estimate. In this case, the ETg amount for the HA not having a separate estimate was calculated by subtracting the separately reported ETg estimate for the other HA from the total ETg estimate given in the multi-HA report (Auxiliary 3I—Case 2).

Nichols (2000) developed water-budget estimates for 16 HAs in east-central Nevada. Some of the HAs that Nichols studied were revisited by Moreo and others (2007) and Welch and others (2007). Moreo and others (2007) estimated ETg on the basis of measurements of ET over specific vegetation

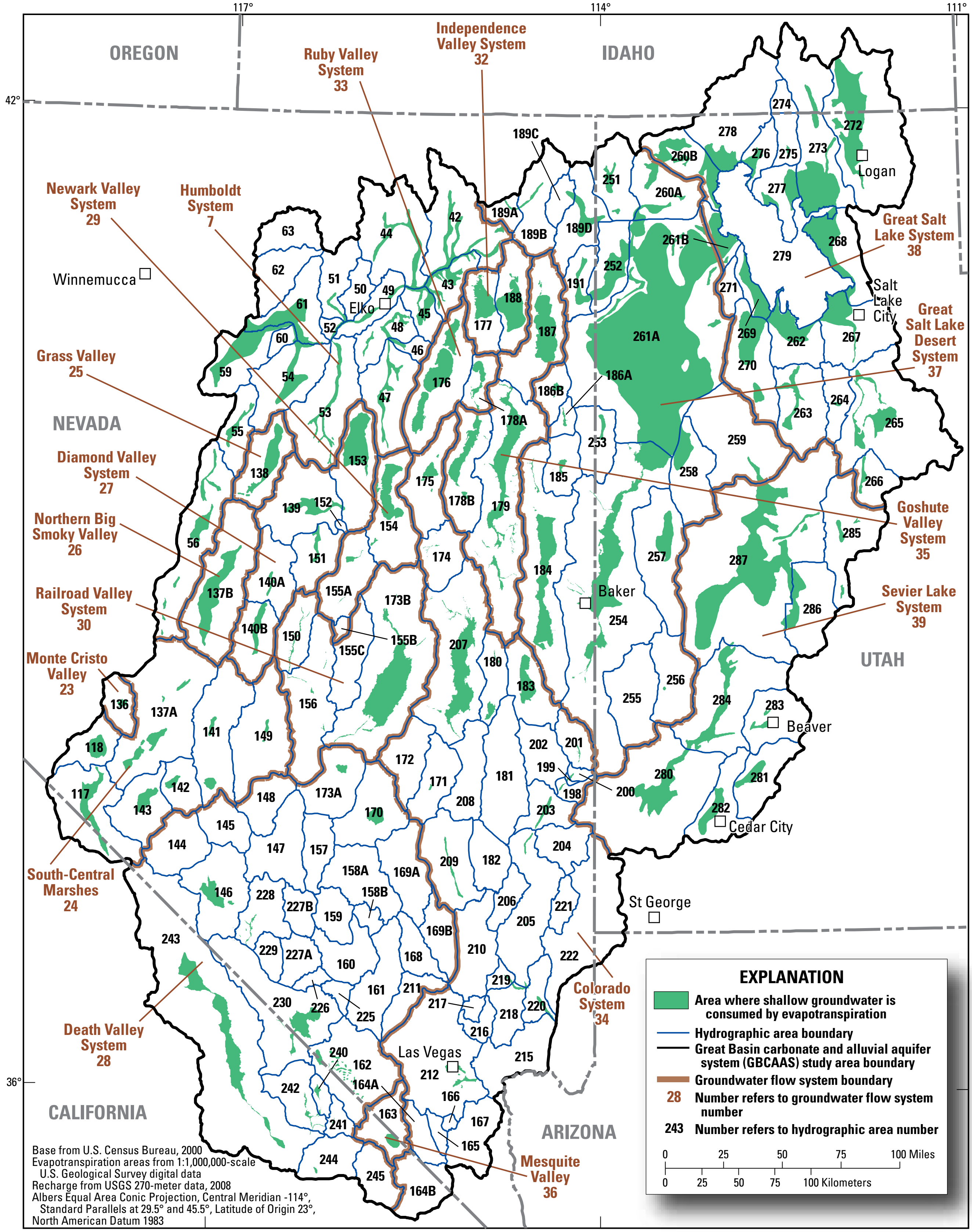

Figure D–12. Areas of groundwater evapotranspiration (ETg) in the Great Basin carbonate and alluvial aquifer system study area.

units. Moreo and others (2007) and Welch and others (2007) did extensive comparisons and uncertainty analyses on their data, as well as data published in previous studies, including Nichols (2000). Nichols's (2000) estimates of ETg generally are on the upper end of the range of reported values and are as much as two times that of the more detailed measurements and estimates made by Moreo and others (2007) and Welch and others (2007). Therefore, Nichols's (2000) ETg estimates were not used to determine ETg in the current study.

Six of the HAs within the study area had mapped ETg areas but no previous ETg estimates. These HAs include Grass Valley (HA 138), Coal Valley (HA 171), Valjean Valley (HA 244), Great Salt Lake Desert-East Part (HA 261B), Great Salt Lake (HA 279), and Sevier Desert (HA 287). As a first step in estimating the volume of ETg for these HAs, the mapped ETg areas were compared to imagery from the U.S. Department of Agriculture National Agricultural Imagery Program (NAIP) Compressed County mosaics (CCM) for Utah (2006b), Nevada (2006a), and California (2005); and the Southwest Regional Gap Analysis Project (SWReGAP) data from the RS/GIS Laboratory, College of Natural Resources, Utah State University (2004). From the NAIP imagery and SWReGAP data, it was determined that ETg areas within all of these HAs, except Great Salt Lake (HA 279), predominantly were playa. Reported ETg rates for playas within the study area generally range from 0.1 to 0.5 ft/yr (Zones, 1961, p. 21; Hood and Rush, 1965, table 6; Harrill and Lamke, 1968, table 8; Hood and Waddell, 1968, table 6; Harrill, 1971, table 5; Van Denburgh and Rush, 1974, table 8; Lines, 1979, p. 88; Malek and others, 1990, table 5; Handman and Kilroy, 1997, table 9; DeMeo and others, 2003, table 4; Welch and others, 2007, Appendix A), with the most commonly reported ETg rate for playas being 0.1 ft/yr. Therefore, ETg estimates for these HAs were determined by applying an ETg rate of 0.1 ft/yr over the ETg area within each HA.

For Great Salt Lake (HA 279), the mapped ETg areas only occur along the shoreline of the Great Salt Lake. The area of this terminal lake varies widely as lake levels fluctuate because of variations in climate and weather conditions from year to year; therefore, the ETg areas along the shoreline may or may not be inundated by the Great Salt Lake at any one point in time. It was not within the scope of this study to determine if evapotranspiration is supported by surface water or groundwater. Because of the relatively fine-grained playa deposits along the lake shore, however, and lack of evidence of inflow of freshwater into the lake along its margins (Dave Naftz, U.S. Geological Survey, oral commun., 2009; Stolp and Brooks, 2009), it is assumed that ET is mainly surface-water supported and, therefore, ETg was assumed to be negligible within this HA. Any ETg along the edge of Great Salt Lake is probably included in the estimates of groundwater discharge to Great Salt Lake.

Many of the previous reports used to derive the ETg estimates include spring discharge in the reported ETg. It was assumed in these reports that all spring discharge from the basin fill ultimately was consumed through evapotranspiration. Because groundwater discharge to springs is a separate component of the groundwater budget in the current study, spring discharge was subtracted from the ETg estimates that included spring discharge. For previous reports in which the amount of spring discharge contributing to ETg was specified, the reported amount of spring discharge was subtracted from the ETg estimate. Very few of the previous reports, however, explicitly define the magnitude of spring discharge or identify which springs in the HA were included in the ETg estimates. The current study assumes that any spring or group of springs within 2 mi of an ETg area (as this distance generally encompasses all springs that discharge within the basin fill) contributes to ETg within that HA. Discharge from these springs ("Estimated/Reported spring discharge in reported ETg" column in Auxiliary 3H) was subtracted from the ETg estimates for those reports that include spring discharge in the reported ETg but that do not specify the amount of spring discharge included. Springs that discharge less than about 300 gal/min (500 acre-ft/yr) are not counted explicitly in the groundwater budget in this study; discharge to small springs within the basin fill can be assumed to be included in the estimates of ETg.

Total estimated predevelopment groundwater discharge to ETg in the current study is 1,800,000 acre-ft/yr (table D–2) and accounts for 43 percent of the total predevelopment discharge for the study area. The Great Salt Lake (38), Great Salt Lake Desert (37), Humboldt (7), and Sevier Lake (39) groundwater flow systems have the highest amounts of discharge to ETg and account for 69 percent of the total estimated annual ETg for the study area. These four groundwater flow systems generally are wetter and host large areas of phreatophytic vegetation (fig. D–12). In contrast, Monte Cristo Valley (23), Mesquite Valley (36), and Grass Valley (25) groundwater flow systems are drier and smaller and have much less annual ETg. ETg estimates for each of the HAs are given in Appendix 5.

Discharge to Surface Water

Within the GBCAAS study area, groundwater discharge to surface water is an important component of the groundwater budget (table D–2). This includes discharge to streams (both mountain and basin-fill streams), as well as discharge to lakes and reservoirs. Groundwater discharge to springs is discussed separately in the "Discharge to Springs" section below.

Discharge to Mountain Streams

In the current study, groundwater budgets for entire HAs, including the mountains, are estimated, and discharge to mountain streams (also referred to as "baseflow") is a component of these budgets. Few previously published reports estimated groundwater discharge to mountain streams; these estimates, therefore, were derived for the current study using records from USGS gaging stations. Some of the baseflow becomes recharge from streams, canals, and irrigated fields on the basin fill as discussed in the “Recharge from Mountain Stream Baseflow” section of this report. For mountain streams that begin flowing in a watershed (that is, no flow in the upgradient part of the stream channel), only one gage is necessary to determine if a stream is gaining because any baseflow in that stream must be derived from groundwater discharge to the stream within the drainage area. It is assumed baseflow estimates do not include streamflow inputs from surface-water runoff or from streams flowing from an upgradient watershed. While there may be both gaining and losing reaches, this gaged baseflow represents net groundwater discharge upstream of the gage location.

A simplified approach for determining baseflow for gaged mountain streams was used in the current study, whereby the annual groundwater discharge was estimated to be the minimum mean daily discharge at each gage for the period of record multiplied by 365 days per year. The use of minimum daily discharge to estimate baseflow represents a minimum value because baseflow changes seasonally and annually (during periods of higher streamflow, baseflow will correspondingly increase). Rigorous hydrograph separation methods for estimating groundwater discharge to streams (Hall, 1968; Zecharias and Brutsaert, 1988; Tallaksen, 1995; Rutledge, 1998) were not used, these methods were not developed for application in snowmelt-dominated streams prevalent in the GBCAAS. Modifying these baseflow separation techniques was beyond the scope of the current study.

USGS streamflow data from the USGS’ NWIS database (Mathey, 1998) and from published reports were used to develop current study estimates of groundwater discharge to streams in the mountains (table D–2, Appendix 5). Streamflow records from 105 USGS stream gages (pl. 1 and Auxiliary 3J) were chosen on the basis of the following criteria: (1) the minimum mean daily discharge was greater than 0, (2) the gage was located within 0.25 mi of consolidated rock, and (3) the station had at least 365 continuous days of streamflow record. The minimum flow limitation was used to eliminate nonperennial streams. Although groundwater discharge from regional and locally perched sources may occur to ephemeral and intermittent streams, this amount of discharge was considered to be negligible at the scale of the current study. The geographic limitation (0.25 mi from consolidated rock) was used to minimize the effects of diversions and stream loss on alluvial fans or other deposits. It was assumed that streamgages within 0.25 mi of consolidated rock were located above all diversions and above substantial stream loss to basin-fill deposits. Where multiple gages exist along a stream, groundwater discharge between the gages was assumed to be the minimum mean daily flow at the lower gage minus the minimum mean daily flow at the upper gage to better evaluate the location of this discharge.

Groundwater likely discharges to some ungaged perennial mountain streams within the study area, particularly in eastern Nevada (Randell J. Laczniak, U.S. Geological Survey, written commun., 2009). Determining the number of these streams and associated baseflow of these streams, however, was beyond the scope of the current study. While the National Hydrography Dataset (NHD) classifies streams as either intermittent or perennial, this classification is subject to error. The NHD classification is based primarily on digitized intermittent and perennial streams from USGS 1:24,000 topographic maps. The water features on these maps were determined as follows: *“Field personnel would look at the particular stream and would attempt to determine if the stream flowed year round (except in the dry season), or flowed part of the year (intermittent). We would talk to local personnel and ask them to determine if the flow we were seeing was typical… this is a rather subjective method as opposed to a scientific method”* (William J. Smith, U.S. Geological Survey National Mapping Division, written commun., 2010). Furthermore, a perennial stream is defined as a stream that *“contains water throughout the year, except for infrequent periods of severe drought”* (National Hydrography Dataset, February 2000, accessed January 2010 at http://nhd.usgs.gov/chapter1/index.html). This implies that many streams classified as perennial in the NHD dataset dry up during drought periods and, thus, are not likely connected to the regional aquifer system. For these reasons, relying on this dataset for estimating groundwater discharge would be problematic. In addition, no basin characteristic techniques or statistics currently exist to determine baseflow in these ungaged streams (Terry A. Kenney, Surface-Water Specialist, U.S. Geological Survey, oral commun., 2010). Because the number of ungaged perennial streams and the amount of discharge from these ungaged streams could not be quantified, the current study estimate of groundwater discharge to mountain streams is a minimum estimate.

Estimates of baseflow for individual gaged mountain streams range from 10 to 57,000 acre-ft/yr (Auxiliary 3J). Mean annual streamflow for individual gaged mountain streams ranges from 270 to 140,000 acre-ft/yr (Auxiliary 3J). For individual streams, the percentage of mean annual flow that is estimated as baseflow ranges from less than 1 to 85 percent.

On the basis of historical streamgage records, total estimated predevelopment groundwater discharge to mountain streams for the current study is 450,000 acre-ft/yr and accounts for 11 percent of the total discharge for the entire study area (table D–2). Generally, mountain ranges with greater amounts of precipitation (fig. D–2) have greater amounts of discharge to mountain streams. The Great Salt Lake (38) and Sevier Lake (39) groundwater flow systems have the highest amounts of discharge to mountain streams and account for 91 percent of the estimated discharge to mountain streams for the entire study area (table D–2). These groundwater flow systems include mountainous regions with more precipitation and larger total lengths of perennial stream reaches than the other groundwater flow systems (pl. 1). Only four HAs in the Great Salt Lake (38) and Sevier Lake (39) groundwater flow systems account for 71 percent of the total estimated discharge to mountain streams (Appendix 5). The Humboldt groundwater flow system (7) accounts for about 3 percent of the total discharge to mountain streams. The remaining 6 percent of discharge to mountain streams is distributed between nine other groundwater flow systems. Five of the groundwater flow systems and 121 HAs within the study area have no gaged perennial mountain streams. Because there are ungaged perennial streams in these areas and elsewhere, the total estimated groundwater discharge to mountain streams for the GBCAAS study area is considered a minimum value.

Discharge to Basin-Fill Streams/Lakes/Reservoirs

Current study estimates of groundwater discharge to basin-fill streams, lakes, and reservoirs (Auxiliary 3K) were derived by compiling and re-evaluating data from more than 100 previous studies, including USGS reports, Nevada DNR reconnaissance reports, Utah DNR technical publications, and journal articles (Auxiliary 2). Each reported estimate was examined in detail to ensure that the data were in agreement with gage data and other conditions (for example, groundwater levels at or above stream altitude); if the data were in agreement, these estimates were used as the current study estimate. If more than one reported discharge estimate existed for an HA, and there was no definitive reason to choose one estimate over another, then the average of the estimates was used. If the previously reported discharge estimate was not in agreement with gage data and other conditions, adjustments were made to the estimate on the basis of gage data or seepage data from other studies (Auxiliary 3K). For example, in Upper Reese River Valley (HA 56), Berger (2000) reported groundwater discharge to the Reese River of 1,000 acre-ft/yr (Auxiliary 3K); however, streamgages from NWIS showed the river losing in the basin fill, not gaining. The current study estimate of groundwater discharge to basin-fill streams, lakes, and reservoirs, therefore, was 0 acre-ft/yr for this HA. Gage data were used to estimate groundwater discharge to streams in a few HAs for which there was no previously reported groundwater discharge estimate. Some previous estimates of groundwater discharge to basin-fill streams were misreported as spring discharge and vice versa (see “Comments” column in Auxiliary 3K). In the current study, (1) groundwater discharge to streams that was incorrectly reported as spring discharge and (2) spring discharge that was incorrectly reported as groundwater discharge to streams were both reclassified under the correct discharge component (Auxiliary 3K and 3L).

Total estimated predevelopment groundwater discharge to basin-fill streams, lakes, and reservoirs for the current study is 660,000 acre-ft/yr (table D–2) and accounts for 16 percent of the estimated total discharge for the study area. The Great Salt Lake (38), Colorado (34), and Sevier Lake (39) groundwater flow systems have the highest amount of discharge to basin-fill streams, lakes, and reservoirs, and account for 98 percent of the total estimated for the entire study area. Seven HAs account for about 97 percent of the total estimated discharge to basin-fill streams, lakes, and reservoirs (Appendix 5). The remaining 3 percent is distributed among 10 other HAs, each having less than 10,000 acre-ft/yr of discharge to basin-fill streams, lakes, and reservoirs. There are 148 HAs with no estimated groundwater discharge to basin-fill streams, lakes, or reservoirs.

Discharge to Springs

Estimates of groundwater discharge to springs were derived for the current study using both spring data compiled from the USGS’ NWIS database (Mathey, 1998) and measurements of individual springs from published reports (Auxiliary 3L). Previously reported total spring discharge estimates by HA were not used in the current study because these estimates often (1) included discharge only from the largest regional springs, (2) did not include discharge to mountain springs, and (or) (3) did not separate spring discharge from ETg discharge estimates.

Within the GBCAAS study area, there are about 300 individual springs or groups of springs having discharge greater than 300 gal/min. Only springs with discharge greater than 300 gal/min (about 500 acre-ft/yr) are included because smaller springs are less likely to be perennial than larger springs. Exceptions are made when several small springs are clustered together to create a total discharge of greater than 300 gal/min. Springs that discharge less than 300 gal/min account for only about 8 percent of the total flow (about 77,000 acre-ft/yr) from springs reported in the NWIS database, and fewer than 2 percent of the total discharge for the study area, which is well within the uncertainty of 30 percent assumed for discharge estimates. For most springs, the mean flow for the entire period of record was used as the predevelopment discharge. Discharge from springs that contributes to a gaged perennial stream was assumed to be included in the gaged baseflow and was not accounted separately. In areas where groundwater withdrawals are known to have affected spring discharge, only discharge measurements before the affected period were used. For springs with data in both NWIS and a published report, only data that more accurately presented predevelopment long-term discharge were used.

The distribution of spring discharge is different from the spatial distribution of gaged perennial mountain streams (pl. 1). In particular, the east-central part of Nevada (Kobeh Valley, HA 139; Diamond Valley, HA 153; Newark Valley, HA 154; Railroad Valley-Northern Part, HA 173B; Ruby Valley, HA 176; Butte Valley-Northern Part, HA 178A; Steptoe Valley, HA 179; Lake Valley, HA 183; Spring Valley, HA 184; White River Valley, HA 207; and Snake Valley, HA 254) has many large springs, yet a relatively small number of gaged streams. The near-surface geology of this area (fig. B–3) is dominated by permeable carbonate rocks. This area has relatively high BCM estimated in-place recharge rates (fig. D–5) and low runoff rates (fig. D–6). The permeable rocks have subdued mounding of the potentiometric surface (less discharge to mountain streams) and transmit this high recharge to both nearby and distant springs. In contrast, the eastern portion of the Sevier Lake (39) groundwater flow system (Parowan Valley, HA 281; Cedar City Valley, HA 282; and Pavant Valley, HA 286) and the central portion of the Humboldt (7) groundwater flow system (Starr Valley Area, HA 43; Lamoille Valley, HA 45; Susie Creek Area, HA 50; Maggie Creek Area, HA 51; and Boulder Flat, HA 61) have few large springs, yet a relatively large number of perennial gaged streams. The surficial geology of these areas is dominated by less permeable siliciclastic and volcanic rocks (tables B–1 and A3–1), resulting in mounding of the potentiometric surface beneath these mountains (more discharge to mountain streams).

Total estimated predevelopment groundwater discharge to springs (in both the mountain block and basin fill) for the current study is 990,000 acre-ft/yr (table D–2) and accounts for 24 percent of the total discharge for the study area (table D–2). This is a minimum estimate because it does not include discharge from springs that have not been measured. Seventy-five percent of the total is discharged from the Great Salt Lake (38), Colorado (34), and Great Salt Lake Desert (37) groundwater flow systems. Ten HAs account for about one-half of the total estimated discharge to springs (Appendix 5), 59 other HAs have less than about 30,000 acre-ft/yr of estimated spring discharge each, and the remaining 96 HAs have no estimated spring discharge.

Discharge to Subsurface Outflow

As with subsurface inflow, subsurface outflow was not estimated for the current study because of (1) the large uncertainty in groundwater-budget components for using water-balance methods, and (2) the sparsity of hydraulic information for using Darcy flux methods. Previous estimates of subsurface outflow were compiled by HA (Auxiliary 3M) and by groundwater flow system (Auxiliary 3N). The estimates compiled by groundwater flow system account only for subsurface outflow that exits a groundwater flow system and do not account for subsurface outflow between HAs within a groundwater flow system. As discussed above in “Recharge from Subsurface Groundwater Inflow,” these previous estimates could not be used in the current study because in many of these studies balancing groundwater budgets in the upgradient or downgradient HAs or groundwater flow systems was not considered.

Figure D–9 shows groundwater-budget imbalances and arrows where the potentiometric contours, likelihood of hydraulic connection across HA boundaries (pl. 2), and groundwater-budget information all indicate possible groundwater subsurface flow between groundwater flow systems. Subsurface outflow is possible from all of the groundwater flow systems except Mesquite Valley (36). Subsurface outflow is likely in the Monte Cristo Valley (23), Grass Valley (25), and Diamond Valley (27) groundwater flow systems, where estimated recharge exceeds predevelopment discharge by more than 30 percent (table D–2). Although subsurface outflow is possible from the other 13 groundwater flow systems, these fluxes are not required to balance predevelopment groundwater budgets in these groundwater flow systems.

The only possible discharge to subsurface outflow leaving the GBCAAS study area occurs in the Humboldt groundwater flow system (7), which is the only partial groundwater flow system in the study area. Potentiometric contours and the likelihood of hydraulic connection across HA boundaries (pl. 2) indicate the potential for subsurface outflow toward the northwest to sections of the Humboldt groundwater flow system (7) outside of the GBCAAS study area (fig. D–9).

Adjustment to Natural Discharge for Well Withdrawals

A number of the previously reported discharge estimates include well withdrawals. Because well withdrawals may affect natural discharge, and because these previously reported discharge estimates were used to calculate previous predevelopment budget estimates, well-withdrawal estimates from these reports were taken into account in establishing a predevelopment groundwater budget for each groundwater flow system and HA. For the current study, it is assumed that previously reported well withdrawals greater than 10 percent of the total reported discharge affect natural discharge (Auxiliary 3O). The effects of withdrawals less than this likely are too small to detect and cannot be differentiated from fluctuations and errors in natural discharge.

Adjustments were only needed in a total of 16 HAs within the Great Salt Lake (38), Sevier Lake (39), Humboldt (7), and Great Salt Lake Desert (37) groundwater flow systems (Auxiliary 3O). All other HAs within the GBCAAS study area either had reported predevelopment groundwater discharge estimates or well withdrawals that were less than 10 percent of total reported natural discharge. In the HAs where adjustments were needed, it was assumed that net well withdrawals (reported well withdrawals minus irrigation return flow) were 70 percent of total reported well withdrawals (see “Recharge of Unconsumed Irrigation and Public Supply Water from Well Withdrawals” section below). Although well withdrawals may have different effects on the various components of natural discharge, the distribution of these effects amongst the individual discharge components (ETg, surface water, springs, and subsurface outflow) is not known. These net well withdrawals, therefore, are represented in table D–2 and Appendix 5 in the column “Adjustment to natural discharge for well withdrawals.” This is a maximum estimate that assumes all discharge from well withdrawals captures groundwater that would otherwise discharge naturally from the system, and it does not account for groundwater that may be released from storage within the aquifer.

The total estimated adjustment to natural discharge for well withdrawals for the current study is 330,000 acre-ft/yr (table D–2) and accounts for 8 percent of the total predevelopment groundwater discharge estimate. The largest adjustments are to the Great Salt Lake (38) and Sevier Lake

(39) groundwater flow systems. Smaller adjustments are to the Humboldt (7) and Great Salt Lake Desert (37) groundwater flow systems. No adjustments were made in the other 13 groundwater flow systems. Six HAs account for 81 percent of the total adjustment to natural discharge (Appendix 5). These HAs incorporate the heavily populated Wasatch Front area that was highly developed as early as the 1950s and 1960s, before the first detailed groundwater studies were conducted. The remaining 19 percent of the total adjustment to natural discharge is distributed among 10 other HAs; 148 HAs required no adjustment to natural discharge, either because reported withdrawals were a small portion of groundwater discharge, or because predevelopment estimates of discharge were previously reported.

Previously Published Estimates of Groundwater Discharge

Previously reported discharge estimates from regional and HA-based groundwater studies were used to derive many of the current study discharge estimates for predevelopment conditions (Appendix 5), and they also were compiled for comparison to current study groundwater-budget estimates (table D–2; Auxiliary 3P). Unfortunately, these previous studies (from the 1940s through the 2000s) were sometimes conducted in HAs undergoing extensive groundwater development, and the natural discharge reported from those studies may be less than it was prior to development. Total previously reported annual discharge for the entire study area ranged from 3,400,000 to 4,200,000 acre-ft/yr (table D–2).

Summary of Discharge Components for Predevelopment Conditions

The current study estimate of total discharge for predevelopment conditions in the GBCAAS study area is 4,200,000 acre-ft/yr (table D–2). Discharge from the Great Salt Lake groundwater flow system (38) accounts for more than 50 percent of the discharge from the entire study area. Discharge from the Great Salt Lake Desert (37), Sevier Lake (39), Humboldt (7), and Colorado (34) groundwater flow systems each account for 5 to 11 percent of total discharge. Discharge for all remaining groundwater flow systems each account for less than 5 percent of the total discharge. Estimated groundwater evapotranspiration, ETg, is the largest form of discharge and accounts for 43 percent of total discharge, followed by discharge to springs (24 percent), discharge to basin-fill streams, lakes, and reservoirs (16 percent), discharge to mountain streams (11 percent), and the adjustment to natural discharge for well withdrawals (8 percent). The relative magnitude of each discharge component by groundwater flow system is shown on figure D–13. Except for the Great Salt Lake (38) and Colorado (34) groundwater flow systems, ETg is the most important form of groundwater discharge from all groundwater flow systems, accounting for about 50–100 percent of total discharge from these flow systems (figs. D–13 and D–14). Discharge to basin-fill streams, lakes, and reservoirs is the largest component in the Great Salt Lake groundwater flow system (38), accounting for 26 percent of discharge in this flow system. Discharge to springs is the largest component in the Colorado groundwater flow system (34), accounting for 57 percent of discharge.

Total groundwater discharge estimated for groundwater flow systems in the current study generally fall within the ranges of the compiled previous estimates (table D–2). Current discharge estimates for the Humboldt (7), Colorado (34), Great Salt Lake (38), and Sevier Lake (39) groundwater flow systems, however, exceed the maximum of the previous estimate compilations by 76, 10, 10, and 14 percent, respectively. Previous estimates for the Humboldt (7) and Sevier Lake (39) groundwater flow systems were missing for various HAs within these flow systems, which explains, in part, why current estimates exceed the compiled numbers from previous estimates. Discharge in the Colorado (34), and Great Salt Lake (38) groundwater flow systems are higher than previous estimates because the previous estimates do not include discharge to mountain streams and springs.

Total groundwater-discharge estimates for HAs in the current study also generally are similar to previous estimates. Where only a minimum previously reported discharge estimate is listed in Appendix 5, this indicates that only one previous study had HA-based total discharge measurements. Previous total groundwater discharge estimates have been reported for 106 of the 165 HAs within the GBCAAS study area; 59 HAs have no previously estimated total groundwater discharge. Of the 106 HAs, only 37 have more than one estimate of total groundwater discharge. In four of these 37 HAs, the current study exceeds or underestimates the previously reported ranges by more than 30 percent. For Jakes Valley (HA 174), Dugway-Government Creek Valley (HA 259), and Cache Valley (HA 272), the current study estimates exceed the previously reported ranges by 90, 61, and 64 percent, respectively. This difference is primarily because the current study estimate includes groundwater discharge to mountain streams and mountain springs, which was not quantified in these previous studies. For Pine Valley (HA 255), the current study estimates no groundwater discharge, compared to a range of 7,000 to 7,100 acre-ft/yr from previous reports. This is because (1) the previous estimates of ETg of 5,500 acre-ft/year (Stephens, 1976; Gates and Kruer, 1981) were not used in the current study estimate because it appears that this ET is surface-water supported, on the basis of stream proximity and (or) a deep water table; (2) the 940 acre-ft/yr of reported discharge to Sheep, Indian, and Pine Grove Creeks (Stephens, 1976) was not used in the current study estimate because flow is intermittent in these streams and, therefore, were not considered gaining streams in the basin-fill; and (3) the current study estimate did not include the 650 to 1,600 acre-ft/yr of previously reported spring discharge (Stephens, 1976; Gates and Kruer, 1981) because either (1) the instantaneous discharge measured at each spring was less than 300 gal/min (Stephens, 1976), or (2) previously reported spring discharge

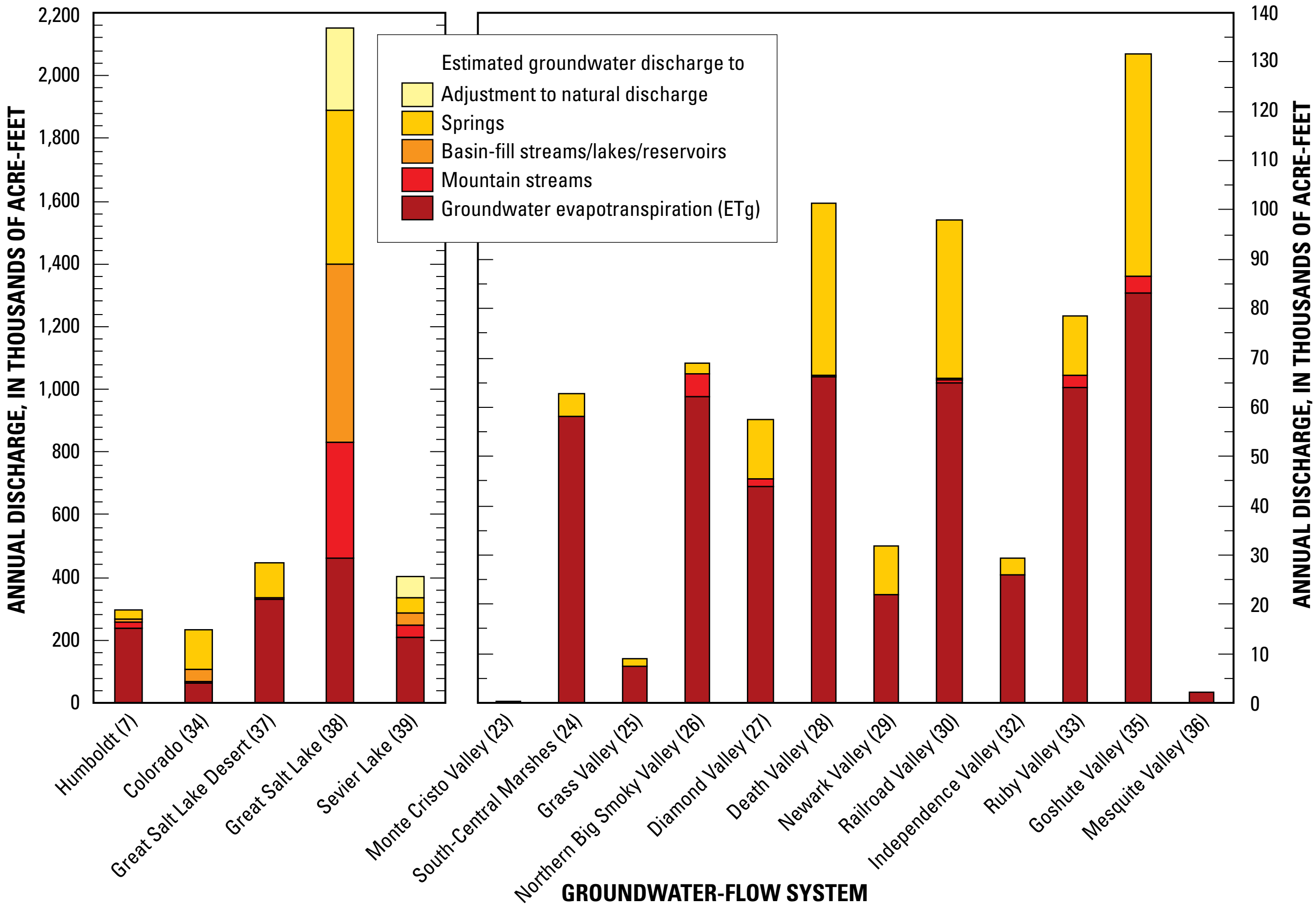

Figure D–13. Estimated groundwater-discharge components for predevelopment conditions for the 17 groundwater flow systems of the Great Basin carbonate and alluvial aquifer system study area.

measurements also included discharge from wells (Gates and Kruer, 1981).

Of the 69 HAs with only one previous estimate of total groundwater discharge, the current study exceeds or underestimates these previously reported estimates by more than 30 percent in 13 HAs (Appendix 5). For three of these HAs (South Fork Area, HA 46; Lida Valley, HA 144; and Indian Springs Valley, HA 161), the current study estimate is larger and includes groundwater discharge to mountain streams and (or) mountain springs, which was not quantified in the previous studies. For Marys Creek Area (HA 52), the current study estimate is larger because it includes both groundwater discharge to mountain streams and 9,500 acre-ft/yr of discharge to the Humboldt River not included in the previous estimate. Current study discharge estimates for the other nine HAs (Antelope Valley-Southern Part, HA 186A; Goshute Valley, HA 187; Las Vegas Valley, HA 212; California Wash, HA 218; Lower Moapa Valley, HA 220; Sink Valley, HA 271; Promontory Mountains Area, HA 277; Beryl-Enterprise Area, HA 280; and Milford Area, HA 284) are less than previously reported estimates for a variety of reasons including (1) for Antelope Valley-Southern Part (HA 186A), previously reported discharge was entirely as subsurface outflow, which is not considered at the HA level in the current study; (2) for Goshute Valley (HA 187), California Wash (HA 218), Lower Moapa Valley (HA 220), and Sink Valley (HA 271), previously reported ETg is likely supported by surface water and is too high; (3) for Las Vegas Valley (HA 212), Beryl-Enterprise Area (HA 280), and Milford Area (HA 284), the previous studies were conducted during groundwater development and did not report discharge for predevelopment conditions; and (4) for Promontory Mountains Area (HA 277), the previously reported estimate of discharge to springs is not consistent with NWIS data and is likely too high.

Recent (2000) Groundwater Budgets

The groundwater budgets presented in previous sections of this report were developed for conditions prior to groundwater development. Significant changes in the groundwater budgets as a result of development since the 1940s include discharge by well withdrawals, recharge from irrigation with groundwater, recharge from imported water (Las Vegas Valley; HA 212), decreased natural discharge, and declines

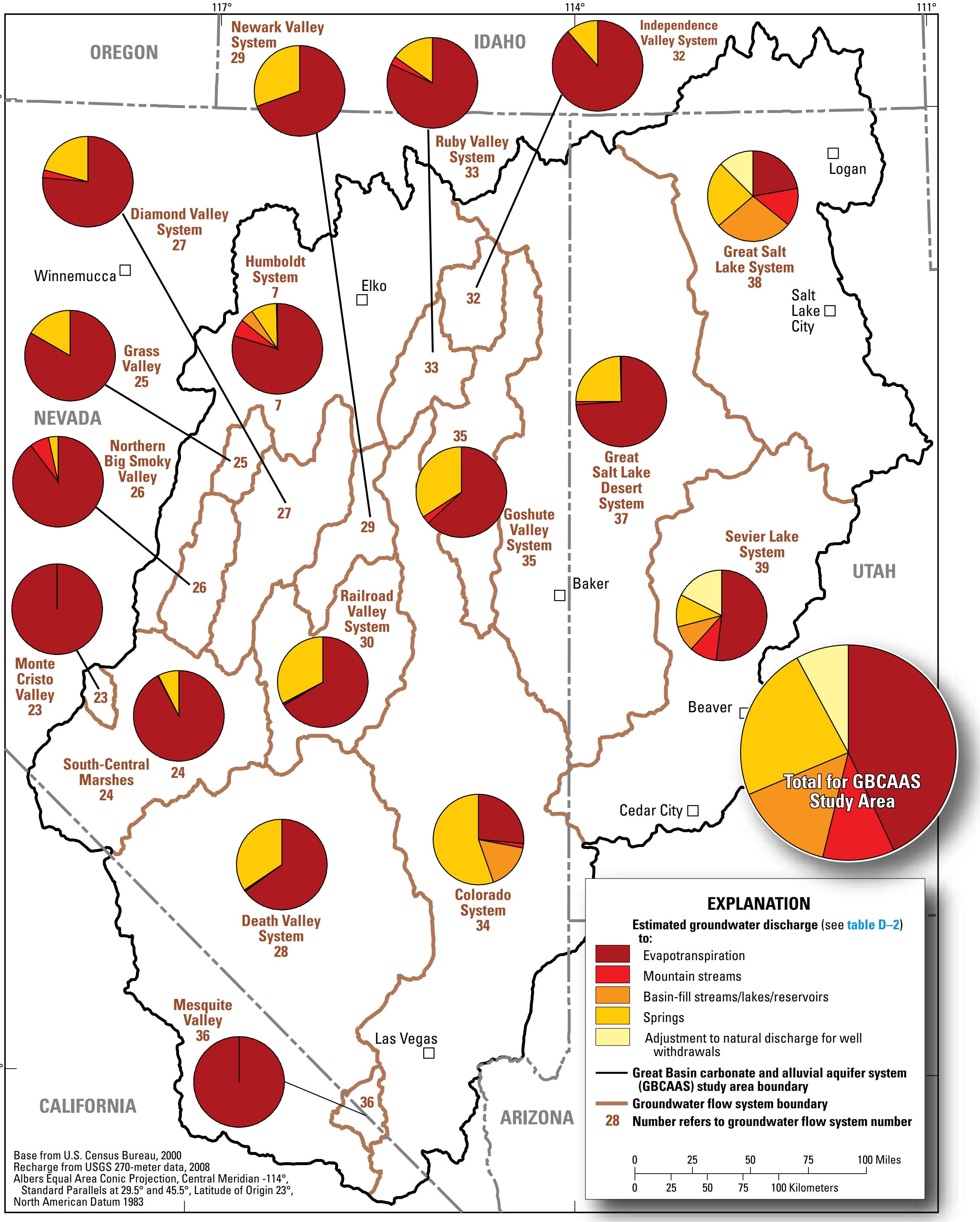

Figure D–14. Groundwater-discharge components for predevelopment conditions for the 17 groundwater flow systems of the Great Basin carbonate and alluvial aquifer system study area.

in groundwater storage (table D–3 and Appendix 7). The following sections quantify recent groundwater components for the study area.

Well Withdrawals

Well withdrawals have had the largest effect on changes in groundwater budgets during the past century. The State of Utah has compiled well withdrawals on an annual basis since 1963 (Arnow and others, 1964). The most complete compilation for the State of Nevada is for the year 2000 (pumpage and crop inventories from http://water.nv.gov; Lopes and Evetts, 2004; Matt Dillon, Nevada Division of Water Resources [NDWR], written commun., 2008; Moreo and Justet, 2008). More recent compilations by Moreo and Justet (2008), Matt Dillon (NDWR, written commun., 2008), and pumpage and crop inventories from the NDWR website (http://water.nv.gov) include very few HAs. Recent budget component estimates for the entire GBCAAS study area, therefore, are based on well withdrawals for the year 2000.

Water development in the eastern Great Basin began shortly after significant numbers of settlers arrived in the 1840s. Early water development used surface water from many of the mountain-front streams and rivers. Within the GBCAAS study area, the largest amount of surface-water development occurred in the Great Salt Lake groundwater flow system (38). Groundwater development by early settlers initially was limited to springs. For example, the settlement in the Las Vegas area was around a large spring complex. Shortly after the first settlers arrived, however, shallow hand-dug wells were developed. The oldest documented well in Salt Lake Valley was completed in 1848 (Gates, 2004). Through the late 1800s, many small-diameter flowing wells were constructed by driving or jetting casing in areas with groundwater at shallow depths (Richardson, 1906; Gates, 2004). Mechanical drilling of larger diameter wells and the installation of pumps began around 1900 and groundwater extraction accelerated. The first successful wells in the Las Vegas area were drilled around 1906 (Malmberg, 1964). The rate of construction of large-diameter wells increased during drought periods between the 1920s and the 1940s. By the late 1930s, areas of both Nevada and Utah were experiencing groundwater level declines in the more developed basins. Groundwater withdrawals have continued to increase as drilling technologies have improved and as water demand by agriculture and public supply has increased.

In Las Vegas Valley (HA 212), measurable subsidence associated with groundwater withdrawals began in the 1930s, with total subsidence exceeding 2 ft between 1935 and 1963 (Malmberg, 1964), and nearly 6 ft since 1935 (Pavelko and others, 1999). In recent years, however, the rate of subsidence has decreased, and, in some sections of the basin, land-surface altitudes have rebounded slightly (generally less than 1.5 in.) because of direct-well injection for aquifer storage and recovery operations that began in 1988, and decreases in well withdrawals (Hoffman and others, 2001; Bell and others, 2008).

Total annual groundwater withdrawals in Utah for 1939 and 1963–2004 were compiled by Gates (2007, p. 130) on the basis of available data (Utah State Engineer, 1940) and the “Ground-water conditions in Utah” reports beginning in 1963 (Arnow and others, 1964). About 90 percent of these withdrawals in Utah, or more than 820,000 acre-ft/yr of the total 920,000 acre-ft/yr reported for water year 2004 (Burden and others, 2004), occur within the GBCAAS study area. Similar historical well withdrawals are not available for most areas of Nevada. Patterns and changes in groundwater withdrawals in Utah over time, however, are assumed to be representative of changes that have occurred throughout the entire GBCAAS study area. Gates (2007) compiled annual total, irrigation, and public-supply groundwater withdrawals in Utah for the period 1963–2002 (fig. D–15). Total Utah groundwater withdrawals for 1939 and withdrawals from six western Utah areas during 1945–1962 also were estimated. These six western Utah areas (Beryl-Enterprise Area, HA 280; Parowan Valley, HA 281; Cedar City Valley, HA 282; Milford Area, HA 284; Pavant Valley, HA 286; and Sevier Desert, HA 287) were selected because they have large withdrawals and groundwater level declines. Withdrawals have been updated through 2006 by Burden and others (2004, 2005, 2006, 2007). Withdrawals for industrial and domestic/stock use (not shown on fig. D–15) account for the difference between total withdrawals and the sum of irrigation plus public-supply withdrawals. Historically, total annual groundwater withdrawals in Utah generally have increased and range from 220,000 acre-ft in 1939 to a peak of 947,000 acre-ft in 2002. Annual withdrawals for irrigation are about two-thirds of total annual withdrawals and have an inverse relation with annual precipitation (fig. D–15). During years with above average precipitation, groundwater withdrawals decrease as irrigators use more abundant surface-water resources. During 1963–2006, withdrawals for irrigation decreased slightly, yet withdrawals for public supply more than tripled, reflecting the population growth in Utah. Some of these withdrawals for public supply have occurred through the transfer of water rights from agriculture. The conversion of agricultural to public-supply use is expected to continue as additional water supplies are needed to serve a growing population in the region.

In order to evaluate general groundwater development trends within the GBCAAS study area, historical annual well withdrawals for the period of 1940–2006 were estimated on the basis of the compilation and interpolation of existing well withdrawal data (Appendix 8). Historical estimates were developed for the 78 HAs with more than 500 acre-ft of well withdrawals in the year 2000 (Auxiliary 4). Historical withdrawals were not estimated for the other 87 HAs, and withdrawals for these HAs were not included in the summation of yearly withdrawals within the groundwater flow system; these HAs accounted for less than 0.4 percent of the total withdrawals in 2000 (Appendix 7).

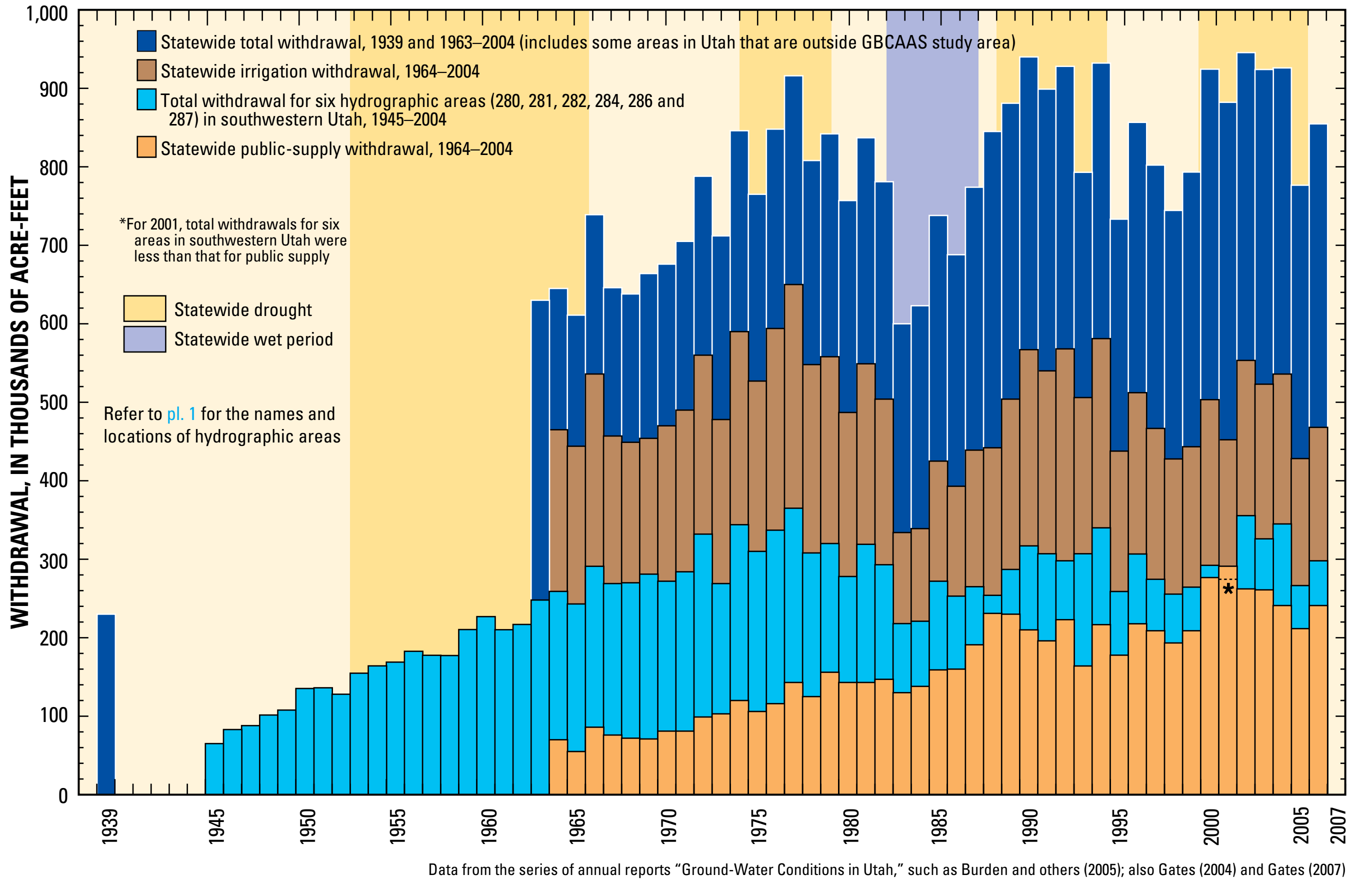

Figure D–15. Groundwater withdrawals from wells in Utah, 1939 and 1945–2006.

The estimated total annual well withdrawals by HA for 1940–2006 are given in Auxiliary 4. These estimates include withdrawals for mining, irrigation, and public supply. Figure D–16 shows historical estimated well withdrawals for 7 of the 17 groundwater flow systems (those with maximum annual withdrawals greater than 50,000 acre-ft) and for the entire study area. Withdrawals for each groundwater flow system were computed by summing yearly estimated withdrawals from each HA within the groundwater flow system. Recent (2000) well withdrawal estimates by groundwater flow system are given in table D–3. The total estimated amount of well withdrawals during the year 2000 for the GBCAAS study area is 1,500,000 acre-ft. The greatest amount of estimated withdrawal during 2000 was from the Great Salt Lake groundwater flow system (38), followed in decreasing order by the Sevier Lake (39), Humboldt (7), and Colorado (34) groundwater flow systems. Both the Great Salt Lake (38) and Colorado (34) groundwater flow systems have had increases in withdrawals through the 1990s and 2000s, associated with rapid population growth during the past two decades along the Wasatch Front and in Las Vegas and Mesquite. The Humboldt groundwater flow system (7) has experienced increasing withdrawals since the 1970s and 1980s, mainly related to gold mining along the Carlin trend. In contrast, groundwater development in the South-Central Marshes (24), Diamond Valley (27), Death Valley (28), and Sevier Lake (39) groundwater flow systems has not increased substantially since the 1980s (fig. D–16). Well withdrawals in these areas have stabilized because of more efficient irrigation practices and the change from agricultural to municipal water use.

To determine the HAs in which recent (2000) pumping significantly affects natural hydrologic conditions, estimated net well withdrawals were compared with estimated natural predevelopment discharge. Net well withdrawals were calculated as the total well withdrawals minus the recharge from unconsumed irrigation and public supply water from well withdrawals in each HA (Appendix 7). Fifteen HAs had estimated net well withdrawals exceeding estimated natural predevelopment discharge by at least 1,000 acre-ft/yr (fig. D–17, Appendix 7). The buffer of 1,000 acre-ft/yr was chosen in order to highlight HAs where pumping clearly exceeds natural discharge and to acknowledge uncertainties in both the discharge and withdrawal estimates. In the HAs with withdrawals exceeding natural discharge, predominant water uses generally are mining (Maggie Creek Area, HA 51; Crescent Valley, HA 54; Lower Reese River Valley, HA 59; and Boulder Flat, HA 61), agricultural (Diamond Valley,

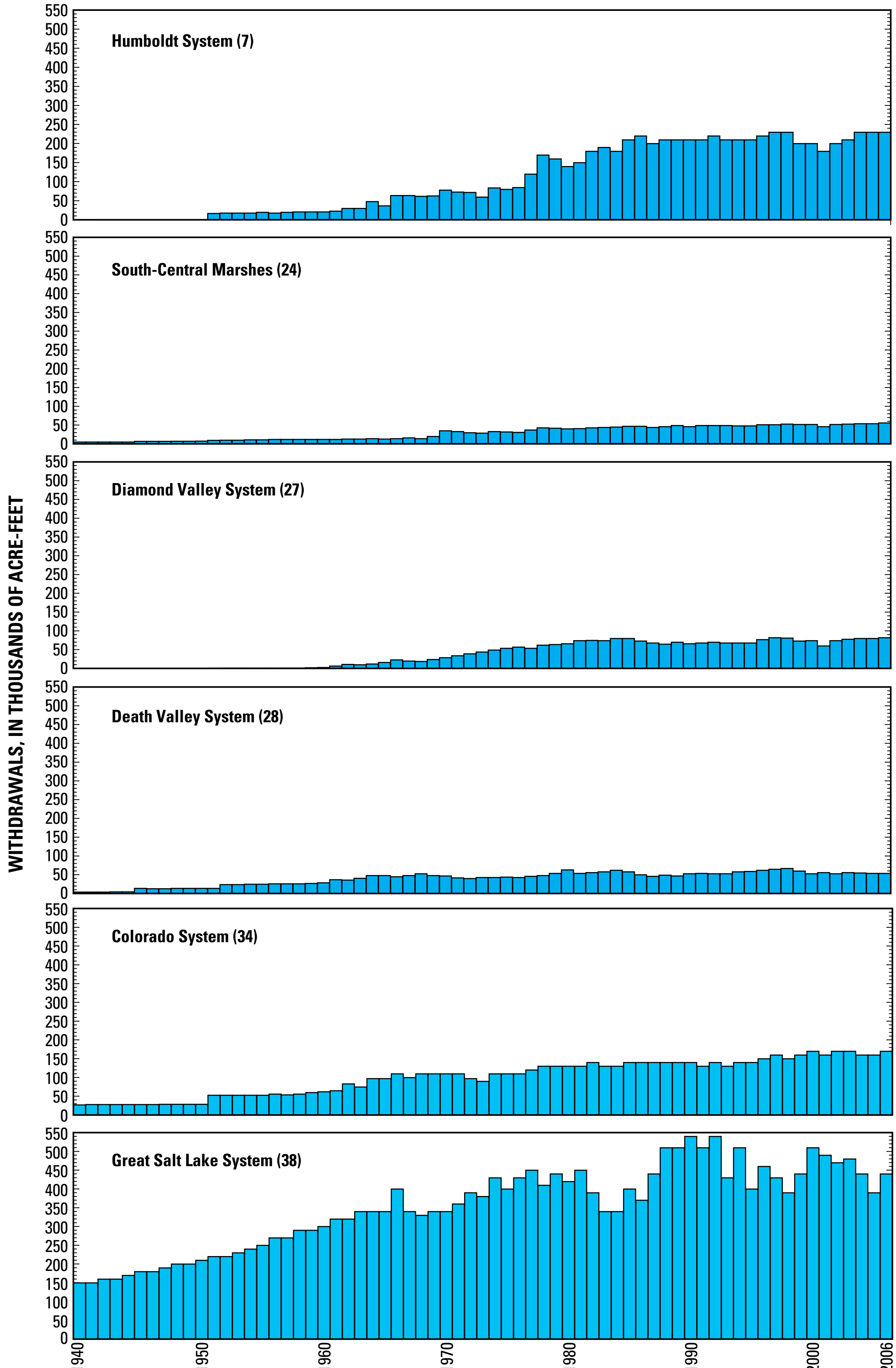

Figure D–16. 1940–2006 estimated annual well withdrawals for groundwater flow systems that have maximum annual withdrawals greater than 50,000 acre-feet and total well withdrawals for the entire Great Basin carbonate and alluvial aquifer system study area.

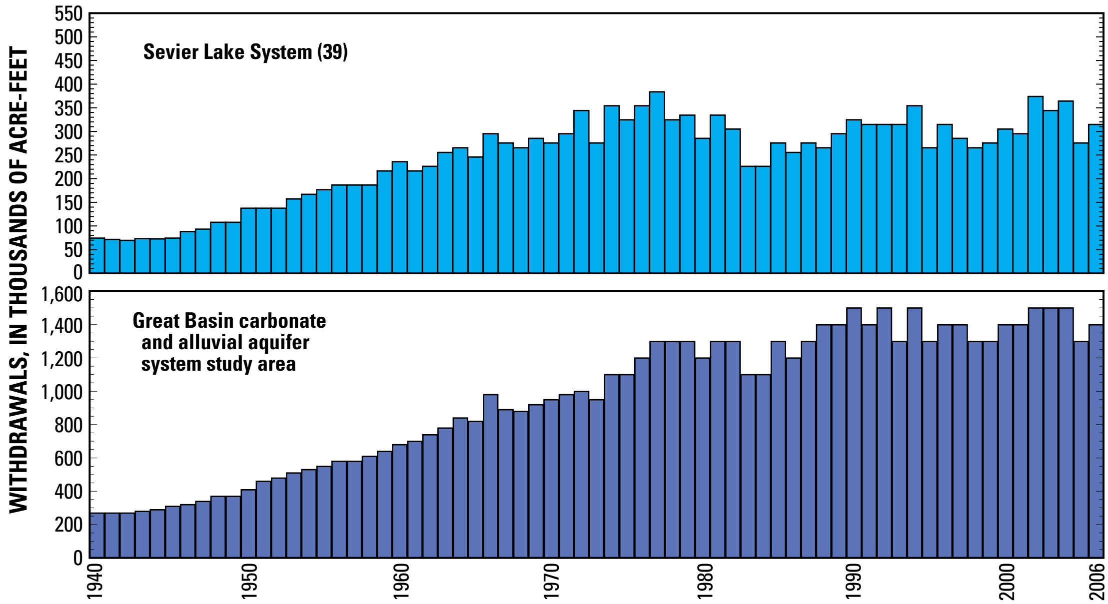

Figure D–16. 1940–2006 estimated annual well withdrawals for groundwater flow systems that have maximum annual withdrawals greater than 50,000 acre-feet and total well withdrawals for the entire Great Basin carbonate and alluvial aquifer system study area.—Continued

HA 153; Pahrump Valley, HA162; Mesquite Valley, HA 163; Penoyer Valley, HA 170; Dry Valley, HA 198; Patterson Valley, HA 202; Cedar Valley, HA 264; Curlew Valley, HA 278; Beryl-Enterprise Area, HA 280, and Milford Area, HA 284), and public supply (Virgin River Area, HA 222). Total estimated well withdrawals from these 15 HAs was 550,000 acre-ft during 2000, accounting for 37 percent of the total 1,500,000 acre-ft of well withdrawals for the GBCAAS.

In some HAs, groundwater pumping since the 1940s has reduced or eliminated natural discharge and has caused significant water-level declines. Examples of decreased natural discharge include Manse Springs in Pahrump Valley (HA 162), Muddy River Springs in Muddy River Springs Area (HA 219) (fig. D–18), and Las Vegas Springs in Las Vegas Valley (HA 212). Another example is the 80-percent decline in spring discharge at Locomotive Springs (Hurlow and Burk, 2008) in Curlew Valley (HA 278) since the 1960s. These effects are partly attributed to a rapid increase in withdrawals for irrigation. Fourteen HAs also have one or more wells showing long-term water-level declines of more than 50 ft during the latter half of the 20th century that are assumed to be in response to increased well withdrawals (figs. D–17 and D–19). In other HAs, either (1) the impact of groundwater withdrawals is less significant and water levels respond predominantly to climatic variations or climate-driven pumping variations (Gardner and Heilweil, 2009); or (2) insufficient historical data are available to document declining water levels and decreased natural discharge.

Recharge of Unconsumed Irrigation and Public Supply Water from Well Withdrawals

For HAs that have undergone significant groundwater development, recharge from unconsumed irrigation and public supply water from well withdrawals also must be considered. Most well withdrawals are used for irrigation; in addition, much of the well withdrawals used for public supply are applied as irrigation to lawns and gardens (Hely and others, 1971; Mower and Cordova, 1974; Clark and others, 1990; Kariya and others, 1994; Brooks and Mason, 2005; Cederberg and others, 2009; Gardner, 2009). It is assumed that part of this groundwater recharges the aquifer system, either as focused infiltration along irrigation canals or infiltration of unconsumed irrigation water applied to fields, lawns, and gardens. This “recycled” groundwater is difficult to quantify, but it is an important form of groundwater recharge in HAs that have undergone substantial groundwater development. Irrigation return flow studies in the Amargosa Desert (HA 230) and the Milford Area (HA 284) show that recharge from irrigation on sprinkler-irrigated fields ranges from 8 to 16 percent of the applied irrigation (Susong, 1995, table 3; Stonestrom and others, 2003, p. 1) and recharge on flood-irrigated fields can be as high as 50 percent of the applied irrigation (Susong, 1995, table 3). Current study estimates of groundwater recharge of unconsumed irrigation and public supply water from well withdrawals, therefore, were calculated assuming that 30 percent of this applied irrigation and public supply water is recycled back into the aquifer.

Estimated recharge from unconsumed irrigation and public supply water within the study area in the year 2000 was

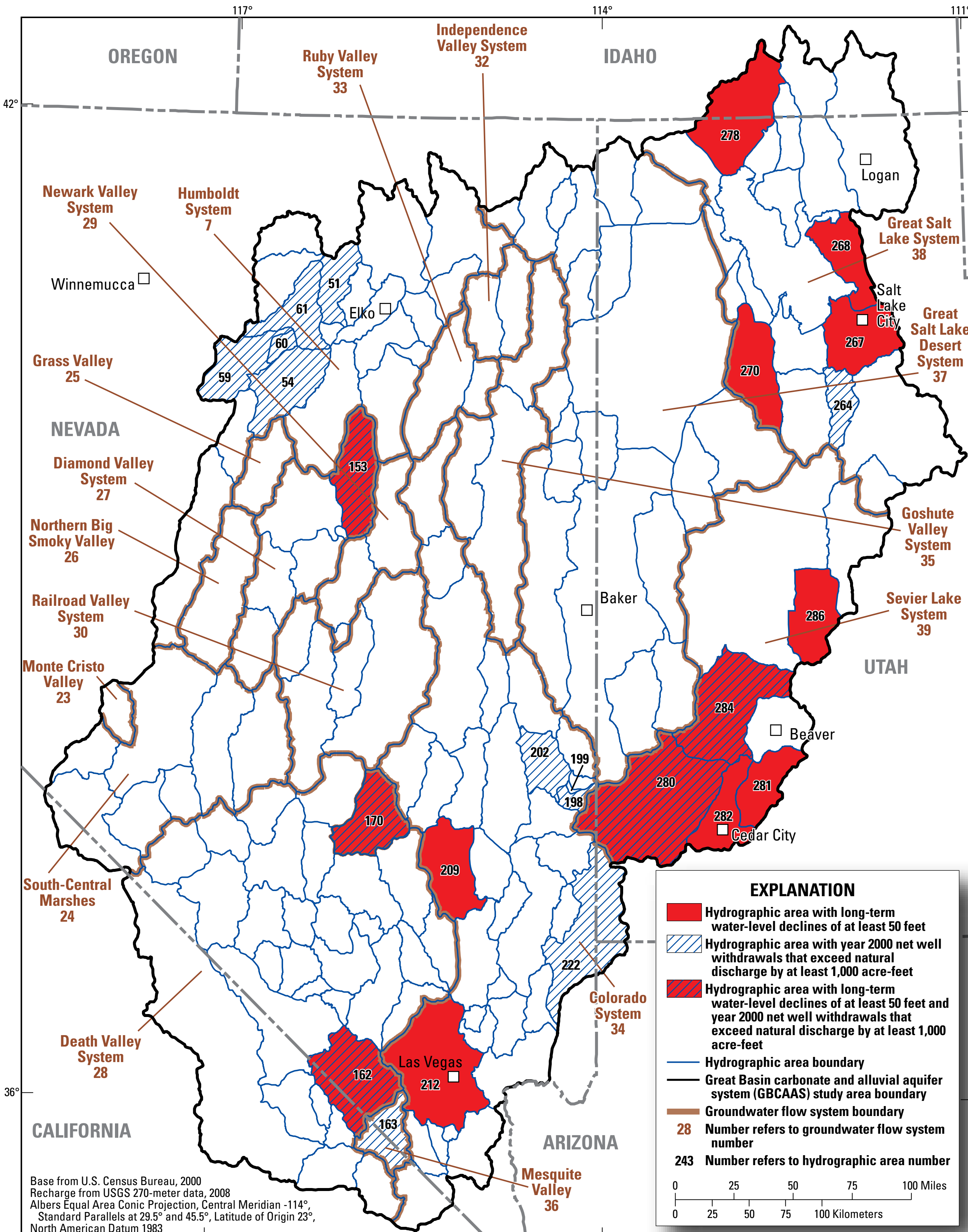

Figure D–17. Hydrographic areas with 2000 estimated net well withdrawals exceeding natural discharge by at least 1,000 acre-feet per year and areas where one or more wells show long-term water-level declines of at least 50 feet during the latter half of the 20th century within the Great Basin carbonate and alluvial aquifer system study area.

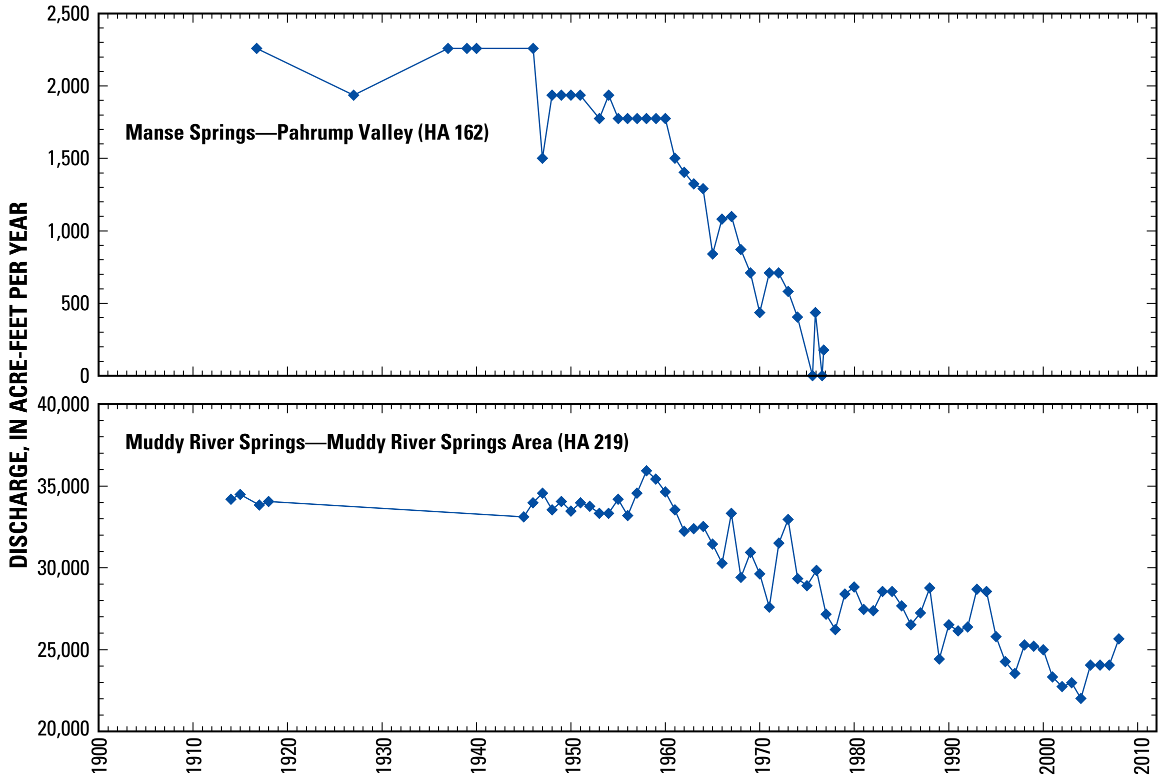

Figure D–18. Declining spring discharge at Manse Springs, in the Pahrump Valley (HA 162), and Muddy River Springs, in the Muddy River Springs Area (HA 219), within the Great Basin carbonate and alluvial aquifer system study area.

470,000 acre-ft. These estimates are presented by groundwater flow system in table D–3 and by HA in Appendix 7. The highest amounts of recharge from unconsumed irrigation and public supply water from groundwater withdrawals occur in the Great Salt Lake (38) and Sevier Lake (39) groundwater flow systems. These two areas account for more than 60 percent of total recharge from irrigation with groundwater within the study area. Both of these groundwater flow systems are highly developed; in the case of the Sevier Lake groundwater flow system (39), there is very little surface water available for irrigation and, therefore, most of the water for irrigation is derived from groundwater resources.

Artificial Recharge and Recharge of Unconsumed Irrigation and Public Supply Water from Lake Mead

In Las Vegas Valley (HA 212), increased recharge also occurs from the importation of Lake Mead water that began in 1942. In the year 2000, a total of 440,000 acre-ft of water was imported from Lake Mead; 30,000 acre-ft was injected in the aquifer directly (NDWR pumpage inventory; http://water.nv.gov, accessed on July 6, 2009). As in other HAs with imported surface water, the same percentage was used to determine the recharge from imported water as was used for determining recharge from runoff (see "Recharge From Imported Surface Water"); therefore, 10 percent (41,000 acre-ft) of the remaining imported water was assumed to become recharge as seepage from lawns and gardens . This results in a 2000 total estimated recharge from imported water for Las Vegas Valley of 71,000 acre-ft; this recharge is included in the "Recharge from unconsumed irrigation and public supply water from well withdrawals" column in table D–3 under the Colorado groundwater flow system (34) and Appendix 7 under HA 212.

Decrease in Natural Discharge and Change in Storage

All water withdrawn from wells in the study area is balanced by some combination of varying amounts of increase in recharge, decrease in natural discharge, and decrease of groundwater in storage. In general, withdrawals reduce groundwater storage by an equivalent amount until

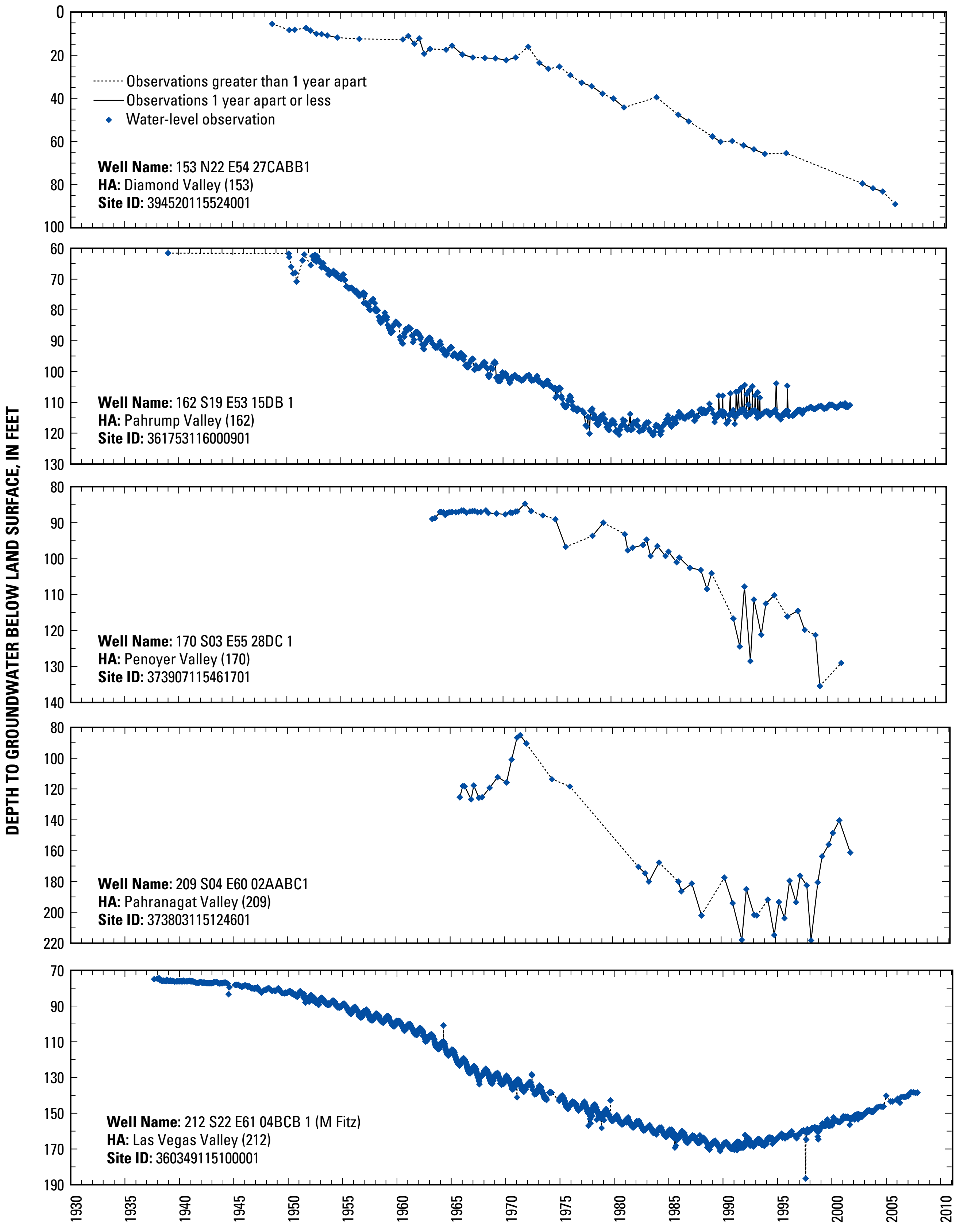

Figure D–19. Examples of well hydrographs from hydrographic areas in the Great Basin carbonate and alluvial aquifer system study area where one or more wells show long-term water-level declines of at least 50 feet during the latter half of the 20th century.

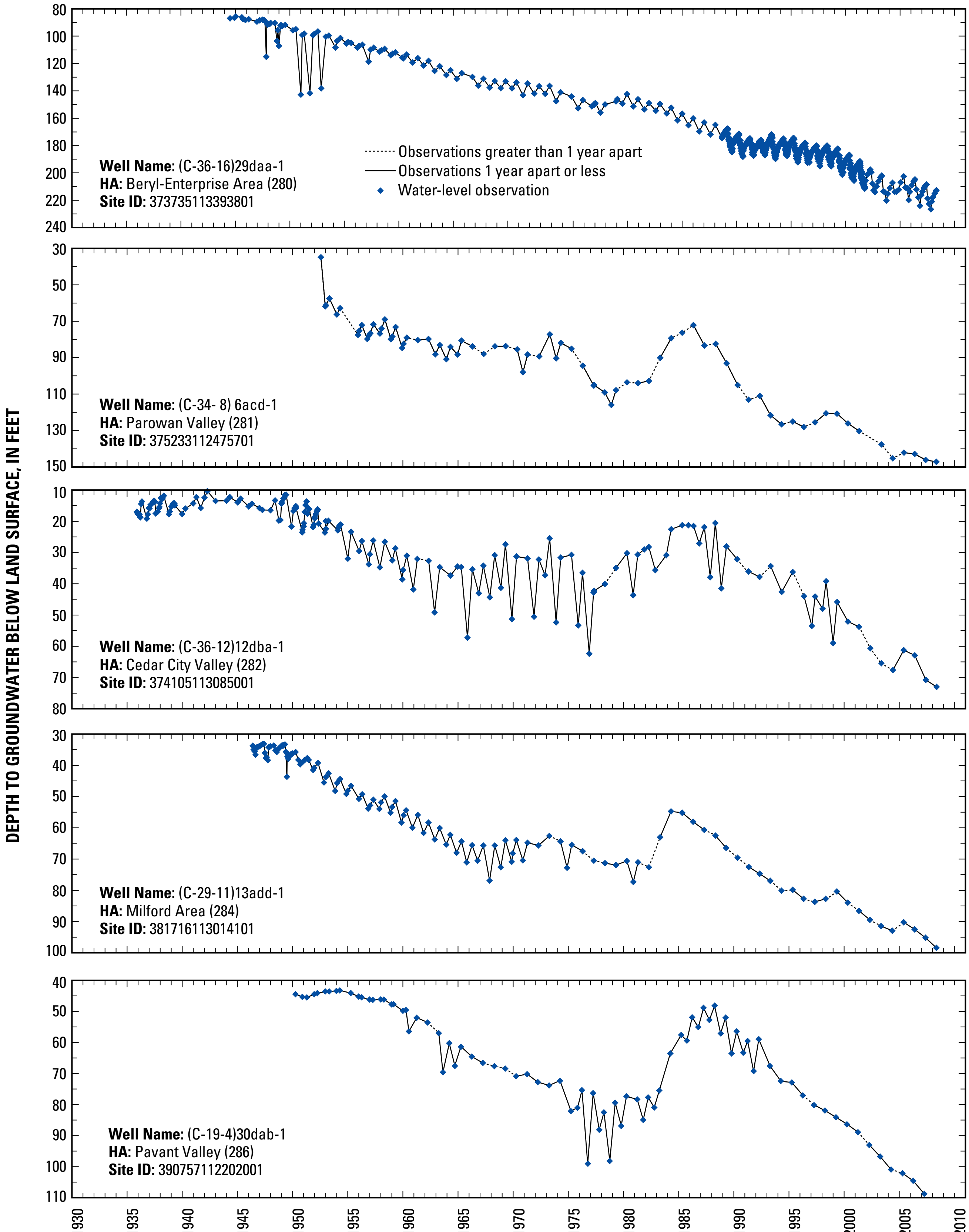

Figure D–19. Examples of well hydrographs from hydrographic areas in the Great Basin carbonate and alluvial aquifer system study area where one or more wells show long-term water-level declines of at least 50 feet during the latter half of the 20th century.—Continued

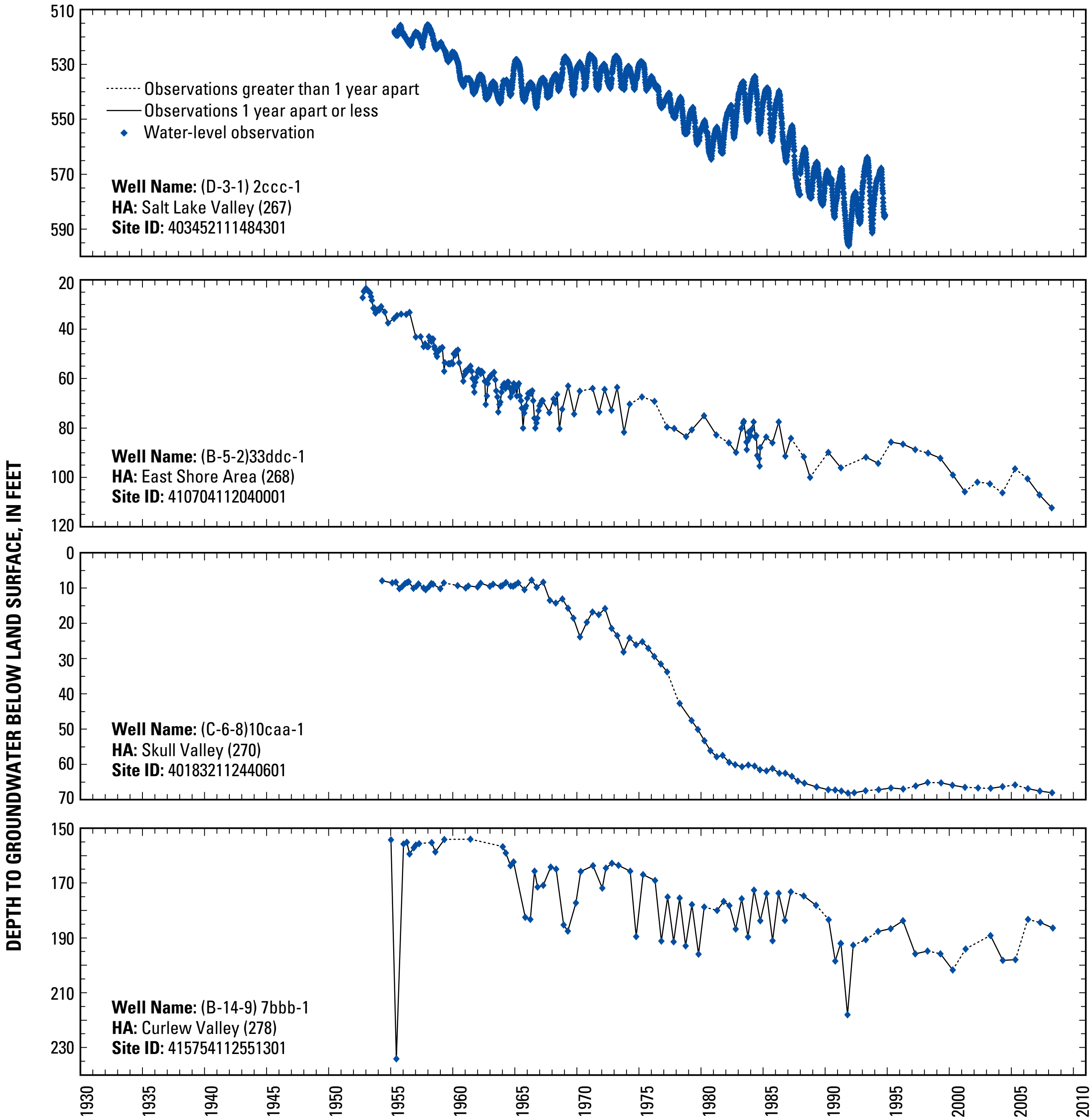

Figure D–19. Examples of well hydrographs from hydrographic areas in the Great Basin carbonate and alluvial aquifer system study area where one or more wells show long-term water-level declines of at least 50 feet during the latter half of the 20th century.—Continued the drawdown from the withdrawals reaches areas of natural discharge or areas of potential recharge. Potential recharge is typically captured from lakes and streams. In the GBCAAS study area, however, the small number of lakes and basin-fill streams are generally in areas of groundwater discharge (hydraulic gradients have not been reversed). Capture of potential recharge, therefore, is not considered in the current study. If sufficient quantities of natural discharge cannot be captured at the rate at which the groundwater is withdrawn, groundwater storage will continue to decrease and groundwater levels will continue to decline. If sufficient quantities of natural discharge can be captured, a new pumping equilibrium will be established such that the change in storage becomes minimal. For most of the HAs that have undergone groundwater development for agriculture, the increase in withdrawals generally occurred between the 1940s and 1980s. Thus, many of the developed HAs have been equilibrating with respect to pumping for decades. The budget calculations assume that the majority of these HAs have equilibrated, except for a few HAs where groundwater levels continue to decline (figs. D–17 and D–19).

Decrease in natural discharge and (or) storage was estimated as the net well withdrawals in each HA. The estimated decrease in groundwater storage in the current study is a minimum value; it assumes that all natural discharge is captured before groundwater storage is reduced, and that groundwater storage is reduced only if net well withdrawals exceed predevelopment groundwater discharge (Appendix 7). Long-term well hydrographs having at least one measurement prior to 1980 were examined to determine whether water levels were declining. If an HA had at least one well in which long-term water levels declined by 50 ft or more that did not appear to be influenced by climate or aquifer testing and had net well withdrawals that exceeded predevelopment groundwater discharge by 1,000 acre-ft or more, it was assumed that well withdrawals were capturing groundwater from storage.

The estimated decreases in natural discharge and (or) groundwater storage and the minimum decrease in storage for each groundwater flow system were calculated as the sum of these components in each HA within the flow system (table D–3). This sum represents the change in the groundwater system caused by well withdrawals. Additional water-level and discharge measurements would help refine these estimates. Unless well withdrawals in a particular HA or groundwater flow system are very large, it is unlikely that this stress will affect discharge and storage in an adjacent HA or groundwater flow system. For that to occur, groundwater levels would need to decline over wide areas. The analysis of water levels did not indicate substantial water-level decline in adjacent basins caused by well withdrawals. It is possible, however, that subsurface outflow to a downgradient HA could be reduced by withdrawals in an upgradient HA or upgradient recharge could be increased.

The estimated decrease in natural discharge and (or) groundwater storage caused by well withdrawals for the year 2000 was 990,000 acre-ft (table D–3). The Great Salt Lake (38), Sevier Lake (39), and Humboldt (7) groundwater flow systems account for 77 percent of the total estimated decrease in natural discharge and (or) groundwater storage for the GBCAAS. The estimated minimum decrease in groundwater storage for the study area in 2000 was 67,000 acre-ft and occurred in only five HAs (Appendix 7) within three groundwater flow systems (table D–3): the Sevier Lake (39) system (34,000 acre-ft), the Diamond Valley (27) system (24,000 acre-ft), and the Death Valley (28) system (9,300 acre-ft).

Uncertainty of Estimated Groundwater Budgets

For the GBCAAS study area, the total estimated predevelopment groundwater recharge of 4,500,000 acre-ft/yr is 7 percent greater than the total estimated predevelopment groundwater discharge of 4,200,000 acre-ft/yr. Because of uncertainty in these estimates, however, recharge and discharge for the entire study area are considered to be about equal. It is estimated that the uncertainty in the total recharge estimate is about ±50 percent, or about ±2,200,000 acre-ft/yr. This was derived predominantly from estimated error in the two largest recharge components: direct infiltration of precipitation and recharge from runoff, both calculated using results from BCM.

It is estimated that the uncertainty in the total predevelopment groundwater-discharge estimate for the GBCAAS study area is about ±30 percent, or about ±1,300,000 acre-ft/yr. This composite uncertainty was derived predominantly from estimated error in the three largest discharge components: ETg, springs, and discharge to basin-fill streams, lakes, and reservoirs, which account for 82 percent of total discharge. Although there are few published estimates of uncertainty with regard to ETg measurements, 12 HAs in Nevada and Utah within the GBCAAS study area have 95-percent confidence intervals of ±22 to ±227 percent of reported estimates (Lundmark and others, 2007, table 2). The estimated uncertainty in gaged stream baseflow used for estimating groundwater discharge to mountain streams (current study does not estimate ungaged stream discharge) and spring discharge measurements was estimated to be ±30 percent. This is based on an assumed ±10 percent error in individual discharge measurements and an additional ±20 percent error to account for (1) temporal averaging of measurements made over a 60-year period, (2) the natural fluctuation in predevelopment discharge associated with climate variability, and (3) general error associated with extrapolating regional estimates from more site-specific studies.

As mentioned in the “Analysis and Adjustment of BCM Results” section of this report, the groundwater-budget differences between recharge estimates calculated using BCM results and estimates of predevelopment discharge were not evenly distributed spatially. There are larger differences between the recharge estimates calculated using BCM results and discharge estimates in the Death Valley (28) and Colorado (34) groundwater flow systems of central and southern Nevada than elsewhere in the GBCAAS study area. The adjustments to recharge calculated using BCM results for groundwater flow systems or subareas do not necessarily result in balanced recharge and discharge within each HA (fig. D–20). Some of the imbalances may be caused by budget uncertainties and some by the adjustment of BCM recharge. Extreme imbalances may indicate areas where subsurface flow occurs between HAs, especially from HAs that have very little or no measured groundwater discharge. These extreme differences are important in each HA, but not in each subarea or groundwater flow system.

Uncertainty in reported discharge probably is not the main reason for the large discrepancies between recharge and discharge in the groundwater flow systems. It is unlikely that large springs, streams, and ETg have been completely overlooked in previous studies. It is also unlikely the reported discharge measurements would have a consistent bias toward underestimation. For example, ETg is the largest component of discharge within the study area; this has been extensively studied, especially in Nevada (Smith and others, 2000; Laczniak and Smith, 2001; Laczniak and others, 2007; Moreo and others, 2007; Smith and others, 2007; and Welch and others, 2007). These ETg estimates are based on mapped phreatophyte and playa areas, and measured ETg rates, both of which have no apparent bias toward underestimation.

Limitations of Estimated Groundwater Budgets

The following limitations should be considered when utilizing the water-budget information presented in Chapter D:

- Previously published recharge estimates (“net” recharge to the basin-fill portion of an HA) typically have been used by regulatory agencies for developing HA-based estimates of perennial yield for allocating water rights. The newer spatially distributed recharge estimates (“total” recharge to an HA) in the current report are typically higher and should not be used for managing water resources without also considering losses associated with groundwater discharge in the mountain block.

- The total estimated predevelopment discharge to mountain streams (450,000 acre-ft/yr) and springs (990,000 acre-ft/yr) are minimum values because they do not account for ungaged perennial streams and unmeasured spring discharge. Additional mountain stream and spring discharge measurements are needed to refine these values.

- The estimated percentages of BCM calculated runoff that recharges the basin fill (30 percent for HAs highly irrigated with surface water; 10 percent for HAs not highly irrigated with surface water) are only approximate. Additional seepage studies along streams and canals, and deep percolation studies of irrigation return flow are needed to improve these estimates.

- The current study summarizes previously published quantities of subsurface flow between HAs, but does not provide new estimates because of the uncertainty in groundwater budgets. The current study also does not quantify subsurface flow between groundwater flow systems; rather such flows only are indicated qualitatively on the basis of water budget, hydraulic gradient, and geological constraints.

Summary

Detailed groundwater budgets were compiled for the GBCAAS study area for average annual conditions before extensive groundwater development began in the middle of the 20th century and for the year 2000. Total estimated predevelopment groundwater recharge is 4,500,000 ± 2,200,000 acre-ft/yr. Predevelopment recharge comprises five components: direct infiltration of precipitation (in-place recharge), infiltration of surface-water runoff, infiltration of mountain stream baseflow, infiltration of imported surface water, and subsurface inflow. Direct infiltration of precipitation and associated snowmelt for the GBCAAS study area is estimated to be about 2,900,000 acre-ft/yr, providing more than 64 percent of groundwater recharge. The majority of this recharge is assumed to occur in the higher altitude mountain ranges as direct infiltration of precipitation. Precipitation that does not infiltrate into the subsurface or is not consumed by evapotranspiration in the mountain block becomes runoff. The majority of runoff generated in the mountains flows into adjacent basins, some portion of which recharges the unconsolidated deposits as infiltration beneath stream channels, irrigation canals, and irrigated fields. Estimated recharge from infiltration of runoff is 570,000 acre-ft/yr. In addition to recharge from runoff, there is recharge from mountain stream baseflow that infiltrates beneath stream channels, irrigation canals, and irrigated fields; this recharge is estimated to be 130,000 acre-ft/yr. Recharge from imported surface water (both natural and through transbasin diversions) is estimated to be 990,000 acre-ft/yr, and is concentrated almost exclusively within the Great Salt Lake groundwater flow system (38). Although subsurface inflow may be an important component of recharge in some HAs and groundwater flow systems, it is less important at the scale of the GBCAAS study area. Estimates of subsurface inflow between groundwater flow systems typically are computed as a residual in groundwater budgets, and because of the large uncertainties in other water-budget components, subsurface inflows are not quantified in this study. Rather, such fluxes between groundwater flow systems are qualitatively described

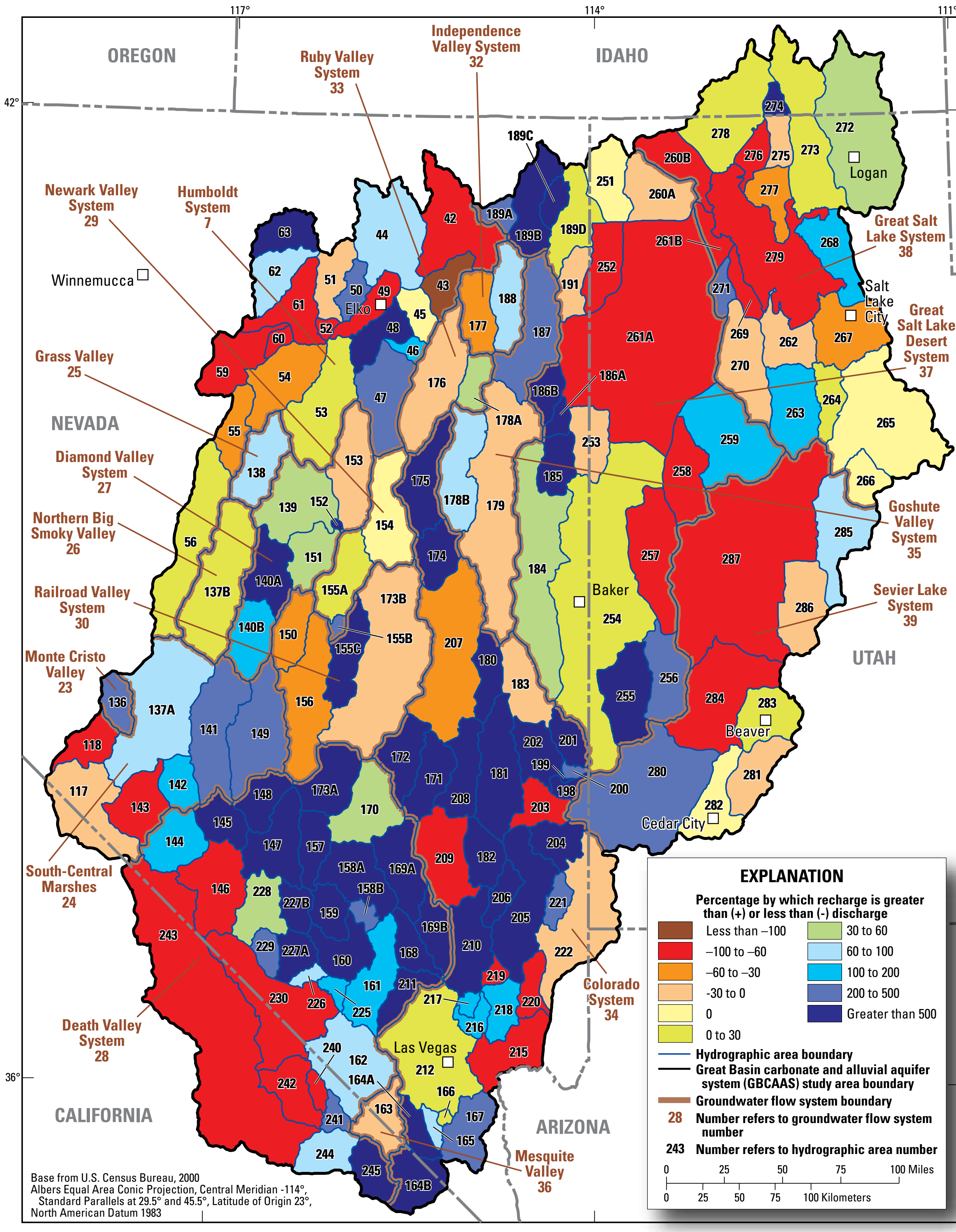

Figure D–20. Predevelopment groundwater-budget imbalances for each hydrographic area in the Great Basin carbonate and alluvial aquifer system study area.

as likely, possible, or unlikely, on the basis of the hydraulic gradients; the likelihood of hydraulic connections across HA boundaries; and whether substantial groundwater-budget imbalances exist. Findings of the current study indicate that subsurface inflow to Railroad Valley groundwater flow system is likely, while subsurface inflow to many other groundwater flow systems within the GBCAAS study area is possible.

Total estimated predevelopment groundwater discharge for the GBCAAS study area is 4,200,000 ±1,300,000 acre-ft/yr. Predevelopment discharge comprises six components: groundwater evapotranspiration (ETg); groundwater discharge to mountain streams; groundwater discharge to basin-fill streams, lakes, and reservoirs; groundwater discharge to springs; adjustment to natural discharge for well withdrawals; and subsurface outflow. Estimated predevelopment groundwater discharge to ETg is 1,800,000 acre-ft/yr and accounts for 43 percent of the total predevelopment discharge for the study area. On the basis of historical streamgage records, estimated predevelopment groundwater discharge to mountain streams is 450,000 acre-ft/yr. Estimated predevelopment groundwater discharge to basin-fill streams, lakes, and reservoirs is 660,000 acre-ft/yr and to springs is 990,000 acre-ft/yr. The estimated adjustment to natural discharge for well withdrawals is 330,000 acre-ft/yr. Although subsurface outflow may be an important component of discharge in some HAs and groundwater flow systems, these fluxes are not quantified in the current study because of uncertainties in the other water-budget components. Such fluxes between groundwater flow systems are qualitatively described as likely, possible, or unlikely on the basis of the same factors described above for subsurface inflow. Findings of the current study indicate that subsurface outflow is likely from the Monte Cristo Valley (23), Grass Valley (25), and Diamond Valley (27) groundwater flow systems; subsurface outflow to many other groundwater flow systems within the GBCAAS study area is possible.

Between 1940 and 2006, groundwater development has occurred in various parts of the GBCAAS study area. Although well withdrawals have been minimal in the majority of HAs and groundwater flow systems, some areas have undergone substantial development, sometimes causing significant water-level declines. Total well withdrawals for the study area increased from less than 300,000 acre-ft/yr in 1940 to almost 1,300,000 acre-ft/yr in the late 1970s. Since the late 1970s, well withdrawals have fluctuated between about 1,100,000 and 1,500,000 acre-ft/yr. Most of the well withdrawals (as much as 900,000 acre-ft/yr) have occurred in Utah. Although the majority of well withdrawals are used for irrigation, there has been a general increase in withdrawals for public supply and a decrease in withdrawals for irrigation (as water use changes from irrigation to public supply and as more efficient irrigation practices are implemented) since the late 1970s. It is assumed that about 30 percent of this water is recycled back to the aquifer as recharge from unconsumed irrigation and public supply water.

The estimated decrease in combined natural discharge and groundwater storage within the GBCAAS study area caused by well withdrawals for the year 2000 was 990,000 acre-ft. The Great Salt Lake (38), Sevier Lake (39), and Humboldt (7) groundwater flow systems account for most of this decrease. The minimum estimated decrease in groundwater storage for the study area in 2000 was 67,000 acre-ft and was limited to only the Sevier Lake (39), Diamond Valley (27), and Death Valley (28) groundwater flow systems.

References Cited

Arnow, T., and others, 1964, Ground-water conditions in Utah, spring of 1964: Utah Water and Power Board (Utah Division of Water Resources) Cooperative Investigations Report no. 2, 104 p.

Belcher, W.R., D'Agnese, F.A., and O'Brien, G.M., 2004, Introduction, chap. A *of* Belcher, W.R., ed., Death Valley regional ground-water flow system, Nevada and California—Hydrogeologic framework and transient ground-water flow model: U.S. Geological Survey Scientific Investigations Report 2004–5205, p. 7–19.

Bell, J.W., Amelung, F., Ferretti, A., Bianchi, M., and Novali, F., 2008, Permanent scatter InSAR reveals seasonal and long-term aquifer-system response to groundwater pumping and artificial recharge: Water Resources Research, v. 44, doi: 10.1029/2007WR006152, accessed January 20, 2009 at http://www.agu.org/pubs/crossref/2008/2007WR006152.shtml.

Berger, D.L., 2000, Water budgets for Pine Valley, Carico Lake Valley, and Upper Reese River Valley hydrographic areas; middle Humboldt River basin, north-central Nevada: Methods for estimation and results: U.S. Geological Survey Water-Resources Investigations Report 99–4272, 43 p.

Bolke, E.L., and Price, D., 1972, Hydrologic reconnaissance of the Blue Creek Valley area, Box Elder County, Utah: Utah Department of Natural Resources Technical Publication 37, 39 p.

Brooks, L.E., and Mason, J.L., 2005, Hydrology and simulation of ground-water flow in Cedar Valley, Iron County, Utah: U.S. Geological Survey Scientific Investigations Report 2005–5170, 127 p.

Burden, C.B., and others, 2004, Ground-water conditions in Utah, spring of 2004: Utah Department of Natural Resources Cooperative Publication 45, 120 p.

Burden, C.B., and others, 2005, Ground-water conditions in Utah, spring of 2005: Utah Department of Natural Resources Cooperative Publication 46, 138 p.

Burden, C.B., and others, 2006, Ground-water conditions in Utah, spring of 2006: Utah Department of Natural Resources Cooperative Publication 47, 128 p.

Burden, C.B., and others, 2007, Ground-water conditions in Utah, spring of 2007: Utah Department of Natural Resources Cooperative Publication 48, 129 p.

Cederberg, J.R., Gardner, P.M., and Thiros, S.A., 2009, Hydrology of Northern Utah Valley, Utah County, Utah, 1975–2005: U.S. Geological Survey Scientific Investigations Report 2008–5197, 114 p.

Clark, D.W., Appel, C.L., Lambert, P.M., and Puryear, R.L., 1990, Ground-water resources and simulated effects of withdrawals in the East Shore area of Great Salt Lake, Utah: Utah Department of Natural Resources Technical Publication 93, 150 p.

Daly, C., Halbleib, M., Smith, J.I., Gibson, W.P., Doggett, M.K., Taylor, G.H., Curtis, J., and Pasteris, P.A., 2008, Physiographically-sensitive mapping of temperature and precipitation across the conterminous United States: International Journal of Climatology, doi: 10.1002/joc.1688, accessed January 20, 2009 at http://onlinelibrary.wiley.com/doi/10.1002/joc.1688/pdf.

Daly, C., Neilson, R.P., and Phillips, D.L., 1994, A statistical-topographic model for mapping climatological precipitation over mountain terrain: Journal of Applied Meteorology, v. 33, p. 140–158.

DeMeo, G.A., Laczniak, R.J., Boyd, R.A., Smith, J.L., and Nylund, W.E., 2003, Estimated ground-water discharge by evapotranspiration from Death Valley, California, 1997–2001: U.S. Geological Survey Water-Resources Investigations Report 03–4254, 27 p.

Dettinger, M.D., 1989, Reconnaissance estimates of natural recharge to desert basins in Nevada, U.S.A., by using chloride-balance calculations: Journal of Hydrology, v. 106, p. 55–78.

Epstein, B.J., 2004, Development and uncertainty analysis of empirical recharge prediction models for Nevada's desert basins: Reno, University of Nevada, M.S. thesis, 131 p.

Flint, A L., and Childs, S.W., 1987, Calculation of solar radiation in mountainous terrain: Journal of Agricultural Forestry Meteorology, v. 40, p. 233–249.

Flint, A.L., and Flint, L.E., 2007a, Application of the basin characterization model to estimate in-place recharge and runoff potential in the Basin and Range carbonate-rock aquifer system, White Pine County, Nevada, and adjacent areas in Nevada and Utah: U.S. Geological Survey Scientific Investigations Report 2007–5099, 20 p.

Flint, L.E., and Flint, A.L., 2007b, Estimation of hourly stream temperatures in unmeasured tributaries to the lower Klamath River, California: Journal of Environmental Quality, v. 37, p. 57–68.

Flint, L.E., and Flint, A.L., 2007c, Regional analysis of ground-water recharge, *in* Stonestrom, D.A., Constantz, J., Ferré, T.P.A., and Leake, S.A., eds., Ground-water recharge in the arid and semiarid southwestern United States: U.S. Geological Survey Professional Paper 1703, p. 29–59.

Gardner, P.M., 2009, Three-dimensional numerical model of ground-water flow in northern Utah Valley, Utah County, Utah: U.S. Geological Survey Scientific Investigations Report 2008–5049, 95 p.

Gardner, P.M., and Heilweil, V.M., 2009, Evaluation of the effects of precipitation on ground-water levels from wells in selected alluvial aquifers in Utah and Arizona, U.S. Geological Survey Scientific Investigations Report 2008–5242, 28 p.

Gates, J.S., 2004, Ground-water development in Utah and effects on ground-water levels and chemical quality, *in* Spangler, L.E., ed., Groundwater in Utah: Resource, protection, and remediation: Utah Geological Association Publication 31, p. 3–26.

Gates, J.S., 2007, Effects of climatic extremes on ground water in western Utah, 1930–2005: U.S. Geological Survey Scientific Investigations Report 2007–5045, 10 p.

Gates, J.S., and Kruer, S.A., 1981, Hydrologic reconnaissance of the southern Great Salt Lake Desert and summary of the hydrology of west-central Utah: Utah Department of Natural Resources Technical Publication 71, 55 p.

Hall, F. R., 1968, Base-flow recession—A review: Water Resources Research, v. 4, p. 973–983.

Handman, E.H., and Kilroy, K.C., 1997, Ground-water resources of northern Big Smoky Valley, Lander and Nye Counties, central Nevada: U.S. Geological Survey Water-Resources Investigations Report 96–4311, 97 p.

Hardman, G., 1936, Nevada precipitation and acreages of land by rainfall zones: Reno, University of Nevada, Agricultural Experiment Station Report, 10 p.

Harrill, J.R., 1971, Water-resources appraisal of the Pilot Creek Valley area, Elko and White Pine Counties, Nevada: Nevada Department of Conservation and Natural Resources Water Resources Reconnaissance Report 56, 46 p.

Harrill, J.R., Gates, J.S., and Thomas, J.M., 1988, Major ground-water flow systems in the Great Basin region of Nevada, Utah, and adjacent states: U.S. Geological Survey Hydrologic Investigations Atlas HA–694–C, 2 sheets, scale 1:1,000,000.

Harrill, J.R., and Lamke, R.D., 1968, Hydrologic response to irrigation pumping in Diamond Valley, Eureka and Elko Counties, Nevada, 1950–65: State of Nevada Department of Conservation and Natural Resources Water Resources Bulletin 35, 85 p.

Harrill, J.R., and Prudic, D.E., 1998, Aquifer systems in the Great Basin region of Nevada, Utah, and adjacent states—Summary report: U.S. Geological Survey Professional Paper 1409–A, 66 p.

Hely, A.G., Mower, R.W., and Harr, C.A., 1971, Water resources of Salt Lake County, Utah: Utah Department of Natural Resources Technical Publication 31, 240 p.

Hevesi, J.A., Flint, A.L., and Flint, L.E., 2003, Simulation of net infiltration and potential recharge using a distributed-parameter watershed model of the Death Valley region, Nevada and California: U.S. Geological Survey Water Resources Investigations Report 03–4090, 161 p.

Hoffman, J., Zebker, H.A., Galloway, D.L., and Amelung, F., 2001, Seasonal subsidence and rebound in Las Vegas Valley, Nevada, observed by synthetic aperture radar interferometry: Water Resources Research, v. 37, p. 1,551–1,566.

Hood, J.W., and Rush, F.E., 1965, Water-resources appraisal of the Snake Valley area, Utah and Nevada: Nevada Department of Conservation and Natural Resources Water Resources Reconnaissance Report 34, 43 p.

Hood, J.W., and Waddell, K.M., 1968, Hydrologic reconnaissance of Skull Valley, Tooele County, Utah: State of Utah Department of Natural Resources Technical Publication 18, 57 p.

Hurlow, H.H., and Burk, N., 2008, Geology and ground-water chemistry, Curlew Valley, northwestern Utah and south-central Idaho—Implications for hydrogeology: Utah Geological Survey Special Study 126, 185 p., 2 pls.

Kariya, K.A., Roark, D.M., and Hanson, K.M., 1994, Hydrology of Cache Valley, Cache County, Utah, and adjacent part of Idaho, with emphasis on simulation of ground-water flow: Utah Department of Natural Resources Technical Publication 108, 120 p.

Kirk, S.T., and Campana, M.E., 1990, A deuterium-calibrated groundwater flow model of a regional carbonate-alluvial system: Journal of Hydrology, v. 119, p. 357–388.

Laczniak, R.J., DeMeo, G.A., Reiner, S.R., Smith, J.L., and Nylund, W.E., 1999, Estimates of ground-water discharge as determined from measurements of evapotranspiration, Ash Meadows area, Nye County, Nevada: U.S. Geological Survey Water-Resources Investigations Report 99–4079, 56 p.

Laczniak, R.J., Moreo, M.T., Smith, J.L., Harper, D.P., and Welborn, T.L., 2007, Potential areas of ground-water discharge in the Basin and Range carbonate-rock aquifer system, White Pine County, Nevada, and adjacent parts of Nevada and Utah: U.S. Geological Survey vector digital data, accessed July 2008 at http://water.usgs.gov/GIS/metadata/usgswrd/XML/sir2007-5087_potgwdischarge.xml.

Laczniak, R.J., and Smith, J.L., 2001, Outer boundary of major discharge areas of Death Valley regional flow system, Nevada and California: U.S. Geological Survey digital data, accessed March 2007 at http://water.usgs.gov/GIS/metadata/usgswrd/XML/darea.xml.

Laczniak, R.J., Smith, J.L., Elliott, P.E., DeMeo, G.A., and Chatigny, M.A., 2001, Ground-water discharge determined from estimates of evapotranspiration, Death Valley regional flow system, Nevada and California: U.S. Geological Survey Water-Resources Investigations Report 2001–4195, 51 p.

Leavesley, G.H., Lichty, R.W., Troutman, B.M., and Saindon, L.G., 1983, Precipitation-runoff modeling system: User's manual: U.S. Geological Survey Water-Resources Investigations Report 83–4238, 207 p.

Lines, G.C., 1979, Hydrology and surface morphology of the Bonneville Salt Flats and Pilot Valley Playa, Utah: U.S. Geological Survey Water-Supply Paper 2057, 107 p.

Lopes, T.J., and Evetts, D.M., 2004, Ground-water pumpage and artificial recharge estimates for calendar year 2000 and average flow by hydrographic area, Nevada: U.S. Geological Survey Scientific Investigations Report 2004–5239, 87 p.

Lundmark, K.W., Pohll, G.M., and Carroll, R.W.H., 2007, A steady-state water budget accounting model for the carbonate aquifer system in White Pine County, Nevada and adjacent areas in Nevada and Utah: Desert Research Institute Publication no. 41235, 56 p.

Lundquist, J.D., and Flint, A.L., 2006, Onset of snowmelt and streamflow in 2004 in the western United States: How shading may affect spring streamflow timing in a warmer world: Journal of Hydrometeorology, v. 7, p. 1,199–1,217.

Malek, E., Bingham, G.E., and McCurdy, G.D., 1990, Evapotranspiration from the margin and moist playa of a closed desert valley: Journal of Hydrology, v. 120, p. 15–34.

Malmberg, G.T., 1964, Land subsidence in Las Vegas Valley, Nevada, 1935–63: Nevada Department of Conservation and Natural Resources Ground-Water Resources—Information Series Report 5, 10 p.

Manning, A.H., and Caine, J.S., 2007, Groundwater noble gas, age, and temperature signatures in an alpine watershed: Valuable tools in conceptual model development: Water Resources Research, v. 43, W04404, doi:10.1029/2006WR005349, accessed January 20, 2009 at http://www.agu.org/pubs/crossref/2007/2006WR005349.shtml.

Manning, A.H., and Solomon, D.K., 2003, Using noble gases to investigate mountain-front recharge: Journal of Hydrology, v. 275, p. 194–207.

Manning, A.H., and Solomon, D.K., 2005, An integrated environmental tracer approach to characterizing groundwater circulation in a mountain block: Water Resources Research v. 41, W12412, 18 p., doi: 10.1029/2005WR004178, accessed January 20, 2009 at http://www.agu.org/pubs/crossref/2005/2005WR004178.shtml.

Markstrom, S.L., Niswonger, R.G., Regan, R.S., Prudic, D.E., and Barlow, P.M., 2008, GSFLOW—Coupled ground-water and surface-water flow model based on the integration of the precipitation-runoff modeling system (PRMS) and the modular ground-water flow model (MODFLOW–2005): U.S. Geological Survey Techniques and Methods 6–D1, 240 p.

Mathey, S.B., ed., 1998, National Water Information System (NWIS): U.S. Geological Survey Fact Sheet 027–98, 2 p., accessed January 14, 2009 at http://pubs.usgs.gov/fs/FS-027-98/fs-027-98.pdf.

Maxey, G.B., and Eakin, T.E., 1949, Ground water in White River Valley, White Pine, Nye, and Lincoln Counties, Nevada: Nevada Office of the State Engineer Water Resources Bulletin no. 8, 59 p.

Medina, R.L., 2005, 1:1,000,000-scale areas of evapotranspiration in the Great Basin: U.S. Geological Survey vector digital data, accessed March 2007 at http://water.usgs.gov/lookup/getspatial?ha694c_et1000gb_p.

Molotch, N., Blanken, P., Williams, M., Turpinseed, A., Monson, R., and Margulis, S.A., 2006, Estimating sublimation of intercepted and sub-canopy snow using eddy covariance systems, in Eastern Snow Conference, 63rd, Newark, Delaware, 2006, Proceedings: Eastern Snow Conference, p. 75–87, accessed January 20, 2009 at http://www.easternsnow.org/proceedings/2006/proceedings_index.html.

Moreo, M.T., and Justet, L., 2008, Update to the ground-water withdrawal database for the Death Valley regional ground-water flow system, Nevada and California, 1913–2003: U.S. Geological Survey Data Series 340, 10 p., with supplemental data. (Available at http://pubs.usgs.gov/ds/340/.)

Moreo, M.T., Laczniak, R.J., and Stannard, D.I., 2007, Evapotranspiration rate measurements of vegetation typical of ground-water discharge areas in the Basin and Range carbonate-rock aquifer system, White Pine County, Nevada and adjacent areas in Nevada and Utah, September 2005–August 2006: U.S. Geological Survey Scientific Investigations Report 2007–5078, 37 p.

Mower, R.W., and Cordova, R.M., 1974, Water resources of the Milford area, Utah, with emphasis on ground water: Utah Department of Natural Resources Technical Publication 43, 106 p.

Nevada Division of Water Resources, 2010, Nevada Water Facts Definitions: accessed March 2010 at http://water.nv.gov.

Nichols, W.D., 2000, Regional ground-water evapotranspiration and ground-water budgets, Great Basin, Nevada: U.S. Geological Survey Professional Paper 1628, 93 p., with optical disc and 4 pls.

Pavelko, M.T., 2007, Spring database for the Basin and Range carbonate-rock aquifer system, White Pine County, Nevada, and adjacent areas in Nevada and Utah: U.S. Geological Survey Data Series 272, 10 p., with supplemental database. (Available at http://pubs.usgs.gov/ds/2007/272/.)

Pavelko, M.T., Wood, D.B., and Laczniak, R.J., 1999, Pt. I: Mining ground water, Las Vegas, Nevada, *in* Galloway, D., Jones, D.R., and Ingebritsen, S.E., eds., Land subsidence in the United States: U.S. Geological Survey Circular 1182, 177 p.

Priestley, C.H.B., and Taylor, R.J., 1972, On the assessment of surface heat flux and evaporation using large-scale parameters: Monthly Weather Review, v. 100, p. 81–92.

Prudic, D.E., Harrill, J.R., and Burbey, T.J., 1995, Conceptual evaluation of regional ground-water flow in the Carbonate-Rock province of the Great Basin, Nevada, Utah, and adjacent states: U.S. Geological Survey Professional Paper 1409–D, 102 p.

Richardson, G.B., 1906, Underground water in the valleys of Utah Lake and Jordan River, Utah: U.S. Geological Survey Water-Supply Paper 157, 81 p.

RS/GIS Laboratory, 2004, 'PROVISIONAL' Digital Landcover Dataset for the Southwestern United States: Utah State University, College of Natural Resources, accessed November 2007 at http://earth.gis.usu.edu/swgap/landcover.html.

Rush, F.E., 1964, Ground-water appraisal of the Meadow Valley area, Lincoln and Clark Counties, Nevada: Nevada Department of Conservation and Natural Resources Ground-Water Resources Reconnaissance Report 27, 42 p.

Rush, F.E., 1968, Water-resources appraisal of the Lower Moapa-Lake Mead area, Clark County, Nevada: Nevada Department of Conservation and Natural Resources Water Resources Reconnaissance Report 50, 66 p.

Rutledge, A., 1998, Computer programs for describing the recession of ground-water discharge and estimating mean ground-water recharge and discharge from streamflow records—Update: U.S. Geological Survey Water-Resources Investigation Report 98–4148, 43 p.

San Juan, C.A., Belcher, W.R., Laczniak, R.J., and Putnam, H.M., 2004, Hydrologic components for model development, chap. C *of* Belcher, W.R., ed., Death Valley regional ground-water flow system, Nevada and California—Hydrogeologic framework and transient ground-water flow model: U.S. Geological Survey Scientific Investigations Report 2004–5205, p. 103–136.

Scott, B.R., Smales, T.J., Rush, F.E., and Van Denburgh, A.S., 1971, Water for Nevada: Nevada Department of Conservation and Natural Resources, Water Planning Report no. 3, 87 p.

Smith, J.L., Laczniak, R.J., Moreo, M.T., and Welborn, T.L., 2007, Mapping evapotranspiration units in the Basin and Range carbonate-rock aquifer system, White Pine County, Nevada, and adjacent areas in Nevada and Utah: U.S. Geological Survey Scientific Investigations Report 2007–5087, 21 p.

Smith, J.L., Reece, B.D., and Medina, R.L., 2000, Data sets and related information used for estimating regional ground-water evapotranspiration in eastern Nevada: U.S. Geological Survey Open-File Report 99–242, CD-ROM.

Stephens, J.C., 1976, Hydrologic reconnaissance of the Pine Valley drainage basin, Millard, Beaver and Iron Counties, Utah: Utah Department of Natural Resources Technical Publication 51, 38 p.

Stolp, B.J., and Brooks, L.E., 2009, Hydrology and simulation of ground-water flow in Tooele and Rush Valleys, Utah: U.S. Geological Survey Scientific Investigations Report 2009–5154, 86 p., 3 appendixes, 1 pl.

Stonestrom, D.A., Prudic, D.E., Laczniak, R.J., Akstin, K.C., Boyd, R.A., and Henkelman, K.K., 2003, Estimates of deep percolation beneath native vegetation, irrigated fields, and the Amargosa-River channel, Amargosa Desert, Nye County, Nevada: U.S. Geological Survey Open-File Report 03–104, 88 p.

Susong, D.D., 1995, Water budget and simulation of one-dimensional unsaturated flow for a flood- and sprinkler-irrigated field near Milford, Utah: U.S. Geological Survey Water-Resources Investigations Report 95–4072, 32 p.

Tallaksen, L., 1995, A review of baseflow recession analysis: Journal of Hydrology, v. 165, p. 349–370.

Thiros, S.A., Stolp, B.J., Hadley, H.K., and Steiger, J.I., 1996, Hydrology and simulation of ground-water flow in Juab Valley, Juab County, Utah: Utah Department of Natural Resources Technical Publication 114, 100 p.

Thomas, J.M., Calhoun, S.C., and Apambire, W.B., 2001, A deuterium mass-balance interpretation of groundwater sources and flows in southeastern Nevada: Desert Research Institute Publication no. 41169, 46 p.

Thomas, J.M., Hudson, G.B., Stute, M., and Clark, J.F., 2003, Noble gas loss may indicate groundwater flow across flow barriers in southern Nevada: Environmental Geology v. 43, p. 568–579.

U.S. Department of Agriculture, 2005, National Agricultural Imagery Program (NAIP), Compressed County mosaics (CCM) for California, accessed February 2009 at http://datagateway.nrcs.usda.gov/GDGHOME.aspx.

U.S. Department of Agriculture, 2006a, National Agricultural Imagery Program (NAIP), Compressed County mosaics (CCM) for Nevada, accessed February 2009 at http://datagateway.nrcs.usda.gov/GDGHOME.aspx.

U.S. Department of Agriculture, 2006b, National Agricultural Imagery Program (NAIP), Compressed County mosaics (CCM) for Utah, accessed February 2009 at http://datagateway.nrcs.usda.gov/GDGHOME.aspx.

Utah State Engineer, 1940, Twenty-second biennial report of the State Engineer to the Governor of Utah: Salt Lake City, 226 p.

Van Denburgh, A.S., and Rush, F.E., 1974, Water-resources appraisal of Railroad and Penoyer Valleys, east-central Nevada: Nevada Department of Conservation and Natural Resources Water Resources Reconnaissance Report 60, 61 p.

Watson, P., Sinclair, P., and Waggoner, R., 1976, Quantitative evaluation of a method for estimating recharge to the desert basins of Nevada: Journal of Hydrology, v. 31, p. 335–357.

Welch, A.H., Bright, D.J., and Knochenmus, L.A., eds., 2007, Water resources of the Basin and Range carbonate-rock aquifer system, White Pine County, Nevada, and adjacent areas in Nevada and Utah: U.S. Geological Survey Scientific Investigations Report 2007–5261, 96 p.

Wilson, J.L., and Guan, H., 2004, Mountain-block hydrology and mountain-front recharge, *in* Hogan and others, eds., Groundwater recharge in a desert environment: The southwestern United States: Washington, D.C., American Geophysical Union, Water Science and Application Series, v. 9, p. 113–137.

Winograd, I.J., and Pearson, F.J., 1976, Major carbon-14 anomaly in a regional carbonate aquifer: possible evidence for megascale channeling, south central Great Basin: Water Resources Research, v. 12, p. 1,125–1,143.

Winograd, I.J., and Thordarson, W., 1975, Hydrogeologic and hydrochemical framework; south-central Great Basin, Nevada-California, with special reference to the Nevada test site: U.S. Geological Survey Professional Paper 712–C, 126 p.

Zecharias, Y.B., and Brutsaert, W., 1988, Recession characteristics of groundwater outflow and base flow from mountainous watersheds: Water Resources Research, v. 24, p. 1,651–1,658.

Zones, C.P., 1961, Ground-water potentialities in the Crescent Valley, Eureka and Lander Counties, Nevada: U.S. Geological Survey Water Supply Paper 1581, 50 p.

Appendix 1: Three-Dimensional Hydrogeologic Framework

By Jay R. Cederberg, Donald S. Sweetkind, Susan G. Buto, and Melissa D. Masbruch

A three-dimensional (3D) hydrogeologic framework was constructed to represent the regional hydrogeologic units (HGUs) and major structures in the Great Basin carbonate and alluvial aquifer system (GBCAAS) study area. A generalized conceptual model of geology, structure, and faulting, incorporating hydrogeologic properties of the HGUs was used to develop a computer generated hydrogeologic framework. The digital 3D-hydrogeologic framework is the physical skeleton that will form the foundation of the groundwater flow model of the study area being developed concurrently (2011).

The 3D-hydrogeologic framework, consisting of nine HGUs with distinct hydraulic properties, was constructed by extracting and combining information from a variety of datasets. The top altitudes of the HGU surfaces were modeled from the input data using a 2.59 km^2 (1 mi^2) grid cell size. The modeled HGU surfaces were constrained by two regional datasets: (1) the National Elevation Dataset Digital Elevation Model (NED DEM) surface (U.S. Geological Survey EROS Data Center, 1999) and (2) the depth-to-basement surface (depth to pre-Cenozoic rocks) (see section “Depth-to-Basement Surface”). The HGU surfaces were combined and stacked together, resulting in the 3D-hydrogeologic framework for the GBCAAS study area. Major fault zones and caldera margins were incorporated to define regional trends and structural controls on the hydrogeology. A detailed description of structural controls and HGU designations within the GBCAAS study area is given in the “Hydrogeologic Units” section of Chapter B.

Interpolation of spatial data points into grids representing the HGU surfaces was processed using Rockware Rockworks14® software. Further modification and interpretation of the gridded HGU surfaces was completed using Environmental Science Research Institute ARC/INFO® geographic information system (GIS) software.

Input Data

Construction of the 3D-hydrogeologic framework utilized data from multiple sources to define the top surface and extent of each HGU. Input data sources include topographic data, geologic maps, borehole logs, previously published geologic cross sections, and digital geophysical models.

Topographic Data

Digital elevation data for the study area consist of seamless 1:24,000-scale National Elevation Data (NED) digital elevation models (DEM) (U.S. Geological Survey EROS Data Center, 1999). Data are in Albers projection North American Datum 1983 with a grid cell spacing of about 30 m.

Geologic Maps

Data from digital state geologic maps of Arizona, California, Idaho, Nevada, and Utah were used as input to the 3D-hydrogeologic framework. Geologic data from the five state maps, ranging in scale from 1:500,000 to 1:1,000,000, were cross-correlated to generate an integrated geologic map database for the Western U.S. (Ludington and others, 1996), including the GBCAAS study area. Each geologic unit from the integrated dataset was assigned to a HGU using the criteria discussed in Chapter B and from published unit descriptions in the primary source data for the digital maps (fig. A1–1 and fig. B–2 of Chapter B).

HGU data from the surficial geologic map were processed in a GIS by locating nodes (points) along adjacent HGU polygon boundaries (fig. A1–1). Each node was assigned an HGU corresponding to the geologically oldest HGU polygon located at that point. Cross-correlating the NED at that point results in the top altitude of the HGU at that point relative to the surficial geologic map. The process assumes younger geologic units overlie older units. In order to simplify and reduce the number of data points from this data source, each HGU point within a radius of 402.3 m (1,320 ft) of another was combined and represented spatially as the geometric mean of the overlapping points.

Well Stratigraphic Data

Stratigraphic log data from 441 wells throughout the GBCAAS study area were compiled and HGU contacts at each well were delineated for input to the 3D-hydrogeologic framework. Well stratigraphic data came from a variety of sources and databases including Nevada and Utah oil and gas exploration wells (Hess and others, 2004; Utah Division

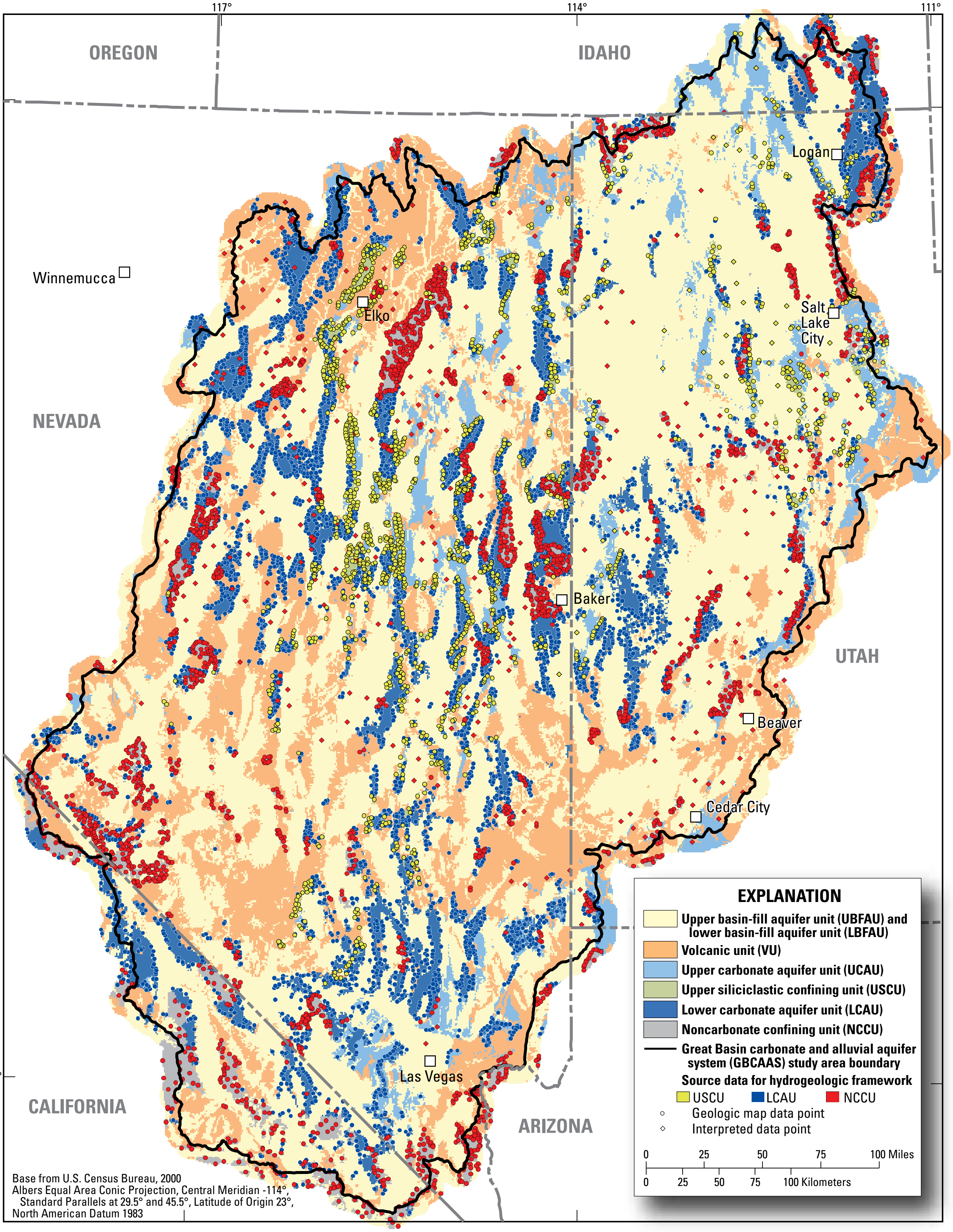

Figure A1–1. Surficial hydrogeologic units and locations of geologic map data used to create the three-dimensional hydrogeologic framework in the Great Basin carbonate and alluvial aquifer system study area.

of Oil, Gas, and Mining, 2008), the MX missile program (Tumbusch and Schaefer, 1996), Southern Nevada Water Authority exploration and production wells (Nevada Division of Water Resources, 2008), and water wells in Utah (Utah Division of Water Rights, 2008). Thousands of wells have been drilled in the study area; however, only a small fraction of these wells have detailed lithologic and stratigraphic data with HGU contact altitudes. Locations of wells used for constructing the hydrogeologic framework are shown in figure A1–2.

Cross Sections

The contacts between HGUs were manually picked from 245 cross sections compiled from 99 separate sources and used as input data for developing the 3D-hydrogeologic framework (fig. A1–2). References for each of the cross sections used are listed in Auxiliary 1. A scanned image of each cross section was scaled and georeferenced in a GIS along the cross-section trace of the digital source map. Geologic units on each cross section were correlated to the HGUs defined for the GBCAAS study area. HGU contacts along the cross-section trace were used to pick points representing the oldest HGU at the contact. The altitude of the top surface of each HGU point represented in cross section was interpolated from the cross section vertical scale.

Existing Geologic Frameworks

The existing 3D-hydrogeologic framework for the Death Valley regional flow system (DVRFS) model (Faunt and others, 2004) was incorporated into the GBCAAS hydrogeologic framework (fig. A1–2). The DVRFS hydrogeologic model consists of 27 separate HGUs. Individual HGUs in the DVRFS model were grouped and assigned to the nine HGUs for this study (table A1–1). The grouped HGU surfaces from the Death Valley framework were resampled to a 2.59 km^2 (1 mi^2) grid cell size used in this study.

Depth-to-Basement Surface

Regional gravity studies were used to delineate the boundary between the pre-Cenozoic basement rocks and the Cenozoic volcanic and sedimentary basin-fill deposits. Gravity data were used to estimate the shape and extent of the Cenozoic basins in three dimensions. There is a large density contrast between the pre-Cenozoic basement rocks and the overlying Cenozoic volcanic rocks and sedimentary basin fill that is used to estimate the depth-to-basement in Cenozoic basins (Saltus and Jachens, 1995). The regional Saltus and Jachens (1995) depth-to-basement surface for Arizona, California, Nevada, and Utah was joined with a depth-to-basement surface for Idaho (Mankinen and others, 2004). The resulting surface was combined with three higher resolution datasets from more recent regional studies of the Basin and Range carbonate-rock aquifer system (BARCAS) (Ponce and others, 2001; Welch and others, 2007), the DVRFS (Belcher, 2004), and geophysical framework investigations in east-central Nevada and west-central Utah (Watt and Ponce, 2007) (fig. A1–3). In areas where the detailed studies overlapped the regional Saltus and Jachens (1995) data, the original Saltus and Jachens data were replaced with the more recent data using a common 500-m^2 grid cell size of the Saltus and Jachens (1995) data. The depth-to-basement surface was compared to the HGU surficial geology map and modified so that the depth-to-basement surface altitude was equal to the NED altitude where pre-Cenozoic rocks outcrop on the HGU map. The final merged map was resampled using a 2.59 km^2 (1 mi^2) grid cell size to be consistent with the HGU map. The end result is a single "depth-to-basement" surface that incorporates multiple datasets to represent the altitude of the pre-Cenozoic rock surface. The final gridded surface used in the hydrogeologic framework defines both the top of pre-Cenozoic rocks and the base of the Cenozoic sedimentary basin-fill deposits and volcanic rocks. The thickness of the Cenozoic rocks was derived by subtracting the depth-to-basement surface from the NED DEM (fig. A1–3).

Fault and Caldera Boundaries

Structural features, including faults and calderas, are abundant within the GBCAAS study area and affect the extent and depth of HGUs (see "Hydrogeologic Units" in Chapter B). Fault boundaries were compiled from and modified after Raines and others (1996), Hintze and others (2000), Potter and others (2002), Workman and others (2002), Page and others (2005), Ludington and others (1996), and Beard and others (2007), and were simplified to represent the regional scale of the study (fig. A1–4).

Caldera boundaries were compiled from numerous published sources (Shawe, 1972; Lindsey, 1982; Steven and others, 1984; Best and Grant, 1987; Best and others, 1989; Loucks and others, 1989; Gans and others, 1989; Ludington and others, 1996; Raines and others, 1996; Williams and others, 1997; Workman and others, 2002; Page and others, 2005; Henry, 2008). Caldera boundaries were also generalized for use at a regional scale (fig. A1–5). The caldera boundary dataset was used to control the extent of pre-Cenozoic HGUs within a caldera boundary. Calderas were assumed to have similar hydrogeologic properties as the noncarbonate confining unit (NCCU); therefore, the area contained within a caldera boundary is designated as NCCU and extends vertically to the base of the volcanic unit (VU).

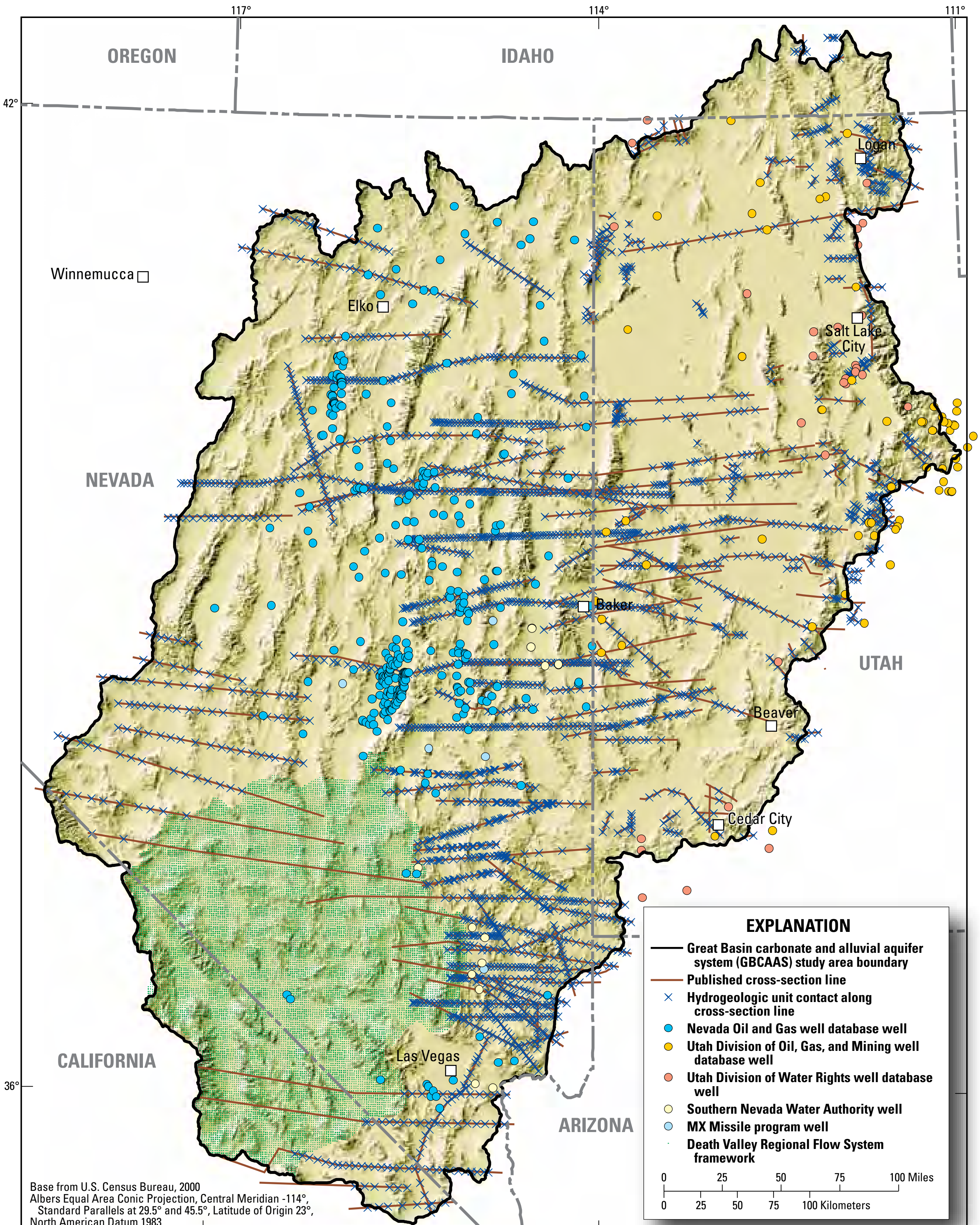

Figure A1–2. Locations of wells and cross sections used to create the three-dimensional hydrogeologic framework in the Great Basin carbonate and alluvial aquifer system study area.

Table A1–1. Correlation of hydrogeologic units between the Great Basin carbonate and alluvial aquifer system study and Death Valley regional flow system study.

[DVRFS HGU designations from Faunt and others, 2004, table E-1. Abbreviations: GBCAAS, Great Basin carbonate and alluvial aquifer system; DVRFS, Death Valley regional flow system; HGU, hydrogeologic unit; UBFAU, upper basin-fill aquifer unit; LBFAU, lower basin-fill aquifer unit; VU, volcanic unit; TLCAU, thrusted lower carbonate aquifer unit; TNCCU, thrusted noncarbonate confining unit; UCAU, upper carbonate aquifer unit; USCU, upper siliciclastic confining unit; LCAU, lower carbonate aquifer unit; NCCU, noncarbonate confining unit; NED, National Elevation Dataset]

GBCAAS HGU	DVRFS HGU	Stacking order	Calculation of top of HGU
UBFAU	YAA, YACU, OAA, OACU, LA, LFU, YVU, Upper VSU	9	Equals altitude of NED grid where UBFAU HGU exists.
LBFAU	YAA, YACU, OAA, OACU, LA, LFU, YVU, Upper VSU	8	Equals altitude of NED minus two-thirds the thickness of the basin-fill deposits (where thickness equals altitude of UBFAU grid minus altitude of depth-to-basement grid).
VU	TMVA, PVA, CHVU, WVU, CFPPA, CFBCU, CFTA, BRU, OVU, Lower VSU	7	Equals altitude of NED grid where VU HGU exists.
TLCAU	LCA_T1	6	Equals altitude of depth-to-basement grid.
TNCCU	LCCU_T1	5	Equals altitude of TLCAU grid minus thickness of TLCAU.
UCAU	SCU, UCA	4	Equals altitude of TNCCU grid minus thickness of TNCCU.
USCU	UCCU	3	Altitude of USCU grid is interpolated. Altitude set equal to UCAU or LCAU if the interpolated grid extended above or below the respective surfaces.
LCAU	LCA	2	Altitude of LCAU grid is interpolated. Altitude set equal to UCAU or NCCU if the interpolated grid extended above or below the respective surfaces.
NCCU	LCCU, XCU, ICU	1	Altitude of NCCU grid is interpolated. Altitude set equal to UCAU if the interpolated grid extended above respective surface.

Hydrogeologic Unit Gridded Surface Construction

In the hydrogeologic framework, individual HGUs are represented by an interpolated gridded surface of the top altitude of each HGU. Gridded surfaces were interpolated from the data described in the previous sections and modified in specific areas where data were limited. Different approaches were used for developing the upper basin-fill and lower basin-fill aquifer units (UBFAU and LBFAU) and the VU surfaces than were used for gridding the pre-Cenozoic HGU surfaces due to differences and limitations of the data. Each of the nine individual HGU gridded surfaces covers the entire GBCAAS study area with an altitude represented in each grid cell. If the HGU does not exist in a cell, the next lower HGU has the same altitude value in that cell, thereby producing a thickness of zero between the HGUs.

Cenozoic Hydrogeologic Units

Cenozoic HGUs include the UBFAU, the LBFAU, and the VU. Point data sources such as geologic contacts from wells and cross sections often do not clearly define contacts between volcanic rock and basin-fill deposits, thereby limiting the accuracy of the interpolated HGU gridded surface. Because of this limitation, the Cenozoic units were delineated using the NED surface, depth-to-basement surface, and surficial HGU map (fig. A1–1). Gridded surfaces were created from the surficial geology of Cenozoic sedimentary and volcanic units shown on the surficial HGU map (fig. A1–1). The altitude of the UBFAU gridded surface, representing the uppermost unit in the hydrogeologic framework, is defined by the NED and bounds the uppermost extent of all the lower HGUs. The two basin-fill aquifer HGUs have a combined thickness equal to the NED minus the depth-to-basement surface (fig. A1–4) where Cenozoic sediments are present on the HGU map (fig. A1–1). Point data sources such as geologic contacts from wells and cross sections rarely delineate volcanic ash deposits, lava flows into valley centers, or semiconsolidated basin-fill deposits at depth; therefore, the basin-fill aquifer HGUs are divided into an upper unit (UBFAU) and a lower unit (LBFAU) to represent potential differences in hydrogeologic properties. The UBFAU is defined as the upper two-thirds of the total basin-fill thickness, and the LBFAU as the lower one-third of the total basin-fill thickness. Wherever VU is present (fig. A1–1), it is represented as the thickness equal to the NED surface minus the depth-to-basement surface (fig. A1–5). The bottom surfaces of the LBFAU and VU are bounded by the depth-to-basement surface.

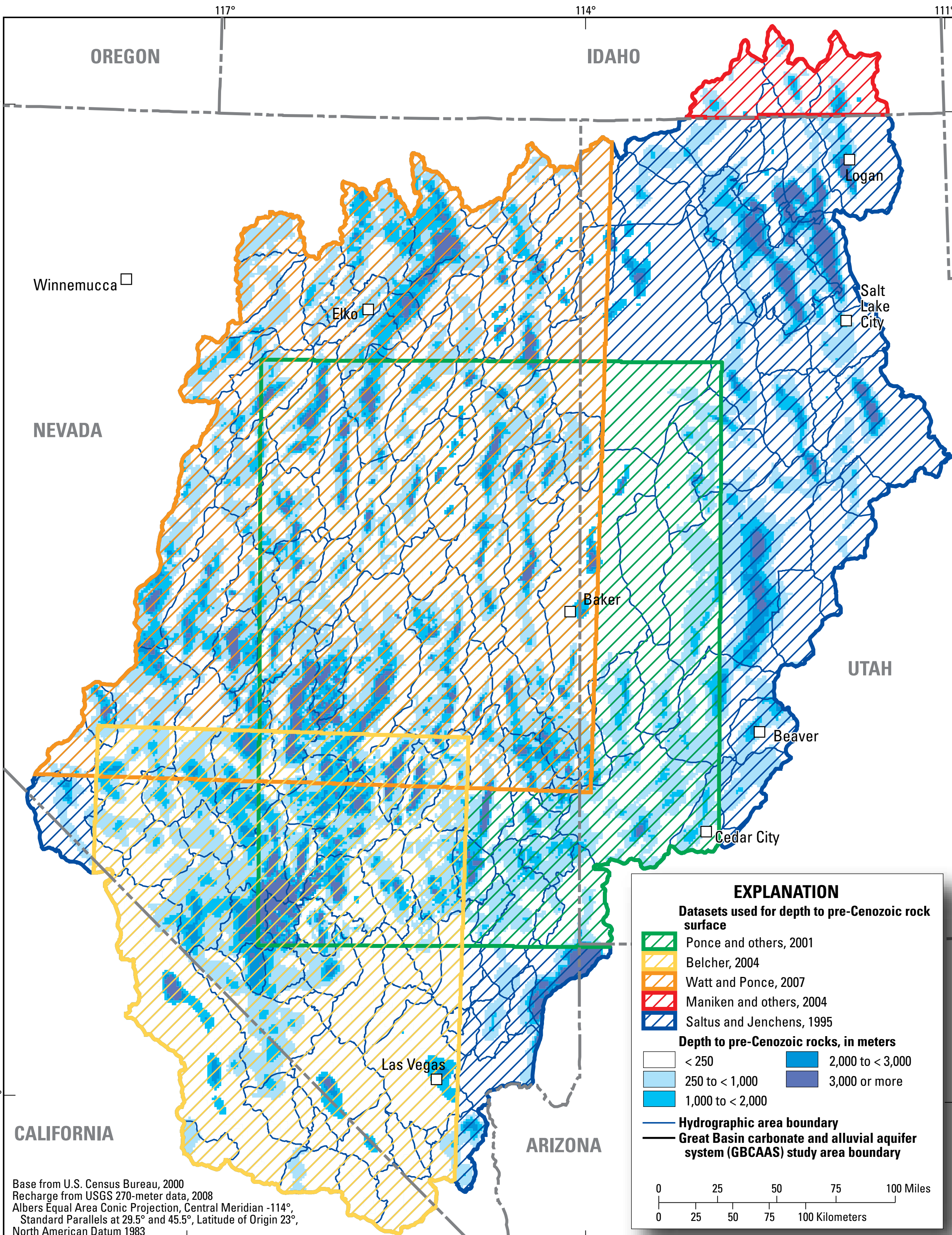

Figure A1–3. Locations of published datasets and estimated thickness of Cenozoic deposits (depth to pre-Cenozoic rocks) in the Great Basin carbonate and alluvial aquifer system study area.

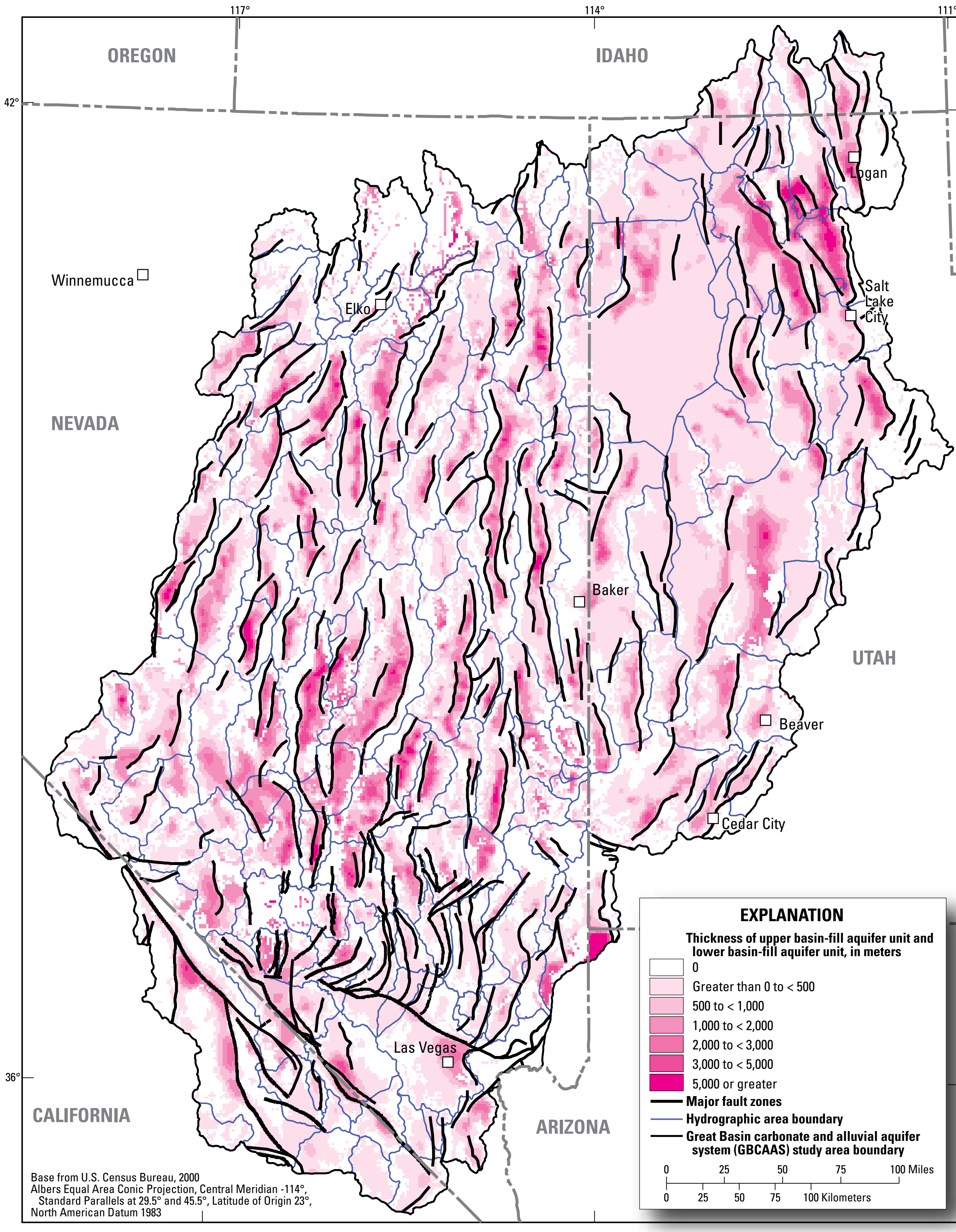

Figure A1–4. Extent and thickness of the upper basin-fill (UBFAU) and lower basin-fill (LBFAU) aquifer units (combined) and major fault zones in the Great Basin carbonate and alluvial aquifer system study area.

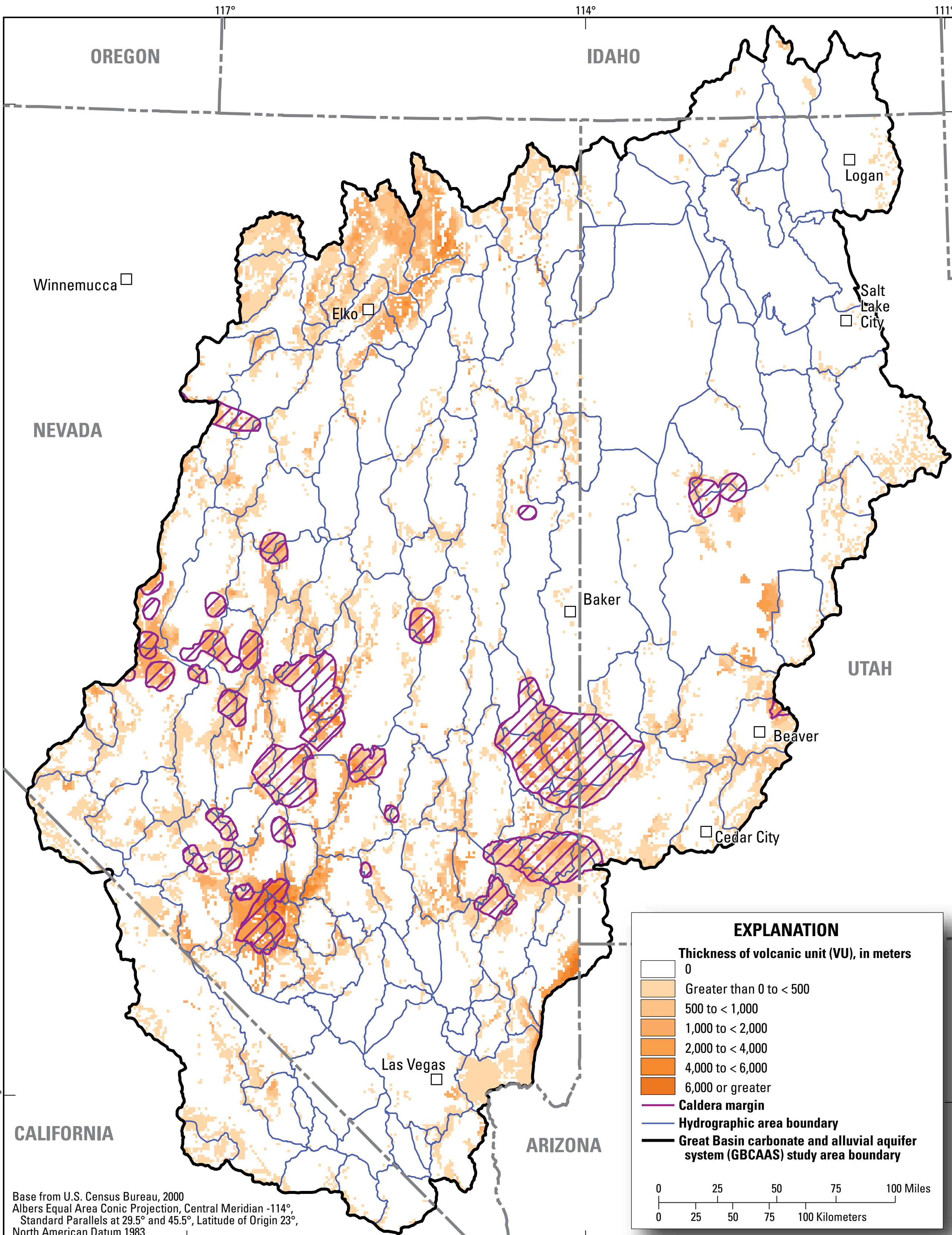

Figure A1–5. Extent and thickness of the volcanic unit (VU) and caldera boundaries in the Great Basin carbonate and alluvial aquifer system study area.

Pre-Cenozoic Units

Surfaces representing the top altitude were created for each of the pre-Cenozoic HGUs—NCCU, the lower carbonate aquifer unit (LCAU), the upper siliciclastic confining unit (USCU), the upper carbonate aquifer unit (UCAU), the thrusted noncarbonate confining unit (TNCCU), and the thrusted lower carbonate aquifer unit (TLCAU). The depth-to-basement surface is the top of the uppermost pre-Cenozoic unit surface (table A1–1).

The TNCCU and TLCAU spatial geometries (fig. A1–6) were interpolated by delineating the extent and thickness of two major thrust belts within the study area, the Roberts Mountain thrust and the Sevier thrust (see Chapter B). The TLCAU thickness was subtracted from the altitude of the depth-to-basement surface to determine the altitude of the top of the TNCCU. Subsequently, the TNCCU thickness was subtracted from the altitude of the top of the TNCCU to determine the altitude of the top of the UCAU gridded surface.

The altitudes of the NCCU, LCAU, and USCU gridded surfaces were interpolated from the data for each HGU using an inverse distance weighted algorithm. The algorithm also uses linear features as x-y pairs to represent major structural controls such as faults that act as barriers in the interpolation routine. The inverse distance weight across the linear feature was increased by a factor of 100, thereby limiting the unit interpolation across these structures.

The NCCU is stratigraphically the lowest unit and is the base of the 3D-hydrogeologic framework; therefore, the altitude of the NCCU surface defines the basal extent of all the pre-Cenozoic HGUs. The NCCU surface was limited by the digital elevation model and the UCAU, TLCAU, and (or) TNCCU surfaces so that it could not extend above the depth-to-basement surface, the thrusted units, or the land surface datum. The NCCU surface within the caldera boundaries was set equal to the depth-to-basement surface because it is assumed that the caldera complexes have hydraulic properties similar to the NCCU HGU.

The LCAU and USCU surfaces are controlled by the altitude of the UCAU gridded surface, so that they cannot extend above the pre-Cenozoic surface. The extent and thickness of the interpolated LCAU HGU are controlled by the altitude of the LCAU surface minus the altitude of the NCCU surface (table A1–1). The thickness of the LCAU was arbitrarily truncated at 6,000 m in areas where the NCCU surface was interpolated to be deeper than is likely. The NCCU surface was sequentially modified to be equal to the LCAU surface minus the LCAU thickness in the truncated areas. The extent and thickness of the interpolated USCU HGU are controlled by the altitude of the USCU surface minus the altitude of the LCAU surface. The extent and thickness of the USCU and LCAU HGUs are shown in figures A1–7 and A1–8, respectively. The extent and thickness of the UCAU are defined by the altitude of the UCAU surface (depth-to-basement minus thrusted units) minus the altitude of the USCU surface (fig. A1–9).

The resulting pre-Cenozoic HGU surfaces were compared to the surficial HGU map (fig. A1–1). Each HGU surface was adjusted so that the top was equal to the NED if the respective HGU occurred on the surficial map at the same point.

Three-Dimensional Hydrogeologic Framework

The final 3D-hydrogeologic framework was compiled by stacking the individual HGU gridded surfaces and allowing the individual HGU surfaces to represent the top altitude of each respective HGU (Z coordinate). The stacking order is defined by the geologic age of the unit, from oldest (Precambrian) to most recent (Quaternary) (table A1–1). An exception to the stacking rule applies to the thrusted surfaces, TNCCU and TLCAU, which are stacked relative to time of movement (Mesozoic) rather than age of deposition. HGU thickness is represented by the difference between altitudes of successive HGU surfaces such that the bottom of an HGU is always equal to the top of the HGU directly below it in the stacking order. Where the thickness is zero at a location, the respective HGU does not exist at that location. Cross sections and fence diagrams of the stacked 3D-hydrogeologic framework are illustrated on figures B–10 and B–11, respectively, in Chapter B.

The hydrogeologic framework is a simplified 3D representation of the hydrogeology of the entire GBCAAS study area, encompassing 165 individual hydrographic areas (HAs). As such, it is suitable for regional analysis at the scale of the GBCASS study but it may not accurately represent smaller scale hydrogeology within individual HAs, as it is not intended to be utilized at that scale.

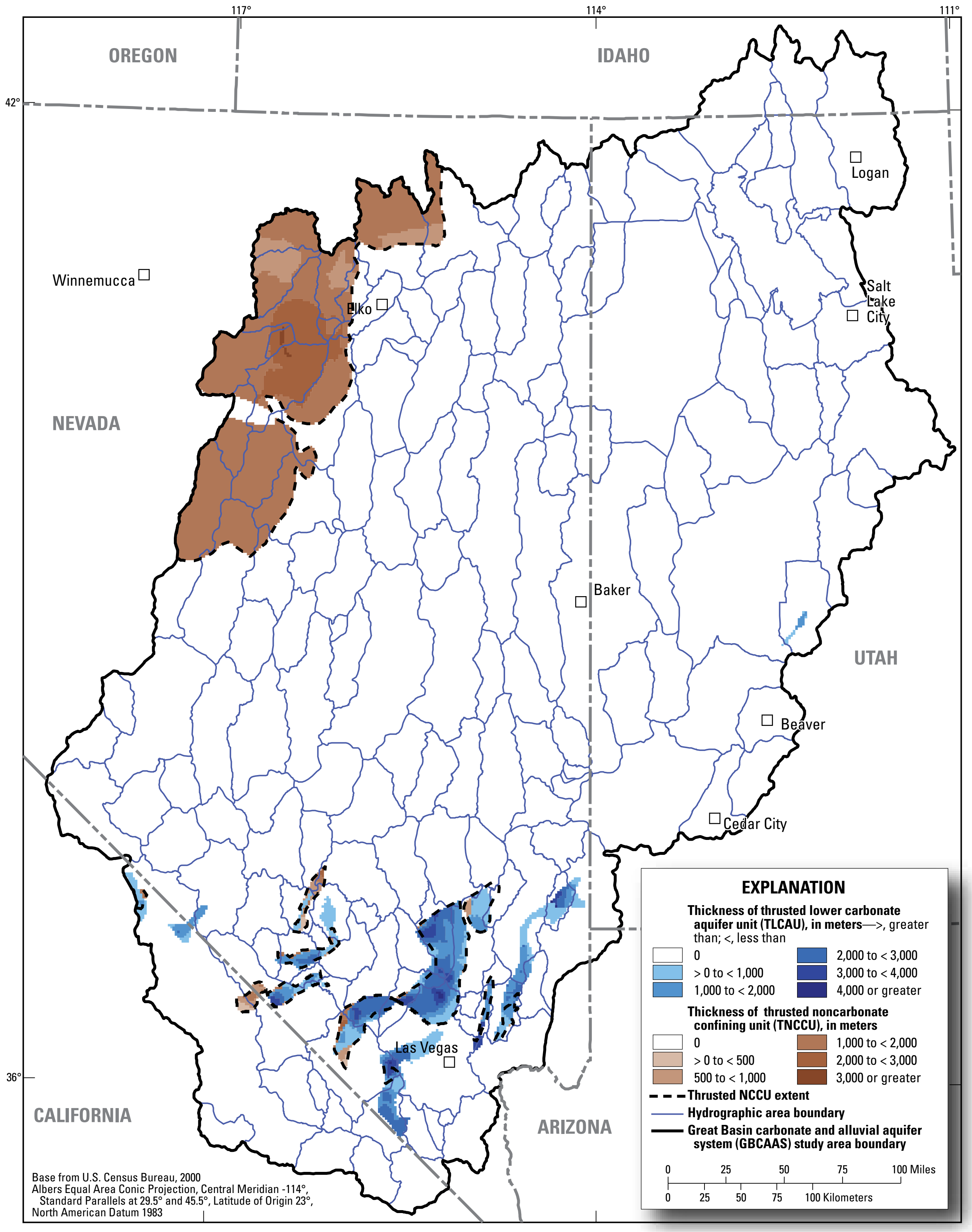

Figure A1–6. Extent and thickness of the thrusted lower carbonate aquifer unit (TLCAU) and thrusted noncarbonate confining unit (TNCCU) in the Great Basin carbonate and alluvial aquifer system study area.

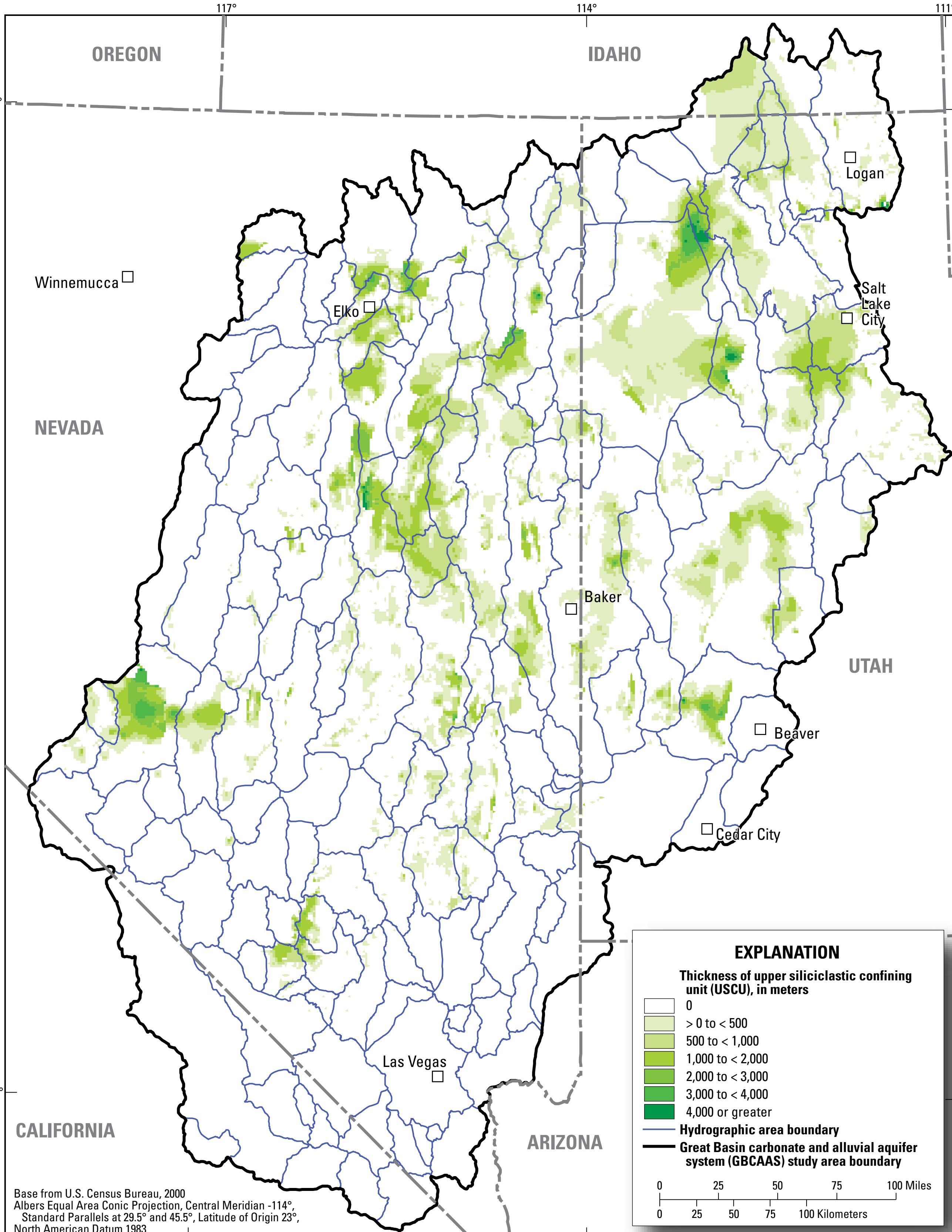

Figure A1–7. Extent and thickness of the upper siliciclastic confining unit (USCU) in the Great Basin carbonate and alluvial aquifer system study area.

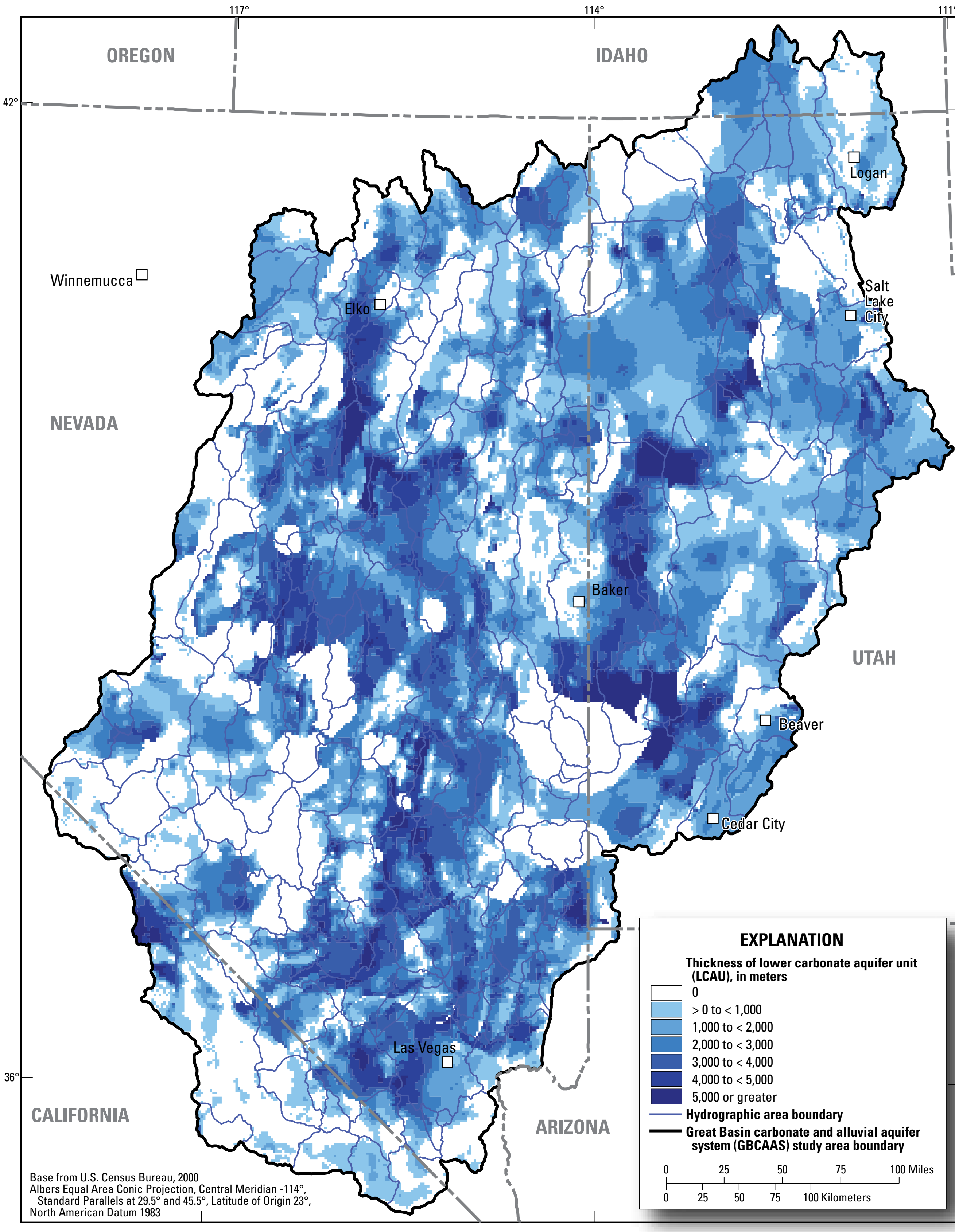

Figure A1–8. Extent and thickness of the lower carbonate aquifer unit (LCAU) in the Great Basin carbonate and alluvial aquifer system study area.

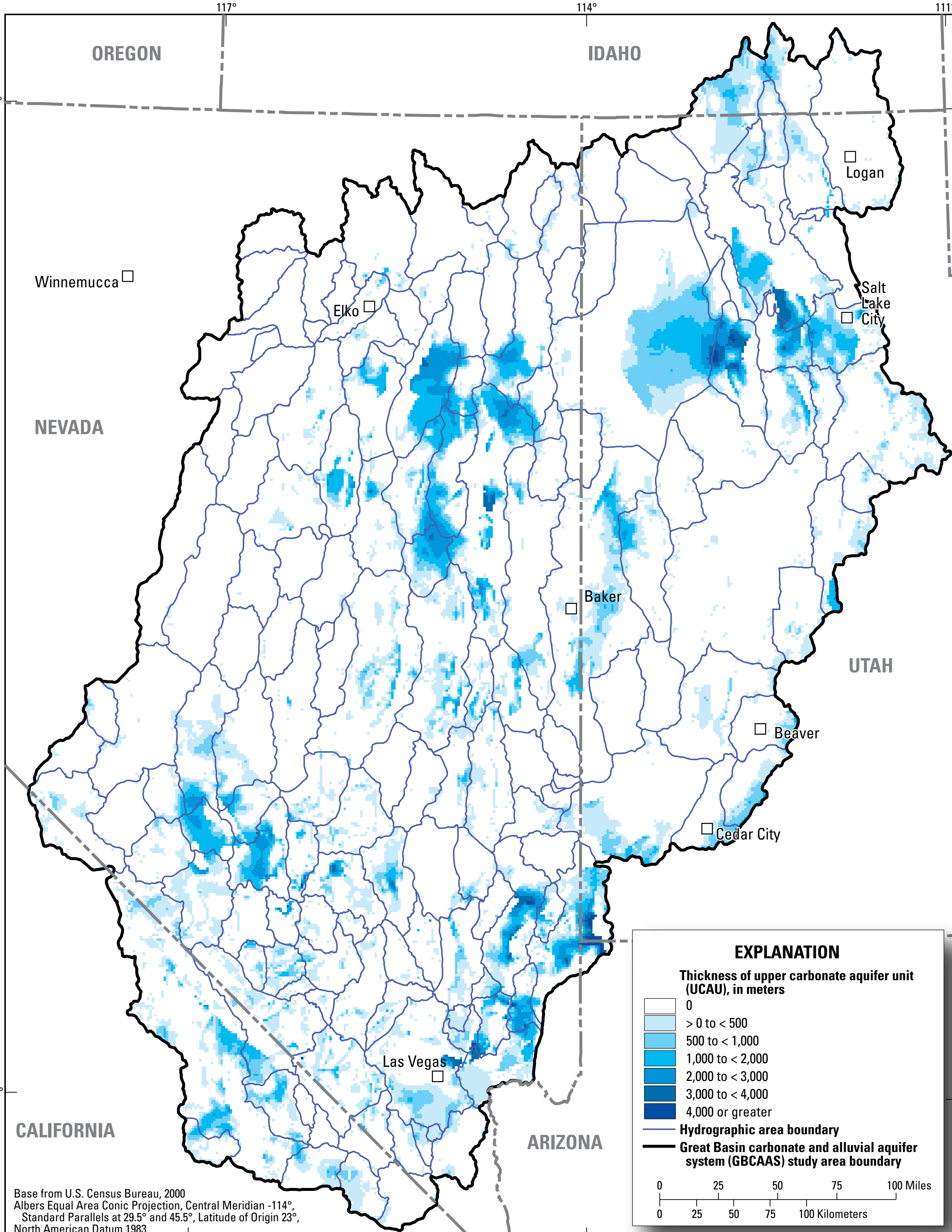

Figure A1–9. Extent and thickness of the upper carbonate aquifer unit (UCAU) in the Great Basin carbonate and alluvial aquifer system study area.

References Cited

Beard, L.S., Anderson, R.E., Block, D.L., Bohannon, R.G., Brady, R.J., Castor, S.B., Duebendorfer, E.M., Faulds, J.E., Felger, T.J., Howard, K.A., Kuntz, M.A., and Williams, V.S., 2007, Preliminary geologic map of the Lake Mead 30' X 60' quadrangle, Clark County, Nevada, and Mohave County, Arizona: U.S. Geological Survey Open-File Report 2007–1010, 109 p., 3 pls., scale 1:100,000.

Belcher, W.R., ed., 2004, Death Valley regional ground-water flow system, Nevada and California—Hydrogeologic framework and transient ground-water flow model: U.S. Geological Survey Scientific Investigations Report 2004–5205, 408 p.

Best, M.G., Christiansen, E.H., Deino, A.L., Grommé, C.S., McKee, E.H., and Noble, D.C., 1989, Excursion 3A: Eocene through Miocene volcanism in the Great Basin of the western United States: New Mexico Bureau of Mines and Mineral Resources Memoir, v. 47, p. 91–133.

Best, M.G., and Grant, S.K., 1987, Stratigraphy of the volcanic Oligocene Needles Range Group in southwestern Utah and eastern Nevada: U.S. Geological Survey Professional Paper 1443–A, 28 p.

Faunt, C.C., Sweetkind, D.S., and Belcher, W.R., 2004, Three-dimensional hydrogeologic framework model, chap. E, *of* Belcher, W.R., ed., Death Valley regional ground-water flow system, Nevada and California—Hydrogeologic framework and transient ground-water flow model: U.S. Geological Survey Scientific Investigations Report 2004–5205, p. 164–255.

Gans, P.B., Mahood, G.A., and Schermer, E., 1989, Synextensional magmatism in the Basin and Range province; A case study from the eastern Great Basin: Geological Society of America Special Paper 233, 53 p.

Henry, C.D., 2008, Ash-flow tuffs and paleovalleys in northeastern Nevada: Implications for Eocene paleogeography and extension in the Sevier hinterland, northern Great Basin: Geosphere, v. , no. 1, p. 1–35, doi: 10.1130/GES00122.1, accessed January 20, 2009 at http://geosphere.gsapubs.org/content/4/1/1.abstract?ijkey=320cabcbba80c521846d115a124126a106e1262a&keytype2=tf_ipsecsha.

Hess, R.H., Fitch, S.P., and Warren, S.N., 2004, Nevada oil and gas well database (NVOILWEL): Nevada Bureau of Mines and Geology Open-File Report 04–1, 242 p.

Hintze, L.F., Willis, G.C., Laes, D.Y.M., Sprinkel, D.A., and Brown, K.D., 2000, Digital geologic map of Utah: Utah Geological Survey Map 179DM, CD-ROM, scale 1:500,000.

Lindsey, D.A., 1982, Tertiary volcanic rocks and uranium in the Thomas Range and northern Drum Mountains, Juab County, Utah: U.S. Geological Survey Professional Paper 1221, 71 p.

Loucks, M.D., Tingey, D.G., Best, M.G., Christiansen, E.H., and Hintze, L.F., 1989, Geologic map of the Fortification Range, Lincoln and White Pine Counties, Nevada: U.S. Geological Survey Miscellaneous Investigations Series Map I–1866, 1 sheet, scale 1:50,000.

Ludington, S., Cox, D.P., Moring, B.C., and Leonard, K.R., 1996, Cenozoic volcanic geology of Nevada: Nevada Bureau of Mines and Geology Open-File Report 96–2, chap. 5, p. 5–1–5–10.

Ludington, S., Moring, B.C., Miller, R.J., Stone, P.A., Bookstrom, A.A., Bedford, D.R., Evans, J.G., Haxel, G.A., Nutt, C.J., Flyn, K.S., and Hopkins, M.J., 2006, Preliminary integrated geologic map databases for the United States, western states: California, Nevada, Arizona, Washington, Oregon, Idaho, and Utah, version 1.2: U.S. Geological Survey Open-File Report 2005–1305, accessed March 2007, at http://pubs.usgs.gov/of/2005/1305/.

Mankinen, E.A., Hildenbrand, T.G., Zientek, M.L., Box, S.E., Bookstrom, A.B., Carlson, M.H., and Larsen, J.C., 2004, Guide to geophysical data for the northern Rocky Mountains and adjacent areas, Idaho, Montana, Washington, Oregon, and Wyoming: U.S. Geological Survey Open-File Report 2004–1413, 34 p.

Nevada Division of Water Resources, 2008, Well log database: accessed February 8, 2008, at http://water.nv.gov/engineering/wlog/wlog.cfm.

Page, W.R., Dixon, G.L., Rowley, P.D., and Brickey, D.W., 2005, Geologic map of parts of the Colorado, White River, and Death Valley groundwater flow systems, Nevada, Utah, and Arizona: Nevada Bureau of Mines and Geology Map 150, 23 p., 1 sheet, scale 1:250,000.

Ponce, D.A., Blakely, R.J., Morin, R.L., and Mankinen, E.A., 2001, Isostatic gravity, aeromagnetic, and depth to pre-Cenozoic basement maps of the Death Valley ground-water model area, Nevada and California: U.S. Geological Survey Miscellaneous Investigations Map MF–2381–C, 1 sheet, scale 1:250,000, with pamphlet.

Potter, C.J., Sweetkind, D.S., Dickerson, R.P., and Killgore, M.L., 2002, Hydrostructural map of the Death Valley ground-water basin, Nevada and California: U.S. Geological Survey Miscellaneous Field Studies Map MF-2372, 2 sheets, scale 1:350,000, with pamphlet.

Raines, G.L., Sawatzky, D.L., and Connors, K.A., 1996, Great Basin geoscience data base: U.S. Geological Survey Digital Data Series DDS–41, 2 CD-ROMs.

Saltus, R.W., and Jachens, R.C., 1995, Gravity and basin-depth maps of the Basin and Range province, Western United States: U.S. Geological Survey Geophysical Investigation Map GP–1012, 1 sheet, scale 1:2,500,000.

Shawe, D.R., 1972, Reconnaissance geology and mineral potential of the Thomas, Keg, and Desert calderas, central Juab County, Utah: U.S. Geological Survey Professional Paper 800–B, p. B67–B77.

Steven, T.A., Rowley, P.D., and Cunningham, C.G., 1984, Calderas of the Marysvale volcanic field, west central Utah: Journal of Geophysical Research, v. 89, p. 8,751–8,764.

Tumbusch, M.L., and Schaefer, D.H., 1996, Selected hydrologic data for and location of MX wells in east-central and southern Nevada, January 1980 through May 1996: U.S. Geological Survey Open-File Report 96–469, 37 p.

U.S. Geological Survey EROS Data Center, 1999, 1 arc-second (30-meter) National Elevation Dataset: accessed June 26, 2005, at http://ned.usgs.gov/.

Utah Division of Oil, Gas, and Mining, 2008, Online oil and gas information system, accessed April 9, 2008, at http://oilgas.ogm.utah.gov/Data_Center/LiveData_Search/main_menu.htm.

Utah Division of Water Rights, 2008, Water distribution/regulation—Distribution system list, accessed January 28, 2008, at http://www.waterrights.utah.gov/cgi-bin/dvrtview.exe?Modinfo=StationView&STATION_ID=2335&RECORD_YEAR=2008.

Watt, J.T., and Ponce, D.A., 2007, Geophysical framework investigations influencing ground-water resources in east-central Nevada and west-central Utah, *with a section on* geologic and geophysical basin-by-basin descriptions by Wallace, A.R., Watt, J.T., and Ponce, D.A.: U.S. Geological Survey Open-File Report 2007–1163, 47 p., 2 pls., scale 1:750,000.

Welch, A.H., Bright, D.J., and Knochenmus, L.A., eds., 2007, Water resources of the Basin and Range carbonate-rock aquifer system, White Pine County, Nevada, and adjacent areas in Nevada and Utah: U.S. Geological Survey Scientific Investigations Report 2007–5261, 96 p.

Williams, V.S., Best, M.G., and Keith, J.D., 1997, Geologic map of the Ursine-Panaca Summit-Deer Lodge area, Lincoln County, Nevada, and Iron County, Utah: U.S. Geological Survey Miscellaneous Investigations Series Map I–2479, 1 sheet, scale 1:50,000.

Workman, J.B., Menges, C.M., Page, W.R., Ekren, E.B., Rowley, P.D., and Dixon, G.L., 2002, Tectonic map of the Death Valley ground-water model area, Nevada and California: U.S. Geological Survey Miscellaneous Field Studies Map MF–2381–B, 1 pl., scale 1:350,000, with pamphlet.

Appendix 2: Descriptive Information for Each Hydrographic Area within the Great Basin Carbonate and Alluvial Aquifer System Study Area

By Victor M. Heilweil and Susan G. Buto

Table A2–1. Descriptive information for each hydrographic area within the Great Basin carbonate and alluvial aquifer system study area.

[Latitude and longitude of centroid: geographic coordinate based on NAD83 horizontal datum. Mean altitude: based on NAVD88 vertical datum. Mean annual precipitation: based on PRISM average annual 1971–2000 precipitation (Daly and others, 2008[1]). Abbreviations: mi^2, square miles; ft, feet; in., inches]

Groundwater flow system name	Groundwater flow system number	Hydro-graphic area number	Hydrographic area name	Hydrographic subarea name	Latitude of centroid	Longitude of centroid	Area (mi^2)	Mean altitude (ft)	Mean annual precipitation (in.)
Humboldt System	7	42	Marys River Area		41.33	-115.17	1,065	6,215	14
		43	Starr Valley Area		40.96	-115.23	326	6,400	18
		44	North Fork Area		41.27	-115.71	1,092	6,281	13
		45	Lamoille Valley		40.79	-115.46	253	6,432	17
		46	South Fork Area		40.56	-115.52	106	7,752	24
		47	Huntington Valley		40.27	-115.72	754	6,273	14
		48	Tenmile Creek Area		40.64	-115.77	386	5,839	13
		49	Elko Segment		40.82	-115.84	317	5,660	11
		50	Susie Creek Area		40.91	-115.99	222	5,953	12
		51	Maggie Creek Area		40.99	-116.16	393	6,076	13
		52	Marys Creek Area		40.68	-116.21	65	5,680	11
		53	Pine Valley		40.19	-116.23	1,023	6,212	13
		54	Crescent Valley		40.35	-116.55	746	5,536	11
		55	Carico Lake Valley		40.04	-116.93	384	5,986	12
		56	Upper Reese River Valley		39.35	-117.26	1,160	6,844	13
		59	Lower Reese River Valley		40.46	-116.96	586	5,294	10
		60	Whirlwind Valley		40.59	-116.60	95	5,403	11
		61	Boulder Flat		40.80	-116.48	551	5,227	10
		62	Rock Creek Valley		40.99	-116.64	452	5,556	12
		63	Willow Creek Valley		41.26	-116.56	399	5,956	14
				Groundwater flow system subtotals			**10,375**	**6,029**	**13**
Monte Cristo Valley	23	136	Monte Cristo Valley		38.34	-117.81	282	6,046	9
				Groundwater flow system subtotals			**282**	**6,046**	**9**
South-Central Marshes	24	117	Fish Lake Valley		37.67	-118.00	993	6,720	9
		118	Columbus Salt Marsh Valley		38.08	-118.01	366	5,483	6
		137A	Big Smoky Valley	Tonopah Flat	38.31	-117.47	1,609	5,854	8
		141	Ralston Valley		38.20	-117.02	969	6,261	8
		142	Alkali Spring Valley		37.85	-117.29	317	5,459	6
		143	Clayton Valley		37.71	-117.60	551	5,568	7
		149	Stone Cabin Valley		38.18	-116.68	985	6,333	9
				Groundwater flow system subtotals			**5,790**	**5,954**	**8**

Table A2-1. Descriptive information for each hydrographic area within the Great Basin carbonate and alluvial aquifer system study area.—Continued

[Latitude and longitude of centroid: geographic coordinate based on NAD83 horizontal datum. Mean altitude: based on NAVD88 vertical datum. Mean annual precipitation: based on PRISM average annual 1971–2000 precipitation (Daly and others, 2008[1]). Abbreviations: mi², square miles; ft, feet; in., inches]

Groundwater flow system name	Groundwater flow system number	Hydro-graphic area number	Hydrographic area name	Hydrographic subarea name	Latitude of centroid	Longitude of centroid	Area (mi²)	Mean altitude (ft)	Mean annual precipitation (in.)
Grass Valley	25	138	Grass Valley		39.84	-116.72	598	6,386	12
				Groundwater flow system subtotals			**598**	**6,386**	**12**
Northern Big Smoky Valley	26	137B	Northern Big Smoky Valley		39.10	-117.02	1,313	6,780	13
				Groundwater flow system subtotals			**1,313**	**6,780**	**13**
Diamond Valley	27	139	Kobeh Valley		39.61	-116.42	881	6,649	12
		140A	Monitor Valley	Northern Part	39.16	-116.63	530	7,385	14
		140B	Monitor Valley	Southern Part	38.76	-116.76	523	7,788	15
		151	Antelope Valley		39.28	-116.29	446	7,129	11
		152	Stevens Basin		39.47	-116.08	20	7,567	17
		153	Diamond Valley		39.82	-115.97	756	6,339	13
				Groundwater flow system subtotals			**3,156**	**7,143**	**13**
Death Valley	28	144	Lida Valley		37.49	-117.31	535	5,571	7
		145	Stonewall Flat		37.63	-116.94	370	5,397	7
		146	Sarcobatus Flat		37.22	-116.98	806	4,843	6
		147	Gold Flat		37.50	-116.50	678	5,749	9
		148	Cactus Flat		37.77	-116.63	382	5,855	8
		157	Kawich Valley		37.49	-116.22	351	6,039	10
		158A	Emigrant Valley	Groom Lake Valley	37.31	-115.87	654	5,385	9
		158B	Emigrant Valley	Papoose Lake Valley	37.08	-115.81	109	4,949	9
		159	Yucca Flat		37.09	-116.08	310	4,779	8
		160	Frenchman Flat		36.85	-115.96	460	4,186	8
		161	Indian Springs Valley		36.69	-115.72	650	4,444	9
		162	Pahrump Valley		36.15	-115.89	1,006	4,090	9
		168	Three Lakes Valley	Northern Part	36.88	-115.43	298	4,433	8
		169A	Tikapoo Valley	Northern Part	37.37	-115.52	615	5,085	10
		169B	Tikapoo Valley	Southern Part	36.98	-115.24	368	4,380	8
		170	Penoyer Valley		37.73	-115.80	698	5,631	9
		173A	Railroad Valley	Southern Part	37.90	-116.09	595	5,896	9
		211	Three Lakes Valley	Southern Part	36.58	-115.49	313	4,391	7
		225	Mercury Valley		36.61	-116.03	108	3,937	8
		226	Rock Valley		36.69	-116.23	86	3,548	6
		227A	Fortymile Canyon	Jackass Flats	36.82	-116.34	283	3,988	6
		227B	Fortymile Canyon	Buckboard Mesa	37.11	-116.34	242	5,763	11
		228	Oasis Valley		37.10	-116.62	467	4,965	9
		229	Crater Flat		36.83	-116.56	183	3,775	6
		230	Amargosa Desert		36.52	-116.49	1,363	3,019	5
		240	Chicago Valley		35.99	-116.14	108	2,617	6
		241	California Valley		35.83	-116.01	139	3,362	7

Table A2-1. Descriptive information for each hydrographic area within the Great Basin carbonate and alluvial aquifer system study area.—Continued

[Latitude and longitude of centroid: geographic coordinate based on NAD83 horizontal datum. Mean altitude: based on NAVD88 vertical datum. Mean annual precipitation: based on PRISM average annual 1971–2000 precipitation (Daly and others, 2008[1]). Abbreviations: mi^2, square miles; ft, feet; in., inches]

Groundwater flow system name	Groundwater flow system number	Hydro-graphic area number	Hydrographic area name	Hydrographic subarea name	Latitude of centroid	Longitude of centroid	Area (mi^2)	Mean altitude (ft)	Mean annual precipitation (in.)
Death Valley—Continued	28	242	Lower Amargosa Valley		35.98	-116.33	466	2,475	6
		243	Death Valley		36.39	-116.99	3,943	2,815	5
		244	Valjean Valley		35.60	-116.06	405	2,152	5
		245	Shadow Valley		35.50	-115.70	371	3,959	7
				Groundwater flow system subtotals			**17,362**	**4,435**	**8**
Newark Valley	29	154	Newark Valley		39.54	-115.67	793	6,518	12
		155A	Little Smoky Valley	Northern Part	39.15	-116.03	590	6,799	10
		155B	Little Smoky Valley	Central Part	38.84	-116.07	63	6,835	9
				Groundwater flow system subtotals			**1,446**	**6,717**	**10**
Railroad Valley	30	150	Little Fish Lake Valley		38.82	-116.43	430	7,518	12
		155C	Little Smoky Valley	Southern Part	38.66	-115.98	502	6,364	8
		156	Hot Creek Valley		38.39	-116.29	1,047	6,412	9
		173B	Railroad Valley	Northern Part	38.64	-115.68	2,141	5,992	10
				Groundwater flow system subtotals			**4,120**	**6,571**	**10**
Independence Valley	32	177	Clover Valley		40.80	-114.97	479	6,239	15
		188	Independence Valley		40.89	-114.72	561	6,176	13
				Groundwater flow system subtotals			**1,040**	**6,208**	**14**
Ruby Valley	33	176	Ruby Valley		40.36	-115.31	1,027	6,627	16
		178A	Butte Valley	Northern Part	40.36	-114.98	273	6,544	13
				Groundwater flow system subtotals			**1,300**	**6,585**	**15**
Colorado	34	164A	Ivanpah Valley	Northern Part	35.75	-115.37	247	3,829	8
		164B	Ivanpah Valley	Southern Part	35.45	-115.38	506	3,789	7
		165	Jean Lake Valley		35.77	-115.25	97	3,384	7
		166	Hidden Valley	South	35.83	-115.16	35	3,333	6
		167	Eldorado Valley		35.75	-114.97	524	2,928	6
		171	Coal Valley		37.93	-115.31	463	5,568	11
		172	Garden Valley		38.06	-115.52	496	6,191	13
		174	Jakes Valley		39.30	-115.28	421	7,018	13
		175	Long Valley		39.76	-115.38	665	6,694	13
		180	Cave Valley		38.57	-114.86	353	6,841	14
		181	Dry Lake Valley		37.96	-114.76	891	5,505	12
		182	Delamar Valley		37.45	-114.88	382	5,278	12
		183	Lake Valley		38.50	-114.57	550	6,531	14
		198	Dry Valley		37.87	-114.22	113	6,061	14
		199	Rose Valley		37.93	-114.24	12	5,789	14
		200	Eagle Valley		37.97	-114.17	54	6,436	16
		201	Spring Valley		38.17	-114.20	285	6,913	16
		202	Patterson Valley		38.09	-114.46	427	6,247	14
		203	Panaca Valley		37.75	-114.43	337	5,514	13
		204	Clover Valley		37.54	-114.29	361	5,803	16
		205	Lower Meadow Valley Wash		37.15	-114.57	975	3,981	11
		206	Kane Springs Valley		37.21	-114.73	234	4,472	12

Table A2-1. Descriptive information for each hydrographic area within the Great Basin carbonate and alluvial aquifer system study area.—Continued

[Latitude and longitude of centroid: geographic coordinate based on NAD83 horizontal datum. Mean altitude: based on NAVD88 vertical datum. Mean annual precipitation: based on PRISM average annual 1971–2000 precipitation (Daly and others, 2008[1]). Abbreviations: mi^2, square miles; ft, feet; in., inches]

Groundwater flow system name	Groundwater flow system number	Hydro-graphic area number	Hydrographic area name	Hydrographic subarea name	Latitude of centroid	Longitude of centroid	Area (mi^2)	Mean altitude (ft)	Mean annual precipitation (in.)
Colorado—Continued	34	207	White River Valley		38.70	-115.15	1,595	6,225	12
		208	Pahroc Valley		37.96	-115.04	515	5,493	11
		209	Pahranagat Valley		37.44	-115.18	768	4,729	10
		210	Coyote Spring Valley		36.90	-114.98	657	3,839	8
		212	Las Vegas Valley		36.24	-115.26	1,537	3,842	8
		215	Black Mountains Area		36.25	-114.66	633	2,026	6
		216	Garnet Valley		36.44	-114.93	157	2,937	7
		217	Hidden Valley	North	36.53	-114.98	77	3,603	8
		218	California Wash		36.51	-114.73	311	2,354	6
		219	Muddy River Springs Area		36.72	-114.78	92	2,519	6
		220	Lower Moapa Valley		36.64	-114.49	253	2,025	6
		221	Tule Desert		37.17	-114.29	184	4,009	12
		222	Virgin River Valley		37.08	-114.11	1,299	3,547	11
						Groundwater flow system subtotals	**16,508**	**4,722**	**11**
Goshute Valley	35	178B	Butte Valley	Southern Part	39.83	-115.09	747	6,780	13
		179	Steptoe Valley		39.62	-114.78	1,958	6,994	12
		187	Goshute Valley		40.68	-114.51	953	6,108	11
						Groundwater flow system subtotals	**3,658**	**6,627**	**12**
Mesquite Valley	36	163	Mesquite Valley		35.81	-115.64	457	3,634	8
						Groundwater flow system subtotals	**457**	**3,634**	**8**
Great Salt Lake Desert	37	184	Spring Valley		39.23	-114.46	1,700	6,771	13
		185	Tippett Valley		39.86	-114.31	347	6,364	11
		186A	Antelope Valley	Southern Part	40.13	-114.30	123	6,232	11
		186B	Antelope Valley	Northern Valley	40.31	-114.40	268	6,160	11
		189A	Thousand Springs Valley	Herrell-Brush Creek	41.40	-114.80	173	6,260	14
		189B	Thousand Springs Valley	Toano-Rock Spring	41.47	-114.51	621	6,021	12
		189C	Thousand Springs Valley	Rocky Butte Area	41.48	-114.34	177	5,875	11
		189D	Thousand Springs Valley	Montello-Crittenden	41.36	-114.18	573	5,690	11
		191	Pilot Creek Valley		40.98	-114.18	329	5,397	11
		251	Grouse Creek Valley		41.61	-113.88	524	5,704	12
		252	Pilot Valley		41.09	-113.93	495	4,732	8
		253	Deep Creek Valley		40.01	-114.04	453	6,214	12
		254	Snake Valley		39.09	-113.95	3,685	6,192	12
		255	Pine Valley		38.44	-113.74	738	6,318	12
		256	Wah Wah Valley		38.55	-113.43	605	5,762	10
		257	Tule Valley		39.31	-113.52	943	5,316	10
		258	Fish Springs Flat		39.78	-113.26	632	4,900	10

Table A2-1. Descriptive information for each hydrographic area within the Great Basin carbonate and alluvial aquifer system study area.—Continued

[Latitude and longitude of centroid: geographic coordinate based on NAD83 horizontal datum. Mean altitude: based on NAVD88 vertical datum. Mean annual precipitation: based on PRISM average annual 1971–2000 precipitation (Daly and others, 2008[1]). Abbreviations: mi^2, square miles; ft, feet; in., inches]

Groundwater flow system name	Groundwater flow system number	Hydro-graphic area number	Hydrographic area name	Hydrographic subarea name	Latitude of centroid	Longitude of centroid	Area (mi^2)	Mean altitude (ft)	Mean annual precipitation (in.)
Great Salt Lake Desert—Continued		259	Dugway-Government Creek Valley		40.02	-112.90	1,171	4,990	11
		260A	Park Valley	West Park Valley	41.53	-113.49	644	4,967	10
		261A	Great Salt Lake Desert	West Part	40.65	-113.57	4,648	4,486	9
				Groundwater flow system subtotals			**18,849**	**5,718**	**11**
Great Salt Lake	38	260B	Park Valley	East Park Valley	41.72	-113.31	502	5,360	12
		261B	Great Salt Lake Desert	East Part	41.26	-113.02	199	4,447	12
		262	Tooele Valley		40.61	-112.43	472	5,159	18
		263	Rush Valley		40.20	-112.38	717	5,924	17
		264	Cedar Valley		40.25	-112.09	316	5,691	17
		265	Utah Valley Area		40.10	-111.64	1,785	6,266	22
		266	Northern Juab Valley		39.74	-111.81	316	6,358	19
		267	Salt Lake Valley		40.66	-111.92	769	5,651	23
		268	East Shore Area		41.15	-112.02	577	4,861	23
		269	West Shore Area		40.94	-112.77	201	4,426	12
		270	Skull Valley		40.47	-112.77	806	5,188	15
		271	Sink Valley		40.93	-112.95	168	4,625	12
		272	Cache Valley		41.90	-111.78	1,889	6,113	26
		273	Malad-Lower Bear River Area		41.91	-112.24	1,252	5,168	20
		274	Pocatello Valley		42.08	-112.49	111	5,532	20
		275	Blue Creek Valley		41.84	-112.46	218	5,150	18
		276	Hansel and North Rozel Flat		41.76	-112.67	234	4,815	15
		277	Promontory Mountains Area		41.50	-112.53	376	4,777	15
		278	Curlew Valley		42.02	-112.87	1,146	5,121	15
		279	Great Salt Lake		41.17	-112.54	1,768	4,222	13
				Groundwater flow system subtotals			**13,823**	**5,243**	**17**
Sevier Lake	39	280	Beryl-Enterprise Area		37.83	-113.61	2,094	5,785	14
		281	Parowan Valley		37.95	-112.73	515	7,080	17
		282	Cedar City Valley		37.77	-113.05	541	6,509	16
		283	Beaver Valley		38.30	-112.63	550	7,298	19
		284	Milford Area		38.43	-113.00	1,294	5,680	12
		285	Leamington Canyon		39.44	-112.02	829	6,023	16
		286	Pavant Valley		38.98	-112.33	683	5,969	17
		287	Sevier Desert		39.28	-112.78	3,969	5,115	11
				Groundwater flow system subtotals			**10,475**	**6,182**	**15**

[1] Daly, C., Halbleib, M., Smith, J.I., Gibson, W.P., Doggett, M.K., Taylor, G.H., Curtis, J., and Pasteris, P.A., 2008, Physiographically-sensitive mapping of temperature and precipitation across the conterminous United States: International Journal of Climatology, doi: 10.1002/joc.1688, accessed January 20, 2009 at http://onlinelibrary.wiley.com/doi/10.1002/joc.1688/pdf.

Appendix 3: Input, Calibration, Uncertainty, and Limitations of the Basin Characterization Model

By Alan L. Flint, Lorraine E. Flint, and Melissa D. Masbruch

An overview of the Basin Characterization Model (BCM) is given in the main text of this report and in Flint, A.L., and Flint, L.E. (2007). Briefly, BCM is a quasi-physical model that simulates the surface-water balance accounting for precipitation, snow accumulation and melt, evapotranspiration, soil moisture, storage, movement, and bedrock saturated hydraulic conductivity to calculate the potential runoff and potential in-place recharge. The model requires spatially distributed data to quantify and simulate each component of the surface-water balance. The flow chart shown in figure A3–1 illustrates the major model components and the relations between components. The following sections describe the input files, model uncertainty, model limitations, and instructions for running the BCM.

Spatially Distributed Input Data

Large scale digital data sets were compiled for the major water-budget components and processes. The sources, resolutions, data components used, and additional processing done on the datasets are described in this section. A digital elevation model (DEM), available as a 30-m resolution DEM (Elevation Derivatives for National Applications, EDNA; http://edna.usgs.gov), was resampled to a 270-m resolution grid. Finer resolution grid dimensions were tested, but required too much computational time for the BCM runs. This grid provides the spatial resolution and extent for the development of all input files that are used to simulate available water for recharge.

Soil properties were extracted from soil maps obtained from the State Soil Geographic Database (STATSGO; http://www.ftw.nrcs.usda.gov/stat_data.html), a state-compiled geospatial database of soil properties that generally are consistent across state boundaries (Soil Conservation Service, 1991). The soil maps for STATSGO are compiled by generalizing more detailed soil survey maps. Mapped soil types are identified in the STATSGO database using a unique map unit identifier (MUID), representing groups of similar soil types. Although the location of a given soil component within a mapped MUID area is not known, the percentage of MUID area covered by each component is defined, and the maximum and minimum thickness of all layers in each component is provided. The database provides soil attributes for each MUID, including porosity, thickness, and percentages of particle sizes for sand, silt, and clay. Soil attributes associated with each MUID were averaged using the combined weight of layer thickness and area for the soil components in each MUID. Soil thickness was obtained directly from STATSGO data for all locations other than where Quaternary basin fill (alluvium) was mapped on geology maps. In locations with alluvium, a total depth of 6 m was chosen on the basis of field observations made in the Mojave Desert of desert plant root penetration into alluvium and bedrock. This assumes that all processes controlling net infiltration occur within the top 6 m of the surficial materials, as shown by Flint and Flint (1995) for Yucca Mountain in the southern Great Basin, and that any water penetrating below 6 m in deep alluvium is recharge. Total soil-water storage capacity was calculated by multiplying soil thickness by soil porosity (Topp and Ferre, 2002). Soil water content at field capacity (-0.01 megapascals (MPa)) and plant wilting point (-6 MPa) were calculated using the average percentage of sand and clay for each MUID and empirical equations from Campbell (1985).

The surficial geologic unit identification is classified broadly for the purpose of assigning saturated hydraulic conductivity values to consolidated surficial bedrock and unconsolidated deposits throughout the region (table A3–1). These geologic units were obtained from geologic maps for each state (California: Jennings, 1977; Idaho: Johnson and Raines, 1996; Nevada: Stewart and others, 2003; Utah: Hintze and others, 2000). The principal geologic units include Quaternary to Tertiary unconsolidated to slightly indurated alluvial, eolian, playa and lacustrine deposits, and volcanic rocks; Mesozoic granitic and other intrusive rocks, sandstone, limestone, and other metasediments, metavolcanic and metamorphic rocks; Paleozoic carbonate and clastic rocks (quartzite, argillite, shale); and Precambrian clastic sedimentary and metamorphic rocks. The surficial geologic units were generalized on the basis of saturated hydraulic conductivity rather than geologic age. The saturated hydraulic conductivity was estimated for each surficial bedrock or unconsolidated surficial unit. Initial saturated hydraulic conductivities were estimated from literature, aquifer-test results, surface-based infiltration experiments, and expert

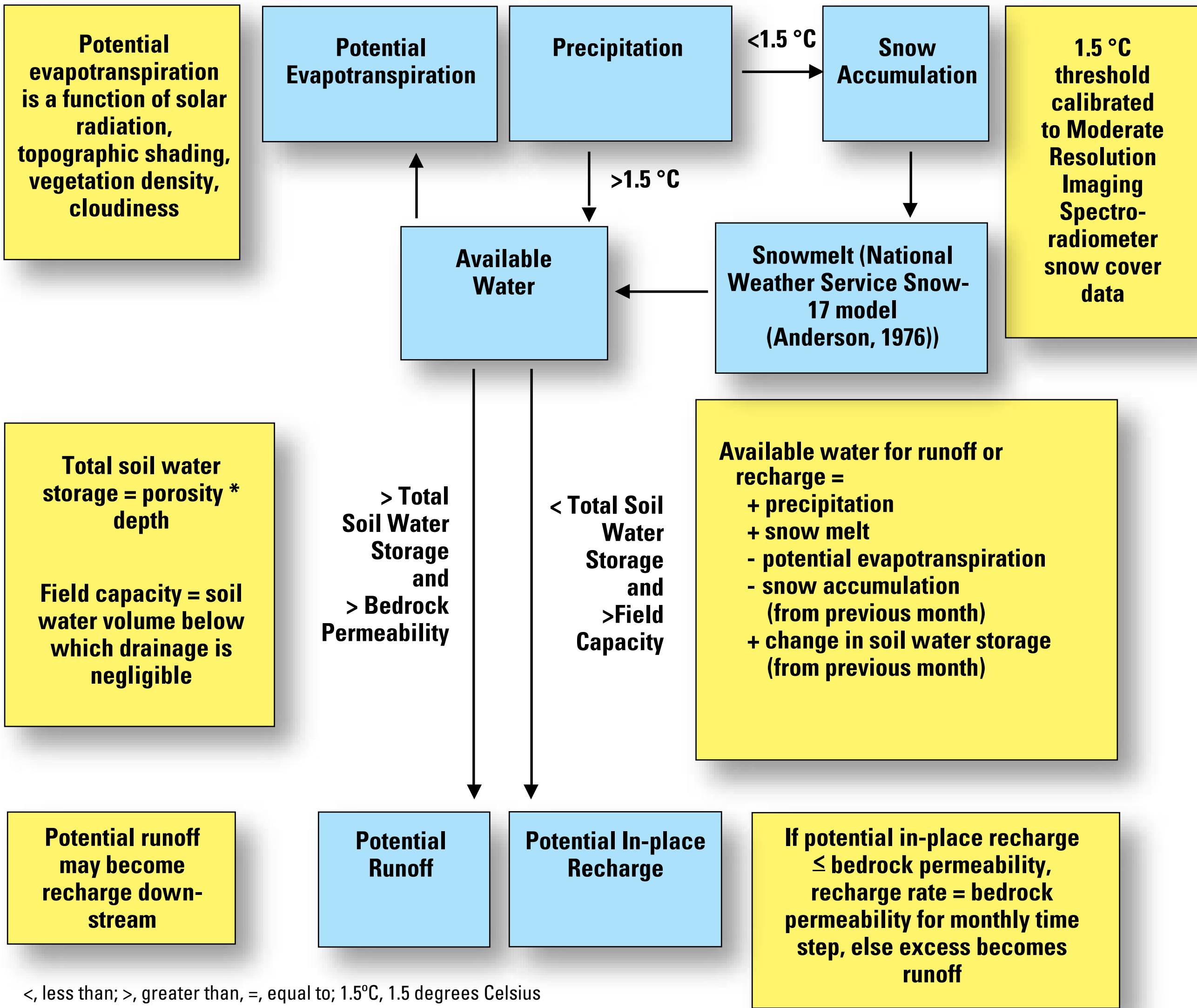

Figure A3–1. Relation of components of the Basin Characterization Model used to calculate potential runoff and in-place recharge at a monthly time step.

opinion from field geologists, and refined during calibration whereby basin runoff estimates were matched to measured streamflow (see "Calibration of Input Data" below). The hydraulic properties of macropores and fractures are incorporated in the bulk estimates of hydraulic conductivity. Hydraulic conductivity estimates of bedrock vary over several orders of magnitude and are uncertain because of the unknown hydraulic properties and spatial distributions of fractures, faults, fault gouge, and shallow infilling materials associated with different bedrock types.

Quaternary basin-fill deposits have the highest saturated hydraulic conductivity in the study area, particularly the eolian deposits and sand and gravel units, whereas finer grained flood-plain deposits, clay-rich lacustrine deposits, and playa deposits generally have the lowest saturated hydraulic conductivity values of the basin-fill deposits. Saturated hydraulic conductivity of surficial bedrock is not equivalent to transmissivity due to surface weathering and infilling of fractures and faults from soils and calcium carbonate development. However, relative estimates among rock types can be derived on the basis of groundwater assessments. Carbonates and sandstones are generally the most permeable of the consolidated rocks (Bedinger and others, 1989), and where fractured and porous have similar permeabilities as the sand and gravel aquifers in the basin fill (Winograd and Thordarson, 1975; Dettinger and others, 2000). Granitic rocks, metamorphic rocks (slates, argillites, marbles, and quartzites), and fine-grained sedimentary rocks (siltstones and shales) typically have very low permeabilities and porosities (Davis and DeWiest, 1966; Freeze and Cherry, 1979). Basalt flows and welded tuffs can be highly permeable and have sufficient porosity to store and transmit large quantities of water

Table A3–1. Surficial bedrock saturated hydraulic conductivity for different geologic units used in the Basin Characterization Model.

[Saturated hydraulic conductivity: ft/d, feet per day, rounded to two significant figures. Abbreviations: ID, identification]

Geologic unit ID	Geologic unit name	Saturated hydraulic conductivity (ft/d)	Percentage of study area
1	Basin fill—ash	1.1E+01	0.000
2	Basin fill—channels	1.1E+01	0.013
3	Basin fill—eolian sand	1.3E+01	0.600
4	Basin fill—glacial till	6.6E-02	0.168
5	Alluvium—gravels	4.5E+00	0.355
6	Alluvium—lake sediments	8.9E-04	8.112
7	Alluvium—landslides	8.2E+00	0.060
8	Alluvium—marshes	1.8E-01	0.522
9	Alluvium—mud and salt flats	9.0E-03	5.770
10	Alluvium—older upland soils	9.0E-01	3.291
11	Alluvium—playas	2.7E-03	1.559
12	Alluvium—valley fill	4.5E+00	38.071
13	Carbonates—dolomite	2.0E-01	2.624
14	Carbonates—Kaibab limestone	2.6E+00	0.287
15	Carbonates—limestone	3.3E-02	6.240
16	Carbonates—travertine	8.9E-04	0.000
17	Chert	3.3E-04	0.558
18	Conglomerate	3.3E-03	4.555
19	Gabbro	8.9E-04	0.000
20	Granite	4.9E-03	1.031
21	Granite—granodiorite	2.0E-02	0.006
22	Granite—mixed	1.6E-03	0.007
23	Granite—quartz monzonite	1.3E-02	0.702
24	Igneous—diabase	9.0E-02	0.027
25	Igneous—dikes and plugs	8.9E-04	0.001
26	Metamorphics—gneiss/schist	1.6E-03	0.862
27	Metamorphics—phyllite	6.6E-03	0.128
28	Metamorphics—serpentinite	3.3E-03	0.001
29	Metasediments	3.3E-02	0.017
30	Metavolcanics	3.3E-04	0.025
31	Quartzite	1.6E-04	1.016
32	Sandstone	1.6E-02	0.483
33	Sandstone—Brushy Basin	9.0E-03	0.004
34	Sandstone—Castle Valle	3.3E-02	0.167
35	Sandstone—Chinle	9.0E-03	0.000
36	Sandstone—Cliff House	2.7E-01	0.000
37	Sandstone—Coconino	1.6E-01	0.000
38	Sandstone—Crazy Hollow	2.7E-01	0.088
39	Sandstone—Dakota	2.7E-01	0.000
40	Sandstone—Moenkopi	4.5E-03	0.150
41	Sandstone—Navajo	1.6E+00	0.595
42	Sandstone—claystone	4.5E-03	0.031
43	Sandstone—fine	3.3E-03	0.795
44	Sandstone—shale	3.3E-04	2.879
45	Sandstone—siltstone	4.5E-03	0.817
46	Sedimentary—shale/limestone	3.3E-01	0.441
47	Sedimentary	4.5E-02	0.000
48	Volcanics—andesites	8.9E-04	0.004
49	Volcanics—andesites (flows and breccias)	1.6E-02	1.366
50	Volcanics—ash-flow tuffs, undifferentiated	6.6E-03	7.750
51	Volcanics—ash-flow tuffs, welded	1.6E-03	1.472
52	Volcanics—ash-flow tuffs, nonwelded	1.6E-02	0.022
53	Volcanics—basalts	2.6E-04	0.392
54	Volcanics—breccias	8.9E-04	0.037
55	Volcanics—lava flows	4.9E-02	3.329
56	Volcanics—pyroclastics	3.3E-03	2.569
57	Volcanics—rhyolites	3.3E-04	0.000

(Glancy, 1986; Winograd and Thordarson, 1975). Typically, volcanic rocks in the desert Southwest are far less porous and permeable than the sand and gravel of the basin fill or the carbonate rocks.

The primary geologic unit exposed at the surface of the GBCAAS study area is alluvium (valley fill), having an estimated saturated hydraulic conductivity of 4.5 ft/d and covering about 38 percent of the study area (table A3–1). Carbonates comprise the second most abundant surficial geologic unit, including both limestone (0.033 ft/d; about 6 percent of study area) and dolomite (0.2 ft/d; about 3 percent of study area). Next are volcanic rocks, including both undifferentiated ash-flow tuffs (0.0066 ft/d; about 8 percent) and welded ash-flow tuffs (0.0016 ft/d; about 1 percent). Other substantial surficial geologic units include alluvium (lake sediments) (0.00089 ft/d; about 8 percent), alluvium (mud and salt flats) (0.009 ft/d; about 6 percent), and conglomerate (0.0033 ft/d, about 5 percent).

Estimated saturated hydraulic-conductivity values used in the BCM range from about 0.00016 ft/d for quartzite to about 13 ft/d for basin fill (eolian sand), but these extremes occur at the surface in only small portions of the GBCAAS study area (table A3–1). Eolian sand covers about 0.6 percent of the study area, primarily in the Great Salt Lake Desert (37) and Sevier Lake (39) groundwater flow systems (fig. B–3). In addition to eolian sand, the highest permeability geologic units include basin-fill ash and channel deposits, both having an estimated hydraulic conductivity of 11 ft/d (table A3–1). The highest hydraulic conductivity values for consolidated rock include the Navajo Sandstone (1.6 ft/d) and the Kaibab

Limestone (2.6 ft/d). The Navajo and Kaibab outcrops in about 6 and 2 percent of the study area, respectively. Both of these permeable bedrock formations are located predominantly in the Great Salt Lake Desert (37), Great Salt Lake (38), and Sevier Lake (39) groundwater flow systems. Low-permeability quartzite outcrops in about 1 percent of the GBCAAS study area. Other low-permeability geologic units include alluvium (lake sediments) (0.00089 ft/d) and shale (0.00033 ft/d), covering about 8 and 3 percent of study area, respectively. These low-permeability formations are primarily located in the Great Salt Lake (38), Great Salt Lake Desert (37), and Sevier Lake (39) groundwater flow systems. Nine of the 57 geologic units in table A3–1 are not present within the GBCAAS study area, but are included in the table, which was generated for the larger areal extent of the BCM model in the western United States.

Temporally Distributed Input Data

Spatially distributed monthly estimates of precipitation, minimum and maximum air temperature, and potential evapotranspiration were used to calculate a surface-water budget and to partition the water available for runoff and in-place recharge on the basis of the spatially distributed estimates of soil-water storage capacity and saturated hydraulic conductivity of the underlying consolidated rock and basin-fill deposits. Locations and quantities of excess water were estimated on a monthly basis. Spatially distributed estimates of monthly precipitation and maximum and minimum monthly air temperatures were approximated using monthly climate data from 1940 to 2006, available at 4,000-m grid spacing (Daly and others, 2008; available from http://www.prism.oregonstate.edu/products/matrix.phtml). The centroids of the grids were used in the downscaling of the data to the 270-m grid by applying a model from Nalder and Wein (1998) that combines a spatial gradient plus inverse-distance squared weighting (GIDS) using multiple regression with northing, easting, and elevation (Flint, L.E., and Flint, A.L, 2007). The long-term record was used in a transient analysis that is conducted to include the effects of antecedent soil moisture and, thus, better reflect the impact of historical climatic trends on hydrologic response.

For this study the Priestley-Taylor equation was used to estimate potential evapotranspiration (PET; Priestley and Taylor, 1972):

$$PET = \alpha \bullet s / (s + \gamma) \bullet (Rn - G) / \lambda \qquad \text{(A1–1)}$$

where

- α is the Priestley-Taylor coefficient and is set to 1.26,
- s is the slope of the vapor deficit curve,
- γ is the psychometric constant,
- Rn is net radiation,
- G is soil heat flux, and
- λ is the latent heat of vaporization.

G is calculated from monthly air temperature using the method of Shuttleworth (1993, equation 4.2.17) and Rn is calculated using the radiation balance equation:

$$Rn = K\downarrow \bullet (1 - a) + L\downarrow + L\uparrow \qquad \text{(A1–2)}$$

where

- $K\downarrow$ is incoming solar radiation, a is surface albedo,
- $L\downarrow$ is incoming long wave radiation, and
- $L\uparrow$ is outgoing long wave radiation.

Incoming solar radiation ($K\downarrow$) is the main energy source for evapotranspiration but it can be reduced or enhanced by the slope and aspect of the site being modeled relative to the sun's elevation and azimuth, determined on an hourly basis. In addition, the solar radiation can be greatly reduced in mountainous terrain by topographic shading (determined by the sun's elevation and azimuth and the elevation of the surrounding topography that will block the sun during the day) (Flint and Childs, 1987). Solar radiation is reduced by atmospheric water vapor, ozone, aerosols, and air molecules, which are accounted for in the solar radiation model of Flint and Childs (1987) and used in this study. Clouds also reduce incoming solar radiation and are estimated for average months using the National Radiation Energy Laboratory (NREL) database from 1960 to 1990 (http://rredc.nrel.gov/solar/old_data/nsrdb/1961-1990/). Albedo (a) is varied monthly and distributed spatially using an inverse-distance squared method and data from Iqbal (1983). Incoming and outgoing long wave radiation (L↓ and L↑) are determined using the Stefan-Boltzmann radiative emission equation:

$$L\downarrow \text{ or } L\uparrow = \varepsilon\, \sigma\, T^4 \qquad \text{(A1–3)}$$

where

- T is air temperature (for L↓) or surface temperature (for L↑), in degrees Kelvin;
- σ is the Stefan-Boltzmann constant; and
- ε is atmospheric emissivity for clear sky for calculating (L↓) and was determined using the equation of Swinbank (1963).

$$\varepsilon = 0.0000092\, T^2 \qquad \text{(A1–4)}$$

where

- T is air temperature for outgoing long wave radiation (L↑), in degrees Kelvin; and
- ε is surface emissivity assumed to be 0.98 for all surfaces.

Clouds have an emissivity of 1, so ε will range from the value calculated by Swinbank (1963) for clear sky to a value of 1 for full cloudy sky, and is proportional between clear sky emissivity and full cloudy sky emissivity based on the percent of clouds. This approach uses the monthly average cloudiness from the NREL cloudiness data base discussed above. Evapotranspiration is assumed to occur at the potential rate until there is no additional water available (the soil reaches wilting point), at which point it is zero.

Soil Water Accounting

Where soils are present, soil thickness, porosity, drainage characteristics, and antecedent (previous month) soil moisture determine how much precipitation and snowmelt is added into the soil zone. If the new calculated soil water content exceeds soil water storage, excess water is allowed to infiltrate into the underlying material at a rate equal to the saturated hydraulic conductivity of the underlying material, assuming a unit vertical hydraulic gradient. If the saturated hydraulic conductivity (ft/day) of the underlying material is less than the excess water (ft) for the month (for the number of days in the month), then the maximum infiltration is calculated as in-place recharge and the excess is calculated as runoff for that month. If the new calculated soil water content does not exceed soil-water storage capacity, but does exceed field capacity, then excess water is allowed to infiltrate at a rate equal to the saturated hydraulic conductivity of the underlying material, with any remaining water allowed to stay in the soil profile until the following month.

Calibration of the Basin Characterization Model

BCM input data and the final BCM results are calibrated or verified in various steps. The solar radiation calculations in the submodel for potential evapotranspiration compared very well to measured average monthly cloud-free data from the Natural Renewable Energy Laboratory for 1960–1990 (http://rredc.nrel.gov/solar/old_data/nsrdb/1961-1990/) and corrections were then added to the submodel to correlate with the average monthly cloudiness data. The resultant potential evapotranspiration was compared with ETo, the calculation for reference crop evapotranspiration, calculated from measured data for the state of California (http://wwwcimis.water.ca.gov/cimis/) and the state of Arizona (http://ag.arizona.edu/azmet/). Simulated monthly potential evapotranspiration using the BCM compares well to monthly ETo from these networks, with slight overestimates in June, July, and August on the order of approximately 10 percent. No ETo data was available for Utah or Nevada, however, estimates of potential evaporation calculated from meteorological data in Nevada compared well with the BCM (Flint and others, 2008), suggesting the detailed calibration in California and Arizona were adequate for the study area.

BCM snow accumulation and snowmelt were compared to Moderate Resolution Imaging Spectroradiometer (MODIS) snowcover remotely sensed data (https://lpdaac.usgs.gov/lpdaac/products/modis_products_table) for visual comparison of snowcover extent, and was adjusted by varying the temperature threshold at which melt occurs (Lundquist and Flint, 2006). Energy and mass balance calculations for snow accumulation and ablation were adapted by Lundquist and Flint (2006) from the operational Snow–17 model (Anderson, 1976; Shamir and Georgakakos, 2005) of the National Weather Service (NWS). Snow–17 is a snowpack energy balance model that uses minimum, maximum, and average air temperature (changing at 6 hour intervals) and an empirical melt factor that varies with day of year to increase or decrease the heat deficit in the snowpack. Once it rises above 0ºC degrees Celsius, snow can melt. The adapted Snow–17 model is applied to every model grid cell so that the spatial distribution, as well as snow water equivalent, is calculated over the modeling domain at each time step. Calibration was performed by varying the air temperature threshold below which precipitation was in the form of snow; this was determined to be 1.5ºC. Sublimation of snow was calculated as a standard rate (5 mm/month), and snowmelt was based on the snowpack energy balance when air temperatures were above freezing. Although snow distribution at maximum snowpack is over- and underestimated to some degree, the calculation of snowmelt reasonably represents snowmelt during the predominant period of runoff. Examples of measured and predicted snowcover for maximum accumulation and snowmelt periods are illustrated in Flint and Flint (2007).

Runoff calibration and recharge calculation by the BCM were done by changing the bedrock saturated hydraulic conductivity values used for the various geologic units. The bedrock saturated hydraulic conductivity values were modified by optimizing the match between modeled runoff and estimated runoff from streamflow records of 67 gages located in 44 hydrographic areas within the study area that have distinct surficial bedrock geology (table A3–2). Estimated runoff was determined by subtracting baseflow (mean annual minimum discharge for period of record) from the total discharge (mean discharge for the period of record) for each gage. Optimizing saturated hydraulic conductivity for each of the geologic units was difficult because: (1) each watershed used in the calibration contained mixed geology, and, thus, the runoff-producing geologic unit listed in table A3–2 was not necessarily the dominant surficial geologic unit within the watershed; instead it was generally the lowest permeability rock type found in the highest precipitation zone (highest altitude); and (or) (2) a geologic unit may occur in more than one watershed used for the calibration, however, the hydraulic conductivity for each geologic unit had to be consistent across the GBCAAS study area. For example, increasing the bedrock permeability from 0.1 to 1 mm/day for volcanic rhyolites results in reductions in simulated BCM runoff of between 170 and 260 percent for four watersheds near Beaver, Utah (Three Creeks, Beaver River, South Creek, and North Fork North Creek). The reduced BCM runoff more closely matched estimated runoff at three stream gages, whereas the reduced BCM runoff was too low for Beaver River. This illustrates the complexity of calibrating the BCM to streamflow measurements when using regional geology maps with multiple geologic units of varying percentages in different basins.

Table A3–2. Comparison of estimated runoff from streamflow records to BCM runoff used for calibration of surficial bedrock saturated hydraulic conductivity.

[Site number, U.S. Geological Survey gaging site number. Latitude and Longitude: in decimal degrees, datum NAD83. Mean annual discharge: for period of record. Baseflow: mean annual minimum discharge for period of record. Estimated runoff: calculated as the difference between mean annual discharge and baseflow. BCM as percent of estimated runoff: BCM runoff divided by estimated runoff. Abbreviations: ID, identification; ft, feet; acre-ft/yr, acre-feet per year]

Stream gage station number	Station name	Hydrographic area number	Dominant runoff-producing geologic unit ID	Dominant runoff-producing geologic unit name
10104700	Little Bear River below Davenport Creek near Avon, Utah	272	12	Alluvium—valley fill
10102300	Summit Creek above diversions near Smithfield, Utah	272	13	Carbonates—dolomite
10109000 and 10108400	Combined flow of Logan River above State Dam and Logan, Hyde Park & Smithfield Canal at head, near Logan, Utah	272	13	Carbonates—dolomite
10145000	Mill Creek at Mueller Park near Bountiful, Utah	268	15	Carbonates—limestone
10166430	West Canyon Creek near Cedar Fort, Utah	264	15	Carbonates—limestone
10172791	Settlement Creek above reservoir near Tooele, Utah	262	15	Carbonates—limestone
10251890	Peak Spring Canyon Creek near Charleston Peak, Nevada	162	15	Carbonates—limestone
10249280	Kingston Creek below Cougar Canyon near Austin, Nevada	137B	17	Chert
10317400	North Fork Humboldt River near North Fork, Nevada	44	17	Chert
10146000	Salt Creek at Nephi, Utah	266	18	Conglomerate
10148400	Nebo Creek near Thistle, Utah	265	18	Conglomerate
10148500	Spanish Fork at Thistle, Utah	265	18	Conglomerate
10219200	Chicken Creek near Levan, Utah	285	18	Conglomerate
10233000	Meadow Creek near Meadow, Utah	286	18	Conglomerate
10233500	Corn Creek near Kanosh, Utah	286	18	Conglomerate
10244720	Franklin River near Arthur, Nevada	176	20	Granite
10244745	Overland Creek near Ruby Valley, Nevada	176	20	Granite
10316500	Lamoille Creek near Lamoille, Nevada	45	20	Granite
10141500	Holmes Creek near Kaysville, Utah	268	26	Metamorphics—gneiss/schist
10142000	Farmington Creek above diversions near Farmington, Utah	268	26	Metamorphics—gneiss/schist
10142500	Ricks Creek above diversions near Centerville, Utah	268	26	Metamorphics—gneiss/schist
10143000	Parrish Creek above diversions near Centerville, Utah	268	26	Metamorphics—gneiss/schist
10143500	Centerville Creek above diversions near Centerville, Utah	268	26	Metamorphics—gneiss/schist
10144000	Stone Creek above diversions near Bountiful, Utah	268	26	Metamorphics—gneiss/schist
10164500	American Fork above Upper Powerplant near American Fork, Utah	265	26	Metamorphics—gneiss/schist
10168500	Big Cottonwood Creek near Salt Lake City, Utah	267	26	Metamorphics—gneiss/schist
10172700	Vernon Creek near Vernon, Utah	263	26	Metamorphics—gneiss/schist
10172870	Trout Creek near Callao, Utah	254	26	Metamorphics—gneiss/schist
10172952	Dunn Creek near Park Valley, Utah	260B	26	Metamorphics—gneiss/schist
10224100	Oak Creek above Little Creek near Oak City, Utah	287	26	Metamorphics—gneiss/schist
10172800	South Willow Creek near Grantsville, Utah	262	31	Quartzite
10172805	North Willow Creek near Grantsville, Utah	262	31	Quartzite
10243240	Baker Creek at Narrows near Baker, Nevada	254	31	Quartzite
10104900	East Fork Little Bear River above reservoir near Avon, Utah	272	43	Sandstone—fine
10105000	East Fork Little Bear River near Avon, Utah	272	43	Sandstone—fine
10148200	Tie Fork near Soldier Summit, Utah	265	43	Sandstone—fine
10242000	Coal Creek near Cedar City, Utah	282	43	Sandstone—fine
9415515	Water Canyon Creek near Preston, Nevada	207	44	Sandstone—shale
10099000	High Creek near Richmond, Utah	272	44	Sandstone—shale
10111700	Blacksmith Fork below Mill Creek near Hyrum, Utah	272	44	Sandstone—shale
10113500	Blacksmith Fork above Utah Power & Light Company's Dam, near Hyrum, Utah	272	44	Sandstone—shale

Table A3–2. Comparison of estimated runoff from streamflow records to BCM runoff used for calibration of surficial bedrock saturated hydraulic conductivity.—Continued

[Site number, U.S. Geological Survey gaging site number. Latitude and Longitude: in decimal degrees, datum NAD83. Mean annual discharge: for period of record. Baseflow: mean annual minimum discharge for period of record. Estimated runoff: calculated as the difference between mean annual discharge and baseflow. BCM as percent of estimated runoff: BCM runoff divided by estimated runoff. Abbreviations: ID, identification; ft, feet; acre-ft/yr, acre-feet per year]

Latitude	Longitude	Altitude (ft)	Number of years	Mean annual discharge (acre-ft/yr)	Baseflow (acre-ft/yr)	Estimated runoff (acre-ft/yr)	BCM runoff (acre-ft/yr)	BCM runoff as percentage of estimated runoff
41.512436	-111.811885	5,020	32	41,543	12,756	28,787	20,956	72.80
41.869374	-111.759110	5,371	18	14,320	2,860	11,460	9,731	84.91
41.744375	-111.784387	4,680	85	178,181	63,897	114,285	53,240	46.59
40.863834	-111.836880	5,240	18	4,660	609	4,050	3,910	96.53
40.405226	-112.100496	5,620	30	2,717	276	2,441	2,180	89.33
40.505500	-112.290502	5,380	10	2,306	435	1,870	1,905	101.85
36.244407	-115.720020	6,900	14	1,417	213	1,204	607	50.36
39.212429	-117.113422	6,480	40	6,548	2,638	3,910	4,058	103.78
41.576072	-115.914956	6,700	16	7,529	218	7,311	3,929	53.74
39.713012	-111.804376	5,280	42	17,891	3,969	13,921	8,346	59.95
39.871624	-111.570196	5,720	10	11,100	3,620	7,481	9,297	124.28
39.999400	-111.499356	5,027	58	64,502	18,682	45,820	38,686	84.43
39.552180	-111.829928	5,540	33	5,698	745	4,953	2,349	47.44
38.891354	-112.327436	5,800	10	5,055	935	4,119	3,689	89.54
38.774134	-112.399659	5,300	10	12,878	3,482	9,396	9,923	105.61
40.821394	-115.135461	6,567	19	8,246	865	7,380	6,571	89.03
40.458262	-115.392550	6,450	13	8,199	699	7,499	3,342	44.56
40.690761	-115.477003	6,240	70	32,638	2,504	30,134	13,388	44.43
41.054944	-111.895218	5,095	16	2,671	986	1,684	2,554	151.64
41.001333	-111.873272	5,100	26	9,669	1,484	8,184	11,814	144.35
40.940223	-111.867438	4,860	16	1,608	339	1,269	2,082	164.10
40.923556	-111.864660	4,600	19	1,139	184	955	1,536	160.77
40.916334	-111.862993	4,680	38	2,149	678	1,471	2,473	168.13
40.894390	-111.845214	5,080	16	2,287	294	1,993	2,810	140.99
40.447730	-111.682147	5,950	62	40,862	8,368	32,494	27,245	83.84
40.618559	-111.781876	4,990	59	50,074	11,440	38,634	39,090	101.18
39.979391	-112.380230	6,200	48	2,712	1,543	1,168	6,051	517.98
39.744108	-113.889994	6,200	40	4,115	909	3,205	1,357	42.33
41.858530	-113.327219	6,250	32	3,936	654	3,283	1,299	39.57
39.356346	-112.232717	6,480	33	2,149	232	1,917	2,690	140.34
40.496331	-112.574403	6,360	43	4,842	1,767	3,076	850	27.63
40.532720	-112.572736	5,960	13	3,996	1,369	2,626	1,170	44.56
38.990780	-114.206661	6,750	15	6,578	687	5,892	6,555	111.27
41.518270	-111.714382	5,390	23	29,043	4,738	24,305	25,240	103.85
41.516603	-111.750773	5,250	12	26,306	6,498	19,809	20,717	104.58
39.949958	-111.216839	6,120	33	4,034	1,140	2,894	3,063	105.82
37.672199	-113.034670	6,000	72	24,791	4,435	20,356	20,721	101.79
38.987720	-114.958350	6,400	11	1,413	532	881	839	95.26
41.977705	-111.745222	5,250	18	24,324	4,847	19,477	13,000	66.74
41.594382	-111.567433	5,545	11	42,586	32,447	10,139	22,250	219.44
41.623545	-111.738829	5,021	87	91,335	44,261	47,074	64,590	137.21

Table A3–2. Comparison of estimated runoff from streamflow records to BCM runoff used for calibration of surficial bedrock saturated hydraulic conductivity.—Continued

[Site number, U.S. Geological Survey gaging site number. Latitude and Longitude: in decimal degrees, datum NAD83. Mean annual discharge: for period of record. Baseflow: mean annual minimum discharge for period of record. Estimated runoff: calculated as the difference between mean annual discharge and baseflow. BCM as percent of estimated runoff: BCM runoff divided by estimated runoff. Abbreviations: ID, identification; ft, feet; acre-ft/yr, acre-feet per year]

Stream gage station number	Station name	Hydrographic area number	Dominant runoff-producing geologic unit ID	Dominant runoff-producing geologic unit name
10172200	Red Butte Creek at Fort Douglas near Salt lake City, Utah	267	44	Sandstone—shale
10241600	Summit Creek near Summit, Utah	281	44	Sandstone—shale
10244950	Steptoe Creek near Ely, Nevada	179	44	Sandstone—shale
10321590	Susie Creek at Carlin, Nevada	51	44	Sandstone—shale
10321950	Maggie Creek at Maggie Creek Canyon near Carlin, Nevada	51	44	Sandstone—shale
10245445	Illipah Creek near Hamilton, Nevada	174	49	Volcanics—andesites (flows and breccias)
10234000	Three Creeks near Beaver, Utah	283	50	Volcanics—ash-flow tuffs
10234500	Beaver River near Beaver, Utah	283	50	Volcanics—ash-flow tuffs
10235000	South Creek near Beaver, Utah	283	50	Volcanics—ash-flow tuffs
10317500	North Fork Humboldt River at Devils Gate near Halleck, Nevada	44	50	Volcanics—ash-flow tuffs
10147500	Payson Creek above diversion near Payson, Utah	265	51	Volcanics—ash-flow tuffs, welded
10245900	Pine Creek near Belmont, Nevada	140B	51	Volcanics—ash-flow tuffs, welded
10245910	Mosquito Creek near Belmont, Nevada	140B	51	Volcanics—ash-flow tuffs, welded
10249300	South Twin River near Round Mountain, Nevada	137B	51	Volcanics—ash-flow tuffs, welded
10325500	Reese River near Ione, Nevada	56	51	Volcanics—ash-flow tuffs, welded
9413900	Beaver Dam Wash near Enterprise, Utah	222	52	Volcanics—ash-flow tuffs, nonwelded
9417500	Meadow Valley Wash at Eagle Canyon near Ursine, Nevada	200	52	Volcanics—ash-flow tuffs, nonwelded
10236000	North Fork North Creek near Beaver, Utah	283	52	Volcanics—ash-flow tuffs, nonwelded
10236500	South Fork North Creek near Beaver, Utah	283	52	Volcanics—ash-flow tuffs, nonwelded
10241400	Little Creek near Paragonah, Utah	281	52	Volcanics—ash-flow tuffs, nonwelded
10241430	Red Creek near Paragonah, Utah	281	52	Volcanics—ash-flow tuffs, nonwelded
10241470	Center Creek above Parowan Creek near Parowan, Utah	281	52	Volcanics—ash-flow tuffs, nonwelded
10245925	Stoneberger Creek near Austin, Nevada	140A	52	Volcanics—ash-flow tuffs, nonwelded
10246846	Lower Currant Creek near Currant, Nevada	173B	57	Volcanics—rhyolites
10246930	Sixmile Creek near Warm Springs, Nevada	156	57	Volcanics—rhyolites
10313400	Marys River below Orange Bridge near Charleston, Nevada	42	57	Volcanics—rhyolites

Table A3-2. Comparison of estimated runoff from streamflow records to BCM runoff used for calibration of surficial bedrock saturated hydraulic conductivity.—Continued

[Site number, U.S. Geological Survey gaging site number. Latitude and Longitude: in decimal degrees, datum NAD83. Mean annual discharge: for period of record. Baseflow: mean annual minimum discharge for period of record. Estimated runoff: calculated as the difference between mean annual discharge and baseflow. BCM as percent of estimated runoff: BCM runoff divided by estimated runoff. Abbreviations: ID, identification; ft, feet; acre-ft/yr, acre-feet per year]

Latitude	Longitude	Altitude (ft)	Number of years	Mean annual discharge (acre-ft/yr)	Baseflow (acre-ft/yr)	Estimated runoff (acre-ft/yr)	BCM runoff (acre-ft/yr)	BCM runoff as percentage of estimated runoff
40.779946	-111.806045	5,400	43	3,056	829	2,227	4,943	221.99
37.786921	-112.916335	6,313	23	3,412	605	2,807	3,061	109.05
39.201539	-114.689161	7,440	40	4,904	2,214	2,690	689	25.61
40.726029	-116.077855	4,910	14	7,367	12	7,355	3,245	44.11
40.803248	-116.200081	5,095	17	17,237	324	16,913	10,368	61.30
39.317764	-115.395058	6,840	11	2,446	1,400	1,046	1,242	118.78
38.294417	-112.428544	8,550	14	7,013	1,195	5,818	3,121	53.64
38.280526	-112.568271	6,200	92	37,691	10,214	27,478	14,359	52.26
38.190249	-112.552437	6,900	11	2,278	192	2,086	1,952	93.58
41.178753	-115.492575	5,370	51	54,889	3,729	51,160	45,668	89.27
39.969400	-111.693816	5,670	15	9,167	2,823	6,344	5,370	84.64
38.794376	-116.854524	7,560	28	3,977	642	3,335	3,348	100.38
38.806043	-116.679520	7,200	27	1,671	182	1,490	1,606	107.82
38.887430	-117.245367	6,400	41	5,086	811	4,275	4,895	114.51
38.857217	-117.475986	7,100	29	8,983	658	8,324	14,836	178.22
37.469975	-114.046646	4,740	15	7,345	229	7,116	6,737	94.68
38.004129	-114.206927	5,670	15	5,697	1,283	4,414	3,208	72.67
38.345527	-112.551604	6,800	11	3,930	592	3,337	2,372	71.06
38.338611	-112.537222	6,800	11	13,012	1,612	11,400	5,764	50.56
37.905530	-112.709107	6,740	21	1,378	194	1,184	177	14.91
37.856920	-112.675773	7,800	10	1,237	496	741	74	10.01
37.793032	-112.816054	6,900	23	4,763	2,358	2,405	2,259	93.94
39.140008	-116.721164	6,880	19	1,219	183	1,036	4,923	475.34
38.847159	-115.367526	6,700	24	2,405	172	2,233	869	38.92
38.573083	-116.314228	—	10	420	6	414	15	3.55
41.549913	-115.306729	5,940	15	34,820	226	34,595	27,880	80.59

Model Uncertainty

Uncertainties in BCM results pertain most significantly to uncertainties in the spatial distribution of input data such as soil type, soil thickness, soil water storage, bedrock saturated hydraulic conductivity, precipitation, and temperature. Although the estimation of bedrock saturated hydraulic conductivity introduces the most uncertainty in the final model results, it is not possible to quantify these uncertainties at a regional level. However, using changes in bedrock saturated hydraulic conductivity to calibrate the model to measured runoff reduces the total model uncertainty.

A thorough uncertainty analysis of the Parameter-elevation Regressions on Independent Slopes Model (PRISM) data used for precipitation in the BCM is available in Daly and others (2008). The authors noted that although the western mountain and desert regions are the most uncertain because of lower data density, monthly mean absolute difference in precipitation in the western U.S. on the basis of cross validation calculations comparing measured and modeled values ranged from 4.7 to 12.6 mm, and monthly air temperature ranged from 0.9 to 1.4ºC for minimum and 0.7 to 0.8ºC for maximum.

A sensitivity analysis to various input parameters was conducted for 1 year. It was determined that a year with above-average precipitation would be more appropriate than an average or below-average year because most recharge occurs during wet years. Water year 1996 was chosen because (1) it was a year of above-normal precipitation for the GBCAAS study area (fig. D–3), and (2) detailed infiltration studies during this year at Yucca Mountain were used in the initial development of the BCM (Flint and others, 2004). The parameters chosen for the sensitivity analysis were temperature, precipitation, soil thickness, and sublimation. The values selected were considered to be within the range of possible error or variation for each tested parameter: minimum and maximum monthly air temperature was increased and decreased by 3ºC; precipitation was increased and decreased by 5 percent; soil thickness was increased and decreased by 10 cm.

Limited sublimation rate data is available for the GBCAAS study area. Recently measured sublimation rates in the Sierra Nevada are as high as 15 mm/month (Alan Flint, U.S. Geological Survey, personal commun., 2009). In another study in central Idaho, sublimation rates of up to 30 mm/month have been measured (Danny Marks, U.S. Department of Agriculture, personal commun., 2009). These rates may be even higher during high wind events or during late spring as temperatures begin to warm significantly. Because sublimation is partially dependent on PET, the monthly sublimation rate for the BCM sensitivity analysis was varied by assigning a percentage of the PET rate as the sublimation rate versus the baseline simulation of using a flat rate of 5 mm/month across the entire study area. Percentages of PET tested in the sensitivity analysis ranged from 10 to 50 percent. Average monthly sublimation rates for each of the 17 groundwater flow systems using 10 percent of PET ranged from 8 to 12 mm/month; average monthly sublimation rates using 50 percent of PET ranged from 37 to 59 mm/month.

The results of the sensitivity analysis show that, for the majority of the 17 groundwater flow systems, in-place recharge is generally most sensitive to increased sublimation and increased temperature (fig. A3–2). The increase in sublimation rates to 50 percent of PET resulted in a reduced recharge of between 48 and 90 percent of the baseline simulation. Decreasing sublimation rates to 10 percent of PET resulted in an increase in recharge of between 102 and 137 percent of the baseline simulation. Increasing the monthly minimum and maximum temperature by 3ºC generally resulted in a reduced recharge of between 27 and 96 percent of the baseline simulation, except for four groundwater flow systems (Humboldt, Independence Valley, Ruby Valley, and Goshute Valley), where recharge increased to between 102 and 120 percent of baseline. Although the model was generally least sensitive to decreasing the monthly minimum and maximum temperature by 3ºC, two groundwater flow systems (Death Valley and Mesquite Valley) show substantial increases of 166 and 243 percent of baseline recharge. Decreasing the precipitation by 5 percent resulted in a reduced recharge of of between 72 and 94 percent of baseline. Increasing the precipitation by 5 percent resulted in an increased recharge of between 106 and 130 percent of baseline. Decreasing soil thickness by 10 cm generally resulted in an increased recharge of as much as 172 percent of baseline, while increasing soil thickness by 10 cm modified the recharge to between 44 and 102 percent of baseline. The variations shown by these sensitivity analyses reflect the uncertainties in the input data sets and the necessary simplification of physical processes for the BCM. Individual in-place recharge quantities for the 17 groundwater flow systems generally vary between 50 and 150 percent of the baseline simulation for the 1996 water year (fig. A3–2). This indicates a possible uncertainty in BCM-estimated in-place recharge of about ± 50 percent for the entire GBCAAS study area.

Another evaluation of uncertainty in the BCM in-place recharge estimates was a comparison to the estimated baseflow of 52 gaged perennial mountain streams. Because each of these streams originates within the watershed (no transbasin diversions), it is assumed this baseflow is entirely supported by in-place recharge in the same watershed. Estimated mountain-stream baseflow was calculated for each gaged stream, as described in "Discharge to Mountain Streams" (Chapter D). This analysis showed that 42 of the 52 watersheds with gaged streams had estimated baseflow that was less than or within 50 percent of BCM in-place recharge, indicating that there was sufficient BCM in-place recharge to support these perennial streams.

Mountain-stream baseflow for the remaining 10 watersheds was more than 50 percent greater than BCM in-place recharge. Most of these 10 watersheds are underlain by low permeability geologic units (metamorphic rocks and quartzite), indicating that the BCM may underestimate in-place recharge for these watersheds. These low permeability geologic units are generally fractured and the BCM may be underestimating hydraulic conductivity and overestimating runoff, resulting in insufficient in-place recharge to support

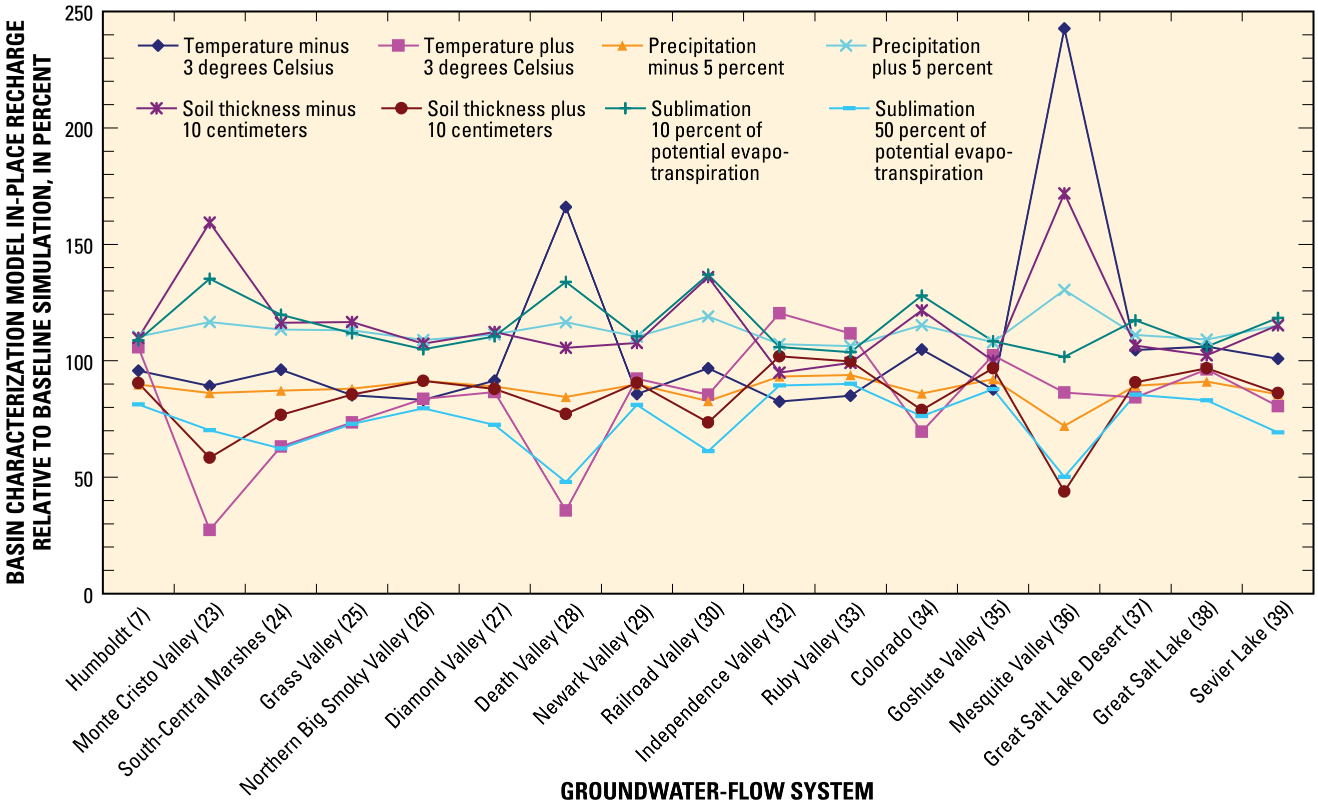

Figure A3–2. Comparison of Basin Characterization Model water year 1996 sensitivity analyses to the baseline simulation (100 percent) for the 17 groundwater flow systems within the Great Basin carbonate and alluvial aquifer system study area.

the observed mountain-stream baseflow. Another possible explanation is that the groundwater catchments for these watersheds may be larger than the surface-water catchments; therefore, the calculated volume of in-place recharge for these watersheds would have been too low.

Model Limitations

One important limitation to the BCM is that the calculation of groundwater recharge assumes that water draining past the root zone becomes recharge within that monthly time step, without consideration of the potential for extended periods of groundwater travel time in the unsaturated zone, which, in the arid and semiarid southwest may be as thick as 500 m. Calculations of groundwater travel time in the southern Great Basin have exceeded 10,000 years (Flint and others, 2000) because of low infiltration rates and unsaturated zone thicknesses exceeding 2,000 m. However, some locations in mountainous areas have shallow unsaturated zones and may recharge to local groundwater within the monthly time step. Another limitation is the use of the 1:500,000-scale geologic maps as the basis for the surficial bedrock saturated hydraulic conductivity input data. Local-scale geology is not represented in any detail at this scale and polygon areas often represent more than one rock type. This introduces error in the recharge calculations, particularly in the mountain block where the majority of in-place recharge and runoff generation occurs.

Instructions for Running the Basin Characterization Model

The BCM is run using a Fortran code, control file, and input files representing potential evapotranspiration, spatially distributed properties of soils and geologic units, and monthly files of spatially distributed climate parameters. All input files are in ASCII format and have been developed to exactly match the extent and grid size of the 270-m DEM. The BCM control file (fig. A3–3) includes input and output file names, saturated hydraulic conductivity corresponding to a surficial geologic unit identification (ID) for each of 57 bedrock geologic types, and period of time for which the model will be run. Input files are ASCII files of soil thickness, soil porosity, soil water content at wilting point and field capacity, surficial geologic unit ID, along with monthly files of precipitation, maximum and minimum air temperature, and potential evapotranspiration.

The Fortran code contains the input and output routines (I/O) to keep track of all the data for each grid cell, including snowpack and soil water storage for the preceding month. Within the Fortran code is the NWS Snow–17 model, which uses the minimum and maximum air temperature and precipitation to accumulate and melt snow that then becomes available for infiltration. Subbasins can be identified by the user and input as ASCII grid files to obtain subbasin statistics of input and output for simple analysis (that is, monthly averages of precipitation, snow, air temperature, runoff, recharge, etc.) The same values can be obtained using the monthly output ASCII grid files and zonal statistics in ArcMap or other user-written codes. Output files include monthly calculations of snow pack, snowmelt, sublimation, soil water stored, excess water (precipitation minus potential evapotranspiration), available water (precipitation minus potential evapotranspiration minus soil water storage at field capacity), potential in-place recharge (precipitation minus potential evapotranspiration minus soil water storage at field capacity plus snowmelt minus snow accumulation, and if recharge is greater than bedrock saturated hydraulic conductivity, recharge is equal to bedrock saturated hydraulic conductivity), and potential runoff (precipitation minus potential evaporation minus porosity plus snowmelt minus snow accumulation plus excess recharge if bedrock saturated hydraulic conductivity is exceeded). The potential in-place recharge and potential runoff are the two monthly files used for most applications.

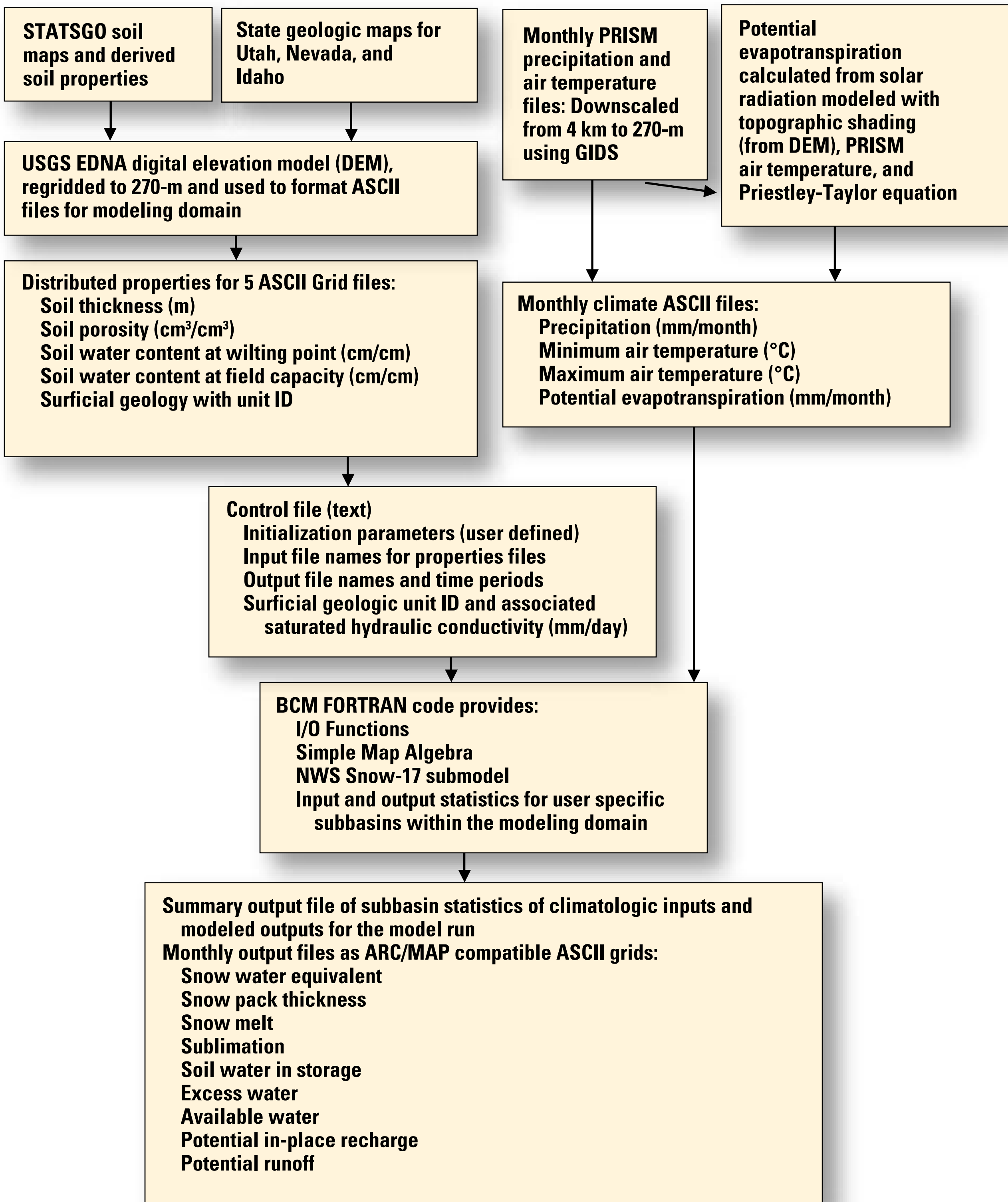

Definitions

BCM = Basin Characterization Model; DEM = Digital Elevation Model; EDNA = Elevation Derivatives for National Applications
GIDS = gradient plus inverse distance squared weighting; ID = identification; I/O = input/output; NWS = National Weather Service
PRISM = Parameter elevation Regressions on Independent Slopes Model; STATSGO = State Soil Geographic Database; m = meter; cm = centimeter; mm = millimeter; km = kilometer; °C = degrees Celsius

Figure A3–3. Flow chart of input files required for operation of the Basin Characterization Model and optional output files resulting from simulations.

References Cited

Anderson, E.A., 1976, A point energy and mass balance model of a snow cover: Silver Spring, Maryland: National Oceanographic and Atmospheric Administration Technical Report NWS 19, 150 p.

Bedinger, M.S., Langer, W.H., and Reed, J.E., 1989, Groundwater hydrology, *in* Bedinger, M.S., Sargent, K.A., and Langer, W.H., eds., Studies of geology and hydrology in the Basin and Range Province, Southwestern United States, for isolation of high-level radioactive waste—Characterization of the Death Valley region, Nevada and California: U.S. Geological Survey Professional Paper 1370–F, p. 28–35.

Campbell, G.S., 1985, Soil physics with BASIC: Transport models for soil plant systems: Amsterdam, Elsevier, Developments in Soil Science, no. 14, 150 p.

Daly, C., Halbleib, M., Smith, J.I., Gibson, W.P., Doggett, M.K., Taylor, G.H., Curtis, J., and Pasteris, P.A., 2008, Physiographically-sensitive mapping of temperature and precipitation across the conterminous United States: International Journal of Climatology, vol. 28, no. 15, p. 2,031–2,064, doi: 10.1002/joc.1688, accessed Januray 20, 2009 at http://onlinelibrary.wiley.com/doi/10.1002/joc.1688/pdf.

Davis, S.N., and DeWiest, R.J.M., 1966, Hydrogeology: New York, John Wiley, 463 p.

Dettinger, M.D., Cayan, D.R., McCabe, G.J., and Marengo, J.A., 2000, Multiscale streamflow variability associated with El Niño/Southern Oscillation, *in* Diaz, H.F. and Markgraf, V., eds., El Niño and the Southern Oscillation, multiscale variability and global and regional impacts: Cambridge, Cambridge University Press, p. 113–147.

Flint, A.L., and Childs, S.W., 1987, Calculation of solar radiation in mountainous terrain: Journal of Agricultural and Forest Meteorology, v. 40, p. 233–249.

Flint, A.L., and Flint, L.E., 2007, Application of the basin characterization model to estimate in-place recharge and runoff potential in the Basin and Range carbonate-rock aquifer system, White Pine County, Nevada, and adjacent areas in Nevada and Utah: U.S. Geological Survey Scientific Investigations Report 2007–5099, 20 p.

Flint, A.L., Flint, L.E., Hevesi, J.A., and Blainey, J.M., 2004, Fundamental concepts of recharge in the Desert Southwest: a regional modeling perspective, *in* Hogan, J.F., Phillips, F.M., and Scanlon, B.R., eds., Groundwater recharge in a desert environment: The Southwestern United States: American Geophysical Union, Water Science and Applications Series, v. 9, p. 159–184.

Flint, A.L., Flint, L.E., Hevesi, J.A., D'Agnese, F.A., and Faunt, C.C., 2000, Estimation of regional recharge and travel time through the unsaturated zone in arid climates, *in* Faybishenko, B., Witherspoon, P., and Benson, S., eds., Dynamics of fluids in fractured rock: American Geophysical Union, Geophysical Monograph, v. 122, p. 115–128.

Flint, A.L., Flint, L.E., and Huntington, J.L., 2008, Regional evaluation of changes in potential evapotranspiration under a changing climate and influences on recharge and runoff, *in* International Conference on Computation Methods in Water Resources, 17th, July 2008, San Francisco, California, Proceedings.

Flint, L.E., and Flint, A.L., 1995, Shallow infiltration processes at Yucca Mountain—Neutron logging data 1984–93: U.S. Geological Survey Water-Resources Investigations Report 95–4035, 46 p.

Flint, L.E., and Flint, A.L., 2007, Estimation of hourly stream temperatures in unmeasured tributaries to the Lower Klamath River, California: Journal of Environmental Quality, v. 37, p. 57–68.

Freeze, R.A., and Cherry, J.A., 1979, Groundwater: Englewood Cliffs, New Jersey, Prentice-Hall, 604 p.

Glancy, P.A., 1986, Geohydrology of the basalt and unconsolidated sedimentary aquifers in the Fallon area, Churchill County, Nevada: U.S. Geological Survey Water Supply Paper 2263, 62 p.

Hintze, L.F., Willis, G.C., Laes, D., Sprinkel, D.A., and Brown, K.D., 2000, Digital geologic map of Utah: Utah Geological Survey Map 179DM, scale 1:500,000.

Iqbal, M., 1983, An introduction to solar radiation: Academic Press, 309 p.

Jennings, C.W., 1977, Geologic map of California: California Division of Mines and Geology Geologic Data Map no. 2, 1 sheet, scale 1:750,000.

Johnson, B.R., and Raines, G.L., 1996, Digital representation of the Idaho state geologic map, a contribution to the Interior Columbia Basin Ecosystem Management Project: U.S. Geological Survey Open-File Report 95–690, 24 p.

Lundquist, J.D., and Flint, A.L., 2006, 2004 onset of snowmelt and streamflow: How shading and the solar equinox may affect spring runoff timing in a warmer world: Journal of Hydrometeorology, v. 7, p. 1,199–1,217.

Nalder, I.A., and Wein, R.W., 1998, Spatial interpolation of climatic normals: Test of a new method in the Canadian boreal forest: Journal of Agricultural and Forest Meteorology, v. 92, no. 4, p. 211–225.

Priestley, C.H.B., and Taylor, R.J., 1972, On the assessment of surface heat flux and evaporation using large-scale parameters: Monthly Weather Review, v. 100, p. 81–92.

Shamir, E., and Georgakakos, K.P., 2005, Distributed snow accumulation and ablation modeling in the American River Basin: Advances in Water Resources, v. 29, no. 4, p. 558–570.

Shuttleworth, W.J., 1993, Evaporation, chap. 4 *of* Maidment, D.R. ed., Handbook of hydrology: New York, McGraw-Hill, p. 4.1–4.53.

Stewart, J.H., Carlson, J.E., Raines, G.L., Connors, K.A., Moyer, L.A., and Miller, R.J., 2003, Spatial digital database for the geologic map of Nevada: U.S. Geological Survey Open-File Report 03–66, version 3.0, 32 p.

Swinbank, W.C., 1963, Long-wave radiation from clear skies: Quarterly Journal of the Royal Meteorological Society, v. 89, p. 339–348.

Topp, G.C., and Ferre, P.A., 2002, Water content, *in* Dane, J.H., and Topp, G.C., eds., Methods of soil analysis, pt. 4, Physical methods: Soil Science Society of America Book Series 5, p. 417–419.

Soil Conservation Service, 1991, State soil geographic data base (STATSGO), data users guide: Washington, D.C., Soil Conservation Service, Miscellaneous Publication 1492, 88 p.

Winograd, I.J., and Thordarson, W., 1975, Hydrogeologic and hydrochemical framework, south-central Great Basin, Nevada-California, with special reference to the Nevada Test Site: U.S. Geological Survey Professional Paper 712–C, 126 p.

Appendix 4: Current Study Groundwater Recharge Estimates for Predevelopment Conditions and Ranges of Previously Reported Estimates of Groundwater Recharge for Each Hydrographic Area within the Great Basin Carbonate and Alluvial Aquifer System Study Area

By Melissa D. Masbruch

Table A4–1. Current study groundwater recharge estimates for predevelopment conditions and ranges of previously reported estimates of groundwater recharge for each hydrographic area within the Great Basin carbonate and alluvial aquifer system study area.

[All values in acre-feet per year rounded to two significant figures. Estimated error in all current study values is ±50 percent. Previously reported total groundwater recharge minimum and maximum: totals adjusted to exclude reported recharge by subsurface inflow (unadjusted estimates are presented in Auxiliary 3G). Abbreviations: HA, hydrographic area; #, number; —, no estimate]

HA #	HA name	Current study groundwater recharge estimates					Previously reported estimates	
		In-place recharge	Runoff	Mountain stream baseflow	Imported surface water	Total groundwater recharge	Total groundwater recharge (minimum)	Total groundwater recharge (maximum)
	Flow System 7: Humboldt System							
42	Marys River Area	31,000	20,000	120	—	51,000	48,000	73,000
43	Starr Valley Area	18,000	24,000	390	—	42,000	26,000	98,000
44	North Fork Area	30,000	15,000	630	—	46,000	56,000	71,000
45	Lamoille Valley	5,900	9,900	1,100	—	17,000	29,000	65,000
46	South Fork Area	8,700	4,200	0	—	13,000	3,300	52,000
47	Huntington Valley	45,000	2,500	0	—	48,000	14,000	180,000
48	Tenmile Creek Area	5,800	2,300	3	20,000	28,000	12,000	18,000
49	Elko Segment	2,900	730	0	—	3,600	7,400	9,500
50	Susie Creek Area	5,200	900	22	—	6,100	6,400	8,000
51	Maggie Creek Area	6,100	2,900	15	—	9,000	12,000	17,000
52	Marys Creek Area	310	180	750	—	1,200	300	1,500
53	Pine Valley	20,000	6,300	0	—	26,000	22,000	66,000
54	Crescent Valley	5,400	880	0	—	6,300	13,000	19,000
55	Carico Lake Valley	4,600	570	0	—	5,200	2,800	20,000
56	Upper Reese River Valley	29,000	21,000	1,300	—	51,000	24,000	91,000
59	Lower Reese River Valley	3,600	1,000	0	—	4,600	10,000	14,000
60	Whirlwind Valley	47	58	0	—	100	1,700	2,000
61	Boulder Flat	1,900	1,300	0	—	3,200	5,200	14,000
62	Rock Creek Valley	1,500	510	[1]110	—	2,100	6,900	9,800
63	Willow Creek Valley	12,000	780	See footnote 1	—	13,000	12,000	15,000
	Flow System 23: Monte Cristo Valley							
136	Monte Cristo Valley	1,200	63	0	—	1,300	400	3,300

Table A4–1. Current study groundwater-recharge estimates for predevelopment conditions and ranges of previously reported estimates of groundwater recharge for each hydrographic area within the Great Basin carbonate and alluvial aquifer system study area.—Continued

[All values in acre-feet per year rounded to two significant figures. Estimated error in all current study values is ±50 percent. Previously reported total groundwater recharge minimum and maximum: totals adjusted to exclude reported recharge by subsurface inflow (unadjusted estimates are presented in Auxiliary 3G). Abbreviations: HA, hydrographic area; #, number; —, no estimate]

HA #	HA name	Current study groundwater recharge estimates					Previously reported estimates	
		In-place recharge	Runoff	Mountain stream baseflow	Imported surface water	Total groundwater recharge	Total groundwater recharge (minimum)	Total groundwater recharge (maximum)
Flow System 24: South-Central Marshes								
117	Fish Lake Valley	22,000	2,000	0	—	24,000	6,100	33,000
118	Columbus Salt Marsh Valley	1,400	74	0	—	1,500	600	3,500
137A	Big Smoky Valley-Tonopah Flat	10,000	1,400	0	—	11,000	12,000	23,000
141	Ralston Valley	7,600	750	0	—	8,400	3,200	25,000
142	Alkali Spring Valley	1,100	45	0	—	1,100	100	1,800
143	Clayton Valley	3,500	100	0	—	3,600	1,500	7,800
149	Stone Cabin Valley	4,600	370	4.6	—	5,000	3,200	28,000
Flow System 25: Grass Valley								
138	Grass Valley	16,000	1,400	0	—	17,000	9,100	31,000
Flow System 26: Northern Big Smoky Valley								
137B	Northern Big Smoky Valley	58,000	28,000	1,400	—	87,000	52,000	78,000
Flow System 27: Diamond Valley System								
139	Kobeh Valley	18,000	550	0	—	19,000	11,000	39,000
140A	Monitor Valley-Northern Part	32,000	2,000	33	—	34,000	6,300	37,000
140B	Monitor Valley-Southern Part	16,000	11,000	360	—	27,000	15,000	47,000
151	Antelope Valley	5,700	190	0	—	5,900	4,100	29,000
152	Stevens Basin	1,400	7.1	0	—	1,400	200	1,000
153	Diamond Valley	21,000	1,600	0	—	23,000	5,900	30,000
Flow System 28: Death Valley System								
Amargosa/Death Valley Subarea								
144	Lida Valley	1,100	44	0	—	1,100	500	5,900
145	Stonewall Flat	1,300	29	0	—	1,300	100	3,800
146	Sarcobatus Flat	2,200	130	0	—	2,300	1,200	6,400
147	Gold Flat	10,000	530	0	—	11,000	2,800	9,300
148	Cactus Flat	1,000	47	0	—	1,000	500	4,600
157	Kawich Valley	5,100	420	0	—	5,500	2,200	6,800
158A	Emigrant Valley-Groom Lake Valley	4,500	300	0	—	4,800	2,200	8,400
158B	Emigrant Valley-Papoose Lake Valley	250	16	0	—	270	4	1,200
159	Yucca Flat	1,700	130	0	—	1,800	600	4,000
160	Frenchman Flat	1,600	19	0	—	1,600	0	5,200
161	Indian Springs Valley	4,300	110	0	—	4,400	3,100	10,000
168	Three Lakes Valley-Northern Part	1,300	32	0	—	1,300	700	3,900
169A	Tikapoo Valley-Northern Part	4,800	78	0	—	4,900	1,900	8,000
169B	Tikapoo Valley-Southern Part	2,000	5.5	0	—	2,000	1,300	5,000
170	Penoyer Valley	5,500	220	0	—	5,700	4,000	14,000
173A	Railroad Valley-Southern Part	3,800	160	0	—	4,000	5,500	8,200
211	Three Lakes Valley-Southern Part	2,500	39	0	—	2,500	4,400	8,700
225	Mercury Valley	140	25	0	—	160	200	1,300
226	Rock Valley	72	2.7	0	—	75	0	900
227A	Fortymile Canyon-Jackass Flats	1,000	66	0	—	1,100	200	2,400

Table A4–1. Current study groundwater-recharge estimates for predevelopment conditions and ranges of previously reported estimates of groundwater recharge for each hydrographic area within the Great Basin carbonate and alluvial aquifer system study area.—Continued

[All values in acre-feet per year rounded to two significant figures. Estimated error in all current study values is ±50 percent. Previously reported total groundwater recharge minimum and maximum: totals adjusted to exclude reported recharge by subsurface inflow (unadjusted estimates are presented in Auxiliary 3G). Abbreviations: HA, hydrographic area; #, number; —, no estimate]

HA #	HA name	Current study groundwater recharge estimates					Previously reported estimates	
		In-place recharge	Runoff	Mountain stream baseflow	Imported surface water	Total groundwater recharge	Total groundwater recharge (minimum)	Total groundwater recharge (maximum)
Flow System 28: Death Valley System—Continued								
Amargosa/Death Valley Subarea—Continued								
227B	Fortymile Canyon-Buckboard Mesa	6,600	420	0	—	7,000	1,100	6,600
228	Oasis Valley	8,400	310	0	—	8,700	250	7,400
229	Crater Flat	320	9	0	—	330	100	2,100
230	Amargosa Desert	600	32	0	—	630	300	27,000
243	Death Valley	10,000	170	0	—	10,000	—	—
Pahrump Valley Subarea								
162	Pahrump Valley	20,000	680	28	—	21,000	17,000	25,000
240	Chicago Valley	150	0.44	0	—	150	—	—
241	California Valley	440	4.3	0	—	440	—	—
242	Lower Amargosa Valley	330	1.4	0	—	330	—	—
244	Valjean Valley	340	4.8	0	—	340	—	—
245	Shadow Valley	830	6.3	0	—	840	—	—
Flow System 29: Newark Valley System								
154	Newark Valley	25,000	1,300	0	—	26,000	13,000	48,000
155A	Little Smoky Valley-Northern Part	7,500	160	0	—	7,700	3,100	23,000
155B	Little Smoky Valley-Central Part	440	17	0	—	460	200	1,400
Flow System 30: Railroad Valley System								
150	Little Fish Lake Valley	3,800	340	0	—	4,100	7,400	37,000
155C	Little Smoky Valley-Southern Part	1,800	68	0	—	1,900	1,400	12,000
156	Hot Creek Valley	4,400	330	4.9	—	4,700	4,800	28,000
173B	Railroad Valley-Northern Part	55,000	2,200	55	—	57,000	35,000	61,000
Flow System 32: Independence Valley System								
177	Clover Valley	10,000	1,800	0	—	12,000	21,000	60,000
188	Independence Valley	16,000	680	0	—	17,000	9,300	50,000
Flow System 33: Ruby Valley System								
176	Ruby Valley	54,000	13,000	750	—	68,000	57,000	160,000
178A	Butte Valley-Northern Part	10,000	560	0	—	11,000	3,000	14,000
Flow System 34: Colorado System								
Lake Mead Subarea								
164A	Ivanpah Valley-Northern Part	1,300	15.0	0	—	1,300	700	1,900
164B	Ivanpah Valley-Southern Part	1,400	45	0	—	1,400	300	7,900
165	Jean Lake Valley	59	5.4	0	—	64	100	1,100
166	Hidden Valley (South)	3.4	2.4	0	—	6	0	400
167	Eldorado Valley	420	30	0	—	450	700	6,400
212	Las Vegas Valley	27,000	500	0	—	28,000	1,600	30,000
215	Black Mountains Area	640	7.9	0	—	650	70	6,900
Muddy River Subarea								
171	Coal Valley	2,200	140	0	—	2,300	2,000	7,800
172	Garden Valley	6,400	210	0	—	6,600	6,100	19,000

Table A4–1. Current study groundwater-recharge estimates for predevelopment conditions and ranges of previously reported estimates of groundwater recharge for each hydrographic area within the Great Basin carbonate and alluvial aquifer system study area.—Continued

[All values in acre-feet per year rounded to two significant figures. Estimated error in all current study values is ±50 percent. Previously reported total groundwater recharge minimum and maximum: totals adjusted to exclude reported recharge by subsurface inflow (unadjusted estimates are presented in Auxiliary 3G). Abbreviations: HA, hydrographic area; #, number; —, no estimate]

HA #	HA name	Current study groundwater recharge estimates					Previously reported estimates	
		In-place recharge	Runoff	Mountain stream baseflow	Imported surface water	Total groundwater recharge	Total groundwater recharge (minimum)	Total groundwater recharge (maximum)
Flow System 34: Colorado System—Continued								
Muddy River Subarea—Continued								
181	Dry Lake Valley	8,700	190	0	—	8,900	4,300	20,000
182	Delamar Valley	4,100	230	0	—	4,300	1,000	10,000
183	Lake Valley	7,000	260	0	—	7,300	8,700	41,000
198	Dry Valley	1,700	49	0	—	1,700	1,300	4,400
199	Rose Valley	81	1.3	0	—	82	100	400
200	Eagle Valley	1,000	15	0	—	1,000	1,100	5,300
201	Spring Valley	7,800	100	0	—	7,900	2,600	16,000
202	Patterson Valley	5,200	200	0	—	5,400	3,000	16,000
203	Panaca Valley	2,900	110	0	—	3,000	1,500	10,000
204	Clover Valley	7,300	840	0	—	8,100	1,700	14,000
205	Lower Meadow Valley Wash	11,000	520	0	—	12,000	1,300	23,000
206	Kane Springs Valley	2,400	210	0	—	2,600	500	7,000
208	Pahroc Valley	4,100	90	0	—	4,200	1,800	45,000
209	Pahranagat Valley	3,800	44	0	—	3,800	1,200	10,000
210	Coyote Spring Valley	2,500	38	0	—	2,500	500	37,000
216	Garnet Valley	160	1.7	0	—	160	0	2,000
217	Hidden Valley (North)	130	0.17	0	—	130	0	1,000
218	California Wash	140	0.38	0	—	140	0	3,500
219	Muddy River Springs Area	120	0.19	0	—	120	0	500
220	Lower Moapa Valley	67	0.46	0	—	67	0	2,600
White River Valley Subarea								
174	Jakes Valley	14,000	830	190	—	15,000	9,200	38,000
175	Long Valley	30,000	1,100	0	—	31,000	5,000	48,000
180	Cave Valley	14,000	610	0	—	15,000	7,600	22,000
207	White River Valley	34,000	2,000	120	—	36,000	35,000	62,000
Virgin River Valley Subarea								
221	Tule Desert	4,200	43	0	—	4,200	200	5,900
222	Virgin River Valley	33,000	1,200	57	—	34,000	3,200	16,000
Flow System 35: Goshute Valley System								
178B	Butte Valley-Southern Part	20,000	880	0	—	21,000	14,000	35,000
179	Steptoe Valley	82,000	3,800	360	—	86,000	45,000	150,000
187	Goshute Valley	19,000	820	0	—	20,000	10,000	41,000
Flow System 36: Mesquite Valley								
163	Mesquite Valley	1,900	14	0	—	1,900	1,000	5,500

Table A4–1. Current study groundwater-recharge estimates for predevelopment conditions and ranges of previously reported estimates of groundwater recharge for each hydrographic area within the Great Basin carbonate and alluvial aquifer system study area.—Continued

[All values in acre-feet per year rounded to two significant figures. Estimated error in all current study values is ±50 percent. Previously reported total groundwater recharge minimum and maximum: totals adjusted to exclude reported recharge by subsurface inflow (unadjusted estimates are presented in Auxiliary 3G). Abbreviations: HA, hydrographic area; #, number; —, no estimate]

HA #	HA name	Current study groundwater recharge estimates					Previously reported estimates	
		In-place recharge	Runoff	Mountain stream baseflow	Imported surface water	Total groundwater recharge	Total groundwater recharge (minimum)	Total groundwater recharge (maximum)
Flow System 37: Great Salt Lake Desert System								
184	Spring Valley	99,000	9,000	48	—	110,000	33,000	100,000
185	Tippett Valley	13,000	680	0	—	14,000	5,100	12,000
186A	Antelope Valley-Southern Part	3,100	240	0	—	3,300	800	3,800
186B	Antelope Valley-Northern Part	10,000	380	0	—	10,000	2,400	10,000
189A	Thousand Springs Valley-Herrell-Brush Creek	5,300	730	26	—	6,100	1,700	7,100
189B	Thousand Springs Valley-Toano-Rock Spring	13,000	990	0	—	14,000	4,200	22,000
189C	Thousand Springs Valley-Rocky Butte Area	8,900	140	0	—	9,000	1,100	5,800
189D	Thousand Springs Valley-Montello-Crittenden	17,000	840	0	—	18,000	2,600	13,000
191	Pilot Creek Valley	4,600	250	0	—	4,800	1,800	7,400
251	Grouse Creek Valley	8,300	4,800	290	—	13,000	14,000	14,000
252	Pilot Valley	1,400	180	0	—	1,600	3,400	3,400
253	Deep Creek Valley	16,000	1,100	0	—	17,000	17,000	17,000
254	Snake Valley	150,000	6,900	280	—	160,000	99,000	120,000
255	Pine Valley	26,000	950	0	—	27,000	21,000	21,000
256	Wah Wah Valley	5,500	460	0	—	6,000	7,000	7,000
257	Tule Valley	13,000	310	0	—	13,000	7,600	7,600
258	Fish Springs Flat	1,500	140	0	—	1,600	4,000	4,000
259	Dugway-Government Creek Valley	11,000	1,800	0	—	13,000	7,000	7,000
260A	Park Valley-West Park Valley	4,300	130	0	—	4,400	—	—
261A	Great Salt Lake Desert-West Part	28,000	600	0	—	29,000	94,000	97,000
Flow System 38: Great Salt Lake System								
260B	Park Valley-East Park Valley	1,600	1,900	330	—	3,800	—	—
261B	Great Salt Lake Desert-East Part	140	55	0	—	200	—	—
262	Tooele Valley	39,000	4,200	2,300	—	46,000	52,000	100,000
263	Rush Valley	66,000	9,300	1,800	—	77,000	34,000	34,000
264	Cedar Valley	27,000	2,000	120	—	29,000	—	—
265	Utah Valley Area	210,000	48,000	33,000	120,000	410,000	280,000	350,000
266	Northern Juab Valley	31,000	6,000	1,000	—	38,000	44,000	44,000
267	Salt Lake Valley	83,000	39,000	10,000	96,000	230,000	360,000	360,000
268	East Shore Area	26,000	42,000	1,900	220,000	290,000	150,000	150,000
269	West Shore Area	330	24	0	—	350	600	600
270	Skull Valley	23,000	2,400	0	—	25,000	40,000	40,000
271	Sink Valley	240	1.8	0	—	240	1,000	1,000
272	Cache Valley	390,000	84,000	57,000	190,000	720,000	210,000	320,000
273	Malad-Lower Bear River Area	90,000	15,000	960	330,000	440,000	380,000	380,000
274	Pocatello Valley	2,100	690	0	—	2,800	—	—

Table A4–1. Current study groundwater-recharge estimates for predevelopment conditions and ranges of previously reported estimates of groundwater recharge for each hydrographic area within the Great Basin carbonate and alluvial aquifer system study area.—Continued

[All values in acre-feet per year rounded to two significant figures. Estimated error in all current study values is ±50 percent. Previously reported total groundwater recharge minimum and maximum: totals adjusted to exclude reported recharge by subsurface inflow (unadjusted estimates are presented in Auxiliary 3G). Abbreviations: HA, hydrographic area; #, number; —, no estimate]

HA #	HA name	Current study groundwater recharge estimates					Previously reported estimates	
		In-place recharge	Runoff	Mountain stream baseflow	Imported surface water	Total groundwater recharge	Total groundwater recharge (minimum)	Total groundwater recharge (maximum)
275	Blue Creek Valley	6,300	21	0	—	6,300	14,000	14,000
276	Hansel and North Rozel Flat	2,400	36	0	—	2,400	8,000	8,000
277	Promontory Mountains Area	5,300	120	0	—	5,400	12,000	12,000
278	Curlew Valley	9,700	2,600	41	—	12,000	76,000	86,000
279	Great Salt Lake	1,300	1,600	0	—	2,900	—	—
Flow System 39: Sevier Lake System								
280	Beryl-Enterprise Area	91,000	3,000	0	—	94,000	48,000	48,000
281	Parowan Valley	31,000	6,900	2,600	—	40,000	—	—
282	Cedar City Valley	19,000	11,000	2,000	—	32,000	40,000	42,000
283	Beaver Valley	62,000	14,000	4,500	—	80,000	56,000	56,000
284	Milford Area	12,000	560	0	—	13,000	56,000	56,000
285	Leamington Canyon	24,000	12,000	360	—	36,000	—	—
286	Pavant Valley	43,000	19,000	1,600	5,400	69,000	65,000	65,000
287	Sevier Desert	30,000	4,300	300	[2]6,600	41,000	53,000	53,000

[1]Total for HAs 62 and 63.

[2]Seepage studies showed 30 percent surface-water irrigation return flow from imported water; however 10% was used for recharge from runoff and mountain-stream baseflow due to small numbers of streams in the HA.

Appendix 5: Current Study Groundwater Discharge Estimates for Predevelopment Conditions and Ranges of Previously Reported Estimates of Groundwater Discharge for Each Hydrographic Area within the Great Basin Carbonate and Alluvial Aquifer System Study Area

By Melissa D. Masbruch

Table A5–1. Current study groundwater discharge estimates for predevelopment conditions and ranges of previously reported estimates of groundwater discharge for each hydrographic area within the Great Basin carbonate and alluvial aquifer system study area.

[All values in acre-feet per year rounded to two significant figures. Estimated error in all current study values is ±30 percent. Previously reported total groundwater discharge minimum and maximum: totals adjusted to exclude groundwater discharge by subsurface outflow (unadjusted estimates are presented in Auxiliary 3P). Abbreviations: HA, hydrographic area; #, number; ETg, groundwater evapotranspiration; —, no estimate]

HA #	HA name	Current study groundwater discharge estimates						Previously reported estimates	
		ETg	Mountain streams	Basin-fill streams/ lakes/ reservoirs	Springs	Adjustment to natural discharge for well withdrawals	Total groundwater discharge	Total groundwater discharge (minimum)	Total groundwater discharge (maximum)
Flow System 7: Humboldt System									
42	Marys River Area	26,000	400	0	1,300	0	28,000	—	—
43	Starr Valley Area	19,000	1,300	0	0	0	20,000	—	—
44	North Fork Area	19,000	2,100	0	3,200	0	24,000	—	—
45	Lamoille Valley	12,000	3,600	0	1,500	0	17,000	—	—
46	South Fork Area	3,000	0	0	1,500	0	[1]4,500	[1,2]3,400	—
47	Huntington Valley	10,000	0	0	3,500	0	14,000	[2]14,000	—
48	Tenmile Creek Area	4,000	10	0	0	0	4,000	[2]4,000	—
49	Elko Segment	2,300	0	0	9,700	0	12,000	—	—
50	Susie Creek Area	1,700	72	See footnote 3	0	0	1,800	[2]1,700	—
51	Maggie Creek Area	9,000	51	See footnote 3	0	0	9,100	[2]9,000	—
52	Marys Creek Area	700	2,500	[3]9,500	4,400	0	[4]17,000	[2,4]3,700	—
53	Pine Valley	17,000	0	5,000	3,200	0	25,000	24,000	54,000
54	Crescent Valley	12,000	0	0	0	600	13,000	[2]14,000	—
55	Carico Lake Valley	7,600	0	0	0	0	7,600	[2]8,200	—
56	Upper Reese River Valley	37,000	4,200	0	0	0	41,000	37,000	57,000
59	Lower Reese River Valley	25,000	0	0	0	0	25,000	—	—
60	Whirlwind Valley	990	0	0	0	0	990	—	—
61	Boulder Flat	30,000	0	0	0	0	30,000	—	—
62	Rock Creek Valley	0	[5]1,100	0	0	0	1,100	—	—
63	Willow Creek Valley	0	See footnote 5	0	0	0	0	—	—
Flow System 23: Monte Cristo Valley									
136	Monte Cristo Valley	400	0	0	0	0	400	[2]400	—

Table A5–1. Current study groundwater-discharge estimates for predevelopment conditions and ranges of previously reported estimates of groundwater discharge for each hydrographic area within the Great Basin carbonate and alluvial aquifer system study area.—Continued

[All values in acre-feet per year rounded to two significant figures. Estimated error in all current study values is ±30 percent. Previously reported total groundwater discharge minimum and maximum: totals adjusted to exclude groundwater discharge by subsurface outflow (unadjusted estimates are presented in Auxiliary 3P). Abbreviations: HA, hydrographic area; #, number; ETg, groundwater evapotranspiration; —, no estimate]

HA #	HA name	Current study groundwater discharge estimates						Previously reported estimates	
		ETg	Mountain streams	Basin-fill streams/ lakes/ reservoirs	Springs	Adjustment to natural discharge for well withdrawals	Total groundwater discharge	Total groundwater discharge (minimum)	Total groundwater discharge (maximum)
Flow System 24: South-Central Marshes									
117	Fish Lake Valley	21,000	0	0	3,600	0	25,000	[2]24,000	—
118	Columbus Salt Marsh Valley	4,000	0	0	0	0	4,000	[2]4,000	—
137A	Big Smoky Valley-Tonopah Flat	6,000	0	0	0	0	6,000	[2]6,000	—
141	Ralston Valley	2,500	0	0	0	0	2,500	[2]2,600	—
142	Alkali Spring Valley	400	0	0	0	0	400	[2]400	—
143	Clayton Valley	23,000	0	0	1,200	0	24,000	[2]24,000	—
149	Stone Cabin Valley	1,500	46	0	0	0	1,500	[2]2,000	—
Flow System 25: Grass Valley									
138	Grass Valley	7,500	0	0	1,500	0	9,000	—	—
Flow System 26: Northern Big Smoky Valley									
137B	Northern Big Smoky Valley	62,000	4,700	0	2,300	0	69,000	64,000	77,000
Flow System 27: Diamond Valley System									
139	Kobeh Valley	12,000	0	0	2,400	0	14,000	[2]15,000	—
140A	Monitor Valley-Northern Part	500	330	0	1,500	0	2,300	[2]2,000	—
140B	Monitor Valley-Southern Part	9,200	1,200	0	0	0	10,000	[2]9,200	—
151	Antelope Valley	3,200	0	0	810	0	4,000	[2]4,200	—
152	Stevens Basin	0	0	0	0	0	0	[2]0	—
153	Diamond Valley	19,000	0	0	7,400	0	26,000	23,000	30,000
Flow System 28: Death Valley System									
Amargosa/Death Valley Subarea									
144	Lida Valley	0	0	0	480	0	[1]480	[1,2]0	—
145	Stonewall Flat	0	0	0	0	0	0	[2]0	—
146	Sarcobatus Flat	13,000	0	0	0	0	13,000	3,000	13,000
147	Gold Flat	0	0	0	0	0	0	—	—
148	Cactus Flat	0	0	0	0	0	0	—	—
157	Kawich Valley	0	0	0	0	0	0	—	—
158A	Emigrant Valley-Groom Lake Valley	0	0	0	0	0	0	—	—
158B	Emigrant Valley-Papoose Lake Valley	0	0	0	0	0	0	—	—
159	Yucca Flat	0	0	0	0	0	0	—	—
160	Frenchman Flat	0	0	0	0	0	0	—	—
161	Indian Springs Valley	0	0	0	1,800	0	[1]1,800	[1,2]660	—
168	Three Lakes Valley-Northern Part	0	0	0	0	0	0	—	—
169A	Tikapoo Valley-Northern Part	0	0	0	0	0	0	—	—
169B	Tikapoo Valley-Southern Part	0	0	0	0	0	0	—	—
170	Penoyer Valley	3,800	0	0	0	0	3,800	3,800	6,400
173A	Railroad Valley-Southern Part	200	0	0	0	0	200	[2]200	—
211	Three Lakes Valley-Southern Part	0	0	0	0	0	0	—	—
225	Mercury Valley	0	0	0	0	0	0	—	—
226	Rock Valley	0	0	0	0	0	0	—	—

Table A5–1. Current study groundwater-discharge estimates for predevelopment conditions and ranges of previously reported estimates of groundwater discharge for each hydrographic area within the Great Basin carbonate and alluvial aquifer system study area.—Continued

[All values in acre-feet per year rounded to two significant figures. Estimated error in all current study values is ±30 percent. Previously reported total groundwater discharge minimum and maximum: totals adjusted to exclude groundwater discharge by subsurface outflow (unadjusted estimates are presented in Auxiliary 3P). Abbreviations: HA, hydrographic area; #, number; ETg, groundwater evapotranspiration; —, no estimate]

HA #	HA name	Current study groundwater discharge estimates						Previously reported estimates	
		ETg	Mountain streams	Basin-fill streams/lakes/reservoirs	Springs	Adjustment to natural discharge for well withdrawals	Total groundwater discharge	Total groundwater discharge (minimum)	Total groundwater discharge (maximum)
Flow System 28: Death Valley System—Continued									
Amargosa/Death Valley Subarea									
227A	Fortymile Canyon-Jackass Flats	0	0	0	0	0	0	—	—
227B	Fortymile Canyon-Buckboard Mesa	0	0	0	0	0	0	—	—
228	Oasis Valley	4,700	0	0	1,300	0	6,000	2,200	6,000
229	Crater Flat	0	0	0	0	0	0	—	—
230	Amargosa Desert	1,400	0	0	18,000	0	19,000	19,000	27,000
243	Death Valley	[6]33,000	0	61	3,700	0	37,000	[2]38,000	—
Pahrump Valley Subarea									
162	Pahrump Valley	1,000	280	0	9,700	0	11,000	10,000	11,000
240	Chicago Valley	[7]430	0	0	0	0	430	[2]430	—
241	California Valley	[8]0	0	0	0	0	0	—	—
242	Lower Amargosa Valley	[9]8,500	0	0	0	0	8,500	[2]8,500	—
244	Valjean Valley	200	0	0	0	0	200	—	—
245	Shadow Valley	0	0	0	0	0	0	—	—
Flow System 29: Newark Valley System									
154	Newark Valley	22,000	0	0	3,600	0	26,000	16,000	60,000
155A	Little Smoky Valley-Northern Part	0	0	0	6,100	0	6,100	4,000	12,000
155B	Little Smoky Valley-Central Part	0	0	0	0	0	0	—	—
Flow System 30: Railroad Valley System									
150	Little Fish Lake Valley	10,000	0	0	0	0	10,000	9,700	9,800
155C	Little Smoky Valley-Southern Part	0	0	0	0	0	0	[2]0	—
156	Hot Creek Valley	5,700	49	300	1,500	0	7,500	5,000	9,000
173B	Railroad Valley-Northern Part	49,000	550	0	31,000	0	81,000	80,000	85,000
Flow System 32: Independence Valley System									
177	Clover Valley	16,000	0	0	3,300	0	19,000	19,000	84,000
188	Independence Valley	9,500	0	0	0	0	9,500	9,500	47,000
Flow System 33: Ruby Valley System									
176	Ruby Valley	58,000	2,500	0	10,000	0	70,000	68,000	170,000
178A	Butte Valley-Northern Part	6,200	0	0	2,200	0	8,400	[2]7,900	—
Flow System 34: Colorado System									
Lake Mead Subarea									
164A	Ivanpah Valley-Northern Part	0	0	0	0	0	0	[2]0	—
164B	Ivanpah Valley-Southern Part	0	0	0	0	0	0	[2]0	—
165	Jean Lake Valley	0	0	0	0	0	0	[2]0	—
166	Hidden Valley South	0	0	0	0	0	0	—	—
167	Eldorado Valley	0	0	0	0	0	0	—	—
212	Las Vegas Valley	19,000	0	0	5,000	0	[10]24,000	[2,10]67,000	—
215	Black Mountains Area	0	0	100	1,600	0	1,700	[2]1,500	—

Table A5–1. Current study groundwater-discharge estimates for predevelopment conditions and ranges of previously reported estimates of groundwater discharge for each hydrographic area within the Great Basin carbonate and alluvial aquifer system study area.—Continued

[All values in acre-feet per year rounded to two significant figures. Estimated error in all current study values is ±30 percent. Previously reported total groundwater discharge minimum and maximum: totals adjusted to exclude groundwater discharge by subsurface outflow (unadjusted estimates are presented in Auxiliary 3P). Abbreviations: HA, hydrographic area; #, number; ETg, groundwater evapotranspiration; —, no estimate]

HA #	HA name	Current study groundwater discharge estimates						Previously reported estimates	
		ETg	Mountain streams	Basin-fill streams/ lakes/ reservoirs	Springs	Adjustment to natural discharge for well withdrawals	Total groundwater discharge	Total groundwater discharge (minimum)	Total groundwater discharge (maximum)
Flow System 34: Colorado System—Continued									
Muddy River Subarea									
171	Coal Valley	100	0	0	0	0	100	—	—
172	Garden Valley	0	0	0	0	0	0	—	—
181	Dry Lake Valley	0	0	0	0	0	0	—	—
182	Delamar Valley	0	0	0	0	0	0	—	—
183	Lake Valley	2,900	0	0	5,500	0	8,400	6,000	8,500
198	Dry Valley	10	0	0	0	0	10	—	—
199	Rose Valley	10	0	0	0	0	10	—	—
200	Eagle Valley	290	0	0	0	0	290	—	—
201	Spring Valley	1,000	0	0	0	0	1,000	—	—
202	Patterson Valley	0	0	0	0	0	0	—	—
203	Panaca Valley	530	0	0	7,900	0	8,400	—	—
204	Clover Valley	210	0	0	0	0	210	—	—
205	Lower Meadow Valley Wash	1,400	0	0	0	0	1,400	—	—
206	Kane Springs Valley	0	0	0	0	0	0	—	—
208	Pahroc Valley	0	0	0	0	0	0	[2]0	—
209	Pahranagat Valley	0	0	0	26,000	0	26,000	[2]27,000	—
210	Coyote Spring Valley	0	0	0	0	0	0	[2]0	—
216	Garnet Valley	0	0	0	0	0	0	—	—
217	Hidden Valley North	0	0	0	0	0	0	—	—
218	California Wash	0	0	0	0	0	[11]0	[2,11]2,700	—
219	Muddy River Springs Area	0	0	0	35,000	0	35,000	—	—
220	Lower Moapa Valley	0	0	730	0	0	[11]730	[2,11]15,000	—
White River Valley Subarea									
174	Jakes Valley	0	1,900	0	0	0	[1]1,900	[1]500	[1]1,000
175	Long Valley	1,000	0	0	0	0	1,000	1,000	11,000
180	Cave Valley	1,400	0	0	650	0	2,000	0	2,000
207	White River Valley	34,000	1,200	1,500	43,000	0	80,000	35,000	77,000
Virgin River Valley Subarea									
221	Tule Desert	0	0	0	0	0	0	—	—
222	Virgin River Valley	0	570	36,000	2,600	0	39,000	—	—
Flow System 35: Goshute Valley System									
178B	Butte Valley-Southern Part	12,000	0	0	0	0	12,000	12,000	12,000
179	Steptoe Valley	64,000	3,600	0	45,000	0	110,000	70,000	130,000
187	Goshute Valley	6,600	0	0	0	0	[12]6,600	[2,12]42,000	—
Flow System 36: Mesquite Valley									
163	Mesquite Valley	2,200	0	0	0	0	2,200	[2]2,200	—

Table A5–1. Current study groundwater-discharge estimates for predevelopment conditions and ranges of previously reported estimates of groundwater discharge for each hydrographic area within the Great Basin carbonate and alluvial aquifer system study area.—Continued

[All values in acre-feet per year rounded to two significant figures. Estimated error in all current study values is ±30 percent. Previously reported total groundwater discharge minimum and maximum: totals adjusted to exclude groundwater discharge by subsurface outflow (unadjusted estimates are presented in Auxiliary 3P). Abbreviations: HA, hydrographic area; #, number; ETg, groundwater evapotranspiration; —, no estimate]

HA #	HA name	Current study groundwater discharge estimates						Previously reported estimates	
		ETg	Mountain streams	Basin-fill streams/ lakes/ reservoirs	Springs	Adjustment to natural discharge for well withdrawals	Total groundwater discharge	Total groundwater discharge (minimum)	Total groundwater discharge (maximum)
Flow System 37: Great Salt Lake Desert System									
184	Spring Valley	65,000	480	0	17,000	0	82,000	71,000	90,000
185	Tippett Valley	2,000	0	0	0	0	2,000	0	2,900
186A	Antelope Valley-Southern Part	210	0	0	0	0	[13]210	[2,13]0	—
186B	Antelope Valley-Northern Part	100	0	0	0	0	100	[2]100	—
189A	Thousand Springs Valley-Herrell-Brush Creek	1,500	260	0	0	240	2,000	[2]1,800	—
189B	Thousand Springs Valley-Toano-Rock Spring	1,600	0	0	0	0	1,600	[2]1,700	—
189C	Thousand Springs Valley-Rocky Butte Area	1,200	0	0	0	0	1,200	[2]1,200	—
189D	Thousand Springs Valley-Montello-Crittenden	12,000	0	0	2,600	0	15,000	[2]14,000	—
191	Pilot Creek Valley	4,000	0	0	1,400	0	5,400	[2]4,600	—
251	Grouse Creek Valley	11,000	960	0	0	1,400	13,000	[2]13,000	—
252	Pilot Valley	6,900	0	0	480	0	7,400	[2]7,600	—
253	Deep Creek Valley	14,000	0	0	4,400	0	18,000	14,000	17,000
254	Snake Valley	100,000	2,800	0	30,000	0	130,000	82,000	130,000
255	Pine Valley	0	0	0	0	0	[11]0	[11]7,000	[11]7,100
256	Wah Wah Valley	620	0	0	900	0	1,500	1,400	1,500
257	Tule Valley	37,000	0	0	1,000	0	38,000	32,000	40,000
258	Fish Springs Flat	8,000	0	0	26,000	0	34,000	35,000	35,000
259	Dugway-Government Creek Valley	1,000	0	0	5,100	0	[1]6,100	[1]3,800	[1]3,800
260A	Park Valley-West Park Valley	4,100	0	0	1,200	0	5,300	—	—
261A	Great Salt Lake Desert-West Part	56,000	0	0	18,000	0	74,000	[2]83,000	—
Flow System 38: Great Salt Lake System									
260B	Park Valley-East Park Valley	11,000	1,100	0	0	0	12,000	—	—
261B	Great Salt Lake Desert-East Part	7,400	0	0	0	0	7,400	—	—
262	Tooele Valley	17,000	7,800	0	24,000	13,000	62,000	66,000	68,000
263	Rush Valley	27,000	5,900	0	0	3,400	36,000	[2]32,000	—
264	Cedar Valley	0	390	0	3,700	0	4,100	—	—
265	Utah Valley Area	49,000	110,000	81,000	110,000	64,000	410,000	310,000	500,000
266	Northern Juab Valley	4,400	3,400	5,800	13,000	11,000	38,000	[2]41,000	—
267	Salt Lake Valley	60,000	34,000	170,000	20,000	75,000	360,000	[2]360,000	—
268	East Shore Area	8,000	6,200	0	70,000	35,000	120,000	[2]130,000	—
269	West Shore Area	2,400	0	0	4,700	0	7,100	[2]6,800	—
270	Skull Valley	27,000	0	0	4,100	3,500	35,000	[2]35,000	—
271	Sink Valley	0	0	0	0	0	[14]0	[2,14]200	—
272	Cache Valley	63,000	190,000	130,000	130,000	27,000	[1]540,000	[1]280,000	[1]330,000
273	Malad-Lower Bear River Area	130,000	9,600	130,000	86,000	11,000	370,000	[2]370,000	—
274	Pocatello Valley	0	0	0	0	0	0	—	—
275	Blue Creek Valley	700	0	0	7,700	0	8,400	[2]8,500	—

Table A5–1. Current study groundwater-discharge estimates for predevelopment conditions and ranges of previously reported estimates of groundwater discharge for each hydrographic area within the Great Basin carbonate and alluvial aquifer system study area.—Continued

[All values in acre-feet per year rounded to two significant figures. Estimated error in all current study values is ±30 percent. Previously reported total groundwater discharge minimum and maximum: totals adjusted to exclude groundwater discharge by subsurface outflow (unadjusted estimates are presented in Auxiliary 3P). Abbreviations: HA, hydrographic area; #, number; ETg, groundwater evapotranspiration; —, no estimate]

HA #	HA name	Current study groundwater discharge estimates						Previously reported estimates	
		ETg	Mountain streams	Basin-fill streams/ lakes/ reservoirs	Springs	Adjustment to natural discharge for well withdrawals	Total groundwater discharge	Total groundwater discharge (minimum)	Total groundwater discharge (maximum)
Flow System 38: Great Salt Lake System—Continued									
276	Hansel and North Rozel Flat	7,600	0	0	0	0	7,600	[2]10,000	—
277	Promontory Mountains Area	7,300	0	0	3,800	0	[15]11,000	[2,15]18,000	—
278	Curlew Valley	13,000	410	0	41,000	22,000	76,000	[2]93,000	—
279	Great Salt Lake	0	0	57,000	1,500	0	58,000	—	—
Flow System 39: Sevier Lake System									
280	Beryl-Enterprise Area	26,000	0	0	0	0	[10]26,000	[2,10]86,000	—
281	Parowan Valley	12,000	8,800	0	0	22,000	43,000	—	—
282	Cedar City Valley	22,000	6,700	0	3,300	0	32,000	39,000	40,000
283	Beaver Valley	18,000	15,000	2,200	26,000	6,900	68,000	[2]56,000	—
284	Milford Area	33,000	0	0	0	0	[10]33,000	[2,10]81,000	—
285	Leamington Canyon	15,000	1,200	See footnote 16	3,100	0	19,000	—	—
286	Pavant Valley	24,000	5,500	0	0	42,000	72,000	[2]84,000	—
287	Sevier Desert	59,000	3,000	[16]35,000	15,000	0	110,000	—	—

[1]Current study estimate exceeds previously reported value by more than 30 percent as current study estimate includes discharge to mountain springs and (or) mountain streams not quantified in previous report.

[2]Only one previously reported total discharge estimate for this HA.

[3]Estimate is total for HAs 50, 51, and 52.

[4]Current study estimate exceeds previously reported value as current study estimate includes discharge to the Humboldt River not included in previously reported estimate.

[5]Estimate is total for HAs 62 and 63.

[6]Estimate does not include ETg from Tecopa area, which is listed under HA 242.

[7]Estimate is for northern portion of HA only.

[8]Small amount of ETg for this HA is included in estimate as part of the Tecopa and California Valley areas reported in HA 242.

[9]Estimate is for Tecopa/California Valley, which includes ETg from HAs 240, 241, 242, and 243; majority in HA 242 and Shoshone areas.

[10]Prveiously reported values exceed current study estimate by more than 30 percent as previously reported estimate includes groundwater discharge to well withdrawals that would not have been occurring under predevelopment conditions; total discharge estimates for predevelopment conditions were not included in previous report.

[11]Previously reported value exceeds current study estimate by more than 30 percent as estimates of ETg from previous report appear to be surface-water supported, and were not used in current study estimate.

[12]Previously reported value exceeds current study estimate by more than 30 percent as previous estimate is from Nichols (2000), which is suspected to be too high; Nichols (2000) estimate was not used in current study estimates; see text for explanation).

[13]Current study estimate exceeds previously reported value by more than 30 percent as previous report includes discharge only from subsurface outflow, which is not quantified at the HA level in the current study.

[14]Previously reported value exceeds current study estimate by more than 30 percent as previously reported ETg was very small, and there was no previously mapped ETg area for the HA; ETg from the previous study, therefore, was not used in current study estimate.

[15]Previously reported value exceeds current study estimate because previous study estimate of spring discharge is suspected to be too high.

[16]Estimate includes some groundwater that discharges to the Sevier River within HA 285.

Appendix 6: Description of Spatial Datasets Accompanying the Conceptual Model of the Great Basin Carbonate and Alluvial Aquifer System

By Susan G. Buto

The U.S. Geological Survey (USGS) Water Resources Discipline (WRD) maintains a clearinghouse for publicly available geographic information system (GIS) data on the USGS WRD National Spatial Data Infrastructure (NSDI) node. The NSDI is a physical, organizational, and virtual network designed to enable the development and sharing of digital geographic information resources (Federal Geographic Data Committee, 2007). GIS datasets created in conjunction with the Great Basin carbonate and alluvial aquifer system (GBCAAS) study have been placed on the WRD NSDI node for public access. Brief descriptions of the datasets are included below. Complete dataset descriptions including source documentation and processing steps can be accessed in the metadata documents accompanying the datasets on the WRD NSDI node. The datasets are in GIS format and require specialized software to view.

Estimated Outer Extent of Areas of Groundwater Discharge to Evapotranspiration

This dataset consists of vector polygons mapped at 1:1,000,000 scale. The polygons represent the outermost extent of areas where groundwater discharge as evapotranspiration likely occurs within the GBCAAS study area. The data are based on 1:1,000,000-scale boundaries updated with more recent, larger scale data where available. The boundaries were not independently field verified during the course of this study. Because of the scale of this dataset, horizontal positional error in these boundaries may exceed ±1,600 ft. This dataset can be downloaded from the WRD NSDI node at http://water.usgs.gov/GIS/metadata/usgswrd/XML/sir2010_5193_GWdisch1000.xml.

Basin Characterization Model Data

Total estimated groundwater recharge from the Basin Characterization Model (BCM) is the summation of in-place recharge and an assigned percentage of runoff (Flint and Flint, 2007). The data are output from the BCM described in Appendix 3 of this report. The BCM is a distributed-parameter, water-balance accounting model that is run on a monthly time step. The BCM incorporates spatially distributed parameters (monthly precipitation, monthly minimum and maximum air temperature, monthly potential evapotranspiration, soil-water storage capacity, and saturated hydraulic conductivity of bedrock and alluvium) to determine where excess water is available in a basin and if the excess water is stored in the soil or infiltrates downward into underlying bedrock.

BCM In-Place Recharge

This dataset represents average annual 1940–2006 BCM in-place recharge for the GBCAAS study area. In-place recharge is calculated as the annual volume of water that can drain from the soil zone directly into consolidated bedrock or unconsolidated deposits. This dataset can be downloaded from the WRD NSDI node at http://water.usgs.gov/GIS/metadata/usgswrd/XML/sir2010_5193_BCM.xml. Estimated in-place recharge values output from the BCM were adjusted for water-balance calculations used in the GBCAAS study. Details of the adjustments can be found in Chapter D and table Auxiliary 3A of this report.

BCM Runoff

This dataset represents average annual 1940–2006 BCM runoff for the GBCAAS study area. Runoff is calculated as the annual volume of water that runs off the mountain front or becomes streamflow. This dataset can be downloaded from the WRD NSDI node at http://water.usgs.gov/GIS/metadata/usgswrd/XML/sir2010_5193_BCM.xml. Estimated runoff values output from the BCM were adjusted for water-balance calculations used in the GBCAAS study. Details of the adjustments can be found in Chapter D and table Auxiliary 3A of this report.

BCM Saturated Hydraulic Conductivity

This dataset represents the spatial distribution of saturated hydraulic conductivity (K) of bedrock and unconsolidated basin fill in the GBCAAS study area, which is temporally invariable input data for the BCM (Flint and Flint, 2007). The dataset was developed by applying assumed K values to geologic formations derived from 1:500,000-scale digital geologic maps for Nevada (Stewart and others, 2003), Utah (Hintze and others, 2000), Oregon (Walker and others, 2002), Idaho (Johnson and Raines, 1996), and Arizona (Hirshberg and Pitts, 2000) and 1:750,000-scale digital geologic maps for California (Saucedo and others, 2000). Saturated K values in the study area range between 0.05 and 4,100 mm / day. This dataset can be downloaded from the WRD NSDI node at http://water.usgs.gov/GIS/metadata/usgswrd/XML/sir2010_5193_BCM.xml.

Hydrogeologic Framework

This dataset represents the modeled top surface altitude and extent for each of the hydrogeologic units within the study area. The dataset was constructed from a variety of data sources including digital elevation data, digital geologic map and hydrogeologic framework data from previous studies, drill-hole stratigraphic data, geologic map cross-section contacts, and regional geophysical depth to basement datasets. See Appendix 1 of this report for a detailed description of the dataset sources and framework construction. The information is also outlined in detail in the metadata accompanying the digital dataset on the WRD NSDI node at http://water.usgs.gov/GIS/metadata/usgswrd/XML/sir2010_5193_3D_HGF.xml.

Hydrographic Areas and Hydraulic Flow Boundaries

This dataset consists of vector polygons and lines mapped at 1:1,000,000 scale. The data represent hydrographic area (HA) polygons and boundary lines. The data are modified from HAs published in paper map form by the U.S. Geological Survey (Harrill and others, 1988) and later released in digital GIS format (Buto, 2009). The subsurface hydrogeologic framework layers described above were used as a basis to infer the likelihood of hydraulic connections accross HA boundaries. An attribute identifying relative likelihood of hydraulic connection is included with the HA boundary lines. This dataset can be downloaded from the WRD NSDI node at http://water.usgs.gov/GIS/metadata/usgswrd/XML/sir2010_5193_ha1000.xml.

Potentiometric Contours and Control Points

This dataset consists of vector lines and points mapped at approximately 1:1,000,000 scale. The line data represent the potentiometric contours or groundwater altitude in the study area. The point data represent control points used to draw the contours.

The control points are based on well and spring locations and water-level measurements from the USGS National Water Information System (NWIS; Mathey, 1998) in addition to estimates of water-level altitudes in select mountain streams from National Hydrography Dataset (USGS, 1999) stream reaches and stream-gage information from NWIS. The water-level altitudes from NWIS were averaged for the period of record. This dataset can be downloaded from the WRD NSDI node at http://water.usgs.gov/GIS/metadata/usgswrd/XML/sir2010_5193_potentiometric1000.xml.

References Cited

Buto, S.G., 2009, Digital representation of 1:1,000,000-scale Hydrographic Areas of the Great Basin: U.S. Geological Survey Data Series Report 457, 5 p., available at http://pubs.usgs.gov/ds/457/.

Federal Geographic Data Committee, 2007, accessed December 4, 2008 at http://www.fgdc.gov/.

Flint, A.L., and Flint, L.E., 2007, Application of the Basin Characterization Model to estimate in-place recharge and runoff potential in the Basin and Range carbonate-rock aquifer system, White Pine County, Nevada and adjacent areas in Nevada and Utah: U.S. Geological Survey Scientific Investigations Report 2007–5099, 30p.

Harrill, J.R., Gates, J.S., and Thomas, J.M., 1988, Major ground-water flow systems in the Great Basin region of Nevada, Utah, and adjacent states: U.S. Geological Survey Hydrologic Investigations Atlas HA–694–C, 2 sheets, scale 1:1,000,000.

Hintze, L.F., Willis, G.C., Laes, D., Sprinkel, D.A., and Brown, K.D., 2000, Digital geologic map of Utah: Utah Geological Survey Map 179DM.

Hirshberg, D.M., and Pitts, S.G., 2000, Digital geologic map of Arizona: A digital database derived from the 1983 printing of the Wilson, Moore, and Cooper 1:500,000-scale map: U.S. Geological Survey Open File Report 00–409, 67 p., 3 sheets, also available at http://geopubs.wr.usgs.gov/open-file/of00-409/.

Johnson, B.R., and Raines, G.L., 1996, Digital representation of the Idaho state geologic map, a contribution to the Interior Columbia Basin Ecosystem Management Project: U.S. Geological Survey Open-File Report 95 –690, 24 p with two datasets, available at http://pubs.usgs.gov/of/1995/of95-690/.

Mathey, S.B., ed., 1998, National Water Information System (NWIS): U.S. Geological Survey Fact Sheet 027–98, 2 p., accessed January 14, 2009 at http://pubs.usgs.gov/fs/FS-027-98/fs-027-98.pdf.

Saucedo, G.J., Bedford, D.R., Raines, G.L., Miller, R.J., and Wentworth, C.M., 2000, GIS data for the geologic map of California: California Geological Survey, CD 2000–07.

Stewart, J.H., Carlson, J.E., Raines, G.L., Connors, K.A., Moyer, L.A., and Miller, R.J., 2003, Spatial digital database for the geologic map of Nevada: U.S. Geological Survey Open-File Report 03–66, version 3.0, 32 p. 2 sheets, with database, available at http://pubs.usgs.gov/of/2003/of03-66/.

Soil Conservation Service, 1991, State soil geographic data base (STATSGO), data user’s guide: Washington, D.C., Miscellaneous Publication 1492, 88 p.

U.S. Geological Survey, 1999, National Hydrography Dataset: U.S. Geological Survey Fact Sheet 106–99, accessed March 2007 at http://erg.usgs.gov/isb/pubs/factsheets/fs10699.html.

Walker, G.W., MacLeod, N.S., Miller, R.J., Raines, G.L., and Connors, K.A., 2002, Spatial digital database for the geologic map of Oregon: U.S. Geological Survey Open-File Report 03–67, version 2.0, 21 p., available at http://pubs.usgs.gov/of/2003/of03-067/.

Appendix 7: Comparison of Predevelopment and Recent (2000) Groundwater Budget Estimates for Each Hydrographic Area within the Great Basin Carbonate and Alluvial Aquifer System Study Area

By Melissa D. Masbruch

Table A7–1. Predevelopment and recent (2000) groundwater budget estimates for each hydrographic area within the Great Basin carbonate and alluvial aquifer system study area.

[All values in acre-feet per year rounded to two significant figures. Estimated error in recharge values is ±50 percent. Estimated error in discharge values is ±30 percent. Values in blue are for predevelopment conditions. Values in red are for recent (2000) conditions. Decrease in natural discharge and/or storage: calculated as the difference of well withdrawals and recharge from unconsumed irrigation and public supply water from well withdrawals. Minimum decrease in groundwater storage: calculated as the difference of the decrease in natural discharge and/or change in storage and groundwater discharge under predevelopment conditions, if the difference is greater than zero. Abbreviations: HA, hydrographic area; #, number; —, no estimate]

HA #	HA name	Groundwater recharge for pre-development conditions	Recharge from unconsumed irrigation and public supply water from well withdrawals (2000)	Groundwater recharge for recent (2000) conditions	Groundwater discharge for pre-development conditions	Well withdrawals (2000)	Decrease in natural discharge and/or storage (net well withdrawals) (2000)	Minimum decrease in groundwater storage (2000)	Groundwater discharge for recent (2000) conditions
				Flow System 7: Humboldt System					
42	Marys River Area	51,000	630	52,000	28,000	2,100	1,500	—	29,000
43	Starr Valley Area	42,000	300	42,000	20,000	1,000	700	—	20,000
44	North Fork Area	46,000	[1]0	46,000	24,000	1,700	1,700	—	24,000
45	Lamoille Valley	17,000	360	17,000	17,000	1,200	840	—	17,000
46	South Fork Area	13,000	24	13,000	4,500	80	56	—	4,500
47	Huntington Valley	48,000	140	48,000	14,000	470	330	—	14,000
48	Tenmile Creek Area	28,000	1,000	29,000	4,000	3,400	2,400	—	5,000
49	Elko Segment	3,600	2,500	6,100	12,000	8,300	5,800	—	14,000
50	Susie Creek Area	6,100	87	6,200	1,800	290	200	—	1,900
51	Maggie Creek Area	9,000	[1]0	9,000	9,100	18,000	18,000	—	9,100
52	Marys Creek Area	1,200	220	1,400	17,000	740	520	—	17,000
53	Pine Valley	26,000	45	26,000	25,000	150	100	—	25,000
54	Crescent Valley	6,300	[1]0	6,300	13,000	32,000	32,000	—	13,000
55	Carico Lake Valley	5,200	140	5,300	7,600	460	320	—	7,700
56	Upper Reese River Valley	51,000	1,400	52,000	41,000	4,700	3,300	—	42,000
59	Lower Reese River Valley	4,600	[1]3,000	7,600	25,000	32,000	29,000	—	28,000
60	Whirlwind Valley	100	1,800	1,900	990	6,100	4,300	—	2,800
61	Boulder Flat	3,200	[1]13,000	16,000	30,000	90,000	77,000	--	43,000
62	Rock Creek Valley	2,100	18	2,100	1,100	60	42	—	1,100
63	Willow Creek Valley	13,000	48	13,000	0	160	110	—	50
				Flow System 23: Monte Cristo Valley					
136	Monte Cristo Valley	1,300	6.0	1,300	400	20	14	—	410

Table A7–1. Predevelopment and recent (2000) groundwater-budget estimates for each hydrographic area within the Great Basin carbonate and alluvial aquifer system study area.—Continued

[All values in acre-feet per year rounded to two significant figures. Estimated error in recharge values is ±50 percent. Estimated error in discharge values is ±30 percent. Values in blue are for predevelopment conditions. Values in red are for recent (2000) conditions. Decrease in natural discharge and/or storage: calculated as the difference of well withdrawals and recharge from unconsumed irrigation and public supply water from well withdrawals. Minimum decrease in groundwater storage: calculated as the difference of the decrease in natural discharge and/or change in storage and groundwater discharge under predevelopment conditions, if the difference is greater than zero. Abbreviations: HA, hydrographic area; #, number; —, no estimate]

HA #	HA name	Groundwater recharge for pre-development conditions	Recharge from unconsumed irrigation and public supply water from well withdrawals (2000)	Groundwater recharge for recent (2000) conditions	Groundwater discharge for pre-development conditions	Well withdrawals (2000)	Decrease in natural discharge and/or storage (net well withdrawals) (2000)	Minimum decrease in groundwater storage (2000)	Groundwater discharge for recent (2000) conditions
Flow System 24: South-Central Marshes									
117	Fish Lake Valley	24,000	8,700	33,000	25,000	29,000	20,000	—	34,000
118	Columbus Salt Marsh Valley	1,500	6.0	1,500	4,000	20	14	—	4,000
137A	Big Smoky Valley-Tonopah Flat	11,000	2,200	13,000	6,000	7,300	5,100	—	8,200
141	Ralston Valley	8,400	110	8,500	2,500	370	260	—	2,600
142	Alkali Spring Valley	1,100	9.0	1,100	400	30	21	—	410
143	Clayton Valley	3,600	4,200	7,800	24,000	14,000	9,800	—	28,000
149	Stone Cabin Valley	5,000	480	5,500	1,500	1,600	1,100	—	2,000
Flow System 25: Grass Valley									
138	Grass Valley	17,000	3.0	17,000	9,000	10	7.0	—	9,000
Flow System 26: Northern Big Smoky Valley									
137B	Northern Big Smoky Valley	87,000	[1]270	87,000	69,000	5,900	5,600	—	69,000
Flow System 27: Diamond Valley System									
139	Kobeh Valley	19,000	810	20,000	14,000	2,700	1,900	—	15,000
140A	Monitor Valley-Northern Part	34,000	10	34,000	2,300	35	25	—	2,300
140B	Monitor Valley-Southern Part	27,000	10	27,000	10,000	35	25	—	10,000
151	Antelope Valley	5,900	15	5,900	4,000	50	35	—	4,000
152	Stevens Basin	1,400	0	1,400	0	0	0	—	0
153	Diamond Valley	23,000	21,000	44,000	26,000	71,000	50,000	24,000	71,000
Flow System 28: Death Valley System									
Amargosa/Death Valley Subarea									
144	Lida Valley	1,100	0.42	1,100	480	1.4	1.0	—	480
145	Stonewall Flat	1,300	3	1,300	0	10	7.0	—	3
146	Sarcobatus Flat	2,300	5	2,300	13,000	18	13	—	13,000
147	Gold Flat	11,000	15	11,000	0	50	35	—	15
148	Cactus Flat	1,000	12	1,000	0	41	29	—	12
157	Kawich Valley	5,500	0	5,500	0	0	0	—	0
158A	Emigrant Valley-Groom Lake Valley	4,800	84	4,900	0	280	200	—	80
158B	Emigrant Valley-Papoose Lake Valley	270	1.3	270	0	4.3	3.0	—	1.3
159	Yucca Flat	1,800	30	1,800	0	100	70	—	30
160	Frenchman Flat	1,600	130	1,700	0	420	290	—	130
161	Indian Springs Valley	4,400	200	4,600	1,800	650	450	—	2,000
168	Three Lakes Valley-Northern Part	1,300	6.0	1,300	0	20	14	—	6
169A	Tikapoo Valley-Northern Part	4,900	13	4,900	0	44	31	—	13
169B	Tikapoo Valley-Southern Part	2,000	7.8	2,000	0	26	18	—	8
170	Penoyer Valley	5,700	3,900	9,600	3,800	13,000	9,100	5,300	13,000
173A	Railroad Valley-Southern Part	4,000	360	4,400	200	1,200	840	—	560

Table A7–1. Predevelopment and recent (2000) groundwater-budget estimates for each hydrographic area within the Great Basin carbonate and alluvial aquifer system study area.—Continued

[All values in acre-feet per year rounded to two significant figures. Estimated error in recharge values is ±50 percent. Estimated error in discharge values is ±30 percent. Values in blue are for predevelopment conditions. Values in red are for recent (2000) conditions. Decrease in natural discharge and/or storage: calculated as the difference of well withdrawals and recharge from unconsumed irrigation and public supply water from well withdrawals. Minimum decrease in groundwater storage: calculated as the difference of the decrease in natural discharge and/or change in storage and groundwater discharge under predevelopment conditions, if the difference is greater than zero. Abbreviations: HA, hydrographic area; #, number; —, no estimate]

HA #	HA name	Groundwater recharge for pre-development conditions	Recharge from unconsumed irrigation and public supply water from well withdrawals (2000)	Groundwater recharge for recent (2000) conditions	Groundwater discharge for pre-development conditions	Well withdrawals (2000)	Decrease in natural discharge and/or storage (net well withdrawals) (2000)	Minimum decrease in groundwater storage (2000)	Groundwater discharge for recent (2000) conditions
Flow System 28: Death Valley System—Continued									
Amargosa/Death Valley Subarea									
211	Three Lakes Valley-Southern Part	2,500	99	2,600	0	330	230	—	100
225	Mercury Valley	160	0.60	160	0	2.0	1.4	—	0.6
226	Rock Valley	75	3.0	78	0	10	7.0	—	3
227A	Fortymile Canyon-Jackass Flats	1,100	28	1,100	0	94	66	—	28
227B	Fortymile Canyon-Buckboard Mesa	7,000	14	7,000	0	48	34	—	14
228	Oasis Valley	8,700	51	8,800	6,000	170	120	—	6,000
229	Crater Flat	330	39	370	0	130	91	—	39
230	Amargosa Desert	630	4,800	5,400	19,000	16,000	11,000	—	24,000
243	Death Valley	10,000	15	10,000	37,000	50	35	—	37,000
Pahrump Valley Subarea									
162	Pahrump Valley	21,000	6,600	28,000	11,000	22,000	15,000	4,000	22,000
240	Chicago Valley	150	0	150	430	0	0	—	430
241	California Valley	440	0	440	0	0	0	—	0
242	Lower Amargosa Valley	330	8.1	340	8,500	27	19	—	8,500
244	Valjean Valley	340	0	340	200	0	0	—	200
245	Shadow Valley	840	0	840	0	0	0	—	0
Flow System 29: Newark Valley System									
154	Newark Valley	26,000	1,300	27,000	26,000	4,300	3,000	—	27,000
155A	Little Smoky Valley-Northern Part	7,700	720	8,400	6,100	2,400	1,700	—	6,800
155B	Little Smoky Valley-Central Part	460	0	460	0	0	0	—	0
Flow System 30: Railroad Valley System									
150	Little Fish Lake Valley	4,100	9.0	4,100	10,000	30	21	—	10,000
155C	Little Smoky Valley-Southern Part	1,900	0	1,900	0	0	0	—	0
156	Hot Creek Valley	4,700	450	5,200	7,500	1,500	1,000	—	8,000
173B	Railroad Valley-Northern Part	57,000	300	57,000	81,000	1,000	700	—	81,000
Flow System 32: Independence Valley System									
177	Clover Valley	12,000	2,800	15,000	19,000	9,300	6,500	—	22,000
188	Independence Valley	17,000	27	17,000	9,500	90	63	—	9,500
Flow System 33: Ruby Valley System									
176	Ruby Valley	68,000	1,500	70,000	70,000	4,900	3,400	—	72,000
178A	Butte Valley-Northern Part	11,000	290	11,000	8,400	970	680	—	8,700

Table A7–1. Predevelopment and recent (2000) groundwater-budget estimates for each hydrographic area within the Great Basin carbonate and alluvial aquifer system study area.—Continued

[All values in acre-feet per year rounded to two significant figures. Estimated error in recharge values is ±50 percent. Estimated error in discharge values is ±30 percent. Values in blue are for predevelopment conditions. Values in red are for recent (2000) conditions. Decrease in natural discharge and/or storage: calculated as the difference of well withdrawals and recharge from unconsumed irrigation and public supply water from well withdrawals. Minimum decrease in groundwater storage: calculated as the difference of the decrease in natural discharge and/or change in storage and groundwater discharge under predevelopment conditions, if the difference is greater than zero. Abbreviations: HA, hydrographic area; #, number; —, no estimate]

HA #	HA name	Groundwater recharge for pre-development conditions	Recharge from unconsumed irrigation and public supply water from well withdrawals (2000)	Groundwater recharge for recent (2000) conditions	Groundwater discharge for pre-development conditions	Well withdrawals (2000)	Decrease in natural discharge and/or storage (net well withdrawals) (2000)	Minimum decrease in groundwater storage (2000)	Groundwater discharge for recent (2000) conditions
	Flow System 34: Colorado System								
	Lake Mead Subarea								
164A	Ivanpah Valley-Northern Part	1,300	29	1,300	0	98	69	—	29
164B	Ivanpah Valley-Southern Part	1,400	60	1,500	0	200	140	—	60
165	Jean Lake Valley	64	39	100	0	130	91	—	39
166	Hidden Valley South	5.8	24	30	0	80	56	—	24
167	Eldorado Valley	450	960	1,400	0	3,200	2,200	—	1,000
212	Las Vegas Valley	28,000	[2]93,000	120,000	24,000	74,000	[3]-19,000	—	120,000
215	Black Mountains Area	650	510	1,200	1,700	1,700	1,200	—	2,200
	Muddy River Subarea								
171	Coal Valley	2,300	9.0	2,300	100	30	21	—	110
172	Garden Valley	6,600	9.0	6,600	0	30	21	—	9
181	Dry Lake Valley	8,900	18	8,900	0	60	42	—	18
182	Delamar Valley	4,300	9.0	4,300	0	30	21	—	9
183	Lake Valley	7,300	3,900	11,000	8,400	13,000	9,100	—	12,000
198	Dry Valley	1,700	1,600	3,300	10	5,200	3,600	—	1,600
199	Rose Valley	82	420	500	10	1,400	980	—	430
200	Eagle Valley	1,000	0	1,000	290	0	0	—	290
201	Spring Valley	7,900	6.0	7,900	1,000	20	14	—	1,000
202	Patterson Valley	5,400	660	6,100	0	2,200	1,500	—	700
203	Panaca Valley	3,000	2,900	5,900	8,400	9,800	6,900	—	11,000
204	Clover Valley	8,100	36	8,100	210	120	84	—	250
205	Lower Meadow Valley Wash	12,000	140	12,000	1,400	450	310	—	1,500
206	Kane Springs Valley	2,600	9.0	2,600	0	30	21	—	9
208	Pahroc Valley	4,200	9.0	4,200	0	30	21	—	9
209	Pahranagat Valley	3,800	840	4,600	26,000	2,800	2,000	—	27,000
210	Coyote Spring Valley	2,500	60	2,600	0	200	140	—	60
216	Garnet Valley	160	300	460	0	990	690	—	300
217	Hidden Valley North	130	3.0	130	0	10	7.0	—	3
218	California Wash	140	48	190	0	160	110	—	50
219	Muddy River Springs Area	120	2,700	2,800	35,000	8,900	6,200	—	38,000
220	Lower Moapa Valley	67	290	360	730	960	670	—	1,000
	White River Valley Subarea								
174	Jakes Valley	15,000	9.0	15,000	1,900	30	21	—	1,900
175	Long Valley	31,000	12	31,000	1,000	40	28	—	1,000
180	Cave Valley	15,000	12	15,000	2,000	40	28	—	2,000
207	White River Valley	36,000	1,000	37,000	80,000	3,500	2,500	—	81,000

Table A7–1. Predevelopment and recent (2000) groundwater-budget estimates for each hydrographic area within the Great Basin carbonate and alluvial aquifer system study area.—Continued

[All values in acre-feet per year rounded to two significant figures. Estimated error in recharge values is ±50 percent. Estimated error in discharge values is ±30 percent. Values in blue are for predevelopment conditions. Values in red are for recent (2000) conditions. Decrease in natural discharge and/or storage: calculated as the difference of well withdrawals and recharge from unconsumed irrigation and public supply water from well withdrawals. Minimum decrease in groundwater storage: calculated as the difference of the decrease in natural discharge and/or change in storage and groundwater discharge under predevelopment conditions, if the difference is greater than zero. Abbreviations: HA, hydrographic area; #, number; —, no estimate]

HA #	HA name	Groundwater recharge for pre-development conditions	Recharge from unconsumed irrigation and public supply water from well withdrawals (2000)	Groundwater recharge for recent (2000) conditions	Groundwater discharge for pre-development conditions	Well withdrawals (2000)	Decrease in natural discharge and/or storage (net well withdrawals) (2000)	Minimum decrease in groundwater storage (2000)	Groundwater discharge for recent (2000) conditions
Flow System 34: Colorado System—Continued									
Virgin River Valley Subarea									
221	Tule Desert	4,200	6.0	4,200	0	20	14	—	6
222	Virgin River Valley	34,000	12,000	46,000	39,000	40,000	28,000	—	51,000
Flow System 35: Goshute Valley System									
178B	Butte Valley-Southern Part	21,000	810	22,000	12,000	2,700	1,900	—	13,000
179	Steptoe Valley	86,000	1,900	88,000	110,000	6,400	4,500	—	110,000
187	Goshute Valley	20,000	720	21,000	6,600	2,400	1,700	—	7,300
Flow System 36: Mesquite Valley									
163	Mesquite Valley	1,900	3,900	5,800	2,200	13,000	9,100	—	6,100
Flow System 37: Great Salt Lake Desert System									
184	Spring Valley	110,000	1,300	110,000	82,000	4,300	3,000	—	83,000
185	Tippett Valley	14,000	6.0	14,000	2,000	20	14	—	2,000
186A	Antelope Valley-Southern Part	3,300	11	3,300	210	38	27	—	220
186B	Antelope Valley-Northern Part	10,000	25	10,000	100	82	57	—	120
189A	Thousand Springs Valley-Herrell-Brush Creek	6,100	0	6,100	2,000	0	0	—	2,000
189B	Thousand Springs Valley-Toano-Rock Spring	14,000	0	14,000	1,600	0	0	—	1,600
189C	Thousand Springs Valley-Rocky Butte Area	9,000	0	9,000	1,200	0	0	—	1,200
189D	Thousand Springs Valley-Montello-Crittenden	18,000	1,200	19,000	15,000	4,100	2,900	—	16,000
191	Pilot Creek Valley	4,800	90	4,900	5,400	300	210	—	5,500
251	Grouse Creek Valley	13,000	1,200	14,000	13,000	4,100	2,900	—	14,000
252	Pilot Valley	1,600	0	1,600	7,400	0	0	—	7,400
253	Deep Creek Valley	17,000	180	17,000	18,000	600	420	—	18,000
254	Snake Valley	160,000	3,300	160,000	130,000	11,000	7,700	—	130,000
255	Pine Valley	27,000	0	27,000	0	0	0	—	0
256	Wah Wah Valley	6,000	0	6,000	1,500	0	0	—	1,500
257	Tule Valley	13,000	0	13,000	38,000	0	0	—	38,000
258	Fish Springs Flat	1,600	0	1,600	34,000	0	0	—	34,000
259	Dugway-Government Creek Valley	13,000	570	14,000	6,100	1,900	1,300	—	6,700
260A	Park Valley-West Park Valley	4,400	0	4,400	5,300	0	0	—	5,300
261A	Great Salt Lake Desert-West Part	29,000	0	29,000	74,000	0	0	—	74,000
Flow System 38: Great Salt Lake System									
260B	Park Valley-East Park Valley	3,800	780	4,600	12,000	2,600	1,800	—	13,000
261B	Great Salt Lake Desert-East Part	200	0	200	7,400	0	0	—	7,400

Table A7–1. Predevelopment and recent (2000) groundwater-budget estimates for each hydrographic area within the Great Basin carbonate and alluvial aquifer system study area.—Continued

[All values in acre-feet per year rounded to two significant figures. Estimated error in recharge values is ±50 percent. Estimated error in discharge values is ±30 percent. Values in blue are for predevelopment conditions. Values in red are for recent (2000) conditions. Decrease in natural discharge and/or storage: calculated as the difference of well withdrawals and recharge from unconsumed irrigation and public supply water from well withdrawals. Minimum decrease in groundwater storage: calculated as the difference of the decrease in natural discharge and/or change in storage and groundwater discharge under predevelopment conditions, if the difference is greater than zero. Abbreviations: HA, hydrographic area; #, number; —, no estimate]

HA #	HA name	Groundwater recharge for pre-development conditions	Recharge from unconsumed irrigation and public supply water from well withdrawals (2000)	Groundwater recharge for recent (2000) conditions	Groundwater discharge for pre-development conditions	Well withdrawals (2000)	Decrease in natural discharge and/or storage (net well withdrawals) (2000)	Minimum decrease in groundwater storage (2000)	Groundwater discharge for recent (2000) conditions
Flow System 38: Great Salt Lake System—Continued									
262	Tooele Valley	46,000	7,200	53,000	62,000	24,000	17,000	—	69,000
263	Rush Valley	77,000	1,600	79,000	36,000	5,400	3,800	—	38,000
264	Cedar Valley	29,000	1,800	31,000	4,100	6,100	4,300	—	5,900
265	Utah Valley Area	410,000	36,000	450,000	410,000	120,000	84,000	—	450,000
266	Northern Juab Valley	38,000	5,400	43,000	38,000	18,000	13,000	—	43,000
267	Salt Lake Valley	230,000	42,000	270,000	360,000	140,000	98,000	—	400,000
268	East Shore Area	290,000	18,000	310,000	120,000	60,000	42,000	—	140,000
269	West Shore Area	350	0	350	7,100	0	0	—	7,100
270	Skull Valley	25,000	1,700	27,000	35,000	5,700	4,000	—	37,000
271	Sink Valley	240	0	240	0	0	0	—	0
272	Cache Valley	720,000	11,000	730,000	540,000	37,000	26,000	—	550,000
273	Malad-Lower Bear River Area	440,000	7,200	450,000	370,000	24,000	17,000	—	380,000
274	Pocatello Valley	2,800	0	2,800	0	0	0	—	0
275	Blue Creek Valley	6,300	0	6,300	8,400	0	0	—	8,400
276	Hansel and North Rozel Flat	2,400	0	2,400	7,600	0	0	—	7,600
277	Promontory Mountains Area	5,400	600	6,000	11,000	2,000	1,400	—	12,000
278	Curlew Valley	12,000	22,000	34,000	76,000	72,000	50,000	—	98,000
279	Great Salt Lake	2,900	0	2,900	58,000	0	0	—	58,000
Flow System 39: Sevier Lake System									
280	Beryl-Enterprise Area	94,000	25,000	120,000	26,000	84,000	59,000	33,000	84,000
281	Parowan Valley	40,000	9,000	49,000	43,000	30,000	21,000	—	52,000
282	Cedar City Valley	32,000	10,000	42,000	32,000	35,000	25,000	—	42,000
283	Beaver Valley	80,000	2,400	82,000	68,000	8,000	5,600	—	70,000
284	Milford Area	13,000	15,000	28,000	33,000	49,000	34,000	1,000	49,000
285	Leamington Canyon	36,000	2,700	39,000	19,000	9,000	6,300	—	22,000
286	Pavant Valley	69,000	24,000	93,000	72,000	80,000	56,000	—	96,000
287	Sevier Desert	41,000	4,500	46,000	110,000	15,000	10,000	—	120,000

[1]Adjusted to exclude recharge from unconsumed irrigation from well withdrawals for mining operations, which are assumed to not be applied as irrigation and, therefore, do not contribute to groundwater recharge.

[2]Amount includes an additional 30,000 acre-ft of recharge from injected Colorado River water, the Nevada Division of Water Resources (NDWR) pumpage inventory, and 41,000 acre-ft of recharge from imported Colorado River Water (calculated as 10 percent of total imported Colorado water (440,000 acre-ft reported in NDWR pumpage inventory) minus amount injected (30,000 acre-ft)); imported surface water included in this estimate because HA 212 is the only HA with postdevelopment surface water importation.

[3]Due to injection of Colorado River water, amount of groundwater in storage has been increased in this HA and, therefore, estimate is negative.

Appendix 8: Development of Historical Well Withdrawal Estimates for the Great Basin Carbonate and Alluvial Aquifer System Study Area, 1940–2006

By Melissa D. Masbruch and Victor M. Heilweil

To evaluate general groundwater development trends within the Great Basin carbonate and alluvial aquifer system (GBCAAS) study area, historical annual well withdrawals for the period of 1940–2006 were estimated based on the compilation and interpolation of existing well-withdrawal data. Very few of the hydrographic areas (HAs) within the GBCAAS had complete well-withdrawal records for the period 1940–2006. This appendix presents the methodologies used to estimate well withdrawals in areas and for time intervals in which historical withdrawal data do not exist.

Sources of Historical Well Withdrawal Estimates

The state of Utah began compiling well withdrawals on an annual basis in 1963 as part of their "Ground-water conditions in Utah" reports (Arnow and others, 1964). Additionally, in HAs 267, 280, 281, 282, 283, 284, 286 and 287, annual withdrawal estimates extend back to the 1930s, 1940s, and 1950s (fig. A8–1). For irrigation wells, pumping well discharge is generally measured once every 3 years, and power consumption records are used to estimate average annual discharge. Public supply well withdrawals are reported to the state of Utah by each municipality.

For HAs in Nevada and California within the Death Valley groundwater flow system (fig. A8–1), estimates of annual well withdrawals were taken from two groundwater-withdrawal databases developed for the Death Valley regional groundwater flow system (DVRFS) study (Moreo and others, 2003; Moreo and Justet, 2008). Moreo and others (2003) estimate groundwater withdrawals from 1913 to 1998 for the HAs within the Death Valley regional flow system. In an update, Moreo and Justet (2008) estimate groundwater withdrawals for the period 1913–2003. The DVRFS withdrawal databases integrate datasets obtained from: (1) well-log and water-rights databases and pumpage inventories from the Nevada Division of Water Resources (NDWR), (2) data obtained directly from water users, (3) remotely sensed Thematic Mapper imagery, and (4) estimates of potential evapotranspiration (ET). Withdrawals were grouped into three categories: mining, public-supply, and commercial water use; domestic water use; and irrigation water use. Mining, public-supply, and commercial water use were generally estimated from wells that typically are metered. Domestic water use was estimated as the product of the number of domestic wells, which was determined using the NDWR well-log database, and the average annual domestic consumption, which was assumed to be 0.7 acre-ft (Moreo and others, 2003, p. 9). Irrigation water use was estimated as the product of irrigated acreage, which was identified using remote sensing and pumping inventories, and application rate. This rate was estimated by dividing annual crop ET, defined as annual potential ET multiplied by a crop coefficient, by the irrigation efficiency.

A second source of well-withdrawal data used for HAs within Nevada was pumping and crop inventories from the NDWR (http://water.nv.gov; Matt Dillon, NDWR, written commun., 2008). Pumping inventories, available on the NDWR website, have been conducted in 15 HAs generally since the late 1980s, except HAs 162 (1959–2008), 210 (2005–2008), 211 (1989–1991), 212 (1956–2008), 215 and 216 (2001–2008), and 230 (1983–2008). The crop inventories available on the NDWR website, which include estimates of well withdrawals for irrigation, are available only for the years 2006 and 2007. Additional unpublished data from Matt Dillon, NDWR, included withdrawal records for HAs 44, 48, 51 (1996–2006) and 219 (2000–2006),

A third source of well-withdrawal data used for HAs in Nevada was from a compilation of year 2000 groundwater withdrawals for the state of Nevada by Lopes and Evetts (2004). The primary source of data used in this compilation is the previously mentioned pumpage and crop inventories from the NDWR. In the absence of these inventory reports, quarterly and monthly pumpage reports from individuals and geothermal operations were used. If no pumping was reported, well withdrawals for the HA was estimated using Landsat imagery, statistical analysis, and mass-balance calculations.

In addition to these larger inventories and databases, estimates of historical well withdrawals reported in individual HA studies were also used. Auxiliary 4 lists the references and years for which previously reported estimates of well withdrawals were used.

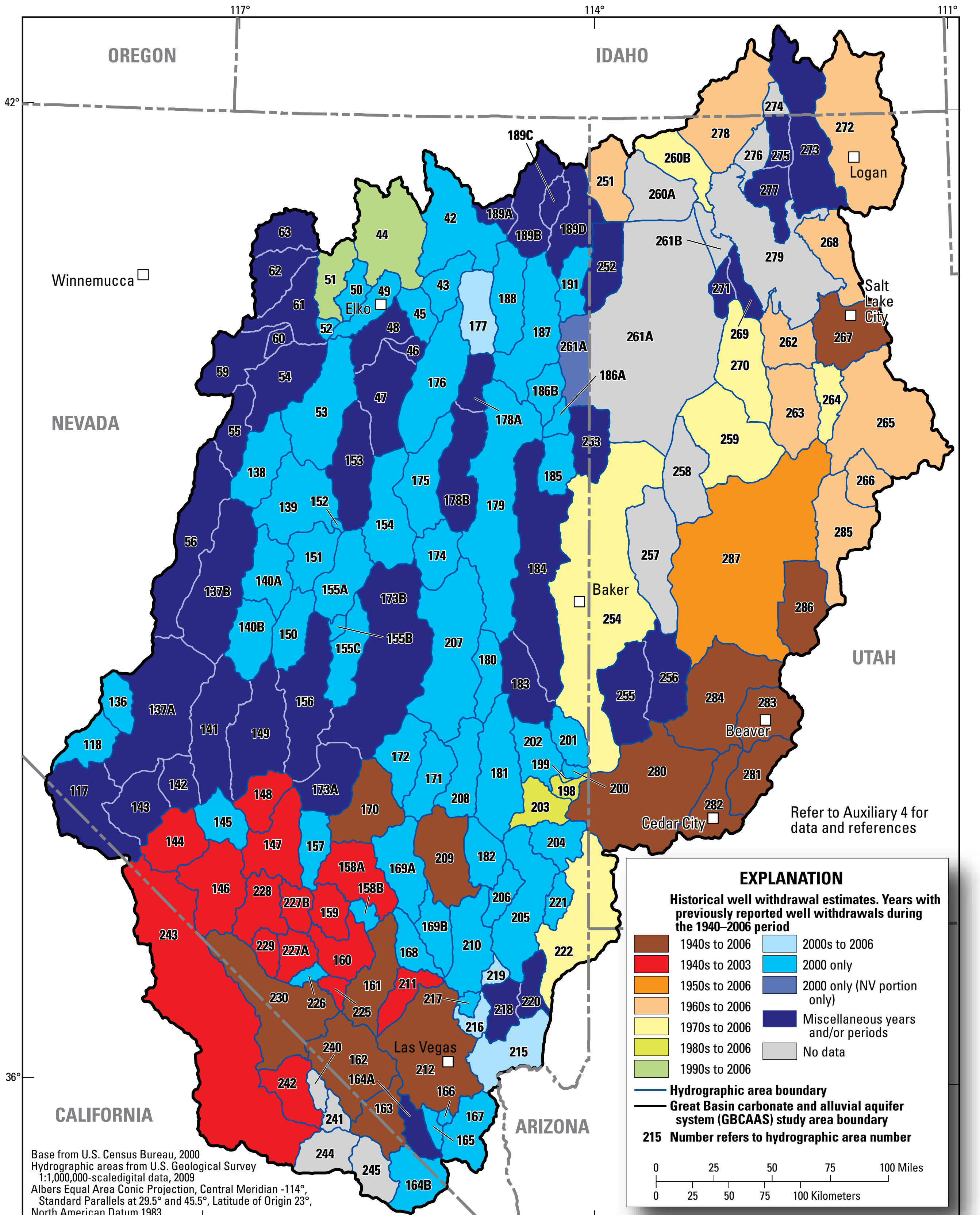

Figure A8–1. Hydrographic areas and time intervals of previously reported historical well-withdrawal estimates during the 1940–2006 period for the Great Basin carbonate and alluvial aquifer system study area.

Methods for Estimating Historical Well Withdrawals

Historical well-withdrawal estimates were developed only for the 78 HAs with more than 500 acre-ft of well withdrawals in the year 2000 (Auxiliary 4). Historical withdrawals were not estimated for the 87 HAs that had less than 500 acre-ft of withdrawals in the year 2000, as these HAs accounted for less than 0.4 percent of the total withdrawals in 2000 (Appendix 7; Auxiliary 4). Because of the differences in sources of historical well-withdrawal data, different methods of interpolating historical well withdrawals were used in different sections of the study area. These methods are described in the following sections.

Hydrographic Areas within Utah

For 19 HAs located entirely within Utah, unpublished data from the U.S. Geological Survey (USGS) Utah Water Science Center were used to develop historical estimates of well withdrawals; the other 12 HAs located entirely within Utah are assumed to have less than 500 acre-ft/yr of withdrawals in 2000 and historical well withdrawals were not estimated for these HAs. A subset of seven of these HAs (267, 280, 281, 282, 283, 284, and 286) has well-withdrawal estimates extending back to the 1930s and 1940s (Auxiliary 4). An inspection of total groundwater withdrawals in these seven HAs indicated that groundwater withdrawal was occurring in most of these seven basins prior to 1940, but that withdrawals began to increase rapidly from the mid-1940s to a peak or plateau during the mid-1970s. On average, 1940 withdrawals for these seven HAs were about 30 percent of the 1970–1979 average annual withdrawals. Therefore, annual withdrawals for HAs that did not have records extending back to 1940 were estimated to increase linearly from 30 percent of the 1970–1979 average in 1940 to the earliest value in their record (Auxiliary 4). In 17 HAs, these estimated withdrawals are less than and increase to about the same amount as the first reported well withdrawals. For Pavant Valley (HA 286) and Sevier Desert (HA 287), however, estimated withdrawals during the 1940s are higher than the subsequently reported well withdrawals beginning in 1946 and 1951, respectively.

Hydrographic Areas That Straddle the Utah-Idaho Border

For the three HAs that straddle the Utah-Idaho border (HAs 272, 273, and 278), assumptions had to be made for well withdrawals from the Idaho portion of these HAs because limited historical well withdrawal data were available. First, for the Utah portion of these HAs, the same linear interpolation methods used for the Utah HAs were applied to these three HAs to estimate the Utah portion of withdrawals for years without previously published estimates (1940–1962 for HA 272; 1940–1994 for HA 273; 1940–1963 for HA 278). Withdrawal estimates for the Utah portion of these HAs were then adjusted in the following ways. For Cache Valley (HA 272), total well withdrawals from 1969 and 1982–1990 (Kariya and others, 1994) were compared to withdrawals for the Utah portion only (USGS Utah Water Science Center data). The comparison indicated that well withdrawals from the Utah portion of Cache Valley accounted for 77 to 85 percent of total Cache Valley well withdrawals in these years. Total withdrawals for Cache Valley, therefore, were estimated by dividing the withdrawals from the Utah portion of the HA by 0.81 for all years except 1969 and 1982–1990 (Auxiliary 4). For Malad-Lower Bear River Area (HA 273), it was assumed that withdrawals from the Idaho portion equaled withdrawals from the Utah portion based on the area of irrigated land being approximately the same. Total withdrawals for Malad-Lower Bear River Area, therefore, were estimated by multiplying withdrawals from the Utah portion (USGS Utah Water Science Center data; Bjorklund and McGreevy (1974) for withdrawals in 1970) by 2 (Auxiliary 4). For Curlew Valley (HA 278), well withdrawals from the Utah portion of the HA (USGS Utah Water Science Center data; Baker, Jr. (1974) for 1964–1972) were compared to total well withdrawals for 1969–1971, for which period Baker, Jr. (1974) reported average withdrawals from the Idaho portion of the HA. The comparison indicated that withdrawals from the Utah portion of Curlew Valley accounted for 54 to 59 percent of total withdrawals from the HA during these years. Total withdrawals for Curlew Valley, therefore, were estimated by dividing the withdrawals from the Utah portion of the HA by 0.57 (Auxiliary 4).

Hydrographic Areas That Straddle the Utah-Nevada Border

For the eight HAs that straddle the Utah-Nevada border (HAs 189D, 222, 251, 252, 261A, 253, 254, and 280), well withdrawals were estimated in the following manner. For the Utah portion of HAs 222, 251, 253 and 254, the same linear interpolation methods used for the Utah HAs were applied to these four HAs to estimate the Utah portion of withdrawals for years with no previously published estimates (1940–1969 for HA 222; 1940–1963 for HA 251; 1940–1968 for HA 253; 1940–1972 for HA 254). Then well withdrawals from the Utah portion of the HA (USGS Utah Water Science Center data) were compared to withdrawals from the Nevada portion of the HA (Lopes and Evetts, 2004) for the year 2000. For Virgin River Valley (HA 222), withdrawals from the Nevada portion for the year 2000 were about 13 percent of withdrawals from the Utah portion; total withdrawals for the HA, therefore, were estimated by adding 13 percent to the Utah portion estimates (Auxiliary 4). For Grouse Creek Valley (HA 251), Deep Creek Valley (HA 253), and Snake Valley (HA 254), withdrawals from the Nevada portion for the year 2000 were only 5 percent or less of withdrawals from the Utah portion; it was assumed, therefore, that withdrawals from the Utah portion closely represented total withdrawals for these HAs (Auxiliary 4). For Pilot Valley (HA 252) and Great Salt Lake Desert-West Part (HA 261A), no withdrawals were reported for the Utah portion, and Lopes and Evetts (2004) reported withdrawals of 320 acre-ft for only the Nevada portion of HA 261A for the year 2000; it was assumed, therefore, that these HAs had less than 500 acre-ft/yr of withdrawals for the year 2000 and historical well withdrawals were not estimated for these HAs. Beryl-Enterprise Area (HA 280) lies mostly within Utah and there were no previous withdrawal estimates from the Nevada portion of the HA. Estimates of withdrawals from the Utah portion of this HA (USGS Utah Water Science Center data), therefore, were assumed to represent total withdrawals from this HA; the same linear interpolation methods used for the Utah HAs were applied to this HA to estimate withdrawals for years with no previously published estimates (1940–1944). Thousand Springs Valley-Montello-Crittenden (HA 189D) lies mostly within Nevada; there were no previously reported estimates of well withdrawals for the Utah portion of the HA. Well-withdrawal estimates for the Nevada portion of this HA are discussed below in the “Method 5: Miscellaneous Reference Years” section of the discussion of Nevada and California well withdrawal estimates.

Hydrographic Areas within Nevada and California

Twenty-three HAs in Nevada and California have historical well-withdrawal estimates that extend back to the 1940s (Auxiliary 4). These include 20 HAs within the Death Valley groundwater flow system, Pahranagat Valley (HA 209), Las Vegas Valley (HA 212), and Mesquite Valley (HA 163) (fig. A8–1). Additionally, 15 other HAs within the Humboldt (7), South-Central Marshes (24), Diamond Valley (27), and Colorado (34) groundwater flow systems have withdrawal estimates for part of the period 1940–2006.

For the 39 HAs in Nevada and California that had more than 500 acre-ft of withdrawals in Nevada in the year 2000 (Lopes and Evetts, 2004; Matt Dillon, NDWR, written commun., 2008; pumpage inventories from NDWR website http://water.nv.gov), but that did not have complete well-withdrawal records from 1940 through 2006, the following methods were used to estimate historical well withdrawals for years with no previously published estimates for the current study. Generally, the methodology used to estimate well withdrawals was the development of yearly ratios between the historical period and a reference year for HAs that had at least partial historical estimates; these yearly ratios were then applied to these HAs for the periods that lacked previously reported estimates of well withdrawals. For the HAs to which this method was applied, the year of the earliest reported withdrawals was used as the reference year. The methods and reference years used are explained in detail below, and the calculations are shown in table A8–1. Except for the determination of yearly ratios for Fish Lake Valley (HA 117), which had an estimate of significant well withdrawals in 1949 (Auxiliary 4), historical estimates of withdrawals for Pahrump Valley (HA 162), Amargosa Desert (HA 230), and Las Vegas Valley (HA 212) were not used in the development of these ratios. These HAs had significant well withdrawals extending back to the 1940s and the use of these HAs in the ratio calculations tended to cause overestimation of withdrawals in the lesser developed HAs.

(Table A8–1 is a Microsoft Excel file, organized by method; available as a separate file)

Table A8–1. 1940–2006 estimated historical well withdrawals for hydrographic areas in Nevada and California that have more than 500 acre-ft of withdrawals in the year 2000 (organized by method).

Method 1: Reference Year 2000

This method was applied to 29 HAs (table A8–1). It is based on historical well-withdrawal estimates from 26 HAs in the Humboldt (7), Death Valley (28), Colorado (34), and Mesquite Valley (36) groundwater flow systems that have a withdrawal estimate for the year 2000 in addition to the estimates reported by Lopes and Evetts (2004). Lopes and Evetts (2004) estimates are less than withdrawal estimates provided by the NDWR (Matt Dillon, NDWR, written commun., 2008) for HAs in the Humboldt groundwater flow system (7) and, therefore, were not used in the following ratio calculation. Historical estimates from each of these 26 HAs were used to develop a multiplication factor that was a ratio of the sum of the withdrawals for each year from 1940 to 2006 for a subset of these HAs to the sum of the withdrawals in 2000 for the same subset (table A8–1). For example, in 1951, 19 out of the 26 HAs have a withdrawal estimate. The multiplication factor for this year was calculated as the sum of withdrawals from these 19 HAs in 1951 divided by the sum of withdrawals from these 19 HAs in 2000. The multiplication factors were then applied to the withdrawal estimates in 2000 for 29 HAs to estimate withdrawals from the periods 1940–1999 and 2001–2006, except for the years in which a withdrawal estimate was reported (Auxiliary 4).

Method 2: Reference Year 1996

This method was applied to three HAs (44, 48, and 51). It is based on historical withdrawal estimates from 26 HAs in the Humboldt (7), Death Valley (28), Colorado (34), and Mesquite Valley (36) groundwater flow systems that have withdrawal estimates for the year 1996. Historical estimates for each of these 26 HAs were then used to develop a multiplication factor that was a ratio of the sum of the withdrawals for each year from 1940 to 2006 from a subset of these HAs to the sum of the withdrawals in 1996 from the same subset (table A8–1). The multiplication factors were then applied to the withdrawal estimates in 1996 for these three HAs to estimate withdrawals from the period 1940–1995 (Auxiliary 4).

Method 3: Reference Year 1998

This method was applied to six HAs (54, 56, 59, 60, 61, and 173A). It is based on historical withdrawal estimates from 31 HAs in the Humboldt (7), Death Valley (28), Colorado (34), and Mesquite Valley (36) groundwater flow systems that have withdrawal estimates from the year 1998. Historical estimates for each of these 31 HAs were then used to develop a multiplication factor that was a ratio of the sum of the withdrawals for each year from 1940 to 2006 from a subset of these HAs to the sum of the withdrawals in 1998 from the same subset (table A8–1). The multiplication factors were then applied to the withdrawal estimates in 1998 for these six HAs to estimate withdrawals from the periods 1940–1997 and 1999–2006, except for the years in which a previous withdrawal estimate was reported (Auxiliary 4).

Method 4: Reference Year 1989

This method was applied to three HAs (198, 199, and 203). It is based on historical withdrawal estimates from 23 HAs in the Death Valley (28), Colorado (34), and Mesquite Valley (36) groundwater flow systems that have withdrawal estimates from the year 1989. Historical estimates for each of these 23 HAs were then used to develop a multiplication factor that was a ratio of the sum of the withdrawals for each year from 1940 to 2006 from a subset of these HAs to the sum of the withdrawals in 1989 from the same subset (table A8–1). The multiplication factors were then applied to the withdrawal estimates in 1989 for these three HAs to estimate withdrawals from the periods 1940–1988 and 1999–2006 (Auxiliary 4).

Method 5: Miscellaneous Reference Years

This method was used to estimate historical withdrawals for five HAs (56, 117, 215, 216, and 189D) that did not fit into the above categories. For HA 56, historical estimates from 22 HAs were used to develop a multiplication factor that was the ratio of the sum of the withdrawals for each year from 1940 to 2006 from a subset of these HAs to the sum of the withdrawals in 1964 from the same subset (table A8–1). These multiplication factors were then applied to the withdrawal estimate in 1964 for HA 56 to estimate withdrawals for the periods 1940–1963 and 1999–2006 (Auxiliary 4).

For HA 117, historical estimates from 23 HAs were used to develop a multiplication factor that was the ratio of the sum of the withdrawals for each year from 1940 to 2006 from a subset of these HAs to the sum of the withdrawals in 1949 from the same subset (table A8–1). These multiplication factors were then applied to the withdrawal estimate in 1949 for HA 117 to estimate withdrawals for the periods 1940–1948, 1970–1988, and 1990 (Auxiliary 4).

For HAs 215 and 216, historical estimates from 25 HAs were used to develop a multiplication factor that was the ratio of the sum of the withdrawals for each year from 1940 to 2006 from a subset of these HAs to the sum of the withdrawals in 2001 from the same subset (table A8–1). These multiplication factors were then applied to the withdrawal estimate in 2001 for HAs 215 and 216 to estimate withdrawals for the period 1940–2000 (Auxiliary 4).

For HA 189D, historical estimates from 18 HAs were used to develop a multiplication factor that was the ratio of the sum of the withdrawals for each year from 1940 to 2006 from a subset of these HAs to the sum of the withdrawals in 1968 from the same subset (table A8–1). These multiplication factors were then applied to the withdrawal estimate in 1968 for HA 189D to estimate withdrawals for the periods 1940–1967 and 1969–2006 (Auxiliary 4). Although HA 189D straddles the Utah-Nevada border, it lies mainly within Nevada, and therefore it is believed that withdrawals from the Nevada portion represent total withdrawals for this HA.

References

Arnow, T., and others, 1964, Ground-water conditions in Utah, spring of 1964: Utah Water and Power Board (Utah Division of Water Resources) Cooperative Investigations Report no. 2, 104 p.

Baker, Jr., C.H., 1974, Water resources of the Curlew Valley drainage basin, Utah and Idaho: State of Utah Department of Natural Resources Technical Publication 45, 91 p.

Bjorklund, L.J., and McGreevy, L.J., 1974, Ground-water resources of the Lower Bear River drainage basin, Box Elder County, Utah: State of Utah Department of Natural Resources Technical Publication 44, 65 p.

Kariya, K.A., Roark, D.M., and Hanson, K.M., 1994, Hydrology of Cache Valley, Cache County, Utah, and adjacent part of Idaho, with emphasis on simulation of ground-water flow: State of Utah Department of Natural Resources Technical Publication 108, 120 p.

Lopes, T.J., and Evetts, D.M., 2004, Ground-water pumpage and artificial recharge estimates for calendar year 2000 and average flow by hydrographic area, Nevada: U.S. Geological Survey Scientific Investigations Report 2004–5239, 87p.

Moreo, M.T., Halford, K.J., La Camera, R.J., and Laczniak, R.J., 2003, Estimated ground-water withdrawals from the Death Valley regional flow system, Nevada and California, 1913–98: U.S. Geological Survey Water-Resources Investigations Report 03–4245, 28p.

Moreo, M.T., and Justet, L., 2008, Update to the ground-water withdrawal database for the Death Valley regional ground-water flow system, Nevada and California, 1913–2003: U.S. Geological Survey Data Series 340, 10 p.

Heilweil and Brooks—**Conceptual Model of the Great Basin Carbonate and Alluvial Aquifer System**—Scientific Investigations Report 2010–5193